ELECTRON TRANSFER PROCESSES BETWEEN ORGANIC REDOX CENTRES AND ELECTRODES VIA ACTIVE BRIDGES IN SELF-ASSEMBLED MONOLAYERS

Dissertation zur Erlangung des
naturwissenschaftlichen Doktorgrades
der Bayerischen Julius-Maximilians-Universität Würzburg

vorgelegt von
Volker Kriegisch
aus Ingolstadt

Würzburg 2005

Promotionsgesuch eingereicht am:_____
bei der Fakultät für Chemie und Pharmazie

1. Gutachter: _____
2. Gutachter: _____
der Dissertation

1. Prüfer: _____
2. Prüfer: _____
3. Prüfer: _____
des öffentlichen Promotionskolloquiums

Tag des öffentlichen Promotionskolloquiums:_____

Doktorurkunde ausgehändigt am:_____

Die vorliegende Arbeit wurde in der Zeit von Januar 2002 bis August 2005
am Institut für Organische Chemie der Universität Würzburg angefertigt

Mein besonderer Dank gilt

Herrn Prof. Dr. C. Lambert

für die Überlassung des äußerst vielseitigen und interessanten Themas und
das mit vielen Anregungen verbundene Interesse an dieser Arbeit

Es gibt nichts Mächtigeres auf dieser Welt, als eine Idee, für die die Zeit gekommen ist.

Victor Hugo
(1802 – 1885)

meinen Eltern

Table of Contents

List of Abbreviations

AC	Alternating current
CPE	Constant phase elements
DC	Direct current
EN	Energy transfer
ET	Electron transfer
FET	Field-effect transistors
GOD	Glucose oxidase
HTL	High temperature limit
ILIT	Indirect laser-induced temperature jump
IRRAS	Infrared reflection absorption spectroscopy
ITO	Indium tin oxide
IV-CT	Intervalence-charge-transfer
LB	Langmuir-Blodgett
MPC	Monolayer-protected cluster
MRH^+-GOD	Protonated merocyanine-glucose oxidase
NLO	Non-linear optical
OLED	Organic light-emitting diode
OPE	Oligophenyleneethynylene
OPV	Oligophenylenevinylene
PES	Potential energy surface
QCM	Quartz crystal microbalance
SAM	Self-assembled monolayer
SP-GOD	Nitrospiropyran-glucose oxidase
STM	Scanning tunnelling microscopy
XPS	X-ray photoelectron spectroscopy

1 Introduction

The research topic of self-assembled monolayers (SAMs) has witnessed tremendous growth in synthetic sophistication and depth of characterisation over the past 20 years [1]. Functionalised self-assembled monolayers [2-4] have attracted the attention of many scientists because of their potential applications in chemical sensors [5-7], biosensors [8, 9], NLO-systems [10-14], molecular switches [9, 15-20], molecular electronics [21-26], photovoltaic devices [27-29], active surfaces for patterning [30-34] and chemical architecture [35, 36]. Even chromophore SAMs attached to gold nanoparticles [37-56] and to other surfaces such as SiO_2 [1, 3, 57-60] or ITO (indium tin oxide) [18, 61, 62] play an increasingly important role and might surpass bulk gold in many technological aspects.

It is well known that organosulphur compounds react with gold surfaces. In 1982 *Taniguchi et al.* observed the spontaneous formation of pyridine disulphide SAMs on a gold surface [63]. In 1983, *Nuzzo* and *Allara* showed that SAMs of alkanethiolate on gold could be prepared by adsorption of *n*-alkyl disulphides from dilute solutions [64]. This report initiated a rapid growth in SAMs research.

The reasons for the large interest in SAMs are their great advantages compared to Langmuir-Blodgett (LB) films [65, 66]. Although there have been numerous attempts to organise molecules in LB-films, the instability of the physisorbed layers and the defects caused by previously adsorbed material are inherent limitations [67]. On the other hand SAMs are ordered molecular assemblies formed by the adsorption of an active surfactant on a solid surface which includes the formation of a covalent bond of thiol e. g. to gold or silver. This simple process makes SAMs inherently manufacturable and thus technologically attractive. Chemisorption involves relatively large heats of bond formation (40 – 160 kJ/mol) and has two advantages: firstly, the chemical reaction displaces any previously formed physically attached adsorbates or impurities from the surface. Secondly, the adsorbed species, once bonded, is difficult to remove from the surface. However there are three disadvantages of chemisorption: the uncertain degree of coverage, the possibility of further chemical reactions, e. g. thiolates on gold slowly oxidise to sulfoxides in high-humidity environment, and the formation of surface dipoles [67].

While the majority of publications deals with thiols on gold, silanes on hydroxylated surfaces, like silicon, glass, mica or ITO are important systems for many potential applications [3, 56, 68, 69], although high quality SAMs of alkyltrichlorosilane

derivatives are difficult to produce. SAMs of fatty acids are an important link between the Langmuir-Blodgett and the self-assembly techniques [3].

While the early days of SAM research were almost exclusively devoted to the investigation of the formation, structure and physical properties of alkanethiols on gold, in the past decade the function of such SAMs moved into the foreground. In many cases the functionality of SAMs is associated with chromophores or π–systems in the broadest sense. Although one can hardly speak of dyes in the common sense because the colour of these SAM chromophores is invisible to the human eye owing to the low absorptivity of the monolayer, changes of absorptivity, orientation, redox state, electron transfer behaviour etc. can readily be measured by a variety of physical methods and can be used to build up functional units on a monolayer scale. Therefore, if we speak of "chromophores" in this context we simply mean more or less extended functional π–systems.

2 Basic Aspects of SAMs

Owing to the easy preparation, to the well-defined order and also to the relative inertness of the substrate, thiols on gold have become a model system for SAMs. The most studied and probably best understood SAMs are those of alkanethiolates on Au(111) surfaces [3, 70-78]. The following description gives a brief overview of the basics of alkanethiol-SAMs, more information can be obtained from the reviews mentioned above and related literature.

2.1 Structure of Alkanethiol-SAMs

A gold substrate can simply be coated with an organised monolayer by immersing the substrate into a dilute solution of thiol or disulphide. The formation of the SAMs may be considered formally as an oxidative addition of the S-H bond to the gold surface, followed by a reductive elimination of hydrogen. Extensive X-ray photoelectron spectroscopic (XPS) experiments suggest that chemisorption of alkanethiols on gold(0) surfaces yields the gold(I) thiolate ($R\text{-}S^-$) species [79]. The presumed adsorption chemistry is:

$$R\text{-}SH + Au_n^0 \rightarrow R\text{-}S^- - Au^+ + \tfrac{1}{2} H_2 + Au_{n-1}^0$$

The bonding of the thiolate group to the gold surface is very strong (the homolytic bond strength is approximately 160 kJ/mol) [80].

Even though the mechanism of SAM formation is still under debate the structure of the monolayer is well understood. In general, the arrangement of sulphur atoms is hexagonal and commensurate with the underlying gold lattice (**fig. 2-1**, **A**). This imposes an S-S distance of 4.97 Å [3]. Depending on the length of the alkyl chains and their relative orientation superlattices may form as exemplified by the c(4 x 2) superlattice of a $(\sqrt{3} \times \sqrt{3})R30°$ overlay structure of octanethiol on Au(111) (**fig. 2-1**, **B**) [81]. While it is generally believed that the stability of the alkanethiol SAMs increases with increasing chain length owing to increasing van der Waals interactions, *Ulman et al.* suggested two chemisorption modes with 180° surface-S-C angle (sp-hybridisation of S) and 104° surface-S-C angle (sp^3-hybridisation of S), the latter being slightly more stable [82]. Indeed,

Zharinkov et al. demonstrated that hydridisation and thus spatial orientation of the bonding orbitals of sulphur is the determining factor for the orientation and density of the monolayers rather than intermolecular interactions [83].

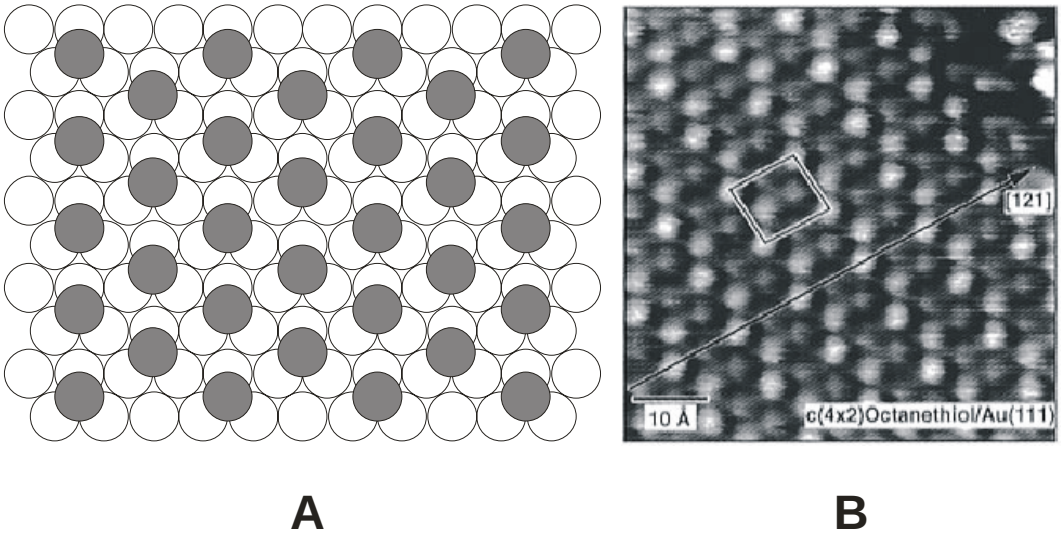

Fig. 2-1 **A**: Hexagonal coverage scheme for alkanethiolates on Au(111). The open circles are gold atoms and the grey circles are sulphur atoms [3]; **B**: Constant-current STM topograph of an octanethiol monolayer on Au(111) which shows a c(4 x 2) superlattice of a $(\sqrt{3} \times \sqrt{3})R30°$ overlay structure. Reprinted with permission from [81]

Because in SAMs the sulphur-sulphur interactions are believed to be minimal and the sulphur-sulphur distance is greater than the minimal distance of the alkyl chains, the latter are tilted in order to maximise the interchain alkyl-alkyl van der Waals interactions. This tilt angle is found to be ~30° with respect to the surface normal towards the nearest neighbour direction (**fig. 2-2**) [70].

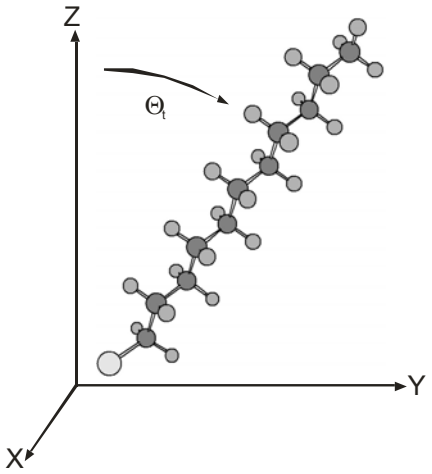

Fig. 2-2 The tilt angle Θ_t of the alkanethiol chain relative to the surface normal [70]

2.2 Important Chromophores in SAMs and their Applications of Self Assembled Dyes on Gold

In recent years organised assemblies e. g. of porphyrins [28, 84-111], phthalocyanines [112-118], fullerene (C_{60}) [27-29, 119-123], aromatic azo compounds [19, 20, 124-128], pyrene chromophores [28, 89, 129-131] and various kinds of other chromophores like merocyanines [132], carotenoids [133-135], helical peptides [136], mixed-valence Ru-Fe complexes [137], quinone dyes [138], cyanine SAMs [87, 88] and perylene bisimide dyes [139] on gold surfaces have attracted considerable attention which was directed towards the development of photovoltaic devices [28, 140], catalysis [96, 141] and photonic sensors [9, 17, 18, 142-145].

2.2.1 Photocurrent generation

One way to convert light energy into electrical energy is to use light sensitive electrodes. Sensitisation of an electrode can be defined as a process by which a heterogeneous interfacial electron transfer (ET) occurs as the consequence of light absorption by a chromophore which is termed photosensitiser. Light absorption of the chromophore sensitiser leads to an excited state which is both a stronger reducing agent and a stronger oxidising agent than the chromophore ground state. The excited sensitiser then oxidises (reduces) an electron donor (acceptor) mediator which serves as a hole (electron) carrier while the sensitiser is concomitantly oxidised (reduced) by the sensitiser supporting electrode. Depending on the relative energy level of sensitiser, Fermi energy of the electrode and redox potential of the mediator an anodic (cathodic) photocurrent is observed. A quantification of the energetic level, thus, is of great importance for the development of photoelectrosynthetic or regenerative cells. One important competitive mechanism to photocurrent generation is the deactivation of the excited sensitiser by energy transfer (EN) to the metal electrode [146].

The ET and EN processes in chromophore SAMs have been widely studied with different systems such as porphyrins [84, 91, 92, 102, 103], fullerenes [29, 120-122], carbazols [136] and pyrenes [89]. SAMs built from molecules consisting of multiple chromophore units in a linear array (dyads, triads etc.) play an important role in the development of devices for photocurrent generation, artifical photosynthesis or current rectification [27, 28, 62, 147-149].

Imahori et al. synthesised a series of dyad and triad chromophore arrays in order to mimic the highly efficient multistep electron transfer in natural photosynthesis [27, 28]. The work of *Imahori et al.* lead to the design of a triad modified SAM which combines all the features for efficient photocurrent generation: a free-base porphyrin as the photosensitiser terminated by C_{60} as covalently attached redox mediator, both bound to the gold electrode by a second redox mediator/relay (ferrocene) which separates the photosensitiser from the metal electrode in order to minimise back electron transfer and excited state quenching. By this way an exceptionally high quantum yield of 25% could be achieved (**fig. 2-3**) [149].

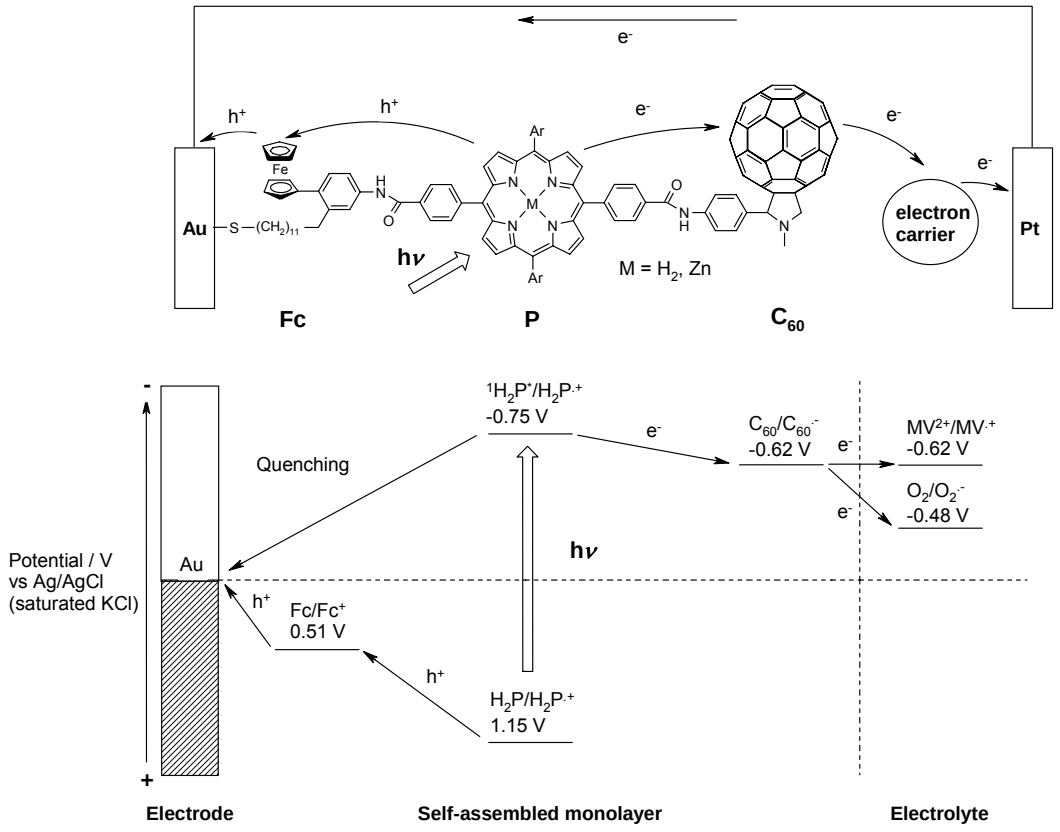

Fig. 2-3 Photoinduced multistep ET at gold electrodes modified with SAMs of ferrocene-porphyrin-C_{60} alkanethiols, electron carrier: oxygen or viologen [28]

2.2.2 Photoswitchable Chromophores as a Route to Optoelectronic Systems

Photostimulation of molecules, macromolecules and biopolymers can lead to changes of their chemical or physical properties which provide the basis for the development of future optoelectronic devices. The photostimulated modification of

biocatalytic and highly specific recognition and binding functions of biomaterials would enable their application in optoelectronic devices [150].

Photostimulation of redox enzymes could transduce recorded optical signals as an amperometric response by their electrical interaction with electrode interfaces. For example, amperometric transduction of recorded optical signals was accomplished using nitrospiropyran-modified glucose oxidase as photoswitchable material (**fig. 2-4**) [15].

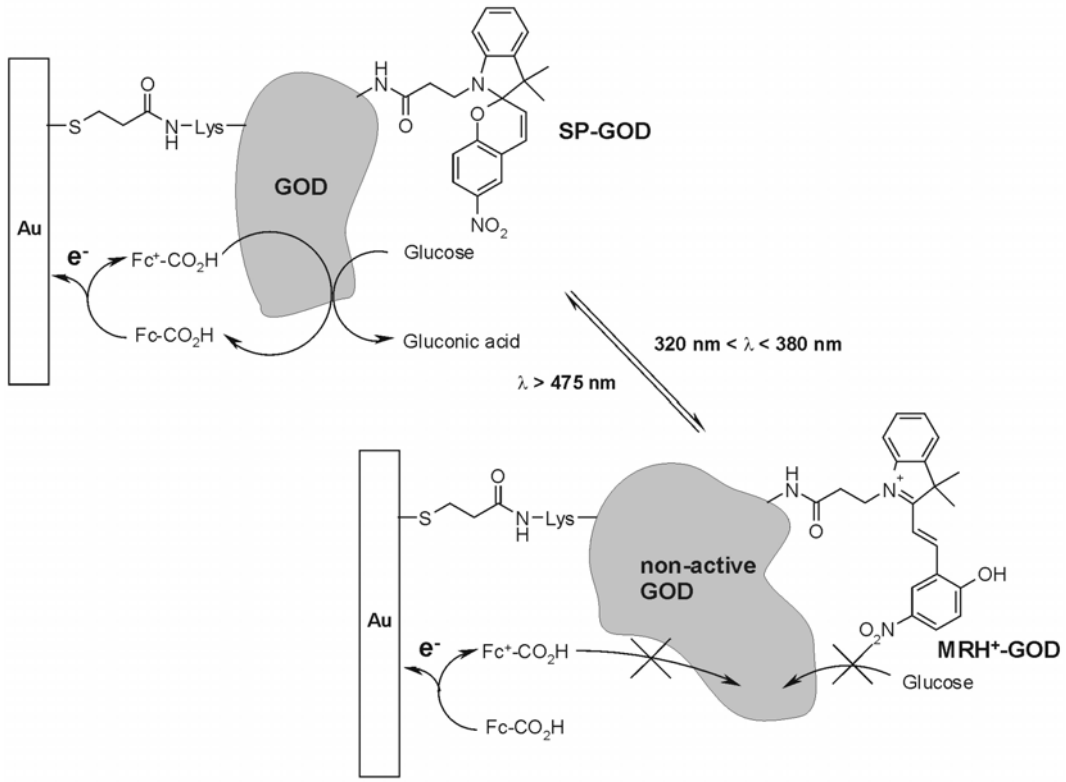

Fig. 2-4 Photoisomerisable nitrospiropyran-functionalised glucose oxidase, SP-GOD, in the active (above) and inactive (below) form in order to mediate the oxidation of glucose [17]

Another application for photoswitchable enzymes attached to gold surfaces is the cytochrome c-mediated biocatalysed reduction of O_2 by cytochrome oxidase, using a functional pyridine-nitrospiropyran photoisomerisable mixed monolayer electrode [9, 17, 18].

Feringa et al. studied the optoelectronic switching of a photochromic molecule using a mechanical break-junction technique and UV/Vis spectroscopy (**fig. 2-5**) [151]. In solution it is possible to switch between the closed and the open state by illuminating the molecule with light of wavelength λ = 546 nm while it can be switched back by using UV-light at λ = 316 nm. If the chromophore is placed between two Au electrodes only the ring opening reaction occurs using visible light. A switch back from the isolating to the conducting state was not possible which is attributed to the quenching of the excited state of the molecule in the open form by the gold electrodes [151].

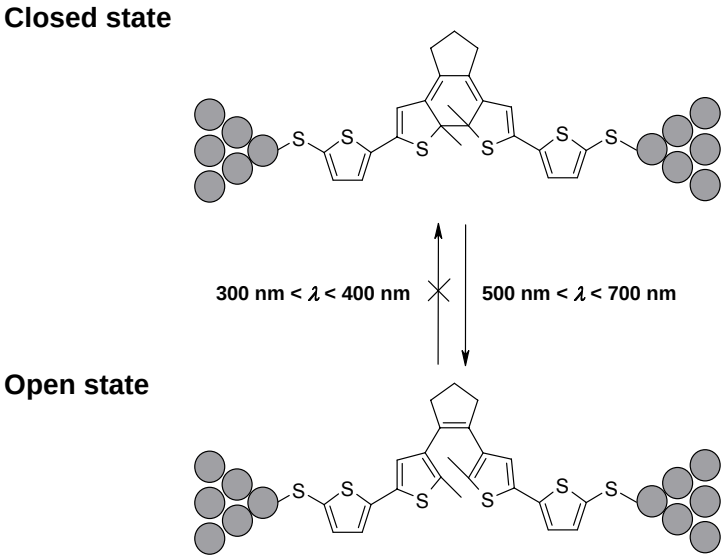

Fig. 2-5 Photochromic molecular switch between two Au contacts in closed state and open state [151]

2.2.3 Self-Assembled Monolayers of Phthalocyanines as Sensors and as Hole-Injection Layers in Organic Light-Emitting Diodes

Phthalocyanines can be used as the chemically active component in both conductometric and optical gas sensors [112, 152]. The technique of self-assembly has the merit of simplicity and from the viewpoint of an application within a sensor, the advantage of providing a monomolecular layer which should exhibit near instantaneous response to a gaseous analyte [153]. Fluorescence quenching by external molecules can, in principal, provide the basis for an optical sensing device. Exposure of a phthalocyanine alkanethiol SAM with a longer chain tether to 200 ppm NO_2 gas showed that the fluorescence is indeed reversibly quenched [154]. In further experiments, changes in the surface plasmon resonance reflectivity signal proportional to the concentration were observed when a phthalocyanine SAM was exposed to NO_2, pointing to a further optical method for the detection of this gas [114].

Another interesting application is to use phthalocyanines as a hole-injection layer in organic light-emitting diodes (OLEDs). *Zhu et al.* demonstrated that a SAM of phthalocyanine thiol (HS-Pc) may act as a hole injection material in OLEDs (**fig. 2-6**). The insertion of a SAM of HS-Pc between the Au anode and the hole-transport layers enhances the hole injection which increases the external quantum efficiency by a factor of ~ 27

compared to the OLED without SAM and decreases the operating voltage from 13 to 8 V [155].

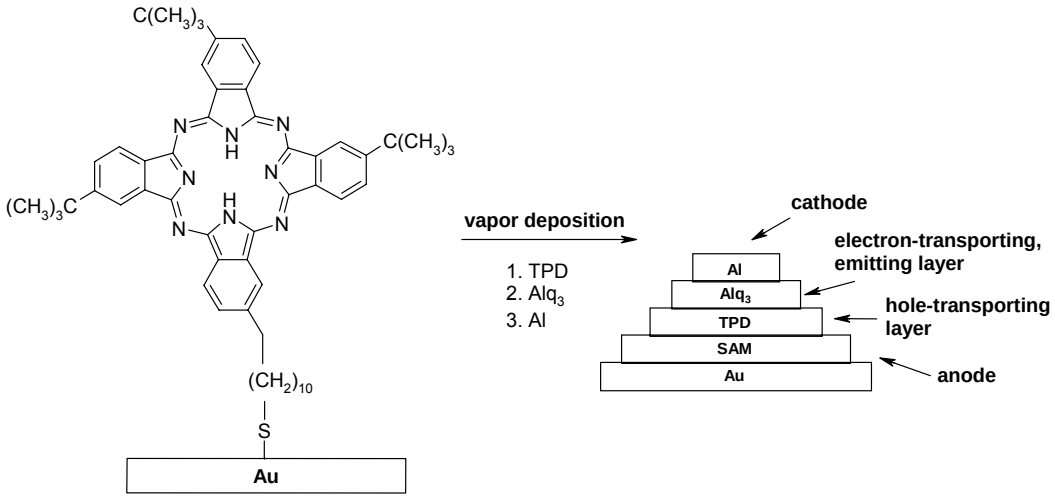

Fig. 2-6 A phthalocyanine SAM as the hole injection layer in a two-layer OLED with *N*,*N*′-bis(3-methylphenyl)-1,1′-biphenyl-4,4′-diamine (TPD) as the hole transport layer and tris(8-hydroxyquinolinato)aluminium (Alq_3) as the electron transport and emitting layer [155]

2.2.4 SAMs as Testing Materials for Molecular Wires

A detailed understanding of how electrons are transferred through organic molecules is an important topic in several areas: rationalising ET in organic conducting and semiconducting materials, biological systems such as the photosynthetic reaction centre, fabricating molecular electronic devices such as organic light emitting diodes (OLED), memory devices or field-effect transistors (FETs) and developing quantum computers on a single-molecular scale [156]. Recent work on the electrochemistry of SAMs on electrodes provides a general route to create surface structures in which redox-active molecules are linked to electrodes via well-defined molecular bridges. One great advantage of this approach is that the distance of the redox centres from the electrode, the chemical surrounding of the redox centres as well as the type of the molecular bridges can be varied systematically. These SAM structures can then serve as excellent model systems for studying bridge mediated ET.

Creager et al. as well as *Chidsey et al.* investigated the ET of ferrocene groups attached to gold electrodes with oligo(phenylenethynylene) bridges of variable length and structure in mixed monolayers with hydroxyalkanethiol dummy molecules (**fig. 2-7**) [157-159]. The conjugated bridges allow a strong electronic coupling between the gold electrode

and the ferrocene redox centre which results in a rapid electron transfer over long distances. Using impedance spectroscopy [160] the effects of bridge length on the ET show an exponential distance dependence of the bridge-mediated ET rates from k_{et} = 350 s^{-1} for the longest bridge (six phenylethynyl units, **E**) to k_{et} = 500000 s^{-1} for the shortest bridge with three phenylethynyl units **A** (**Fig. 2-7**). The effect on the ET rates if two propoxy groups are attached to one of the phenyl rings of the bridge was found to be minimal (cf. **B** vs **C**).

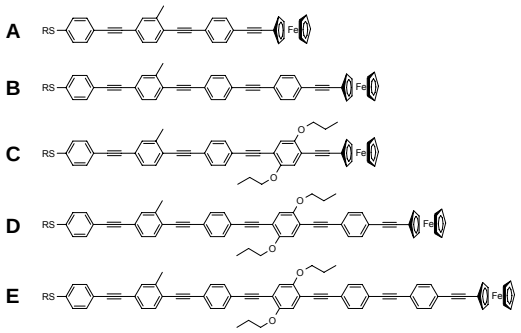

Monolayer components	k_{et} / s^{-1}
A + HO-$(CH_2)_{16}$-SH	5 x 10^5
B + HO-$(CH_2)_{16}$-SH	6 x 10^4
C + HO-$(CH_2)_{16}$-SH	6.5 x 10^4
D + HO-$(CH_2)_{16}$-SH	5 x 10^3
E + HO-$(CH_2)_{16}$-SH	3.5 x 10^2

Fig. 2-7 Structures and rate constants for the heterogeneous ET of ferrocene oligo(phenylenethynylene) thiols in SAMs [158]

In comparison to the above mentioned ferrocene oligo(phenylenethynylene) SAMs, a group of ferrocene-terminated oligo(phenylenevinylene)methane thiols **F** – **J** was prepared and the ET behaviour in the corresponding SAMs was investigated [161]. Studies of the monolayers containing oligomeres of the same length with and without ethoxy

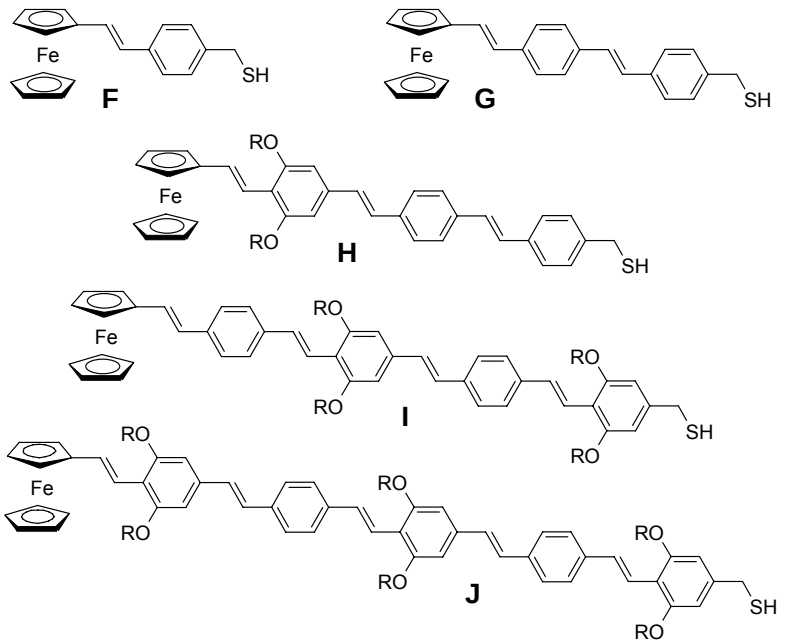

solubilising groups using cyclic voltammetry revealed that both types of oligomers form well-packed SAMs. The position of the solubilising groups in the oligomer chain does not influence the packing in the monolayer significantly. ET measurements were performed on these systems with the indirect laser-induced temperature jump method. The measured ET rate constants are all greater than 5 x 10^5 s^{-1} for the five oligomers **F** – **J** [162].

Other interesting candidates as bridges in molecular wires are oligophenylenevinylene (OPV) chromophores **K** – **Q** with two thioacetyl groups terminating each end [163]. Contact angle, FT-IRRAS and XPS measurements show that molecules with linear hexyloxy-substituted OPV structures **K** – **M** form disordered SAMs. The [2.2]-paracyclophane containing OPVs (**P**, **Q**) form significantly better SAMs than examples with side groups. The best structures for obtaining a monolayer are the unsubstituted OPVs **N** and **O**. Ellipsometry measurements indicate that in the case of

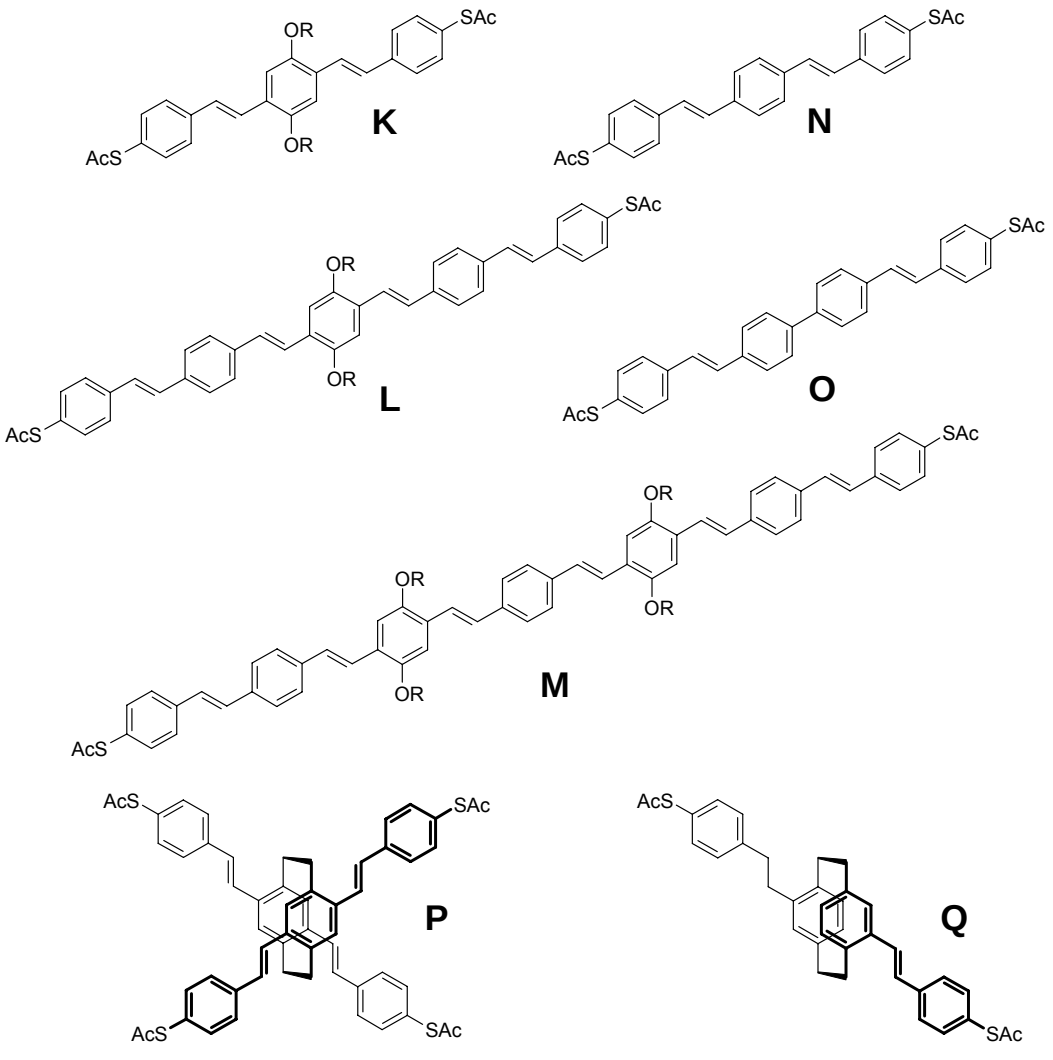

molecules **N** and **O** the orientation of the molecule coincides with the surface normal or is tilted up to 30° from the surface normal. Electrochemical investigations show that these derivatives, especially the [2.2]-paracyclophane-OPVs **P** and **Q** in which through-space and through-bond delocalisation is possible, are promising candidates for molecular wires.

3 Project Aim

The aim of this project is to investigate the influence of "active" bridge units on the electron transfer (ET) mechanism within an organic donor-bridge-electrode array.

Energetical low lying bridge states should support a hopping-mechanism while high lying bridge states facilitate an ET by superexchange. Adjusting the energetical accessible bridge states, the ET-mechanism (superexchange- *vs* hopping-mechanism) and therewith the distance dependence should be varied. Covalent bond donor-bridge-(S)-gold electrode triads are easily accessible as monolayers by self organisation (self-assembled monolayers – SAM). Electrochemical methods are used to investigate the ET behaviour in these systems.

Furthermore the occurance of intervalence-charge-transfer (IV-CT) transitions in organic redoxmolecules bound to gold surfaces should be analysed and interpreted in the context of the *Mulliken-Hush-theory* [164-169].

Basic investigations on the ET of donor-units which are connected to gold electrodes with bridges of different length show an exponential dependence between the chain length and the ET rate (for formulas see chapter 2.2.4 and **fig. 3-1**, **R** and **S**) [157-159, 170, 171]. However, the length dependence may deviate from the exponential "law" by adjusting the energetic states of the bridge units and those of the donor-acceptor-states [172].

The ET in Zn-porphyrin monolayers strongly depends on the surface coverage, independent of the spacer (saturated or unsaturated) used in the experiments (**fig. 3-1**, **T**) [106, 173-176]. The ET rates of the chromophores decrease as the monolayer becomes more densely packed and also when the chain length between the porphyrin and the electrode increases. An alternative to ferrocene or porphyrins to investigate the ET is to change the redox sites, e. g. to use 2,2'-bipyridine rutheniumalkanethiols (**fig. 3-1**, **U**) [170, 177] or to change the spacer functionalities, e. g. oligoglycine spacers instead of alkane spacers (**fig. 3-1**, **V**) [178].

This project should examine the influence of different bridge units onto the ET rate between an organic donor and an electrode (schematic figure: **fig. 3-2**). It is expected to achieve useful information on the ET-mechanism in donor-acceptor units for the use in designing new materials.

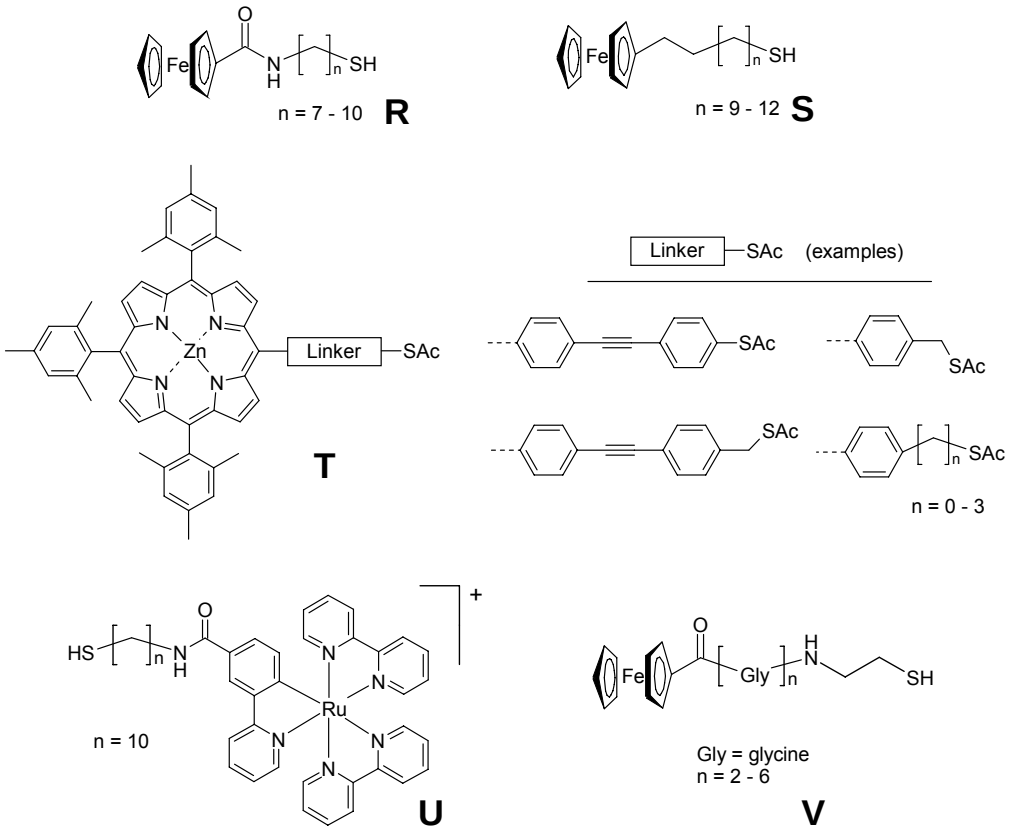

Fig. 3-1 Different donor-units for the investigation of the ET in SAMs on gold

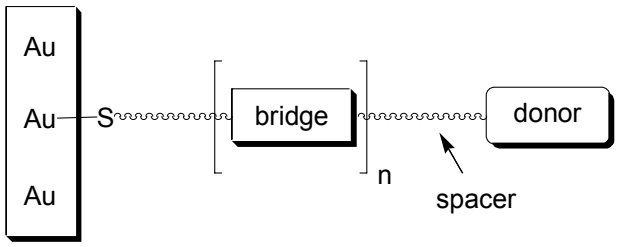

Fig. 3-2 Schematic structure of a donor-bridge-(S)-electrode array

3.1 Diabatic Electron Transfer in SAMs

The conformation of SAMs with thiol-bound organic molecules onto gold surfaces is an established technique to generate highly organised monolayers with a defined electrode-molecule and intermolecular distance for the investigation of basic ET-processes in organic redox molecules. A lot of different methods are used for the characterisation, e. g. chronoamperometry [179-181], cyclic voltammetry (including fast-scan-cyclic voltammetry)

[182-185], AC-voltammetry [158, 186, 187], impedance spectroscopy [159, 188] and the indirect-laser-induced-temperature-jump-method (ILIT) [159, 162, 189].

Investigating the diabatic ET [188], *Feldberg* and *Chidsey et al.* [159] found out that SAMs with oligo(phenyleneethynylene)-units of different chain length and with ferrocene-redox centres show an exponential decay in the ET rate by decreasing the spacer length (see **fig. 2-7**). According to *Creager et al.* using bis(alkoxy)phenylene-spacers instead of unsubstituted phenylene-units had no influence onto the ET [158]. By introducing new donor-acceptor-systems, where the energetic states of the spacers approach those of the donor-acceptor-states, *Wasielewski et al.* [172] showed that the length dependence of the ET deviates from the exponential "law". Because of the low distance dependence of the ET these compounds behave like molecular wires. *Chidsey et al.* [162, 189] obtained comparable results using ferrocene thiols with oligo(phenylenevinylene)-bridges.

3.2 Adiabatic Electron Transfer in SAMs

Inorganic [164, 190] as well as organic model compounds [191, 192], where the coupling between donor and acceptor is large enough compared to k*T and the ET is in the adiabatic region, have also been investigated. In these systems two organic redox centres or metal redox centres with two ligands act as donor and acceptor. In general, these mixed valence systems possess intervalence-charge-transfer-bands (IV-CT) in the NIR-region, which can be attributed to an optically induced ET and which can be analysed by the *Mulliken-Hush-theory* [164-168]. The above mentioned systems exist with two equal or with two different redox centres. Investigations concerning mixed valence compounds as SAMs have not been carried out until now [169].

3.3 Electron Transfer with Active Bridge-Units

The aim of this work is to investigate the influence of bridge energies onto the mechanism and the ET rate in donor-bridge-(S)-electrode arrays with electrochemical and spectroelectrochemical methods. The orbital diagrams and the corresponding state diagrams for the ET between a donor and an electrode are shown in **fig. 3-3**. Changing the ET-mechanism from a superexchange to a hopping-mechanism can be achieved by

variation of the bridge redox potentials. Energetically low lying bridge states should support a hopping-mechanism while high lying bridge states should promote an ET through superexchange [188, 193, 194]. The hopping-mechanism, where the electron is localised for a short time on the bridge units between the redox centres, has the following length dependence: $k_{ET} \propto 1/N$ (N = number of bridge units). Mixing the donor- and acceptor-states by the spacers, an exponential length dependence of the ET rate occurs, the superexchange ($k_{ET} = A \cdot e^{(-\beta r_{DA})}$, where A is a temperature dependent factor, β a structure dependent attenuation factor and r_{DA} the distance between donor and acceptor).

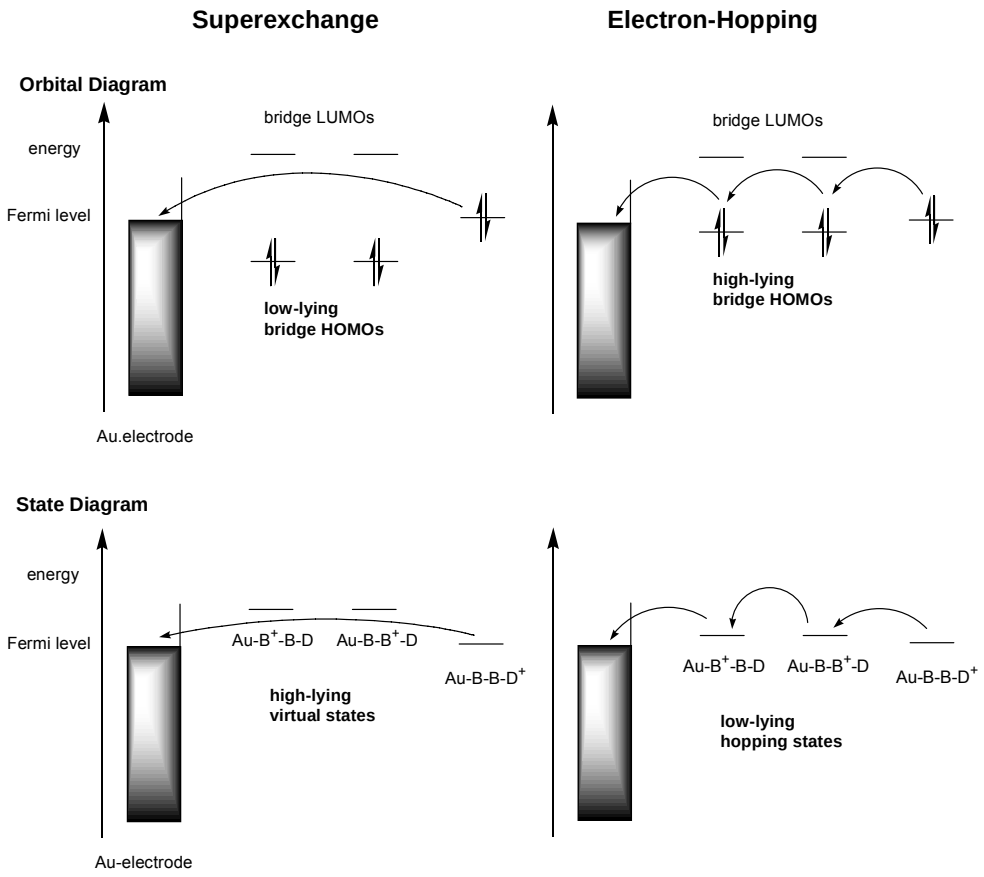

Fig. 3-3 Orbital and state diagrams for an ET-process from a donor via two bridge units to an electrode

The schematic structure of the investigated systems in this work is demonstrated in **fig. 3-4**. Triarylamines or heterodihydroanthracenes should be used as redox centres connected to donor- or acceptor-substituted aromatic bridge units with saturated or unsaturated spacers. The redoxpotential of the triarylamines can be varied over a wide range by exchanging the subtituents R (~ 1000 mV) [195]. The reorganisation energy is quite low (ca. 4000 cm^{-1}) [191], which should lead to a low lying ET-barrier according to the

Mulliken-Hush-theory. Alternatively 5,10-heterodihydroanthracene-derivatives should be tested as donors which possess a relatively large reorganisation energy [196, 197]. The redox potential of the heterodihydroanthracenes can be varied in a wide range of ~ 1300 mV by modifying the hetero atoms in 5- and 10-position. By modifying the different donor-units the influence of the reorganisation energy onto the ET rate should be investigated.

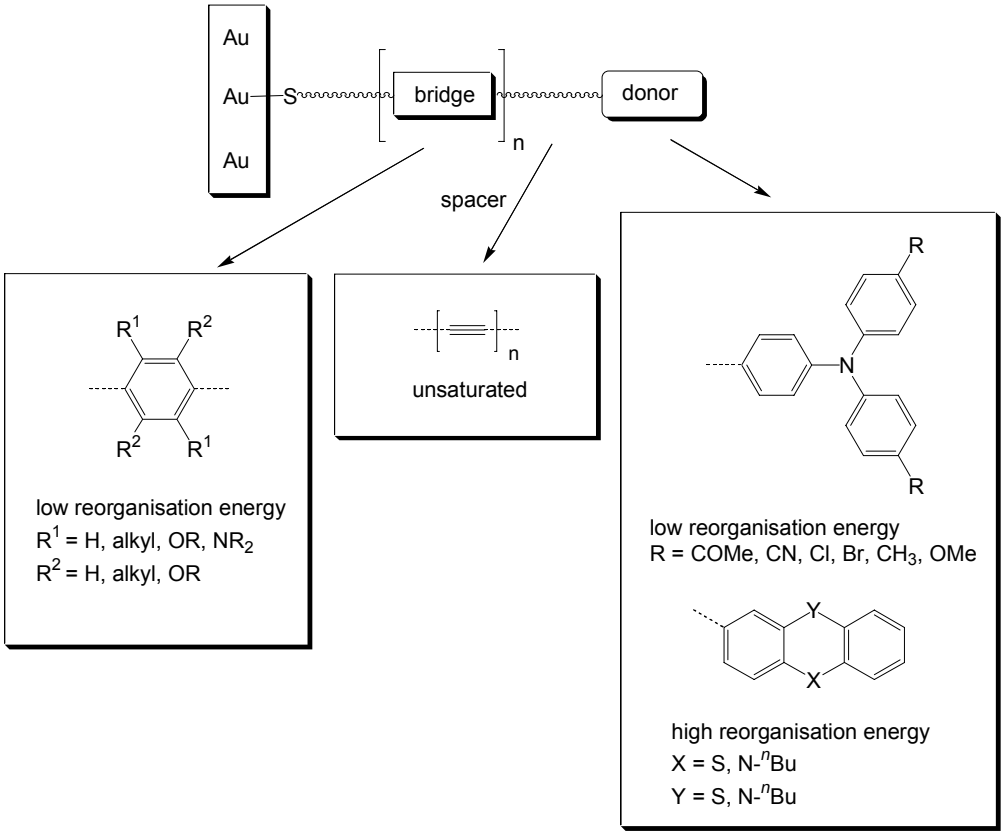

Fig. 3-4 Schematic structure of a donor-bridge-(S)-electrode array and useful units

For a constant ET-distance the ET rate depends on the type of spacer. In this work acetylene units should be used which promote a fast ET because of their strong conjugation.

Furthermore the distance between donor and acceptor plays an important role for the ET rate. Extending the bridge length the rate constant can be varied very easily. In addition, the type of ET (superexchange or hopping) should be changed by modifying the bridge energies. This could be achieved e. g. by using phenylene units with different substituents and therefore different local redox potentials.

The ET behaviour of these compounds should be analysed by impedance spectroscopy and investigations concerning the preparation and the coverage of pure and mixed monolayers with different chromophore systems should be carried out.

4 Theory of Impedance Spectroscopy

In principle it is possible to pass a current through any liquid and solid if a voltage is applied. If an alternating (AC) voltage is applied to the material, the ratio voltage to current (E/I) is known as the impedance, e. g. the impedance is a complex resistance. In many materials, especially those which are not generally regarded as conductors of electricity, the impedance varies with the frequency which depends on the physical structure of the material, the chemical processes within this material or on a combination of both. Thus, if measurements of impedance over suitable frequency ranges are made, it is possible to relate these results to the physical and chemical properties of the material. Since impedance measurement is repeatable, it can provide valuable insights into the behaviour of a huge variety of substances, components and systems. Impedance measurements have many advantages over other techniques including:

- Rapid acquisition of data
- Accurate, repeatable measurements
- Highly adaptability to a wide variety of different applications

4.1 Concept of Complex Impedance[198, 199]

Electrochemical impedance theory is a well-developed branch of AC theory that describes the response of a circuit to an alternating current or voltage as a function of frequency.

In DC (direct current) theory Ohm`s law defines resistance in terms of the ratio between voltage E and current I (**equ. 4-1**).

$$R = \frac{E}{I} \qquad \textbf{equ. 4-1}$$

While this is a well known relationship, its use is limited to only one circuit element - the ideal resistor. In reality the circuit elements exhibit a much more complex behaviour. In AC theory, where the frequency is non-zero, impedance is used as the analogue to resistance (**equ. 4-2**):

$$Z(\omega) = \frac{E(t)}{I(t)}$$ **equ. 4-2**

Electrochemical impedance is usually measured by applying an AC potential $E(t)$ of small amplitude to an electrochemical cell measuring the resulting current $I(t)$ through the cell. Supposing a sinusoidal potential excitation is applied, the response to this potential is an AC current signal, containing the excitation frequency and its harmonics. This current signal can be analysed as a sum of sinusoidal functions (a Fourier series) (**equ. 4-3**, **equ. 4-4**).

$$E(t) = E_0 \cdot \sin(\omega t + \Phi_E)$$ **equ. 4-3**

$$I(t) = I_0 \cdot \sin(\omega t + \Phi_I)$$ **equ. 4-4**

$E(t)$:	actual value of the potential	$I(t)$:	instantaneous current
E_0:	maximum amplitude	I_0:	maximum amplitude
ω:	circuit frequency	t:	time
Φ:	phase shift between potential and current; $\Phi=\Phi_E-\Phi_I$		

Electrochemical impedance is normally measured using a small excitation signal. The cell response is pseudo linear, which means that in a linear (or pseudo-linear) system, the current response to a sinusoidal potential will be a sinusoid at the same frequency but shifted in phase (**fig. 4-1**).

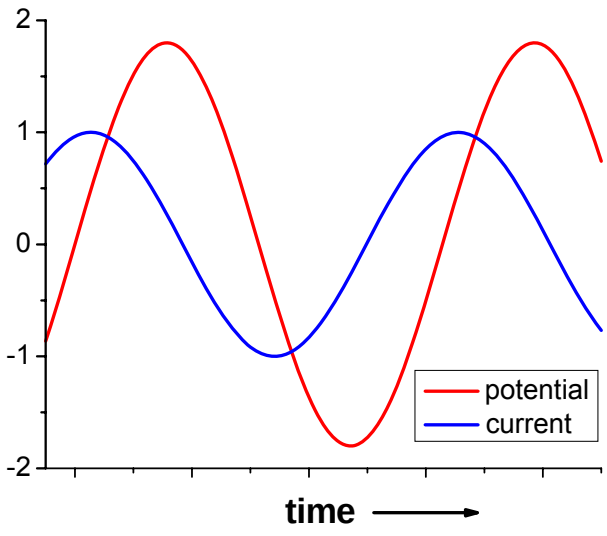

Fig. 4-1 AC waveforms of an applied potential and the resulting current

The impedance spectrum is provided by measuring $Z(\omega)$ over a large frequency range. The impedance is characterised by the amplitude ratio of voltage and current as well as the phase shift between both sinusoidal curves. Therefore a high analytical and mathematical effort for the solution of phase-delayed sinusoidal signals of different amplitudes is involved.

To reduce mathematical calculation, such values are handled like complex values which can be displayed in vector diagrams very easily.

Using the functions for voltage and current and the analytical description for their circulating vectors

$$E(t) = E_0 e^{i(\omega t + \Phi_E)} \quad \text{and} \quad I(t) = I_0 e^{i(\omega t + \Phi_I)} \qquad \textbf{equ. 4-5}$$

as following from **equ. 4-2**:

$$Z(\omega) = \frac{E(t)}{I(t)} = \frac{E_0 e^{i(\omega t + \Phi_E)}}{I_0 e^{i(\omega t + \Phi_I)}} = \frac{E_0}{I_0} \cdot \frac{e^{i\omega t}}{e^{i\omega t}} \cdot \frac{e^{i\Phi_E}}{e^{i\Phi_I}} \qquad \textbf{equ. 4-6}$$

$$Z = \frac{E_0}{I_0} e^{i(\Phi_E - \Phi_I)} = \frac{E_0}{I_0} e^{i(\Phi)} = |Z| e^{i(\Phi)} \qquad \textbf{equ. 4-7}$$

The absolute value $|Z|$ of the vector Z is equal to the apparent resistance, the angle is equal to the phase shift. Using Eulers relationship,

$$e^{i\varphi} = \cos(\varphi) + i \sin(\varphi) \qquad \textbf{equ. 4-8}$$

it is possible to express the impedance as a complex function.

$$Z = Z' + iZ'' = \mathrm{Re}(Z) + i\,\mathrm{Im}(Z) = R + iX \qquad \textbf{equ. 4-9}$$

with the absolute magnitude of the impedance

$$|Z| = \sqrt{(\mathrm{Re}(Z))^2 + (\mathrm{Im}(Z))^2} \qquad \textbf{equ. 4-10}$$

and the phase shift

$$\Phi = \arctan\left(\frac{\mathrm{Re}(Z)}{\mathrm{Im}(Z)}\right) \qquad \textbf{equ. 4-11}$$

A graphic illustration of the real Re(Z) and the imaginary Im(Z) components is shown in **fig. 4-2**, the real part Re(Z) is described as effective resistance, the imaginary part Im(Z) as reactance.

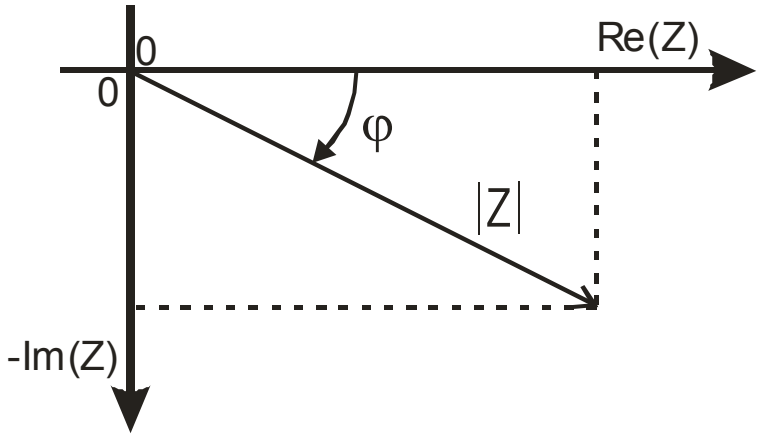

Fig. 4-2 Illustration of impedance as real and imaginary part of the vector

4.2 Equivalent Circuit Elements

The advantage of electrochemical impedance spectroscopy is the use of a purely electronic model to represent an electrochemical cell. These systems can be described with impedance elements like resistances, coils, capacitors, etc. . The combination of these elements results in an analogous electronic circuit where every impedance element represents a specific electrode process.

The kind of different electrode processes leads to a specific connection of the associated impedance elements. A mathematical expression for this mechanism can be used for the electrode impedance, which contains all impedance elements of the single sub-processes and the combination of these elements. Resistance, capacity and inductivity represent the classical impedance elements, which are comparable to the real parts in

electronic like resistance, coil or capacitor. The most common ones are represented in **tab. 4-1** and explained in the following.

Tab. 4-1 Frequently used impedance elements and their characteristics

Circuit element	Symbol	Impedance equation	Phase shift
resistance (R)		$Z = R$	0
coil (L)		$Z_L = i\omega C$	$+\frac{\pi}{2}$
capacitor (C)		$Z_C = \frac{1}{i\omega C}$	$-\frac{\pi}{2}$
constant phase element (CPE)		$Z_{CPE} = \frac{1}{(i\omega)^n A_{CPE}}$	$+n \cdot \frac{\pi}{2}; 0 \le n \le 1$
Warburg-impedance		$Z_W = \frac{W}{(i\omega)^{\frac{1}{2}}}$	$-\frac{\pi}{4}$

As shown in **tab. 4-1** the impedance of a resistor has no imaginary part and is not phase shifted. In this case both, current and impedance, are frequency independent. On the other hand, a capacitor has no real component. Because of the inverse variance of a capacitor's impedance with the frequency, the capacitor acts as a short circuit at high frequencies. At low frequencies the capacitor acts as an open circuit and the impedance tends towards infinity. Another example is the inductor, which acts as a short circuit at low and as a large impedance at high frequencies. The current through an inductor is always 90° out of phase with the voltage.

An empirical approach to explain phenomenons of real systems, which cannot be described with simple impedance elements, is e. g. the implementation of constant phase elements (CPE). The CPE has the effect on the frequency independent phase shift $n \cdot \frac{\pi}{2}$ of the impedance. The variable n is a measure for the surface roughness. If n has the limit one, an ideal plane surface is obtained. An ordinary explanation of the CPE is not possible, because the parameter A_{CPE} contains capacitive and resistive characteristics in the area

between $0 < n < 1$. Just for the borderline cases n = 0, n = 0.5 and n = 1 the CPE leads to a physically interpretation. For n = 1 the CPE acts like an ideal capacitor:

$$Z_{CPE} = \frac{1}{i\omega A_{CEP}} \qquad \text{with} \qquad A_{CPE} = C \qquad \textbf{equ. 4-12}$$

For n = 0 it describes an ohmic resistance,

$$Z_{CPE} = \frac{1}{A_{CEP}} \qquad \text{with} \qquad A_{cpe} = \frac{1}{R} \qquad \textbf{equ. 4-13}$$

and for n = 0.5 the border case of a Warburg impedance results [200].

In a lot of processes the electrode impedance is influenced by concentration variations from the equilibrium state of the electroactive species. Examples are difussion- and absorption-processes as well as heterogeneous or homogeneous chemical reactions. The most common example in this field is the Warburg-impedance. The Warburg-impedance describes the influence of the diffusion onto the electrode impedance. At high frequencies the diffusion of the reactants is not important, because the currents are low and the polarity changes permanently. At low frequencies diffusion plays a relevant role.

The total impedance can be determined by combination of simple elements using the rules for normal resistances. For serial connected resistors or capacitors the total value is the sum of the individual impedance values.

$$Z_s = Z_1 + Z_2 \qquad \textbf{equ. 4-14}$$

For parallel resistors or capacitors the overall value is the addition of the admittance (admittance is the inverse of impedance).

$$\frac{1}{Z_p} = \frac{1}{Z_1} + \frac{1}{Z_2} \qquad \textbf{equ. 4-15}$$

4.3 Plot Analysis

To analyse the data the electrochemical systems can be illustrated with electrical circuit diagrams by using electrochemical impedance spectroscopy. The *Randles* cell is one of the simplest and most common cell models which fits many chemical sytems (**fig. 4-3**). In those systems it is important that the impedance of a resistance is frequency independent while the impedance of a capacitor diminishes as the frequency increases. At high frequencies the impedance of the capacitor C_{dl} is much smaller than of the resistance R_P. But even the capacitor has a very small impedance compared to R_Ω, so that the total impedance at such frequencies is controlled almost entirely by R_Ω. At low frequencies the capacitor C_{dl} acts as an open circuit and the total impedance is given by the combination of R_Ω and R_P.

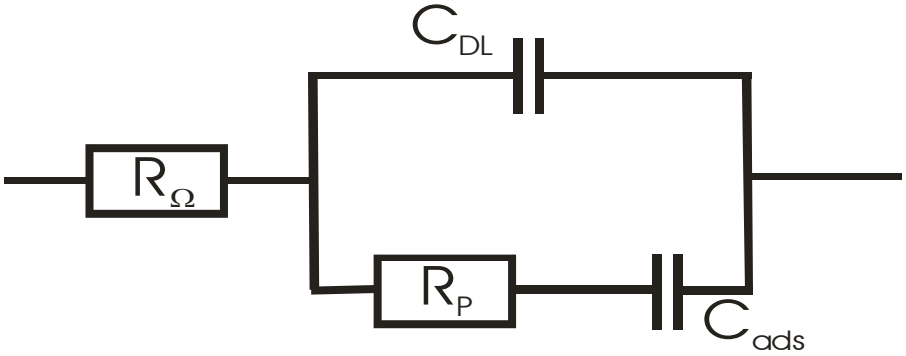

Fig. 4-3 Circuit diagram of the *Randles* cell (R_Ω = ohmic or uncompensated resistance of the solution; C_{dl} = double layer capacitance of the system; R_P = polarization resistance or charge-transfer resistance; C_{ads} = the adsorption capacitance)

4.3.1 Nyquist Plot

A widely used graphical presentation for impedance data is the Nyquist plot (**fig. 4-4**). It is a parametric plot of the real and imaginary part of $Z(\omega)$ in the complex plane as the frequency parameter sweeps through a given interval, plotting the real part on the X-axis and the imaginary part on the Y-axis of a chart. At low frequencies the impedance is caused by R_Ω, while at high frequencies the total impedance is an addition of R_Ω and R_P. On the Nyquist plot the impedance can be represented as a vector of length |Z|. The angle between this vector and the X-axis is φ, where φ = arctan(Z). This plot has some great advantages: first the effects of ohmic resistance is seen very easily, secondly it emphasizes circuit components which are in series. But on the other hand Nyquist plots have one major

shortcoming. The frequency does not appear and therefore the electrode capacitance can be calculated only after frequency information is known.

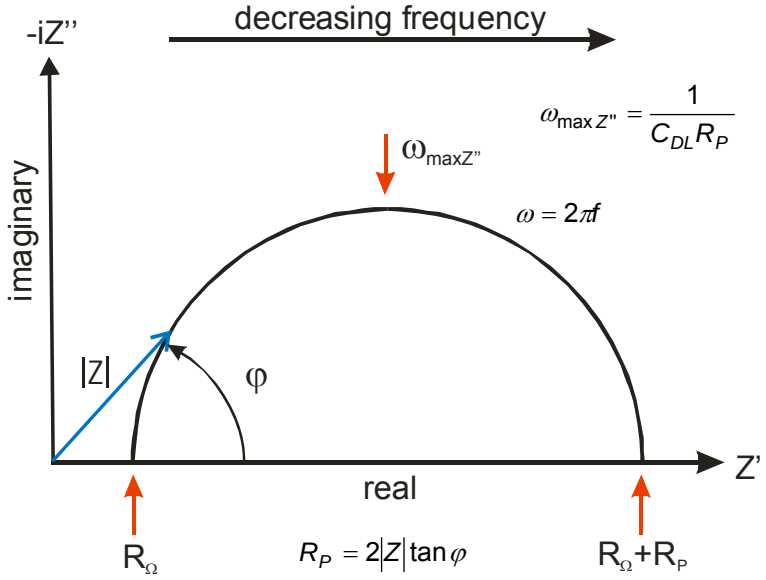

Fig. 4-4 Nyquist plot for a simple electrochemical system - an ET from a dissolved redox component to a metall electrode

4.3.2 Bode Plot

The Bode diagram is also often used for presentation of impedance spectra. The Bode plot of the impedance for an electric circuit is shown in **fig. 4-5**. It explicitly indicates frequency information and to use the logarithm of frequency allows a very wide frequency range. The impedance is plotted with log frequency on the X-axis and both the absolute value of the impedance, |Z|, and phase-shift on the Y-axis. On the other hand it is possible that the shape of the curves can change if the circuit values alter.

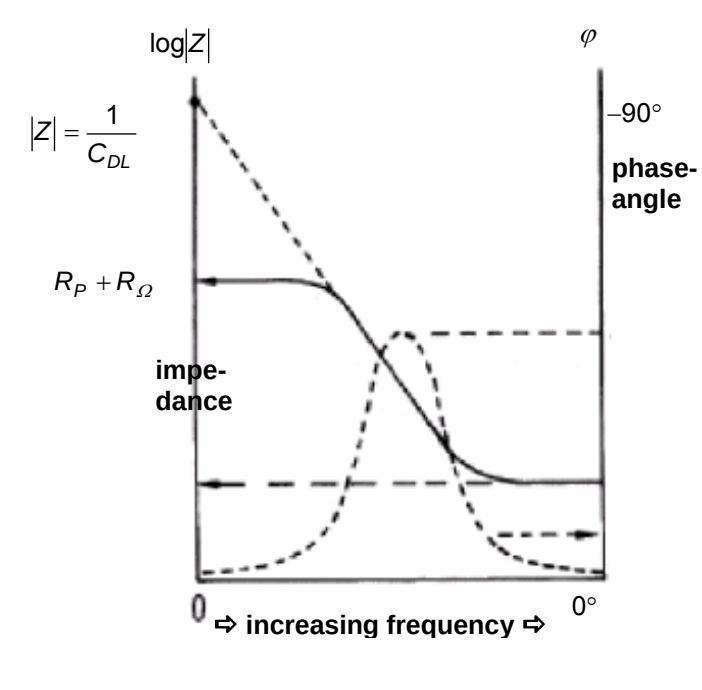

Fig. 4-5 Bode plot for a simple electrochemical system - an ET from a dissolved redox component to a metall electrode

5 Monolayer Preparation

Generally, two different strategies are employed for the formation of SAMs of functional components on gold surfaces. One method is the direct adsorption of a functional component which carries a thiol or disulphide group. This sulphur group is attached to the functional component by a synthetic procedure prior to the SAM formation step (**fig. 5-1**) [28, 110, 136, 147]. The sulphur group itself may either be a thiol, a disulphide, an acetyl protected thiol or [1,2]-dithiolane.

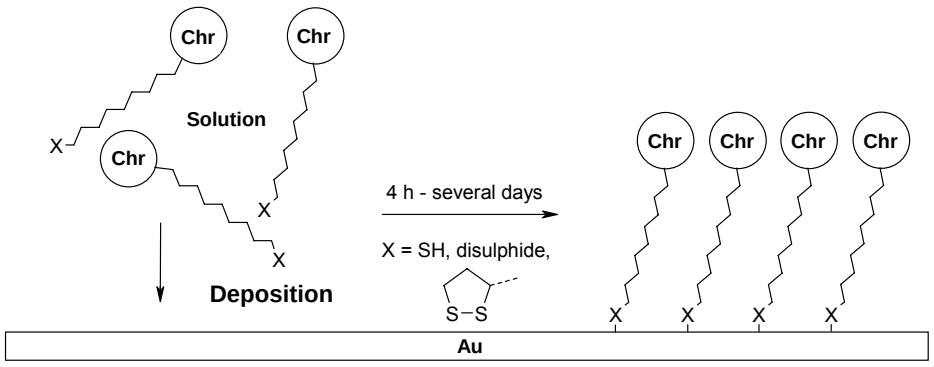

Fig. 5-1 Direct adsorption method of thiolated compounds onto gold (Chr = chromophore)

The alternative method is a covalent attachement of the functional components onto a preformed SAM of ω-functionalised (e. g. –COOH, NH_2) alkanethiols (**fig. 5-2**) [129, 201, 202].

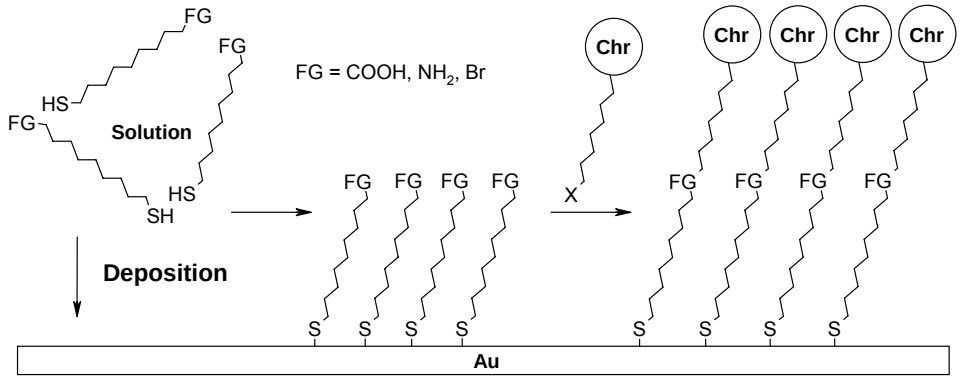

Fig. 5-2 Covalent attachment of the functional components onto preformed SAM of ω-functionalised alkanethiols (Chr = chromophore)

For measuring ET rates the redox active molecules have to be diluted with redox inactive molecules, so called dummy molecules, to ensure that no redox processes between

the redox active molecules appear. The formation of SAMs depends on the solvent and on the different solubilities of the redox active and the dummy molecules. Normally the dummy molecules are long chained alkanethiols, where the length varies with the investigated thiols. The length itself should not exceed the distance between thiol and redox centre so that the redox active part sticks out of the monolayer.

Different strategies for pure or mixed monolayer preparation were used in this work. First, a freshly molten and cleaned gold ball was immersed into a coating solution of redox active and dummy molecules in a special ratio (from 1 : 100 up to 1 : 1) (for more information see chapter 11). The formation of a dissordered monolayer takes place within several minutes, while the organisation requires 24 h (**fig. 5-3**). This procedure was mainly used for the ferrocenealkyl- and ferrocenearylthiol SAMs discussed in chapter 6.

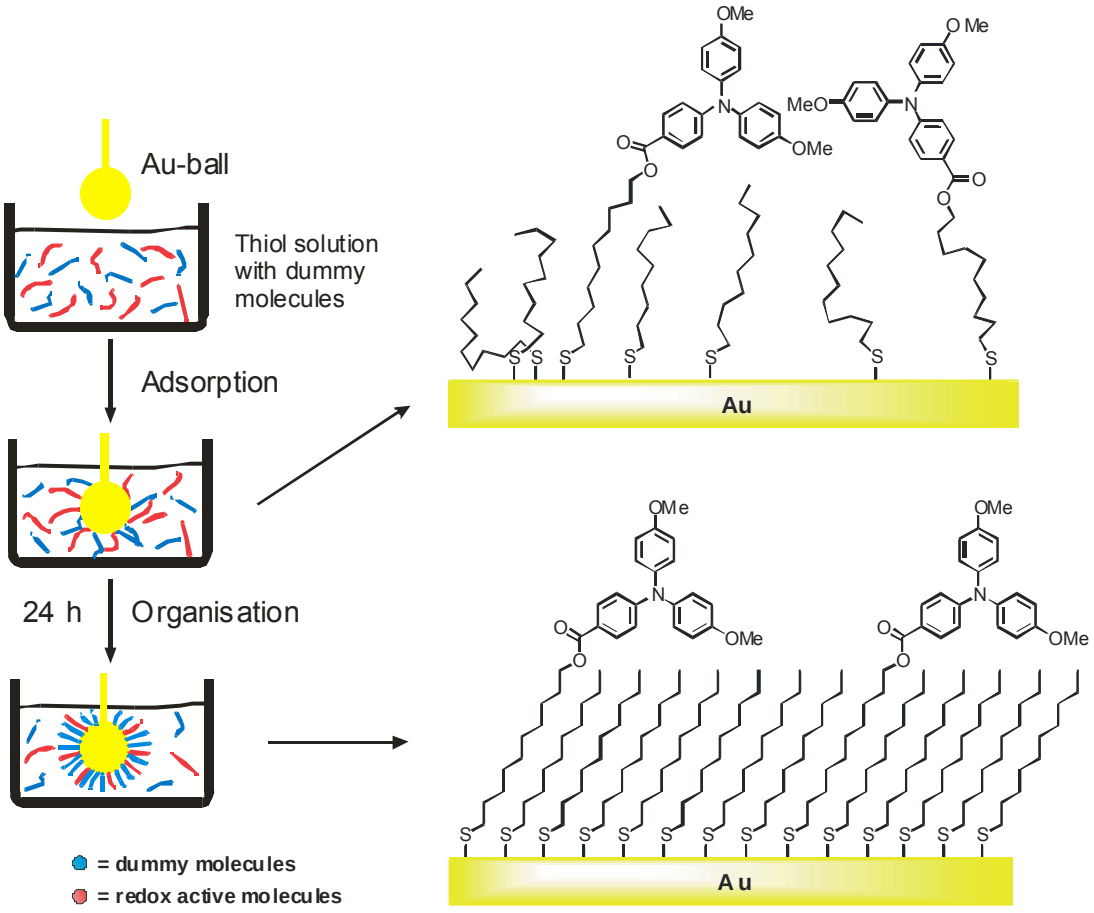

Fig. 5-3 Direct adsorption of redox active and dummy molecules used for ferrocenealkyl- and ferrocenearylthiol SAMs

The second possibility which was used for saturated triarylamine- and phenothiazinealkanethiol SAMs examined in chapter 7 is to dip the gold ball for a short time (10 – 60 seconds) into a solution of dummy molecules. A disordered monolayer with

hole defects is formed. These defects are filled up by immersing this gold ball into a solution with pure redox active molecules for several minutes. For organisation the gold ball is left in a third coating solution containing redox active and dummy molecules for 1 – 2 d to get the mixed monolayer (**fig. 5-4**).

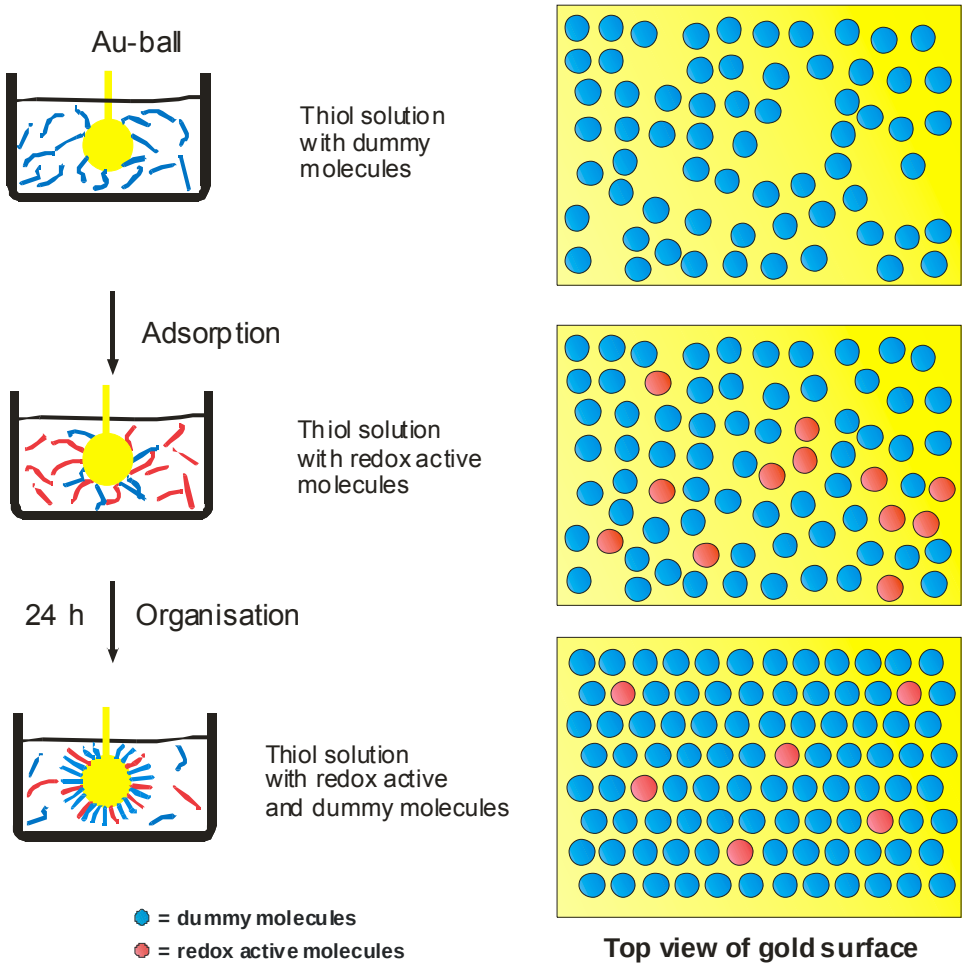

Fig. 5-4 Adsorption of redox active molecules using a monolayer with dummy molecules containing hole defects for the preparation of saturated triarylamine- and phenothiazinealkanethiol SAMs

Third, in case of the unsaturated, pure triarylamine- and phenothiazinealkanethiol SAMs (chapter 8) the gold balls were immersed in a coating solution containing the chromophore and a surplus of diethylamine to deprotect the acetyl-protection group. The electrode was left in the solution for 24 hours.

6 Electron Transfer in Ferrocenealkane- and Ferrocenearylthiol SAMs

In order to obtain experience concerning SAM investigations with impedance spectroscopy [187, 203], measurements on ferrocenealkane- and ferrocenearylthiols (**fig. 6-1**) were carried out in cooperation with the group of PD Dr. A. Terfort (Institut für Anorganische Chemie, Universität Hamburg). The ET rate constants for compounds **1** – **5** were examined using a model developed by *Creager et al.* [158] based on the *Randles Equivalent Circuit*. For these investigations mixed monolayers containing redox active molecules and dummy molecules (alkanethiols) on freshly molten gold balls which possess a Au(111) surface [2] were used.

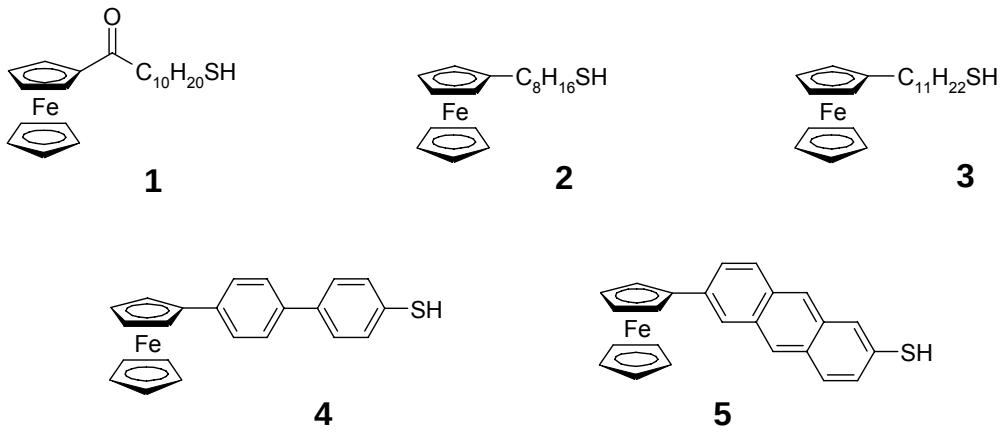

Fig. 6-1 Ferrocenealkane- and ferrocenearylthiols for the investigations in SAMs

6.1 Cyclic Voltammetry and Surface Coverage

The cyclic voltammograms of the diluted monolayers of compounds **1** – **5** are shown in **fig. 6-2**. The redox potential V_{rel} was measured relative to an Ag/AgCl-reference electrode and no calibration with ferrocene as internal standard was carried out. The current of the monolayers of the redox-process is in the nanoampere region which indicates that the redox active molecules are highly diluted by dummy molecules. The cyclic voltammograms show a slight peak separation, indicating that some defects are within the monolayer itself, caused by regions where no molecules are attached to the surface or by

regions where mainly redox active molecules were attached as a domain. In an ideal diluted monolayer no peak separation should occur [204].

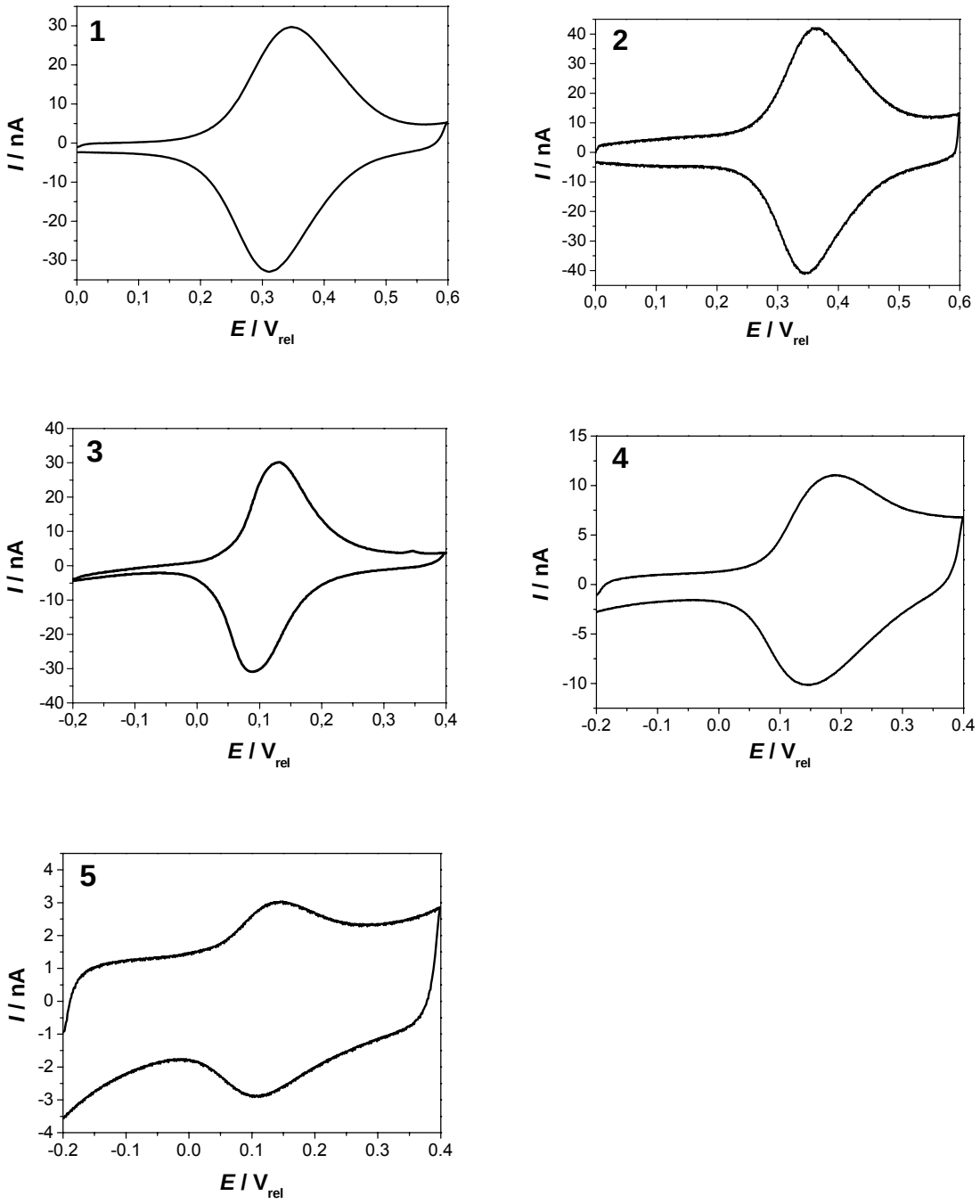

Fig 6-2 Cyclic voltammograms for ferrocenealkane- and ferrocenearylthiols **1** – **5** as SAMs on spherical gold-electrodes. The measurements were carried out in an aqueous 1 M $HClO_4$-solution, scan rate: 50 mV/s

However, it is also important to know the surface coverage for the ET-measurements and the densitiy of the redox-active molecules in the mixed monolayers. This could be achieved by using alkanethiols as dummy molecules which have one or two

methylene units less than the alkane bridge units used for the chromophores so that the redox centre sticks out of the monolayer and that a densiest packing within this monolayer is received (for preparation see chapter 5). A high dilution guarantees that no redox-processes between nearby standing redox-centres occur and therefore wrong ET rates are obtained. One possibility is to calculate the surface coverage Γ of a thin layer by using **equ. 6-1** [198]:

$$\Gamma = \frac{i_P \cdot 4 \cdot \mathrm{R} \cdot T}{n^2 \cdot \mathrm{F}^2 \cdot \nu \cdot A} = 1.053 \cdot 10^{-6} \left[\frac{\mathrm{V} \cdot \mathrm{mol}}{\mathrm{A} \cdot \mathrm{s}} \right] \cdot \frac{i_P}{n^2 \cdot \nu \cdot A} \qquad \textbf{equ. 6-1}$$

where Γ is the surface coverage [mol/cm^2], i_p is the current at the peak maximum of the oxidation or reduction (- background current) in the cyclic voltammogram [A], R is the universal gas constant [J/mol*K], T the temperature [K], n the number of electrons which take part in the redox process, F the Faraday-constant [C/mol], ν the scan rate [V/s] and A the electrode surface [cm^2]. The measured current i_p is directly proportional to the surface coverage. Otherwise it is important to consider a roughness factor or the surface because of the non planar structure of the gold. This roughness factor is typical: $A_{real} = 1.3 * A_{calculated}$ [205]. Investigations which were carried out on pure alkanethiol-SAMs showed a density of $7.8 * 10^{-10}$ mol/cm^2 [205].

The length of the used dummy molecules for the mixed monolayers depends on the length of the saturated spacer between the redox centre and the electrode to get a nearly ideal surface in the mixed monolayers compared to pure alkanethiol-monolayers. It is important that the redox centres stick out of the monolayer otherwise they would be influenced by the surrounding alkane-chains or by diffusion effects. [203] On the other hand these mixed monolayers can be easily compared with the well known surface coverage of densiest packed alkanethiol monolayers.

The coverage of redox active molecules ranges from (2.6 ± 0.3(* 10^{-11} (~ 3 ± 0.4 %) for ferrocenealkanethiol **1** to (5.1 ± 0.7) * 10^{-14} mol/cm^2 (~ (6.5 ± 0.9) * 10^{-3} %) for ferrocenearylthiol **5** and therefore these molecules are diluted quite well (for summary of values see **tab. 6-1**). But we have to keep in mind that the behaviour and the interactions between the alkane dummy molecules and the redox active ferrocenearyl molecules might lead to a different packing where domains of redox-active molecules can occur. In this case STM or AFM measurements would show the homogeneous distributed molecules.

Tab. 6-1 Surface coverage (Γ), dummy molecules, reorganisation energies (λ), double layer capacitance (C_{dl}), uncompensated resistance (R_u) and surface (A_{real}) for compounds **1 - 5**

	Γ / mol/cm^2	surface coverage / %	dummy molecules	λ / eV [183]
1	$(2.6 \pm 0.3) * 10^{-11}$	3 ± 0.4 %	$C_{11}H_{23}SH$	0.85 (H_2O)
2	$(1.3 \pm 0.2) * 10^{-12}$	$(2 \pm 0.3) * 10^{-1}$ %	$C_8H_{17}SH$	0.85 (H_2O)
3	$(1.6 \pm 0.3) * 10^{-12}$	$(2 \pm 0.4) * 10^{-1}$ %	$C_{10}H_{21}SH$	0.85 (H_2O)
4	$(9.3 \pm 1.1) * 10^{-12}$	1.2 ± 0.2 %	$C_7H_{15}SH$	0.85 (H_2O)
5	$(5.1 \pm 0.7) * 10^{-14}$	$(6.5 \pm 0.9) * 10^{-3}$ %	$C_7H_{15}SH$	0.85 (H_2O)

	C_{dl} / F	R_u / Ω	A_{real} / cm^2
1	$(1.4 \pm 0.2) * 10^{-8}$	15.2 ± 2.6	$(2.4 \pm 0.1) * 10^{-2}$
2	$(3.7 \pm 0.7) * 10^{-8}$	80.0 ± 10.3	$(7.0 \pm 0.3) * 10^{-1}$
3	$(1.1 \pm 0.2) * 10^{-8}$	20.0 ± 3.4	$(4.0 \pm 0.2) * 10^{-1}$
4	$(2.8 \pm 0.3) * 10^{-8}$	16.1 ± 3.1	$(2.5 \pm 0.1) * 10^{-2}$
5	$(1.3 \pm 0.2) * 10^{-8}$	22.0 ± 5.0	$(5.0 \pm 0.2) * 10^{-1}$

6.2 Electron Transfer Rates and Bode Plots – Theory and Practice

Because of the difficulty and lots of parameters which are needed to analyse Nyquist and Bode plots, a new protocol developed by *Creager et al.* [186] based on AC voltammetry was used to determine the ET rates. AC voltammetry is an electrochemical technique in which a fixed frequency sinusoidal perturbation (AC signal) is applied and biased with a DC ramp. The resulting AC current and its corresponding phase angle can be plotted vs. the DC potential. The nature of the curve obtained gives information relating to system kinetics. Going from low frequencies to high frequencies the magnitude of the peak current relative to the background in the spectras diminishes (**fig. 6-3**). This phenomenon can be explained by reaching a critical value of the frequency above which the ET cannot keep up longer with the rapidly oscillating potential and therefore the peak diminishes relative to the background.

An alternative for analysing AC data is to plot the ratio of the AC current of the formal potential (I_{peak}, a faradaic current is present) to the background ($I_{background}$, no faradaic processes occur) against the log of frequency for a series of voltammograms recorded over a wide range of frequencies (for detailed experimental description see

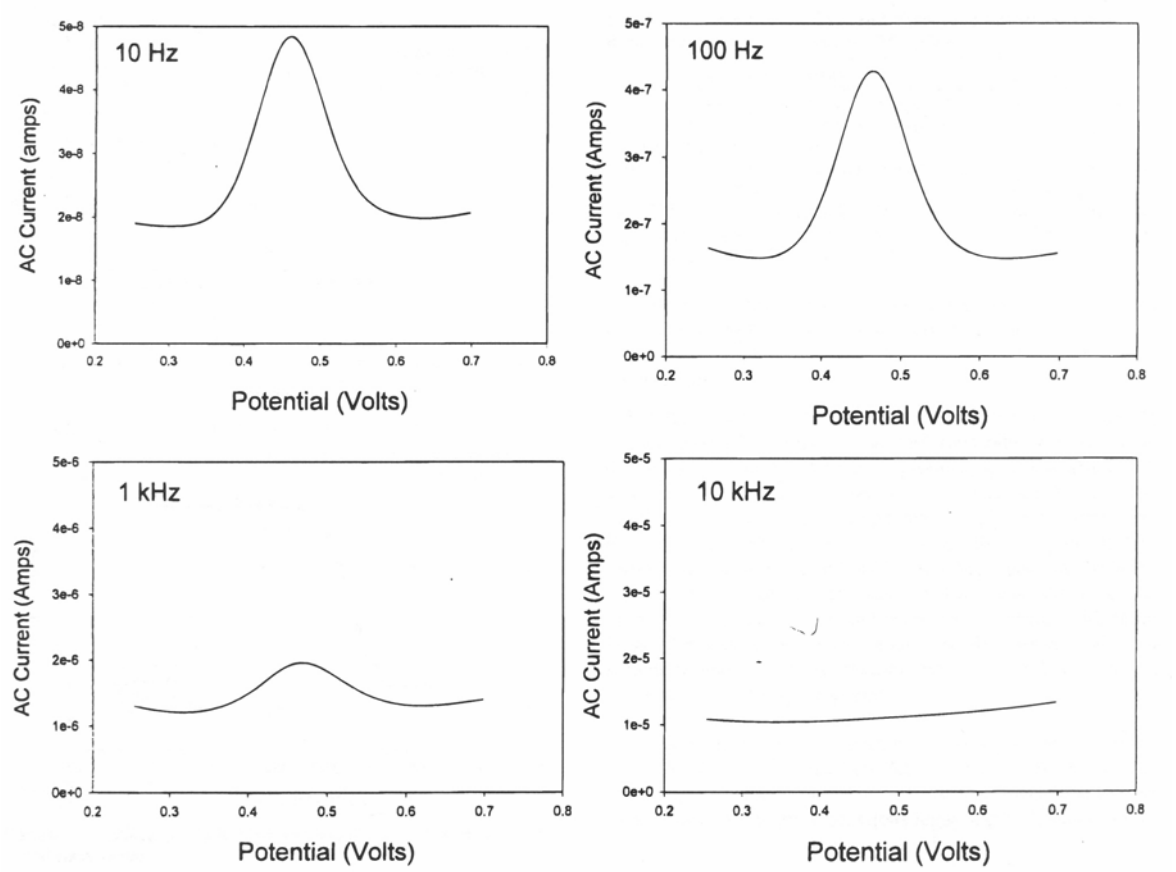

Fig. 6-3 AC voltammograms of a mixed N-(10-mercaptodecyl)ferrocenecarboxamide / 11-mercaptoundecanol monolayer on gold at different frequencies [206]

chapter 11.1.3) [186, 207]. Two spectra have to be recorded, the first one where the potential of the redox peak maximum, obtained from CV of the SAMs, is applied, a second for background measurements at a potential where no redox process occurs. To cause as less perturbation to the system as possible the applied potential is superposed by a small AC potential (10 mV). To circumvent the instability and destruction of the SAMs and the chromophores, the spectra of the redox peak maximum was measured first.

Three regions are important in this plot. At high frequencies, where the redox process cannot follow the applied frequency, the ratio of the current measured on the peak maximum of the redox process compared to the current of the background approaches the value one, while at low frequencies a constant value larger than one is obtained. Between these two regions the current ratio changes rapidly by decreasing the frequency and reaching the ET rate, until the frequency is slow enough and all redox active molecules take part in the redox process and the current reaches a maximum. This sigmoidal curve then can be fitted by using the *Randles equivalent circuit* model in which the different components contribute to the overall impedance and are represented by descrete circuit elements (for graphic see **fig. 4.3**). In this special *Randles equivalent circuit* the charge-

transfer resistance R_{ct} and the adsorption capacitance C_{ads} are in series while the double-layer capacitance C_{dl} is switched parallel. This whole system is connected serial to the uncompensated resistance R_u. The required uncompensated resistance R_u and the double-layer capacitance C_{dl} are determined by using the Bode plot of background impedance measurements (**fig. 6-4**). From the plateau in the high frequency region log R_u can be obtained (blue line), while C_{dl} is an extrapolation of the measured curve with the gradient -1 onto the y-axis $\log|Z|$ at f = 0.16 Hz (red line).

This method involves several advantages compared to analysing the AC data shown in **fig. 6-3**:

- fewer adjustable fitting parameters are required
- fewer fitting parameters lead to a more accurate fit
- no information about the phase of the AC current signal is needed
- data analysis can be performed on extremely small voltammetric peaks

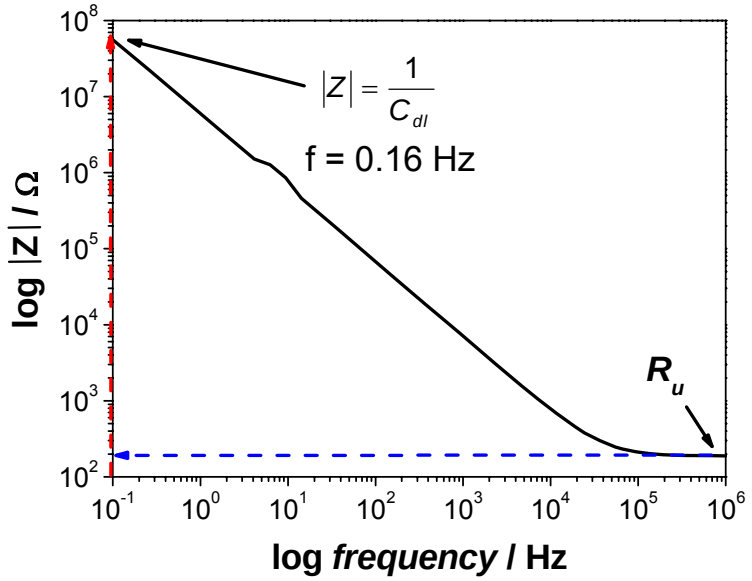

Fig. 6-4 Determination of uncompensated resistance R_u and double-layer capacitance C_{dl} using a Bode plot

In this model the circuit elements C_{dl}, C_{ads} and R_{ct} are related to parameters characterizing the redox-active monolayer-coated electrode (for the used *Randles equivalent circuit* see **fig. 4-3**):

$$C_{dl} = \left(\frac{C}{A}\right) \cdot A \qquad \textbf{equ. 6-2}$$

$$C_{ads} = \frac{F^2 A\Gamma}{4RT}$$ **equ. 6-3**

$$R_{ct} = \frac{2RT}{F^2 A\Gamma k_{et}}$$ **equ. 6-4**

where C_{dl} is the double-layer capacitance, C/A the double-layer capacitance per unit area, A the electrode area, Γ the number of redox-active molecules per unit area, C_{ads} the adsorption capacitance and R_{ct} the charge-transfer resistance. Other constants have been described with **equ. 6-1**. By conversion of these equations the ET rate k_{et} can be readily obtained by

$$k_{et} = \frac{1}{2R_{ct}C_{ads}}$$ **equ. 6-5**

The Bode plots and the fitted curves to determine the ET rate constant for compounds **1** – **5** are shown in **fig. 6-4**. The curve shape of the measured and the fitted curves correlate quite well. The ratio of the current of the peak to the background ranges between 2.6 for **2** over 3.5 for **3** to 17 for **1**. The high ratio of **1** can be explained by a mixed monolayer consisting of a large quantity of redox active molecules and a low amount of dummy molecules compared to ferrocene derivatives **2** - **5**.

The obtained value of $k_{et} = (2.2 \pm 0.3) * 10^3\ s^{-1}$ (lit.: $(2.0 \pm 0.4) * 10^3\ s^{-1}$ [206]) for the ferrocenecarbonyl derivative **1** is in good agreement with literature values (**tab. 6-2**). The ET rates for the ferrocenealkanethiols **2** and **3** of $k_{et} = (4.5 \pm 0.7) * 10^5\ s^{-1}$ (lit.: $(4.4 \pm 0.9) * 10^5\ s^{-1}$ [206]) and $k_{et} = (6.0 \pm 0.8) * 10^3\ s^{-1}$ (lit.: $(4.7 \pm 0.9) * 10^3\ s^{-1}$ [206]) are also in the region of the expected values. In addition, the length dependent decreasing of the ET rate from longer chained (**2**) to shorter chained (**3**) compounds is confirmed (**fig. 6-4**).

The ET rates of the ferrocenarylthiols **4** and **5** are higher compared to the compounds **1 – 3** discussed before due to the strong conjugation of the redox centre and the gold surface caused by the aromatic spacers. The ET rate for the biphenyl derivative **4** is about $k_{et} = (1.0 \pm 0.3) * 10^6\ s^{-1}$. For the anthracene derivative **5** the ET rate is over $10^6\ s^{-1}$ because of the totally conjugated molecules. An exact value could not be obtained and was limited by lacking apparative possibilities and by unfavourable R_u and C_{dl} values with which a good fit was not possible. Using the measured values of R_u and C_{dl} for the fitting

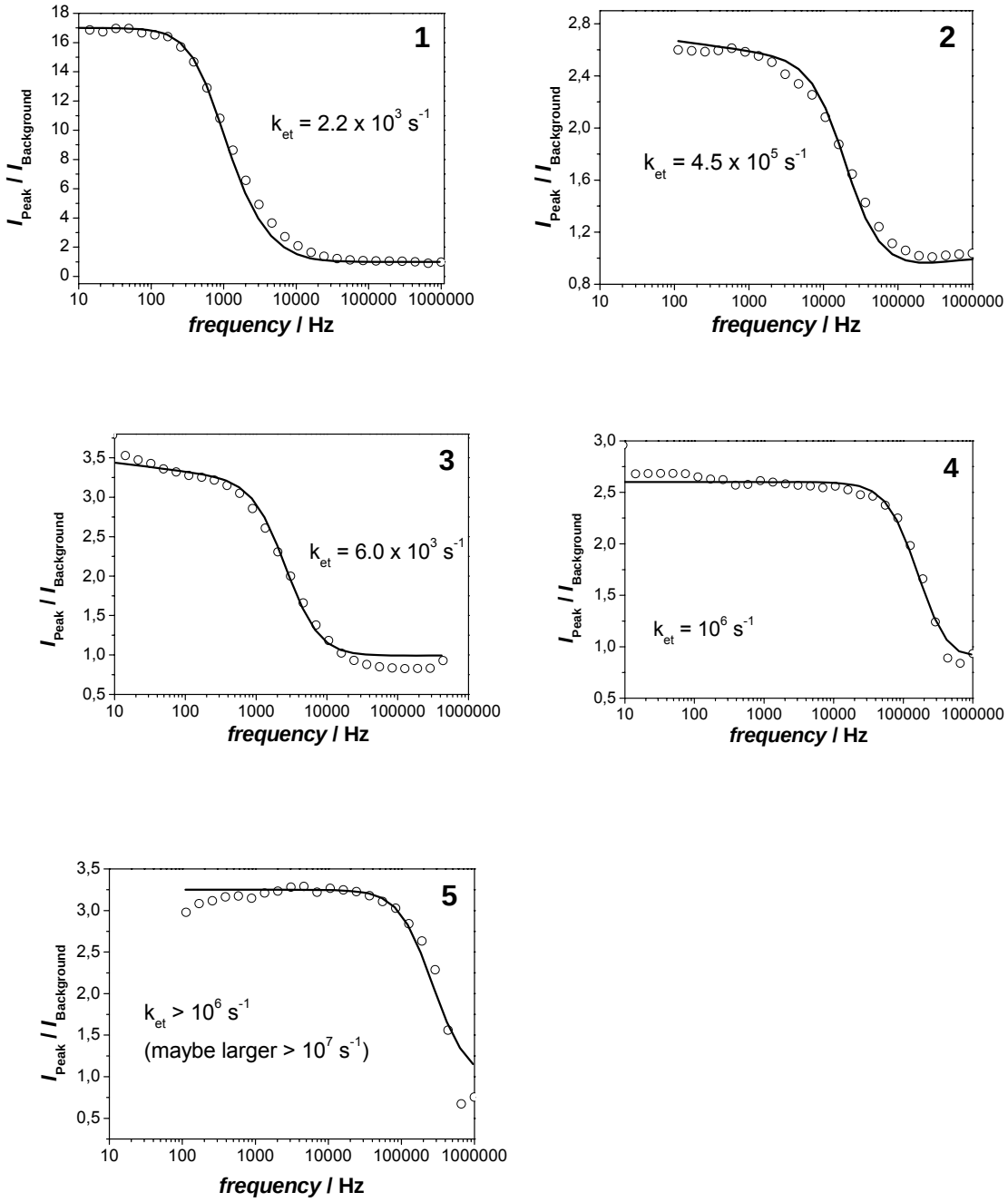

Fig. 6-4 Bode plot for ferrocenealkane- and ferrocenearylthiols **1** – **5** as SAMs on spherical gold-electrodes (Bode-plot: —— fitted curve, ○○○○ measured curve). The measurements were carried out in an aqueous 1 M $HClO_4$-solution, scan rate: 50mV/s

procedure a limiting value was found. By increasing the ET rate manually to test the accuracy of the fit exactly the same curve shape was obtained and no improvement or deterioration was observed. Therefore just a minimum value of $k_{et} = 10^6$ s^{-1} for **5** could be determined.

Tab. 6-2 Rate constants (k_{et}) including literature values, dummy molecules and electronic coupling factors (V) for compounds **1 - 5**

	k_{et} / s^{-1}	lit. values of k_{et} / s^{-1}	dummy molecules	V_{ab} / cm^{-1}
1	$(2.2 \pm 0.3) * 10^3$	$(2.0 \pm 0.4) * 10^3$	$C_{11}H_{23}SH$	1.3 ± 0.3
2	$(4.5 \pm 0.7) * 10^5$	$(4.4 \pm 0.2) * 10^5$ [170]	$C_8H_{17}SH$	17.9 ± 2.2
3	$(6.0 \pm 0.8) * 10^3$	$(4.7 \pm 0.9) * 10^3$ [206]	$C_{10}H_{21}SH$	2.1 ± 0.4
4	$(1.0 \pm 0.3) * 10^6$		$C_7H_{15}SH$	26.7 ± 4.6
5	$>10^6$		$C_7H_{15}SH$	> 26.7

6.3 Electron Coupling Factors of Nonadiabatic Electron Transfer

The electrochemical ET at metal electrodes has been considered as a special case of molecular ET and models have been developed to describe the interfacial ET at electrodes [169, 181-183, 208-210]. The reduction and reoxidation of an electroactive group at a metal electrode is written by

$$Ox + B(e^-) \underset{k_{ox}}{\overset{k_{red}}{\rightleftharpoons}} Red + B$$

where *Ox* is the oxidised and *Red* is the reduced form [169, 181]. B stands for the electronic levels of a metal electrode. The driving force for the electron transfer is:

$$\Delta G^0 = e(E_i - E^0) \qquad \textbf{equ. 6-6}$$

$$E_i = E_F - \frac{\varepsilon_i}{e} \qquad \textbf{equ. 6-7}$$

$$\varepsilon_i = \varepsilon - \varepsilon_F \qquad \textbf{equ. 6-8}$$

where e is the electron charge, E_i the quasi or effective electrode potential of the metal, E_F is the normal electrode potential of the metal, E^0 the formal potential of the electroactive group, ε the energy of a given state in the electrode which corresponds to the energy level in the electrode and ε_F the *Fermi* energy of gold ($4.4 * 10^4$ cm^{-1}; 5.5 eV).

An ET can occur only when the energy of an occupied donor state matches that of an unoccupied receiver state. The rate constants k_{red} and k_{ox} are obtained from the overlaps

of the distribution functions for the molecular reagent (D_{ox}, D_{red} and the electrode ($D_{B(e-)}$, D_B) (**equ. 6-9** and **6-10**).

$$k_{ox} = \frac{4\pi^2}{h}(V_{ab})^2 \int_{-\infty}^{+\infty} D_{B(e^-)} D_{ox}(\varepsilon_i)\mathrm{d}\varepsilon_i = \frac{4\pi^2}{h}(V_{ab})^2 \int_{-\infty}^{+\infty} \rho(\varepsilon_i) f(\varepsilon_i) D_{ox}(\varepsilon_i)\mathrm{d}\varepsilon_i \qquad \textbf{equ. 6-9}$$

$$k_{red} = \frac{4\pi^2}{h}(V_{ab})^2 \int_{-\infty}^{+\infty} D_B D_{red}(\varepsilon_i)\mathrm{d}\varepsilon_i = \frac{4\pi^2}{h}(V_{ab})^2 \int_{-\infty}^{+\infty} \rho(\varepsilon_i)[1-f(\varepsilon_i)] D_{red}(\varepsilon_i)\mathrm{d}\varepsilon_i \qquad \textbf{equ. 6-10}$$

where $\rho(\varepsilon_i)$ is the density of states per energy per atom in the electrode and V_{ab} is the electronic coupling factor between the redox molecule and the electrode. The function $f(\varepsilon_i)$ is the electron occupancy factor given by the *Fermi-Dirac* distribution (**equ. 6-11**):

$$f(\varepsilon_i)_{red} = \frac{1}{1+\exp(\varepsilon_i / kT)} \qquad \textbf{equ. 6-11}$$

Within the Marcus treatment the distribution functions for the oxidised and reduced couple are given by **equ. 6-12** and **6-13**:

$$D_{ox}(\varepsilon_i) = \left[\frac{1}{(4\pi\lambda kT)^{1/2}}\right] \exp\left[-\frac{[\lambda + e(E_i - E^o)]^2}{4\lambda kT}\right] \qquad \textbf{equ. 6-12}$$

$$D_{red}(\varepsilon_i) = \left[\frac{1}{(4\pi\lambda kT)^{1/2}}\right] \exp\left[-\frac{[\lambda - e(E_i - E^o)]^2}{4\lambda kT}\right] \qquad \textbf{equ. 6-13}$$

Thus, the rate constants for the oxidation or reduction of redox molecules at electrodes are obtained by integrating over all of the energy levels of the electrode and are given by **equ. 6-15** and **6-16** [169, 181-183, 208-210], where λ is the reorganisation energy and η the overpotential E_f-E^0 (equal to the applied potential relative to the formal potential of the redox molecule), k is the Boltzmann constant and T is the absolute temperature. The standard ET rate k_0 is obtained from either **equ. 6-15** or **6-16** when the overpotential η is zero (**equ. 6-14**).

$$k_{ox} = k_{red} = k_{et} \qquad \textbf{equ. 6-14}$$

$$k_{ox} = \rho(\varepsilon)|V_{ab}|^2\left(\frac{kT}{\hbar}\right)\sqrt{\frac{\pi}{\lambda kT}}\int_{-\infty}^{\infty}\exp\left[-\frac{(\varepsilon_F-\varepsilon-e\eta+\lambda)^2}{4\lambda kT}\right]\times\left(\frac{\exp[(\varepsilon+\varepsilon_F)/kT]}{1+\exp[(\varepsilon+\varepsilon_F)/kT]}\right)\frac{d\varepsilon}{kT} \qquad \textbf{equ. 6-14}$$

$$k_{red} = \rho(\varepsilon)|V_{ab}|^2\left(\frac{kT}{\hbar}\right)\sqrt{\frac{\pi}{\lambda kT}}\int_{-\infty}^{\infty}\exp\left[-\frac{(\varepsilon_F-\varepsilon+e\eta+\lambda)^2}{4\lambda kT}\right]\times\left(\frac{1}{1+\exp[(\varepsilon+\varepsilon_F)/kT]}\right)\frac{d\varepsilon}{kT} \qquad \textbf{equ. 6-16}$$

Using a value of 6.8 * 10^3 cm^{-1} (0.85 eV; for the reorganisation energy of ferrocene monolayers in water [181, 182] and a value of 3.7 * 10^{-5} states cm (0.3 states eV^{-1}) for the state density of gold near the Fermi energy [183, 209] and solving the integral in **equ. 6-13** numerically, it is possible to calculate $|V_{ab}|$ for the electronic coupling between a redox centre and an electrode via a bridge. As expected the electronic coupling factors are large for short molecules (**2**: V_{ab} = 17.9 ± 2.2 cm^{-1}) and get smaller by increasing the chain length (**3**: V_{ab} = 2.1 ± 0.4 cm^{-1}) or they increase by changing the bridge system from saturated to conjugated ones (**4**: V_{ab} = 26.7 ± 4.6 cm^{-1}). Even here V_{ab} raises by increasing conjugation of the system from **4** to **5**. The electronic coupling factors of compound **1** – **3** are in good agreement with the values of a nonadiabatic ET (**tab. 6-2**) [211].

6.4 Discussion

The ferrocenealkanethiols **1** – **3** and the ferrocenearylthiols **4**, **5** were used to get experience in the monolayer preparation for measuring ET rates and for the measurements itself.

Although some problems, e. g. very high concentrations of the redox active component or no redox active molecules were found in the mixed monolayers, appeared using the preparation techniques of the mixed monolayers with a special ratio of dummy molecules to redox active molecules of the homologeous ferrocene compounds in literature [162, 171, 178, 189, 204, 206, 212], quite well diluted monolayers were achieved in the end. Opposite to *Creager et al.* where very low concentrations of the ferrocenealkanethiols (ferrocenealkanethiols : dummy molecules = 1 : 100) were used [212], increasing the ratio of ferrocenealkanethiols to dummy molecules up to 10 : 1 lead to the expected, well diluted monolayers. The symmetric shape of the cyclic voltammograms of the mixed monolayers

indicate, that they are homogeneously formed [106, 162, 171, 174, 178, 189, 204, 206, 212, 213] and that they are not embedded in the alkylthiol monolayers to influence the ET behaviour due to diffusion effects [203].

For the ferrocenealkylthiols **1** – **3** the ET rates could be confirmed compared to the measured ones done by *Creager et al.* [206]. As expected the ET rate decreases from **2** to **3** by increasing the chain length of the unsaturated spacer. The influence of the carboxy-group between the redox centre and the spacer onto the ET rate in compounds with the same chain length (**1**, **3**) is not very strong. The slightly smaller ET rate of compound **1** might be caused by the higher reorganisation energy of the carboxy ferrocene-centre compared to the directly connected compound **3**. The aromatic ferrocenethiols **4** and **5** show very high ET rates due to the strong conjugated system although the distance between the redox centre and the electrode is comparable to the C_8-alkyl compound **2**. The conjugation in the biphenyl system **4** is smaller than in the anthracene compound **5** because of the less conjugated system of **4**. Although it could be supposed that the biphenyl system of **4** is revolved due to steric hindrance of the hydrogen atoms and therefore lower ET rates are expected, further investigation done by *Terfort et al.* show that the biphenyl system of **4** itself is flat and a strong conjugation can takle place which leads to high ET rates [214].

The electronic coupling factors all indicate a nonadiabatic ET between the redox centre and the electrode. As expected the electronic coupling factors increase with decreasing spacer length or with an enlarged conjugated system.

To sum up, experience in monolayer preparation could be obtained, the measured ET rates for well known ferrocenealkane-compounds **1** - **3** could be verified and the information could be transferred to the conjugated systems **4** and **5**.

7 Electron Transfer in Saturated Triarylamine- and Phenothiazinealkanethiol SAMs

To test the reliability of the impedance measurements for other redox active monolayers apart from ferrocene, the ether- and ester-bridged triarylamine- (**29**, **32**) and phenothiazinealkanethiols (**35**) were synthesised. Because of the saturated alkane spacers a notable slower ET between the redox-donor and the electrode is expected compared to unsaturated bridges with an equal chain length.

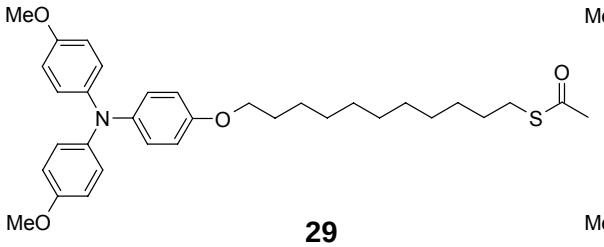

29

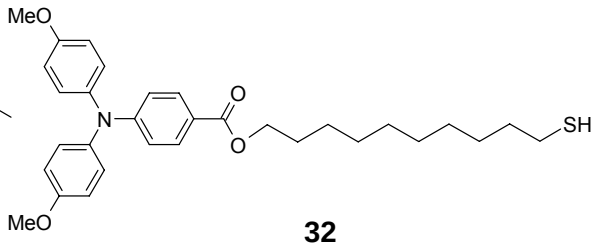

32

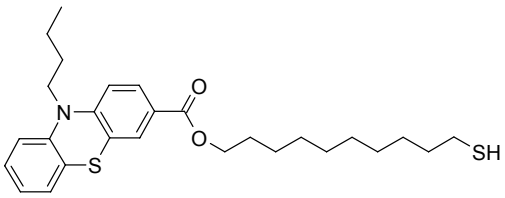

35

7.1 Synthesis

The ether-bridged triarylamine-alkanethiol **29** was synthesised starting from *p*-iodophenole and 9-bromo-1-undecanol to get the ether bridged compound **27** (**scheme 7-1**). After introduction of the thiol function, the redox centre was generated by using a palladium-catalysed aryl-N-coupling reaction to yield product **29**. In the last step the acetyl-protected thiol function was chosen to prevent a deactivation of the catalyst by formation of Pd-S-bonds. The acetyl function can be easily deprotected during monolayer preparation (see chapter 5).

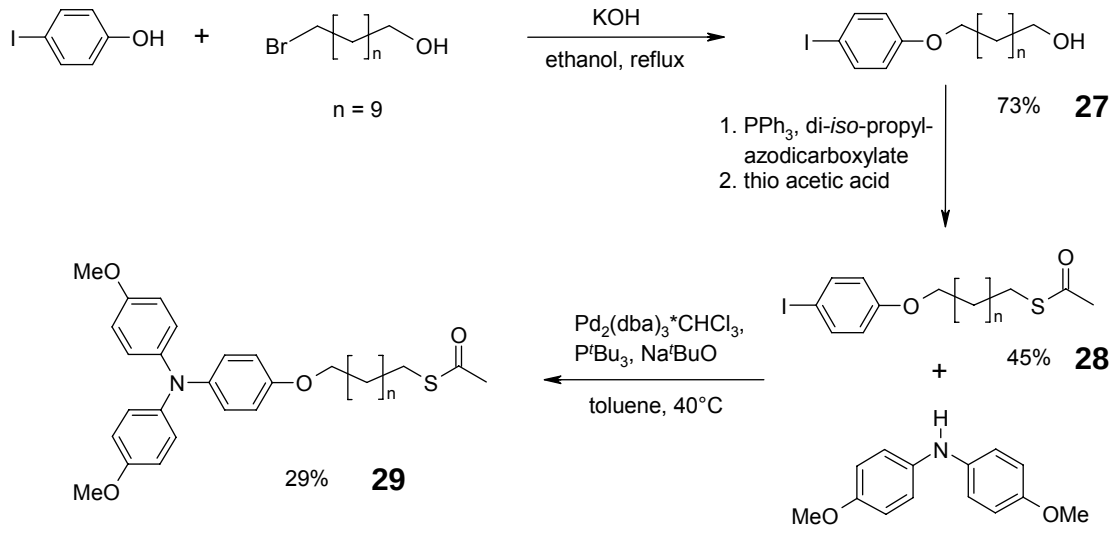

Scheme 7-1 Synthesis of the ether-bridged triarylamine-alkanethiol **29**

The ester-bridged triarylamine- **32** and phenothiazinealkanethiols **35** (**scheme 7-2**) were prepared by an ester condensation reaction starting from the carboxylic acid **30**, in case of the triarylamine compound, and 10-bromo-1-decaneol. The last step includes the generation of the thiol function by using thio urea to obtaine the desired product **32**. The phenothiazine derivative **35** was prepared in an analogous way.

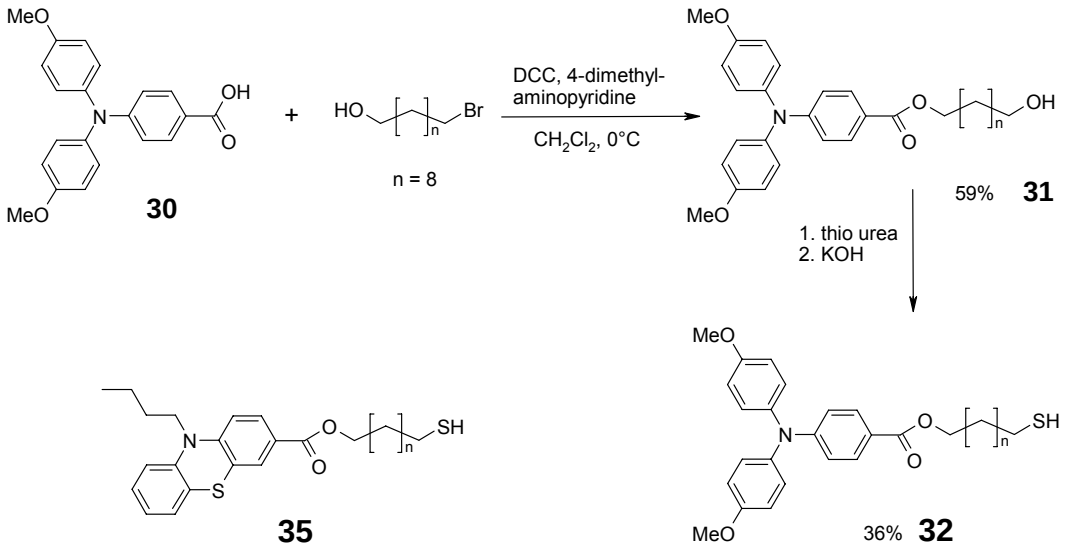

Scheme 7-2 Synthesis of an ester-bridged triarylaminealkanethiol **32**

7.2 ET rates of Triarylaminealkane- and Phenothiazinealkanethiols

7.2.1 Cyclic Voltammetry and Surface Coverage of 29, 32 and 35

The cyclic voltammograms of compounds **29**, **32** and **35** vs Fc / Fc^+ are shown in **fig. 7-1**, the values in **tab. 7-1**. For all CV measurements in solution a glassy carbon instead of a platinum electrode was used to avoid the formation of thiol SAMs on the electrode surface. All three compounds have two oxidation potentials. In all cases the first oxidation is reversible, while an irreversible second oxidation process at higher potential appears. The half wave potential increases from the triarylamine **29** to **32** because of the decreasing electron density caused by the electron rich ether bridge of **29** and the introduction of the ester connected triarylamine **32**. The oxidation potential of the ester connected triarylamine **32** and the phenothiazine **35** do not differ in a wide range. The second oxidation of **29** and **32** is caused by the irreversible oxidation of the sulphur of the thiol function or by the second oxidation of the nitrogen to the dication. The phenothiazine derivative **35** shows a different behaviour. The high current of the second oxidation of **35** compared to **29** and **32** considers that an overlay of the oxidation from the sulphur of the phenothiazine group and the thiol function appears.

Tab. 7-1 Oxidation potential vs Fc / Fc^+ for **29**, **32** and **35** in MeCN / TBAHFP (0.1 M) (for **35**: DCM : MeCN = 1 : 5 / TBAHFP (0.2 M)), scan rate: v = 250 mV/s; working electrode: glassy carbon

	$E_{1/2}^{ox,1}$ / **mV**	$E_{1/2}^{ox,2}$ / **mV**
29	140	830[a]
32	390	1090[a]
35	400	1200[a]

[a] irreversibile process, peak potential

Fig. 7-2 shows the cyclic voltammograms of the diluted SAMs of compounds **29**, **32** and **35** on gold. The peak separation is very small indicating that homogeneous, well ordered monolayers, especially in case of **29**, were formed [204]. The potential measured is relative to an Ag/AgCl-reference electrode and does not reflect the real redox potentials. The ratio of the redox potentials between **29**, **32** and **35** is comparable to the solutions of the same compounds investigated before by cyclic voltammetry. The slight increase of the current between 400 and 700 mV for compounds **32** and **35** points out that domains of triarylamines are formed besides isolated standing redox active molecules and redox processes between the redox active molecules occur.

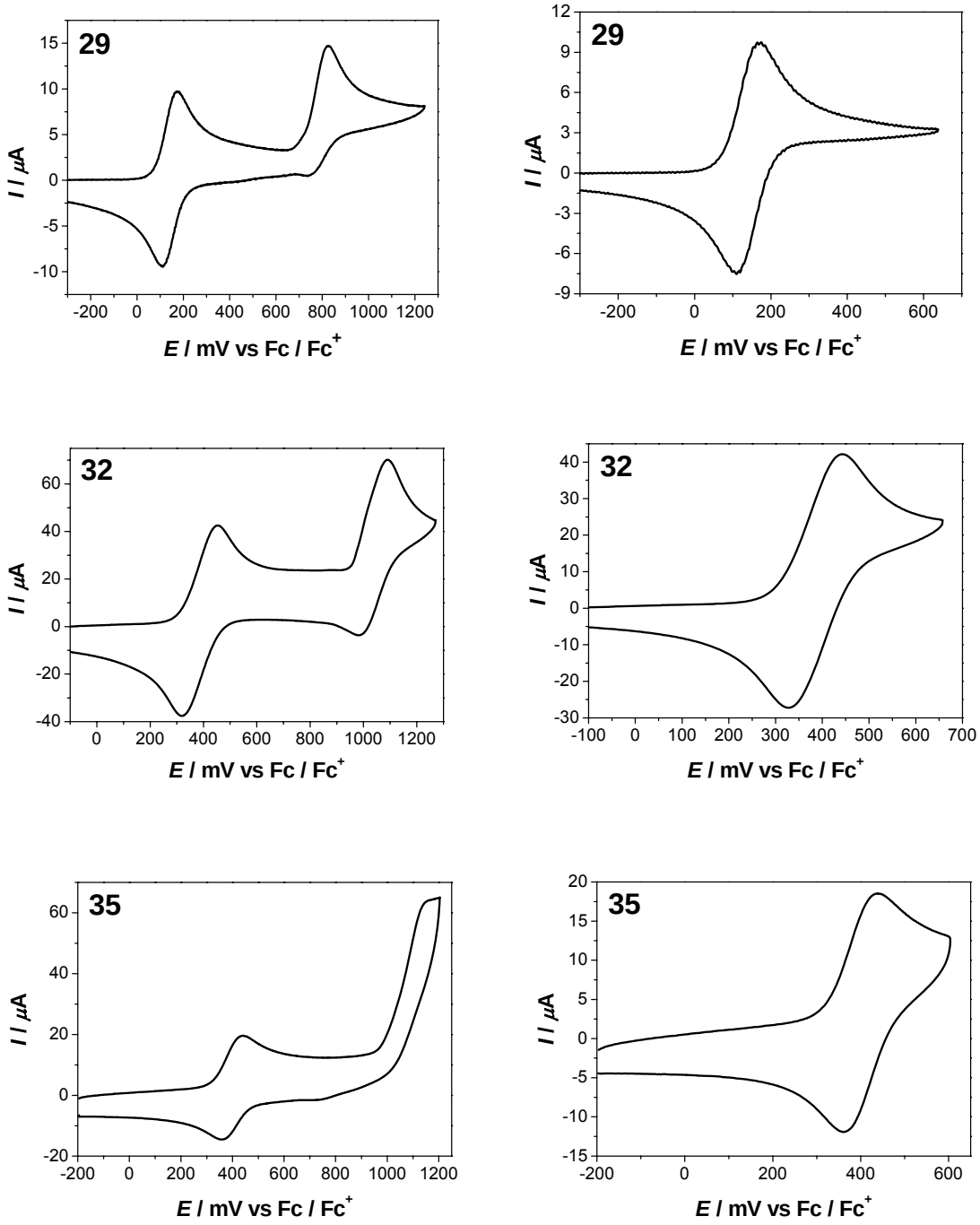

Fig. 7-1 Cyclic voltammograms for triarylamine- and phenothiazinealkanethiols **29**, **32** and **35** in MeCN / TBAHFP (0.1 M) (for **35**: DCM : MeCN = 1 : 5 / TBAHFP (0.2 M)), scan rate: v = 250 mV/s; working electrode: glassy carbon

The surface coverage and the used dummy molecules are depicted in **tab. 7-2**. The surface coverage of the redox active molecules compared to dummy molecules is between 2 ± 0.4 % for **35** and up to 5 ± 1.1 % for **29**. The length of the alkyl chains of the dummy molecules was as chosen so that the redox active molecules stick out of the monolayers to form well ordered SAMs.

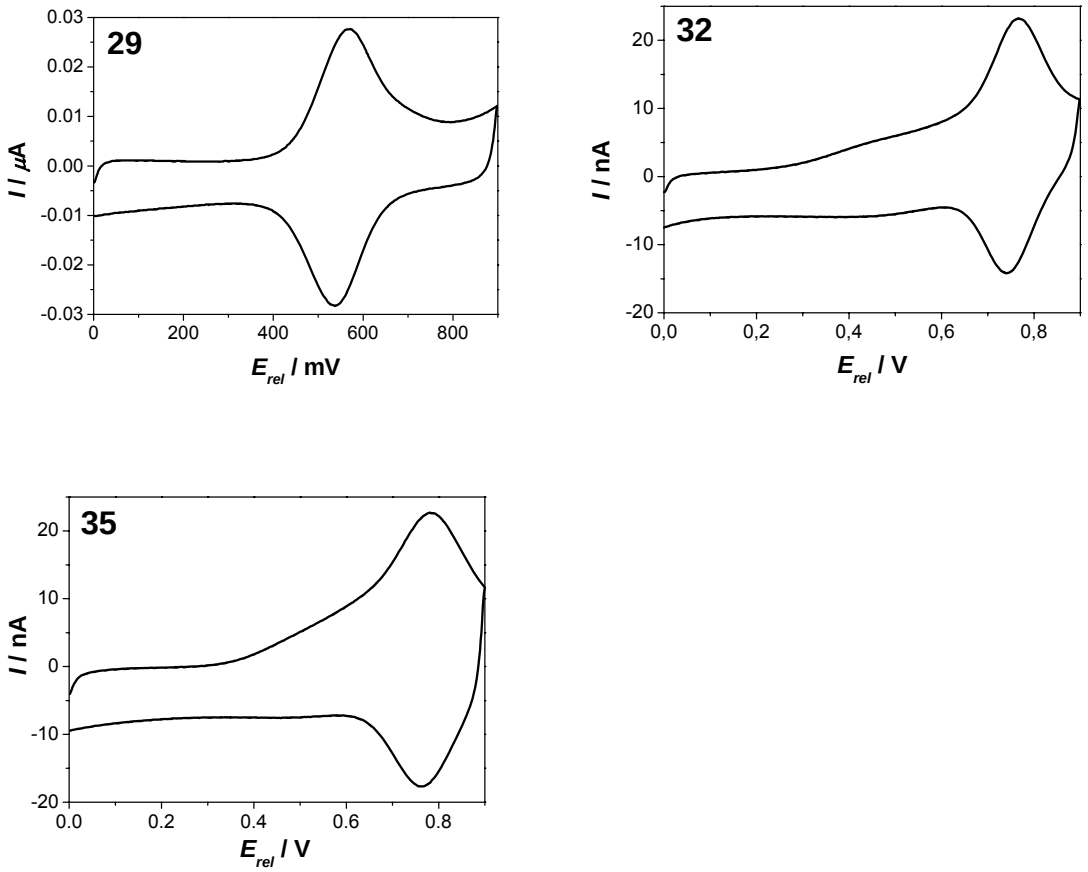

Fig. 7-2 Cyclic voltammograms for triarylamine- and phenothiazinealkanethiols **29**, **32** and **35** as SAMs on spherical gold-electrodes. The measurements were carried out in MeCN / TBAHFP (0.2 M), scan rate: 50 mV/s

Tab. 7-2 Surface coverage (Γ), dummy molecules, reorganisation energies (λ), double layer capacitance (C_{dl}), uncompensated resistance (R_u) and surface (A_{real}) for compounds **29**, **32** and **35**

	Γ / mol/cm^2	surface coverage / %	dummy molecules	λ / eV [215]
29	$(3.1 \pm 0.7) * 10^{-11}$	5.0 ± 1.1 %	$C_{10}H_{21}SH$	0.51 (MeCN)
32	$(1.9 \pm 0.3) * 10^{-11}$	3.0 ± 0.5 %	$C_{10}H_{21}SH$	0.51 (MeCN)
35	$(1.5 \pm 0.3) * 10^{-11}$	2.0 ± 0.4 %	$C_{10}H_{21}SH$	0.60 (MeCN)

	C_{dl} / F	R_u / Ω	A_{real} / cm^2
29	$(4.7 \pm 0.9) * 10^{-8}$	154 ± 25	$(1.4 \pm 0.1) * 10^{-2}$
32	$(5.0 \pm 0.5) * 10^{-8}$	175 ± 16	$(1.6 \pm 0.1) * 10^{-2}$
35	$(5.5 \pm 0.8) * 10^{-8}$	147 ± 24	$(4.9 \pm 0.2) * 10^{-2}$

7.2.2 UV/vis-Spectroscopy of 29, 32 and 35

In **fig. 7-3** the UV/vis-spectra of compounds **29**, **32** and **35** in dichloromethane are displayed, the values are shown in **tab. 7-3**. The absorption spectra of **29**, **32** and **35** have a characteristic intense band between 30900 and 37300 cm^{-1} with shoulders at 28500 cm^{-1} for **29**, 34200 cm^{-1} for **32** and 35000 cm^{-1} for **35**. The absorption band of the ester connected triarylamine **32** shows a bathochromic shift compared to the homologous ether connected triarylamine **29**. The intense almost symmetric band of **29** is caused by an intense HOMO → LUMO ($S_0 \rightarrow S_1$) excitation into a degenerated S_1 state, which is typical for C_3-symmetric triarylamines [216]. In case of the ester connected triarylamine **32** the C_3 symmetry is broken resulting in a splitting of the degenerated LUMO orbitals and a splitting of the degenerated S_1 state. Therefore two absorption bands are visible which are caused by a HOMO → LUMO ($S_0 \rightarrow S_1$) excitation and a HOMO → LUMO + 1 ($S_0 \rightarrow S_2$) excitation [216]. The intensity of **29** compared to **32** is the sum of these two transitions.

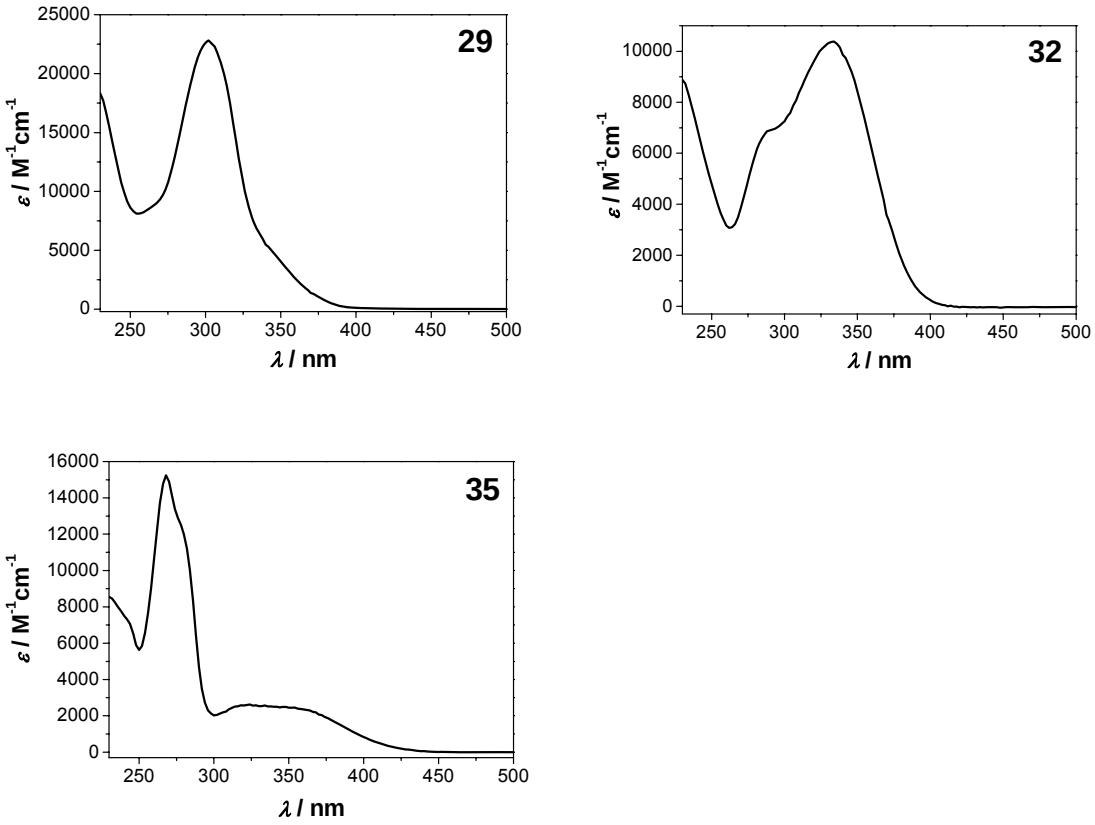

Fig. 7-3 UV/vis-spectra of compounds **29**, **32** and **35** in CH_2Cl_2

Tab. 7-3 UV/vis-maxima of **29**, **32** and **35** in CH_2Cl_2

	λ_1 / nm (cm^{-1})	ε_1 / $M^{-1}cm^{-1}$	λ_2 / nm (cm^{-1})	ε_2 / $M^{-1}cm^{-1}$	λ_3 / nm (cm^{-1})	ε_3 / $M^{-1}cm^{-1}$
29	351(28500)[a]	4100	302 (33100)	22800		
32	334 (29900)	10400	292 (34200)[a]	6900		
35	324 (30900)	2600	279 (35800)[a]	12000	268 (37300)	15200

[a] shoulder

7.2.3 Electron Transfer Rates and Electronic Coupling Factors for 29, 32 and 35

The measured and fitted impedance curves to determine the ET rate in the mixed SAMs are shown in **fig. 7-4**, the rate constants are given in **tab. 7-4**. All curves have a sigmoidal behaviour. At high frequencies, where the redox process cannot follow the applied frequency, the peak ratio between the measured current at the redox peak maximum and the background is one. By decreasing the frequency and reaching the ET rate, a current relative to the background is observed, until the frequency is slow enough so that all redox active molecules take part in the redox process and the current reaches a maximum. The ratio of the current is between 4.8 for **29** and 2.1 for **32**, indicating a good dilution of the redox active molecules compared to the dummy molecules. The rate constants are $k_{et} = (1.8 \pm 0.2) * 10^5\ s^{-1}$ for the ether-bridged triarylamine **29** and $k_{et} = (4.3 \pm 0.7) * 10^4\ s^{-1}$ for the ester-connected one **32**. The phenothiazine derivative **35** has an ET rate of $k_{et} = (1.7 \pm 0.3) * 10^4\ s^{-1}$. The shapes of the curve for **32** and **35** are broader than compared to the fits. Comparable spectra of ferrocenealkanethiol compounds with the same chain length were observed by *Creager et al.* [186, 203] and calculated using a modified *Randles equivalent circuit* [207]. This model analyses impedance spectra of SAMs containing redox active molecules with a distribution of ET rates. The spectra itself get broader if more than one ET rate contribute to the overall rate constant until it reaches a point where a double or triple sigmoidal curve can be observed if the difference between the ET rates are large enough. Therefore different, near adjacent ET rates are measured caused by e. g. domains consisting of only redox active molecules. Another reason for such aberrant curves are monolayers where the redox active part of the molecule is buried in the dummy molecules and therefore no or a poor ion transport, which is important in

ferrocene-alkane-monolayers for the ET, appears [203]. The decay of the curves in the lower frequency region after the current reached a maximum is due to the instability of the monolayer and the redox active molecules. However the ether connected triarylamine **29** shows stability.

The electronic coupling factors are given in **tab. 7-4** and are in the range of 0.9 ± 0.2 cm^{-1} for **32** and **35** up to 1.9 ± 0.3 cm^{-1} for **29** indicating a heterogeneous ET (for detailed information calculating the electronic coupling factors see chapter 6.3).

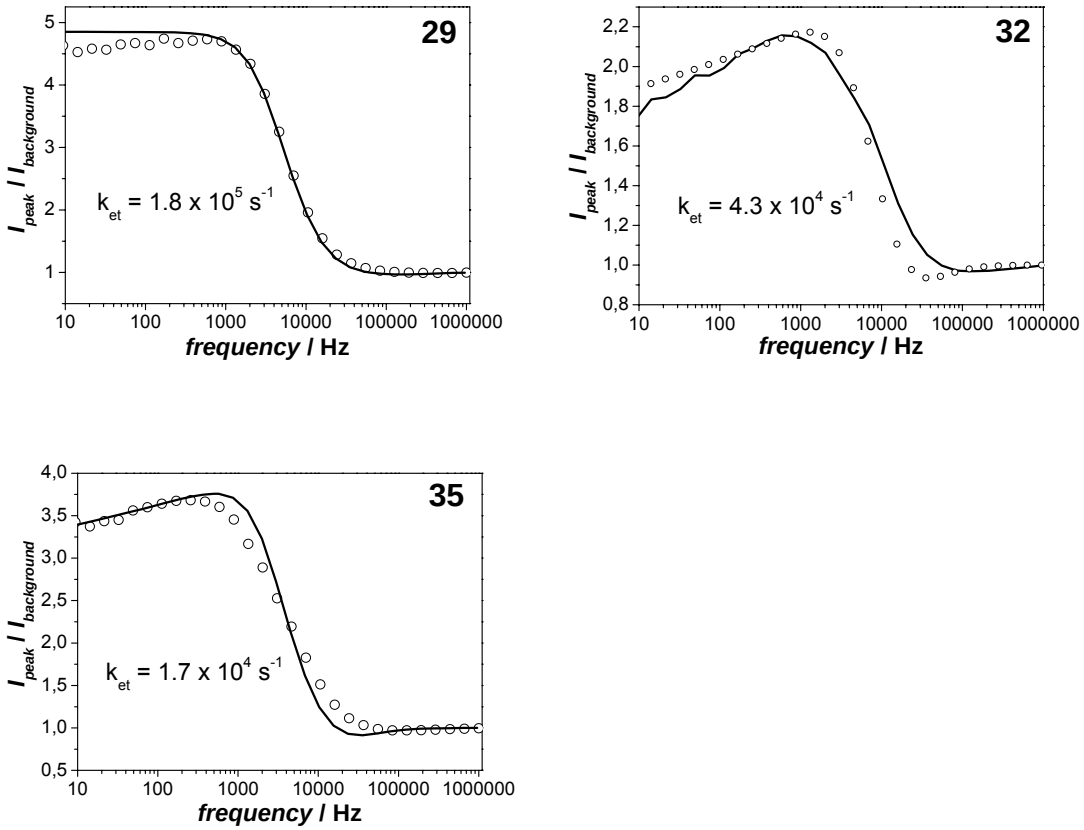

Fig. 7-4 Bode-plot for triarylamine- and phenothiazinealkanethiols **29**, **32** and **35** as SAMs on spherical gold-electrodes (Bode-plot: —— fitted curve, ○○○○ measured curve). The measurements were carried out in MeCN / TBAHFP (0.2 M)

Tab. 7-4 Measured rate constants (k_{et}), dummy molecules and electronic coupling factors (V) used for monolayer preparation of compounds **29**, **32** and **35**

	k_{et} / s^{-1}	dummy molecules	V_{ab} / cm^{-1}
29	(1.8 ± 0.2) * 10^5	$C_{10}H_{21}SH$	1.9 ± 0.3
32	(4.3 ± 0.7) * 10^4	$C_{10}H_{21}SH$	0.9 ± 0.2
35	(1.7 ± 0.3) * 10^4	$C_{10}H_{11}SH$	0.9 ± 0.2

7.3 Discussion

In this chapter the triarylamine- **29**, **32** and the phenothiazinealkanethiol **35** have been examined relative to their ET behaviour in mixed monolayers.

The small peak separation of the redox process in the cyclic voltammograms of the mixed monolayers with alkanethiol dummy molecules indicates homogeneously formed monolayers [106, 162, 171, 174, 178, 189, 204, 206, 212, 213] with some defects regarding to a small increase of the current at lower potential. The low surface coverage of these monolayers compared to pure alkanethiol monolayers also show that diluted well ordered monolayers were formed.

The ET rates of triarylamine- **29** (k_{et} = (1.8 ± 0.2) * 10^5 s^{-1}), **32** (k_{et} = (4.3 ± 0.7) * 10^4 s^{-1}) and the phenothiazinealkanethiols **35** (k_{et} = (1.7 ± 0.3) * 10^4 s^{-1}) are 10 to 100 times higher than compared to ferrocenealkanethiols with equal chain length (12 chain atoms between donor and sulphur) where the ET rate differs from k_{et} = (1.3 ± 0.3) * 10^3 s^{-1} for a carboxamide connected ferrocenealkanethiol up to k_{et} = (1.8 ± 0.4) * 10^3 s^{-1} for a directly connected ferrocenealkanethiol to the alkane bridge [183, 206]. In contrast to the ferrocenealkanethiols nearly the same ET rate of about k_{et} = (4.5 ± 0.9) * 10^4 s^{-1}, compared to compounds **29**, **32** and **35**, was found for the ET in a $[Ru(bpy)2(pp)]^+$-containing monolayer with a saturated bridge of 12 atoms [177]. *Hsu* and *Marcus* point out that two parameters influence the ET rate constant: the matrix element $|V_{ab}|$ describing the electronic coupling between the electrode and the redox centre and the reorganisation energy λ [209] (for large molecules λ is dominated by its outer sphere component λ_{OS} [217]). For $[Ru(bpy)2(pp)]^+$ the reorganisation energy is 0.55 eV which is less than the value for ferrocene derivatives of 0.85 eV [177, 183]. In case of triarylamine **32** and phenothiazine **35** the reorganisation energies are 0.51 eV respectively 0.60 eV [215] resulting in higher or comparable ET rates for the triarylamine compounds and in a lower ET rate for the phenothiazine derivative compared to $[Ru(bpy)2(pp)]^+$ where the reorganisation energy lies in between. *Hortholary* found that λ accounts for about 70% of the rate constant enhancement [177]. In conclusion the ET rate in donor substituted alkanethiols is mainly influenced by the reorganisation energy λ and even small changes have a dramatic effect on the obeserved processes.

The coupling matrix element $|V_{ab}|$ plays a subordinate role in the influence onto the ET rate and does not change significantly, which is easily understood since all molecules

have the same chain length. The electronic coupling factors of **29** (V_{ab} = 2.1 cm^{-1}), **32** (V_{ab} = 0.9 cm^{-1}) and **35** (V_{ab} = 0.9 cm^{-1}) have almost the same values as ferrocenealkanethiols with the same chain length (V_{ab} = 1.0 cm^{-1}) [183]. The small values all indicate a nonadiabatic ET between the redox centre and the electrode.

The high rate constant of the ether connected triarylamine **29** (k_{et} = (1.8 ± 0.2) * 10^5 s^{-1}) compared to its homologeous **35** (k_{et} = (4.3 ± 0.7) * 10^4 s^{-1}) cannot be explained by a difference in the reorganisation energy of the redox centre but by mesomeric effects where the positive charge of the electron rich derivative **29** is more located at the ether function so that the chain is formally shortend by one atom (**fig. 7-5**). Comparison of the ratio of k_{et}(**29**)/k_{et}(**32**) with the ratio of ferrocenecarboxamide alkanethiols (β = 1.1 per methylene unit [183]) of the same chain length and concerning an exponential length dependence of the

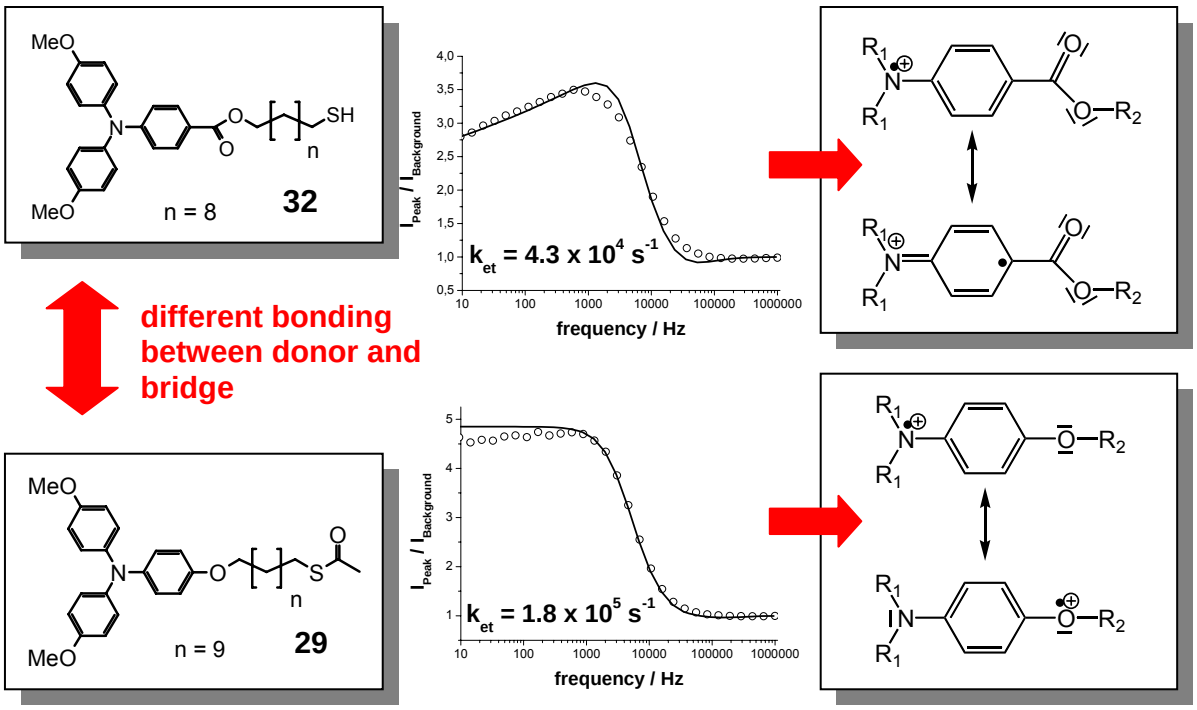

Fig. 7-5 Important mesomeric formula of compounds **29** and **32** for the explanation of the different ET rates while having the same chain length

ET show that the four times higher ET rate of **29** to **32** results formal in a reduction of the alkane chain by 1.1 methylene units and is in good agreement with the above mentioned explanation. The ratio and the formal reduction could be calculated using the equation for k_{et} of the superexchange mechanism ($k_{ET} = A \cdot e^{(-\beta r_{DA})}$, where A is a temperature dependent factor, β a structure dependent attenuation factor per methylene unit and r_{DA} the number of methylene units between donor and aceptor) and the values of k_{et} and β for the ferrocenecarboxamide alkanethiols [183, 206]. *Creager* did not observe such a rate constant

behaviour dependence on the connection between the redox centre and the bridge. Investigations with methylene or carboxamide connected ferrocenealkanethiol SAMs with the same chain lenght always resulted the same ET rates [206].

8 Electron Transfer in Unsaturated Triarylamine- and Phenothiazinethiol SAMs with Conjugated, Active Bridge Units

8.1 Unsaturated Triarylamine- and Phenothiazinethiols with a Single Acetylene Spacers

The triarylamines **36**, **37**, **53** and the phenothiazine derivative **72** were choosen as redox centres in the donor-bridge-(S)Au-arrays because of their strongly varying redox potentials to investigate the ET.

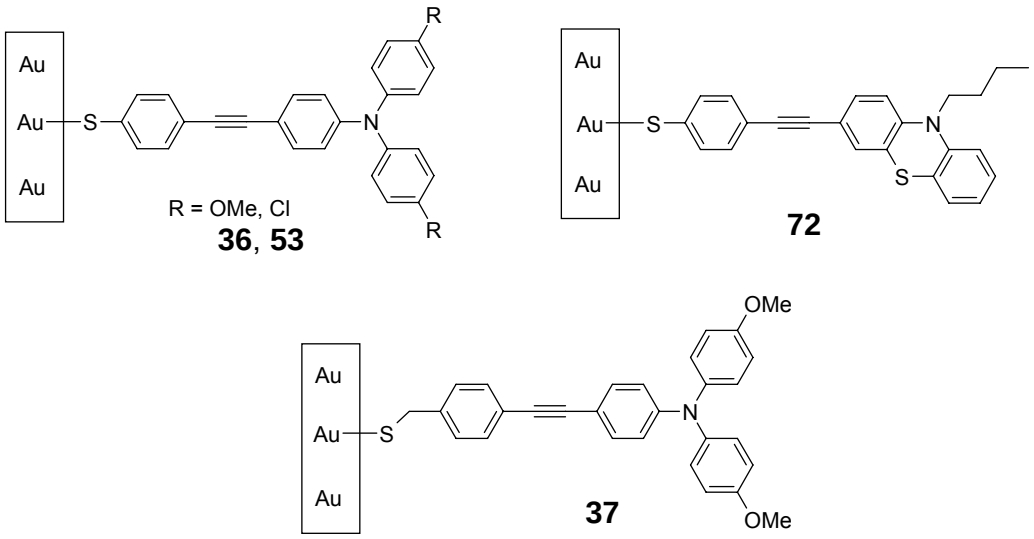

8.1.1 Synthesis

The preparation of the redox units follows a multi step synthesis in order to obtain compounds of type **36** [218-220]. As anchor function for the monolayer preparation on gold the acetyl-protected thiol **17** was used [221]. The easy access as well as the *in situ* elimination of the protection group of the thiol during gold electrode preparation [109] are important advantages. More stable protection groups, like *tert*-butyl ones [222], would have been desirable to start the synthesis of the chromophores from the anchor function and to introduce the redox centres in the last step to get the molecules with as less preparative expense as possible. Nevertheless, the triarylamines were not stable under these deprotection conditions. Starting from the triarylamine **8** and the anchor precursor **17**, a

palladium catalysed *Hagihara*-coupling reaction was used [223] to get the desired compound **36** (**scheme 8-1**). In all cases the thiol-function **17** was introduced in the last step to circumvent deprotection of the acetyl-thiol under the basic conditions of *Hagihara*-

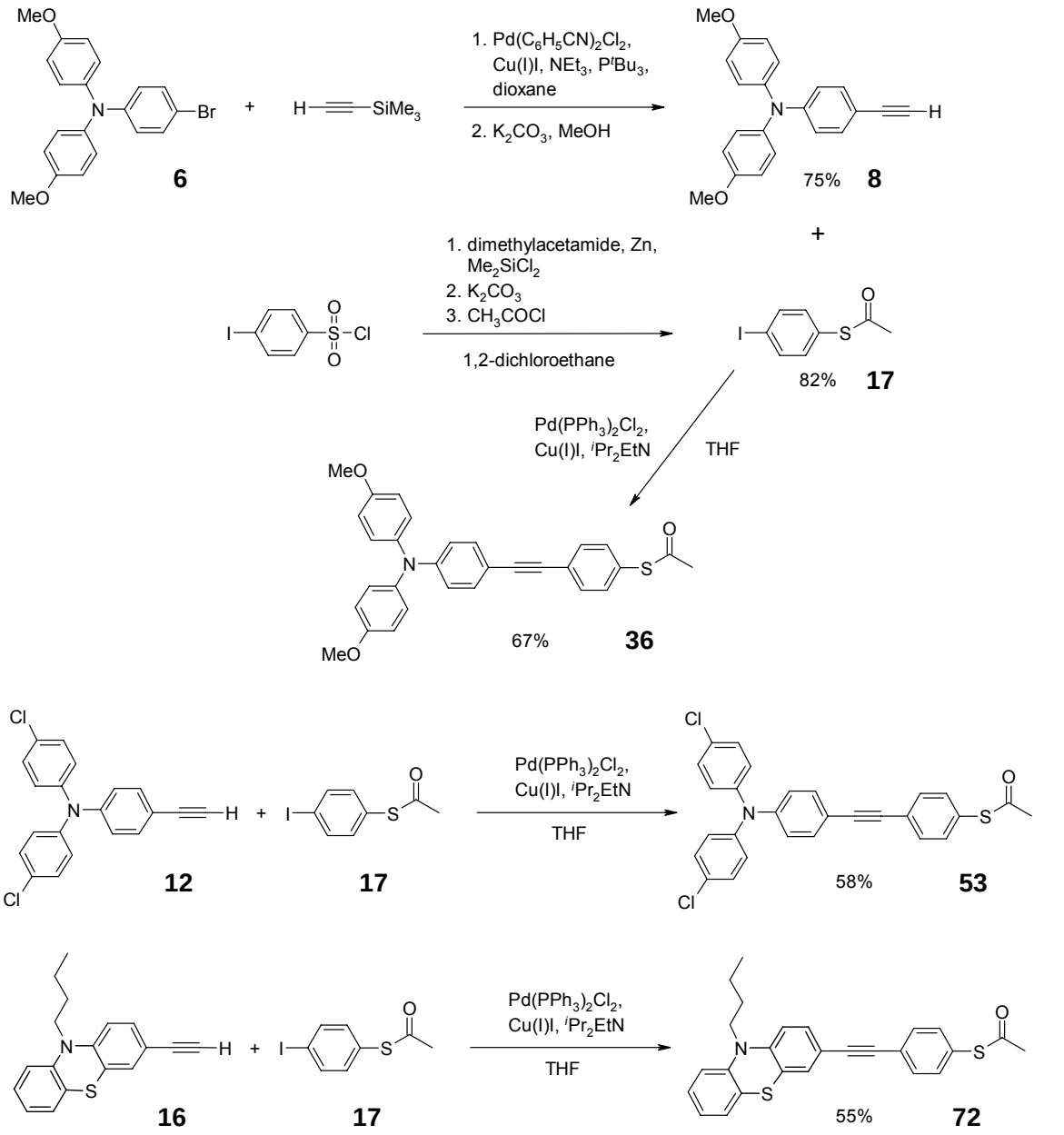

Scheme 8-1 Preparation of donor-bridge-SAc-species **36**, **53** and **72**

coupling reaction when using diethylamine. Three problems appear by the formation of the pure thiol: first the thiol function itself could be oxidised, second the formation of disulphides is possible and third the palladium catalyst could be deactivated by the formation of Pd-S-complexes. To prevent these problems and the deprotection in the last step a non nucleophilic base, di-*iso*-propyl-ethylamine (Hünig's base), was used.

Compounds **53** and **72** were synthesised in an analogous way starting from triarylamine **12** and phenothiazine **16** to obtain the products **53** and **72** by palladium catalysed reaction with anchor function **17**.

As a consequence of the short distance between redox donor and electrode compounds **36**, **53** and **72** should possess a strong electronic coupling. In order to investigate the influence of the bonding on the ET rate between donor and electrode a saturated methylene spacer was introduced between the thiol anchor function and the conjugated systems (compound **37**, **scheme 8-2**). Conductivity measurements of arenethiolate-protected MPCs (monolayer-protected cluster) indicate an electron hopping by introducing saturated spacers between the thiol and the conjugated system [224]. In case of the triarylamine **37** a slower ET rate compared to directly conjugated chromophore **36** is expected. Another reason for using the methylene unit is to get homogeneously ordered monolayers. *Thao et al.* showed that benzyl mercaptans and 4-biphenylmethanethiols compared to its homologous without methylene unit between the thiol and the chromophore form closely packed and well ordered monolayers indicating that the bond angle between the thiolate head group and the π-system influences the packing of the monolayers [225, 226].

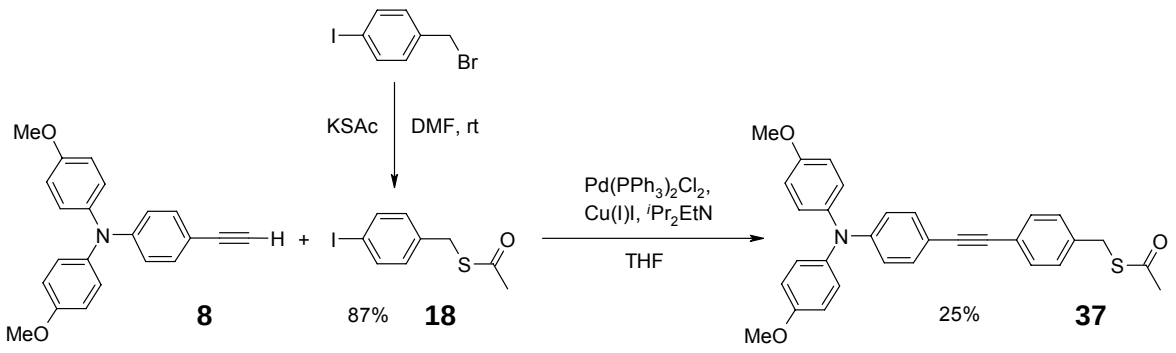

Scheme 8-2 Preparation of donor-bridge-SAc-species **37** with one methylene unit between the thiol function and the conjugated system

8.1.2 Cyclic Voltammetry and UV/vis-Spectroscopy

The cyclic voltammograms of the triarylamine compounds **36**, **37** and **53** and the phenothiazine derivative **72** are depicted in **fig. 8-1**. For all CV measurements in solution a glassy carbon instead of a platinum electrode was used to avoid the formation of thiol

SAMs on the electrode surface. The methoxy substituted triarylamines **36** and **37** and the phenothiazine compound **72** show a first reversible oxidation of the phenothiazine group. In all three cases the second oxidation of the thiol function at higher potential is irreversible. Additional a third irreversible oxidation of **72** is observed. In case of the chlorine substituted triarylamine **53** an irreversible oxidation is observed. The half wave potentials for the first oxidation are 330 mV for **36**, 310 mV for **37**, 690 mV for **53** and 410 mV for **72** measured versus Fc/Fc^+ (**tab. 8-1**). The slightly higher oxidation potential of **36** compared to its homologous **37** is caused by the decreasing influence of the electron withdrawing thioacetyl-function by introducing of one methylene unit between the acetyl-protected sulphur and the conjugated system. As expected, the chloride substituted triarylamine **53** shows a higher redox potential compared to the methoxy substituted ones because of the electron withdrawing groups. As observed in other experiments with IV-CT-derivatives of the chloride type with spacer units, these groups are not very stable [227]. In contrast triarylamines with different chloro-, methoxy or methyl-substituents in the three *para*-positions show a reversible behaviour of the oxidation in the cyclic voltammograms [216].

Tab. 8-1 Oxidation potential vs Fc / Fc^+ for **36**, **37**, **53** and **72** in DCM / TBAHFP (0.1 M) (for **36**: DCM : MeCN = 1 : 5 / TBAHFP (0.2 M)), scan rate: v = 250 mV/s; working electrode: glassy carbon

	$E_{1/2}^{ox,1}$ / mV	$E_{1/2}^{ox,2}$ / mV
36	330	1000[a]
37	310	960[a]
53	690	
72	410	1150[a]

[a] irreversible process, peak potential

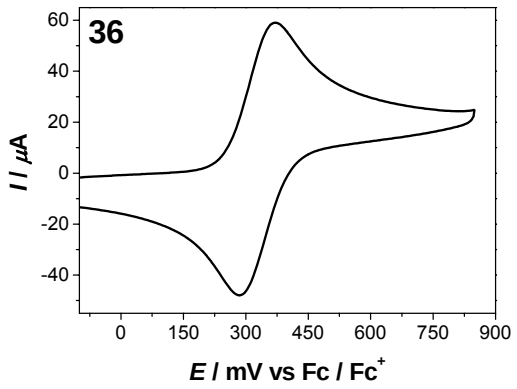

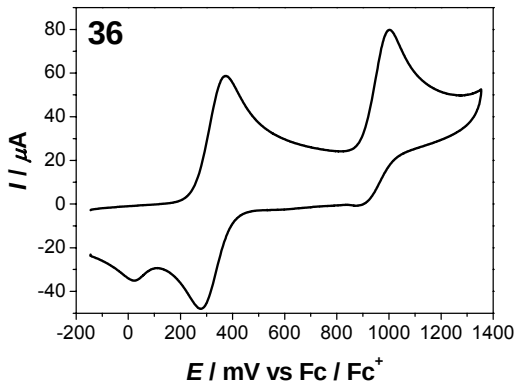

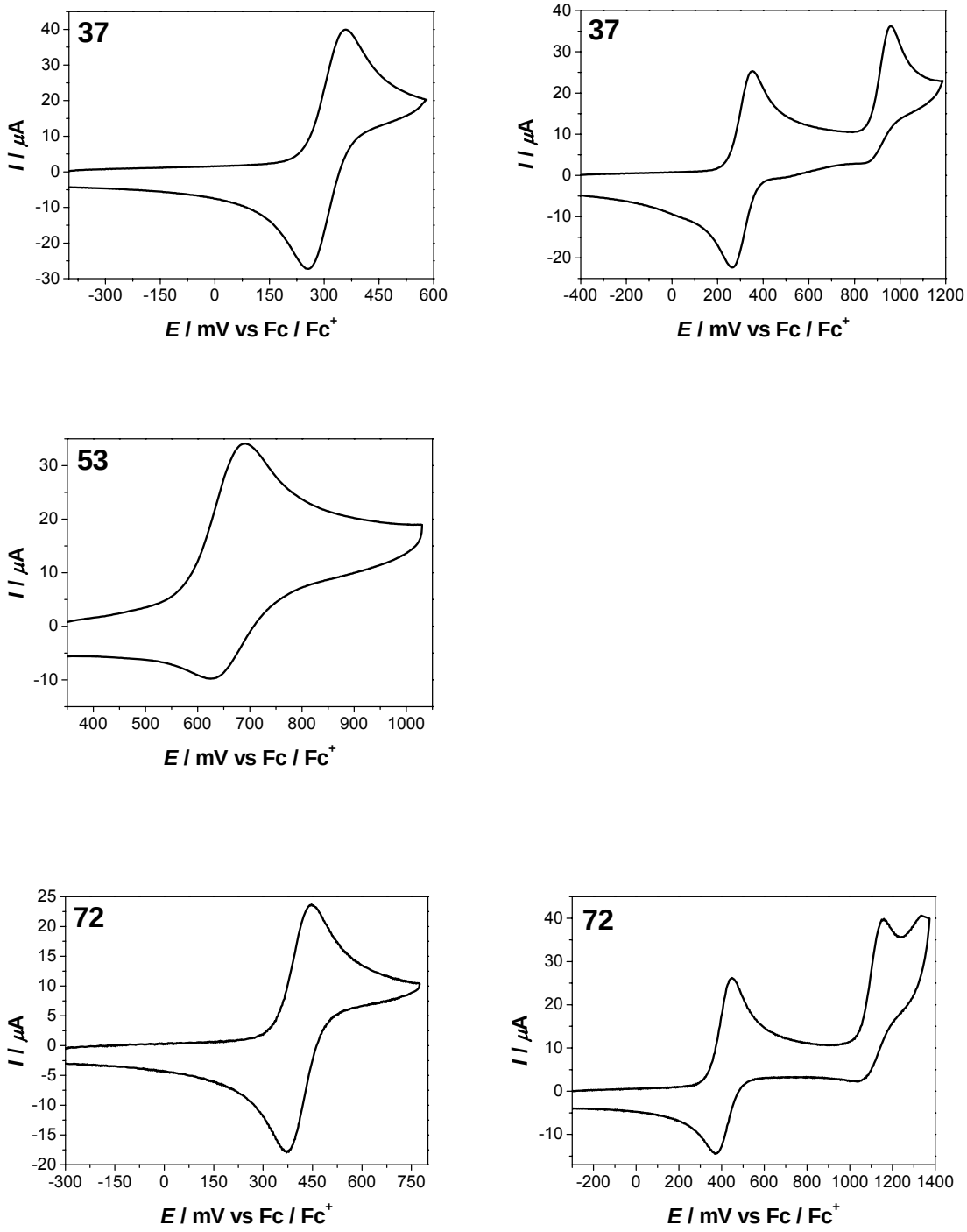

Fig. 8-1 Cyclic voltammograms for triarylamine- and phenothiazinethiols **37**, **53** and **72** in DCM / TBAHFP (0.1 M) (for **36**: DCM : MeCN = 1 : 5 / TBAHFP (0.2 M)), scan rate: v = 250 mV/s; working electrode: glassy carbon

The UV/vis-spectra of the triarylamine- (**36**, **37**, **53**) and the phenothiazine-compound **72** in dichloromethane are shown in **fig. 8-2,** the values are shown in **tab. 8-2**. All compounds have an intensive absorption at ~ 28000 cm^{-1} and a second band at ~ 33000 – 35000 cm^{-1}. Just the intensity of ε inverts comparing phenothiazine **72** with the

triarylamines **36**, **37** and **53**. As in case of the triarylaminealkanethiol **32** (discussed in chapter 7.2.2) the C_3 symmetry of **36**, **37** and **53** is broken resulting in a splitting of the degenerated LUMO orbitals and a splitting of the degenerated S_1 state. Therefore two absorption bands are visible which are caused by a HOMO → LUMO ($S_0 \rightarrow S_1$) excitation and a HOMO → LUMO + 1 ($S_0 \rightarrow S_2$) excitation [216]. The hypsochromic shift of the maximum from **36** ($\tilde{\nu}$ = 27200 cm^{-1}) to **37** ($\tilde{\nu}$ = 28200 cm^{-1}) is due to the influence of the acetyl-protected thiol-function. In case of **37** a methylene-unit between the conjugated system and the thiol-function limits this effect so that the chromophore is less electron rich. Therefore an increasing HOMO-LUMO gap appears which results in an absorbance at higher energy.

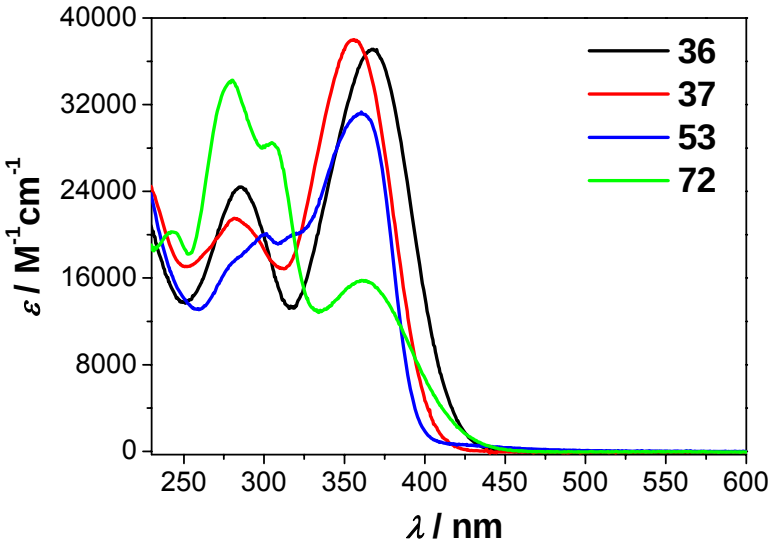

Fig. 8-2 UV/vis-spectra of compounds **36**, **37**, **53** and **72** in CH_2Cl_2

Tab. 8-2 UV/vis-maxima of **36**, **37**, **53** and **72** in CH_2Cl_2

	λ_1 / nm ($\tilde{\nu}_1$ / cm^{-1})	ε_1 / $M^{-1}cm^{-1}$	λ_2 / nm ($\tilde{\nu}_2$ / cm^{-1})	ε_2 / $M^{-1}cm^{-1}$
36	367 (27200)	37100	286 (35000)	24400
37	354 (28200)	37900	281 (35600)	21500
53	360 (27800)	31300	300 (33300)	20000
72	361 (27700)	15800	305 (32800), (280 (35700))	28500 (34300)

8.2 Unsaturated Triarylamine- and Phenothiazinethiol SAMs with Active Bridge Units

The systems with active bridge units between the redox centre and the electrode investigated in this project, are shown in **fig. 8-3**. Triarylamines and phenothiazine, as in the case for the unsaturated triarylamines- and phenothiazinethiols with acetylene spacers (**36**, **37**, **53** and **72**), are used as redox centres which are connected to the electrode via donor- or acceptor-substituted aromatic systems and acetylene spacers.

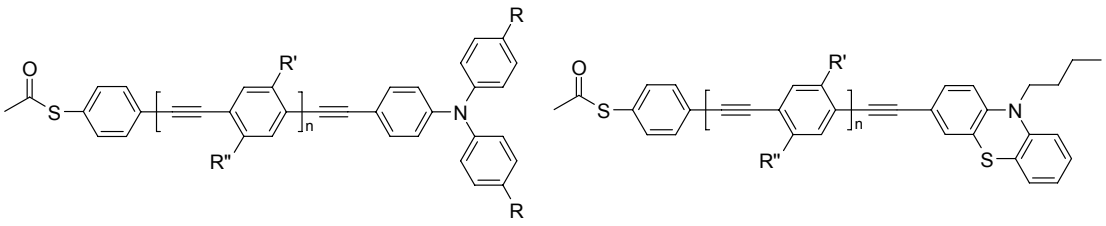

	R = OMe R', R'' = O^{n}Pr	R = OMe R' = CN R'' = H	R = Cl R', R'' = O^{n}Pr	R = Cl R' = CN R'' = H	Phenothiazine R', R'' = O^{n}Pr	Phenothiazine R' = CN R'' = H
n = 1	**40**	**46**	**56**	**65**	**75**	**84**
n = 2		**49**		**68**	**78**	**87**
n = 3		**52**	**62**	**71**	**81**	

Fig. 8-3 Prepared SAMs of donor-bridge-SAc-species to study the ET for n = 1, 2 and 3 bridge units

8.2.1 Synthesis

To limit the high synthetic effort and to get a wide range of chromophores, a repetitive synthesis was chosen. Hereby it is important to use unsymmetrically substituted acetylene bridge units to allow a systematic chain extension.

The conjugated ET-systems with acetylene-bridged units should be prepared according to known synthetic strategies by *Tour et al.* [156, 228] and *Moore et al.* [229]. However, these methods were not practicable because of high synthetic effort and low yields.

The easiest way for a repetitive synthetic strategy is to use unsymmetrically substituted bridge units. The donor substituted compound **23** was synthesised in a five step synthesis in high yields starting from *p*-hydrochinone (**scheme 8-3**) [230, 231]. After

protection of the hydroxyl-groups with alkene functions, compound **19** was mono-brominated followed by an iodation in *para*-position to obtain the unsymmetric substituted bis-halogene compound **21**. A *Hagihara*-coupling reaction with TMSA and a bromo-iodo-exchange gave the desired product **23** in good yields.

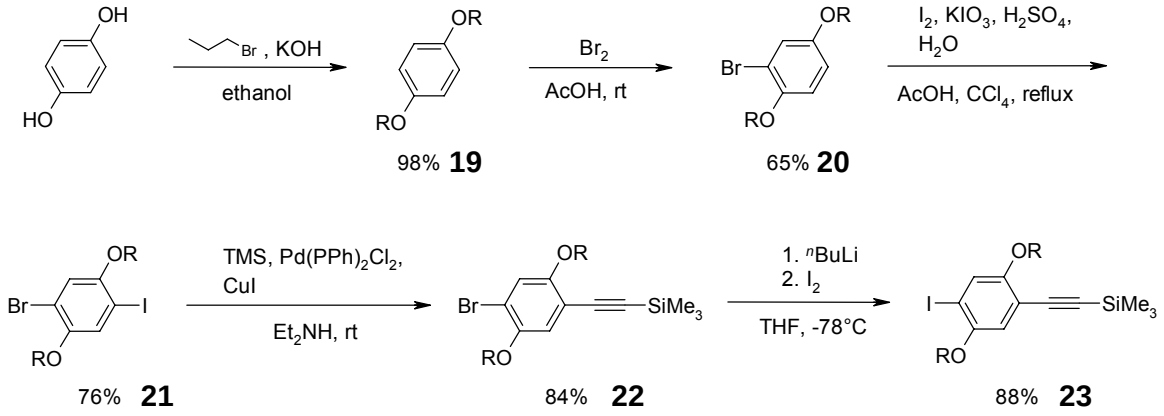

Scheme 8-3 Synthesis of the unsymmetric substituted donor-bridge unit **17** (R = ^{n}Pr)

To vary the energetic state of the bridge in a wide range, a second type of bridge unit with an acceptor substituted nitrile-group, was introduced (**scheme 8-4**). Starting from 2-aminobenzonitrile, **24** was obtained by iodination in *para*-position [232], followed by introduction of the TMSA-group and an amino-iodide-exchange [233] to yield compound **26**.

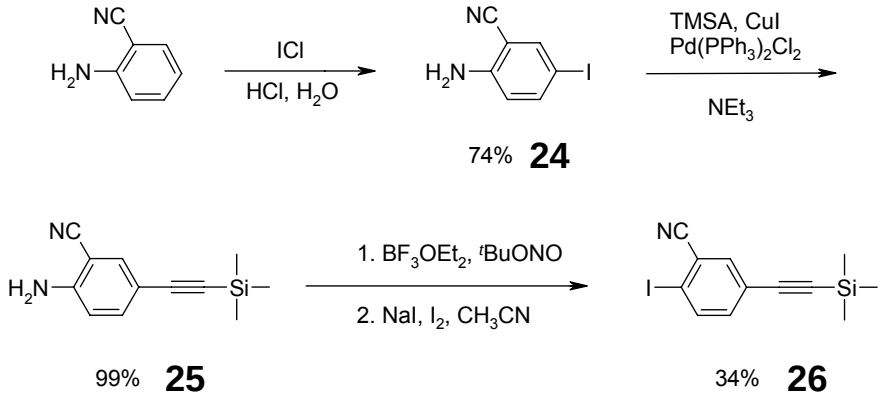

Scheme 8-4 Synthesis of bridge unit **26** with electron withdrawing nitrile functions

The following strategy, which is shown for the phenothiazine compound **75** in **scheme 8-5**, can be used as a general procedure for the preparation of all other comparable derivatives. The palladium-catalysed reaction of the phenothiazine **16** and the bridge unit

23 yielded the phenothiazine derivative **73**, which gave the desired product **75** after removing of the TMS-group and coupling with the anchor function **17** (**scheme 8-5**). A problem in this reaction was the homocoupling of e. g. the acetylene compound **16** to yield the diyne-derivatives. Despite of using other Pd-catalysts, ligands, reaction temperature, solvents and amounts of the used educts this problem could not be solved in a satisfied way. As expected for Pd-catalysed reactions the electron rich bridge unit **23** gave poorer yields than compared to the acceptor substituted bridge group **26**. By introducing the acetyl-protected thiol, a non nucleophilic base, as in case of the compounds **36**, **37**, **53** and **72** depicted in chapter 8.1, di-*iso*-propyl-ethylamine (Hünig's base), had to be used, to prevent deprotection of the acetyl-group. Although this was the best way to introduce the protected thiol, the yields were often very low (down to 5 %). The repetitive sequence of alkyne-arene-coupling and following $SiMe_3$-deprotection was used to built up systems with bridge units up to n = 3.

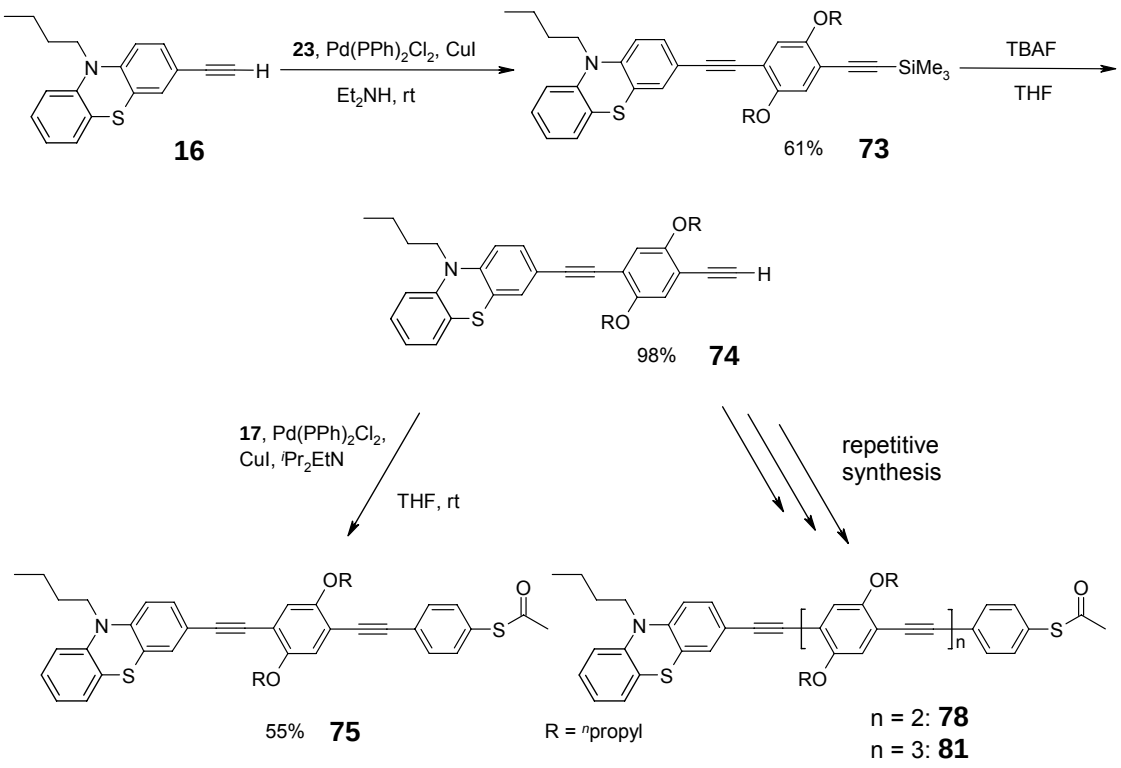

Scheme 8-5 General procedure for the preparation of donor-bridge-SAc-chromophores with n = 1-3 bridge units

8.2.2 Cyclic Voltammetry

The cyclic voltammograms of the methoxy-substituted triarylamines with different conjugated bridge units (**40**, **46**, **49** and **52**) in dichloromethane are shown in **fig. 8-4**, the values are displayed in **tab. 8-3**. For all CV measurements in solution a glassy carbon instead of a platinum electrode was used to avoid the formation of thiol SAMs on the electrode surface. The cyclic voltammogram of the methoxy-substituted triarylamine **40** with a propoxy-substituted phenylene-bridge has a reversible oxidation at 280 mV caused by the nitrogen and two irreversible oxidations at 890 mV and 1000 mV which are attributed to an oxidation of the bridge unit and to an oxidation of the monoradical cation

Tab. 8-3 Oxidation potential vs Fc / Fc^+ for unsaturated triarylamine- and phenothiazinethiols with active bridge units in DCM / TBAHFP (0.1 M), scan rate: v = 250 mV/s; working electrode: glassy carbon

	$E_{1/2}^{ox,1}$ / mV	$E_{1/2}^{ox,2}$ / mV	$E_{1/2}^{ox,3}$ / mV
36	330	1000[a]	
37	310	960[a]	
40	280	890[a]	1000[a]
46	350	980[a]	
49	360	1060[a]	
52	340	990[a]	1520[a]
53	690		
56	590[a]	1080[a]	
62	580[a]	710[a]	1050[a]
65	700		
68	690		
71	710		
72	410	1150[a]	
75	300	890	1320[a]
78	310	780	1270[a]
81	300	750[a]	
84	350	1090[a]	
87	360	1000[a]	1370[a]

[a] irreversible process, peak potential

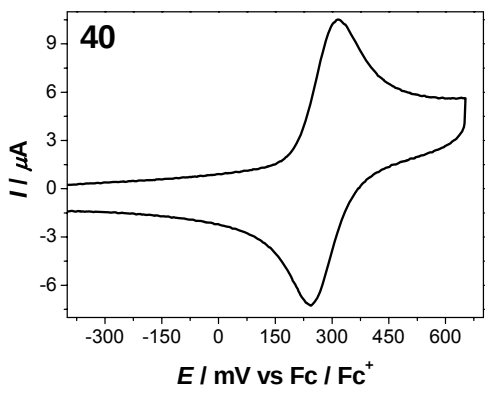
40
I / µA
E / mV vs Fc / Fc+

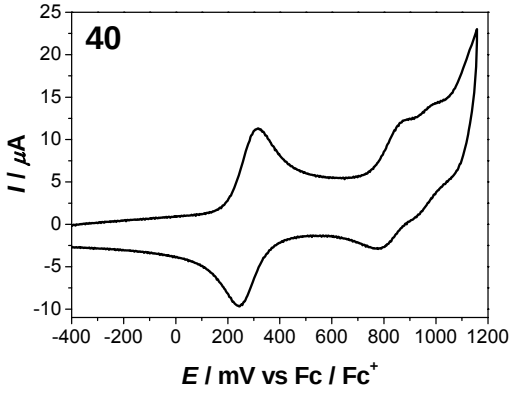
40
I / µA
E / mV vs Fc / Fc+

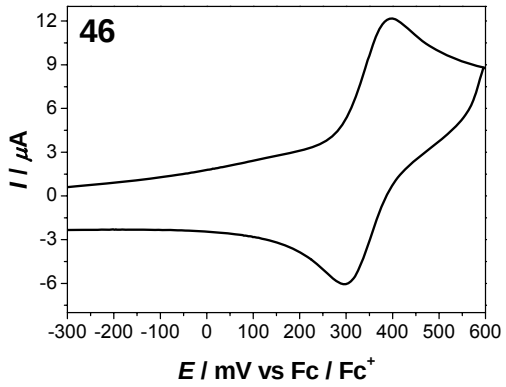
46
I / µA
E / mV vs Fc / Fc+

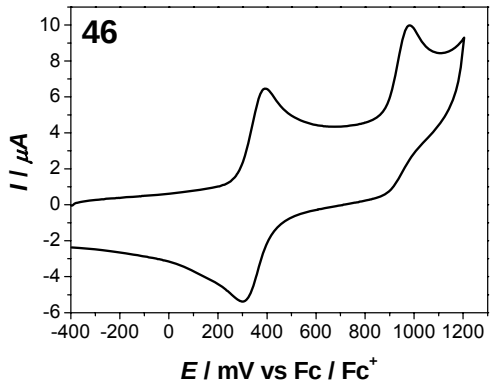
46
I / µA
E / mV vs Fc / Fc+

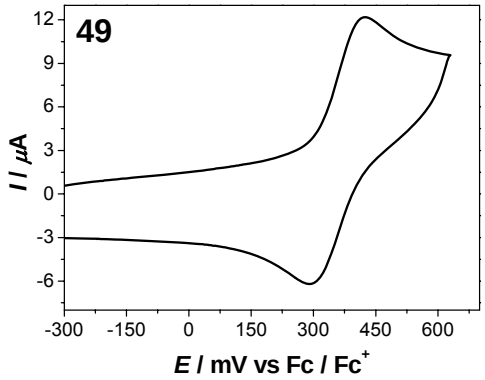
49
I / µA
E / mV vs Fc / Fc+

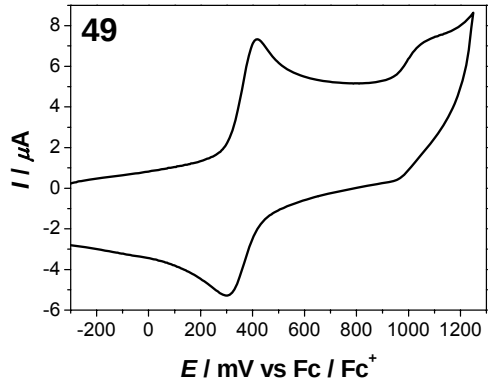
49
I / µA
E / mV vs Fc / Fc+

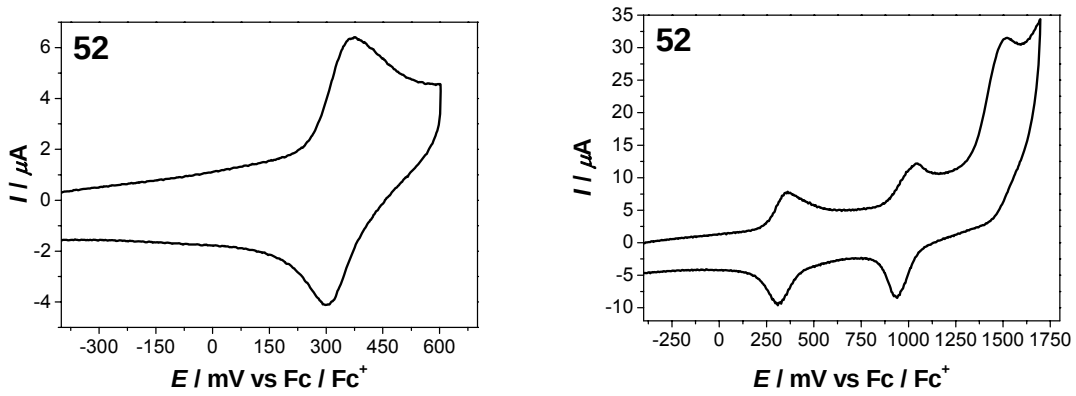

Fig. 8-4 Cyclic voltammograms for the methoxy-substituted triarylamines **40**, **46**, **49** and **52** with different bridge units in DCM / TBAHFP (0.1 M), scan rate: v = 250 mV/s; working electrode: glassy carbon

of the triarylamine group to the dication. Compared to its homologeous (**36**) without bridge unit, the first oxidation occurs at lower potential due to the influence of the electron rich bridge unit. Changing the bridge unit from methoxy- to nitrile-substituted ones, the oxidation potential of the first oxidation slightly increases from 330 mV for no bridge unit (**36**) to 350 mV for one bridge unit (**46**) and up to 360 mV for two bridge units (**49**). This increase is due to the influence of the electron withdrawing nitrile function. Therefore the electron density at the triarylamine decreases which results in higher oxidation potentials. The influence itself gets smaller as longer the bridge is. All three chromophores (**46**, **49** and **52**) have even a second (in case of **52** a third) irreversible oxidation the triarylamine function to the dication. The second oxidation of **52** is caused by the bridge itself.

The cyclic voltammograms of the chloro-substituted triarylamines with different conjugated bridge units (**53**, **56**, **62**, **65**, **68** and **71**) in dichloromethane are shown in **fig. 8-5**, the values are displayed in **tab. 8-4**. As expected, the oxidation of the nitrogen group of the chloro-substituted triarylamines **56** and **62** are shifted to higher potential compared to the methoxy-subsituted ones (**36**, **40**, **46**, **49**, **52**). And even here the influence of the propoxy-substituted bridge unit is remarkable. The potential decreases by 100 mV to 590 mV for 56 (one bridge unit) and to 580 mV for **62** (three bridge units) compared to **53** without bridge unit. This effect is also caused by the electron rich methoxy-substituted bridge units and the influence declines by increasing the bridge length. All oxidations, including the oxidation of the sulphur are irreversible. The second oxidation of **62** at 710 mV again is caused by an irreversible oxidation process of the bridge itself. The influence of the electron withdrawing nitrile is not very remarkable. By increasing the bridge of the chromophore from one (**65**) to two (**68**) bridge units the potential nearly has the same

values compared to **53**. A second oxidation cannot be observed due to solvent oxidation limits.

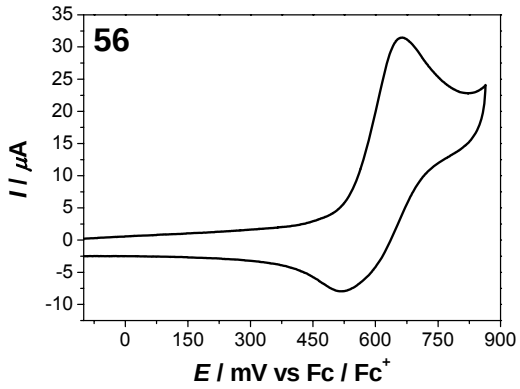

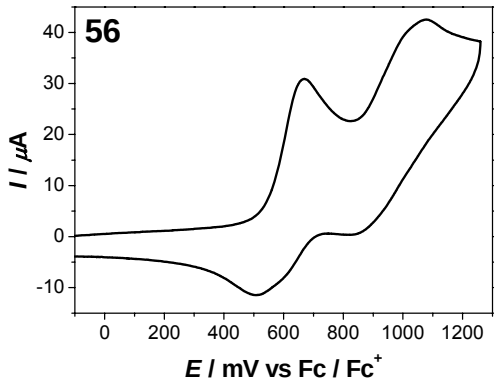

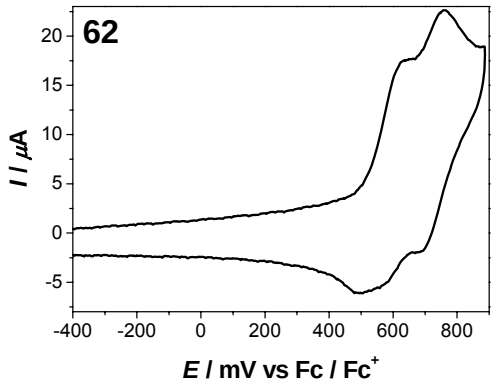

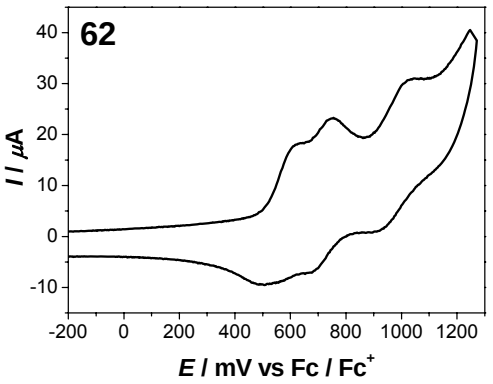

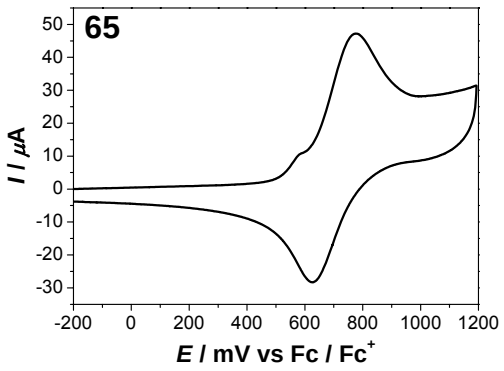

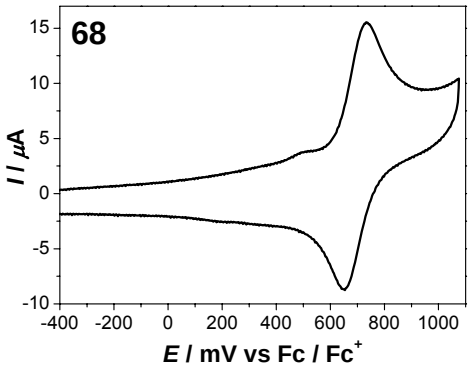

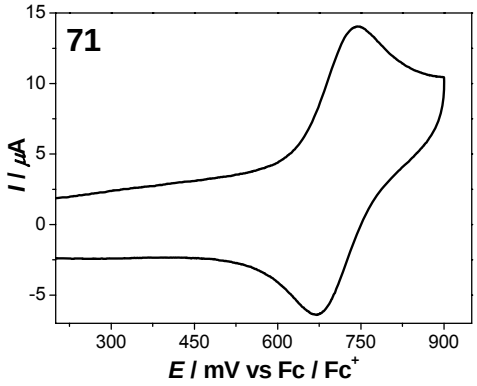

Fig. 8-5 Cyclic voltammograms for the chloro-substituted triarylamines **56**, **62**, **65** and **71** with different bridge units in DCM / TBAHFP (0.1 M), scan rate: v = 250 mV/s; working electrode: glassy carbon

The cyclic voltammograms of the phenothiazines with different conjugated bridge units (**72**, **75**, **78**, **81**, **84** and **87**) in dichloromethane are shown in **fig. 8-6**, the values are displayed in **tab. 8-4**. The methoxy-substituted phenothiazine compounds show the same behaviour as the triarylamines with the same bridge unit - the oxidation potential for the first oxidation decreases (no bridge unit **72**: 410 mV, one bridge unit **75**: 300 mV, two bridge units **78**: 310 mV). Because of the electron rich bridge unit, a second irreversible oxidation can be observed at 890 mV for **75** and 780 mV for **78**. The drop of the oxidation potential can be explained by the introduction of more electron-rich bridge units. An interesting observation is, that by using nitrile substituted bridge units the oxidation potential of the first oxidation even decreases (one bridge unit **84**: 350 mV, two bridge units **87**: 350 mV). The second irreversible oxidation is again caused either by the acetyl-protected sulphur or the sulphur of the phenothiazine. The cyclic voltammogram of **81** shows a different behaviour. The unsymmetric shapes of the curves of the first oxidation to $\mathbf{81}^{1+}$ and of the reduction indicate that presumable an absorption of the oxidised species onto the electrode takes place.

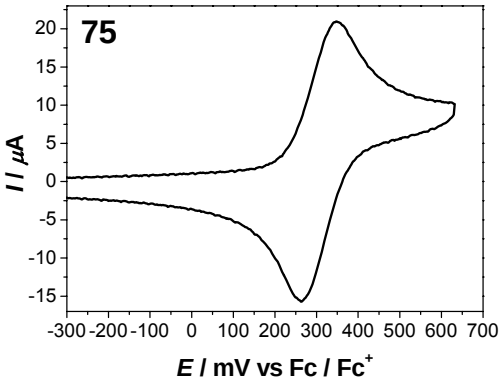
75
I / µA
E / mV vs Fc / Fc+

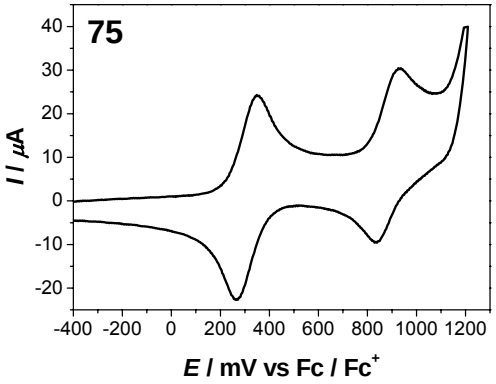
75
I / µA
E / mV vs Fc / Fc+

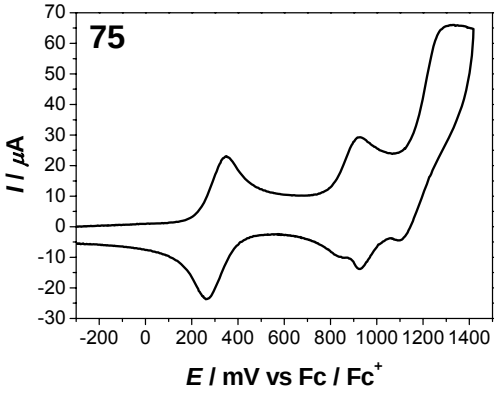
75
I / µA
E / mV vs Fc / Fc+

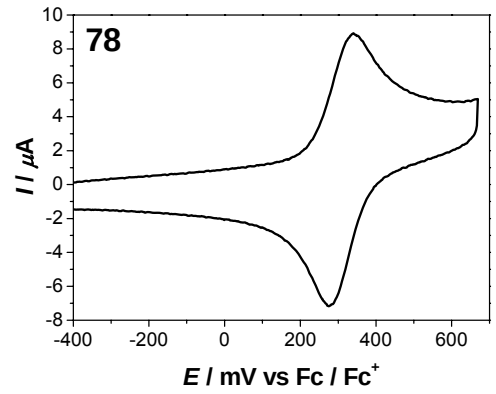
78
I / µA
E / mV vs Fc / Fc+

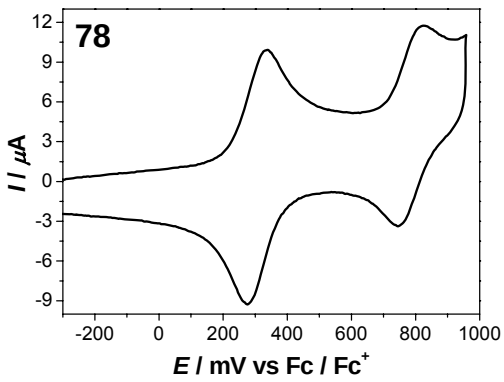
78
I / µA
E / mV vs Fc / Fc+

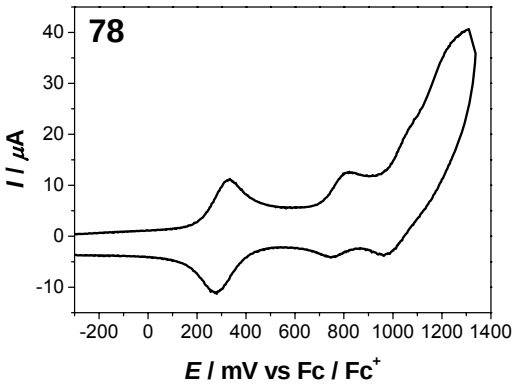
78
I / µA
E / mV vs Fc / Fc+

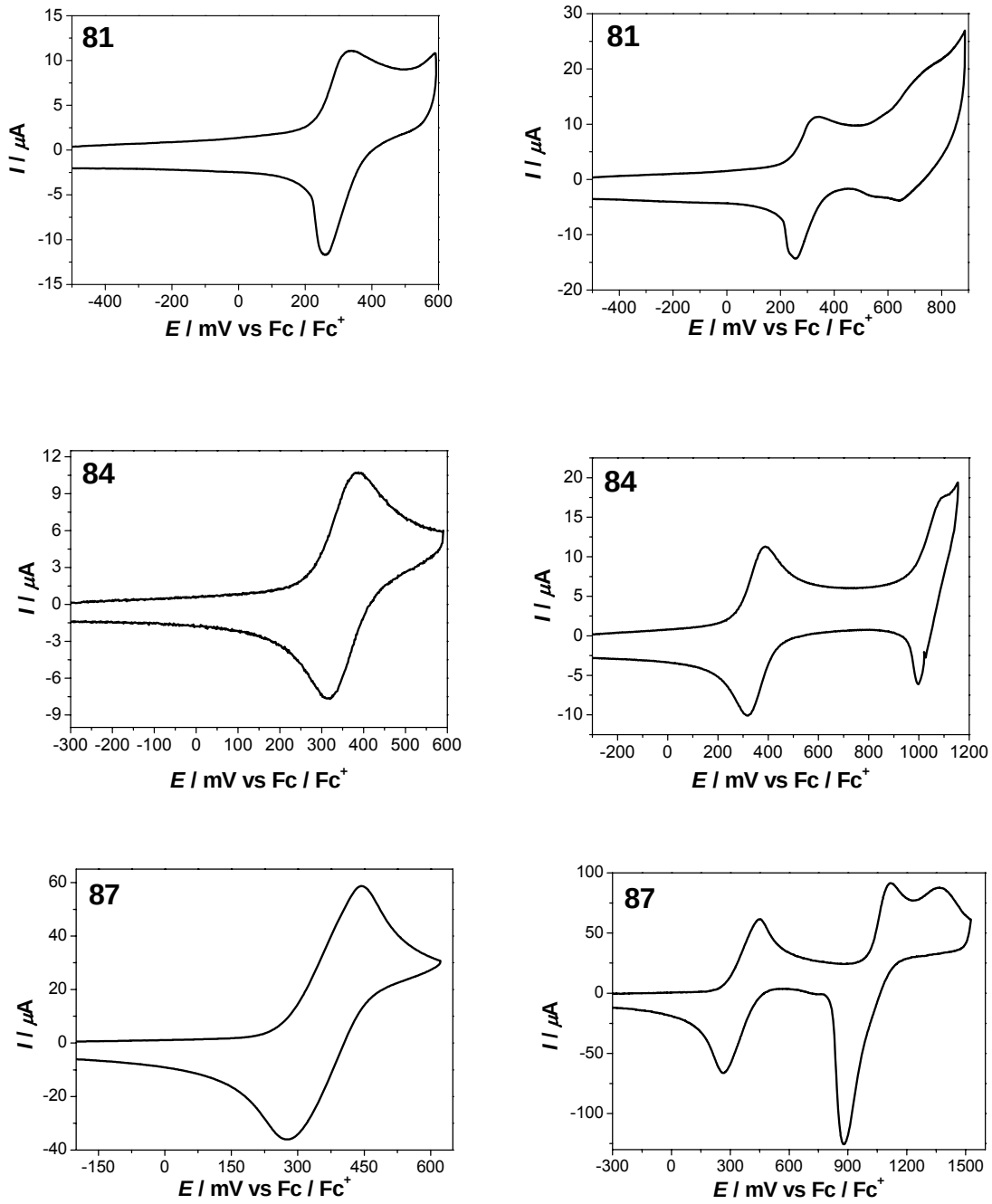

Fig. 8-6 Cyclic voltammograms for the phenothiazine-derivatives **75**, **78**, **84** and **87** with different bridge units in DCM / TBAHFP (0.1 M), scan rate: v = 250 mV/s; working electrode: glassy carbon

8.2.3 UV/vis-Spectroscopy

The UV/vis-spectra of the methoxy- and chloro-substituted triarylamines and phenothiazines with propoxy- and nitrile-substituted bridge units with different chain length are shown in **fig. 8-7** to **8-12**, the values are given in **tab. 8-4**. In all cases within a

homologeous series by increasing the bridge length from n = 0 to n = 3 (e. g. **36**, **46**, **49** and **52**) a slightly bathochromic shift of the wavelength-maxima can be observed. One example should be explained. In case of **36**, **46**, **49** and **52**, the maximum of the absorption band at higher wavelenght shifts from $\tilde{\nu}$ = 27200 cm^{-1} (**36**) to 23800 cm^{-1} by introducing one bridge unit (**46**), to 22900 cm^{-1} (**49**, two bridge-units) and stays nearly constant for **52** with three bridge-units due to the smaller influence of newly introduced bridge units. Even the second band at higher energy shows a bathochromic shift from $\tilde{\nu}$ = 35000 cm^{-1} for **36**, to 31000 cm^{-1} for **46**, over 29200 cm^{-1} for **49**, up to 27100 cm^{-1} for the longest chained chromophore **52**. The reason for this behaviour is due to the increasing π-system which results in a lower excitation energy. The influence is strongest by introducing the first bridge unit.

Tab. 8-4 UV/vis-absorption maxima of unsaturated triarylamine- and phenothiazinethiols with active bridge units in CH_2Cl_2

	λ_1 / nm ($\tilde{\nu}_1$ / cm^{-1})	ε_1 / M^{-1}cm^{-1}	λ_2 / nm ($\tilde{\nu}_2$ / cm^{-1})	ε_2 / M^{-1}cm^{-1}
40	415 (24100)	81800	302 (33100)	52700
46	420 (23800)	37900	323 (31000)	37100
49	436 (22900)	59000	343 (29200)	71700
52	437 (22900)	41000	369 (27100)	53800
56	390 (25600)	54700	312 (32100)	42100
62	414 (24200)	48400	320 (31300)	27100
65	406 (24600)	48800	313 (31900)	42400
68	413 (24200)	40700	352 (24400), (322 (31100))	42000 (42200)
71	409 (24500)	44800	370 (27000), (325 (30800))	56000 (42700)
75	390 (25600)	61000	315 (31700)	57100
78	411 (24300)	69100	318 (31400)	45000
81	415 (24100)	61000	316 (31600)	29100
84	403 (24800)	29300	329 (30400)	40300
87	407 (24600)	36300	327 (30600)	44900

An interesting behaviour is, that by introducing the nitrile-substituted bridge compared to the propoxy-substituted one a stronger bathochromic shift of the absorption of the nitrile-function is observed. As an example the chloro-substituted triarylamine **53**

without bridge unit possesses an absorption maximum at 27800 cm^{-1}, compound **65** with one nitrile-substituted bridge at 24600 cm^{-1} and chromophore **56** with a propoxy-substituted bridge at higher energies (25600 cm^{-1}).

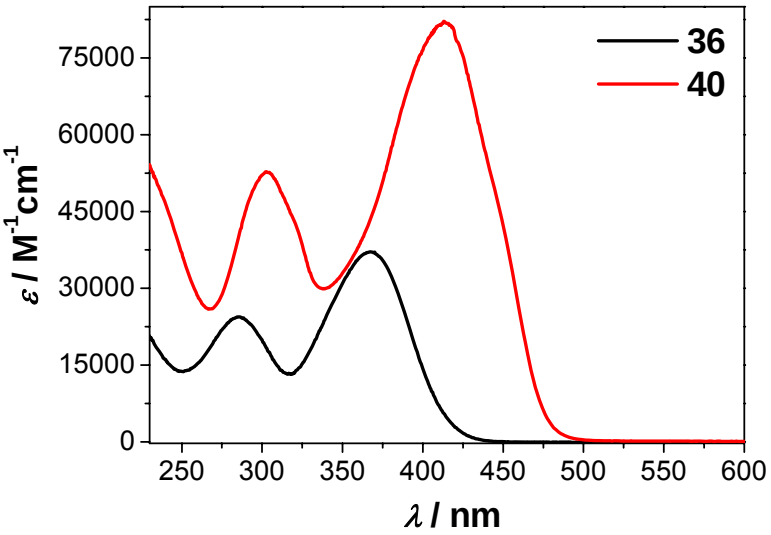

Fig. 8-7 UV/vis-spectra of compounds **36** and **40** in CH_2Cl_2

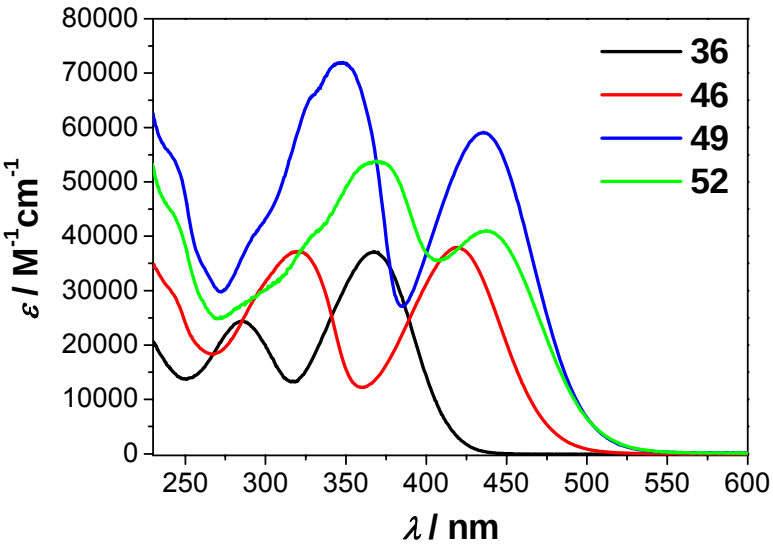

Fig. 8-8 UV/vis-spectra of compounds **36**, **46**, **49** and **52** in CH_2Cl_2

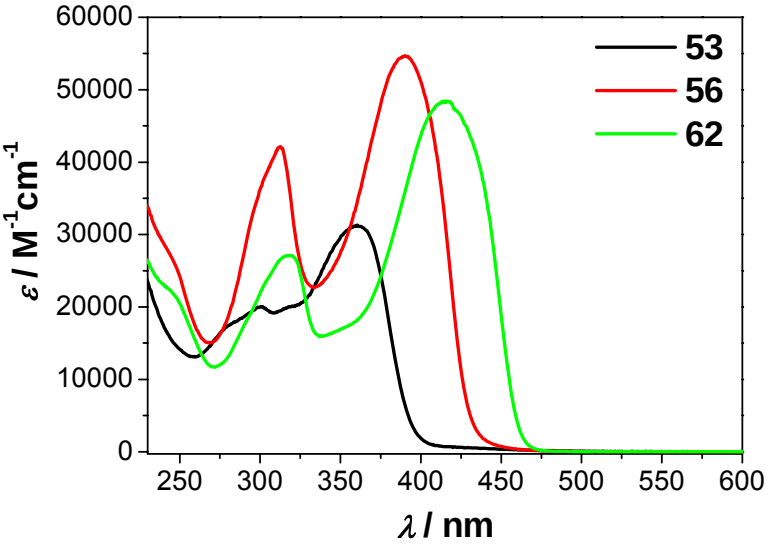

Fig. 8-9 UV/vis-spectra of compounds **53**, **56** and **62** in CH_2Cl_2

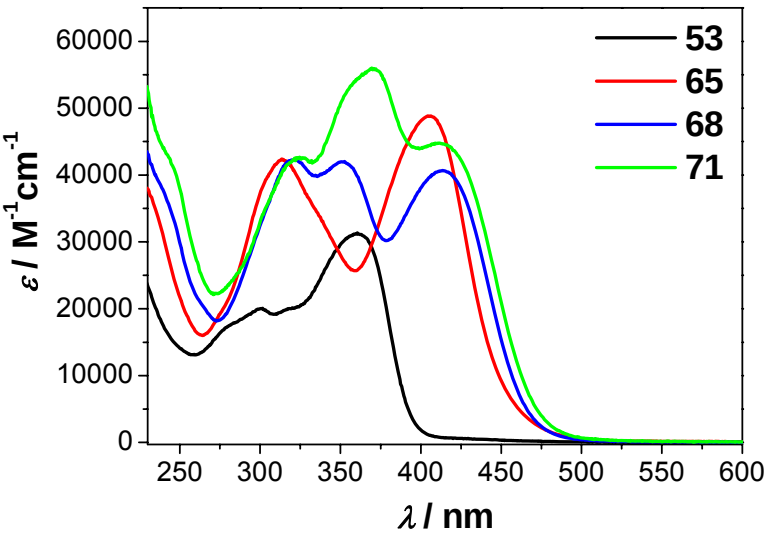

Fig. 8-10 UV/vis-spectra of compounds **53**, **65**, **68** and **71** in CH_2Cl_2

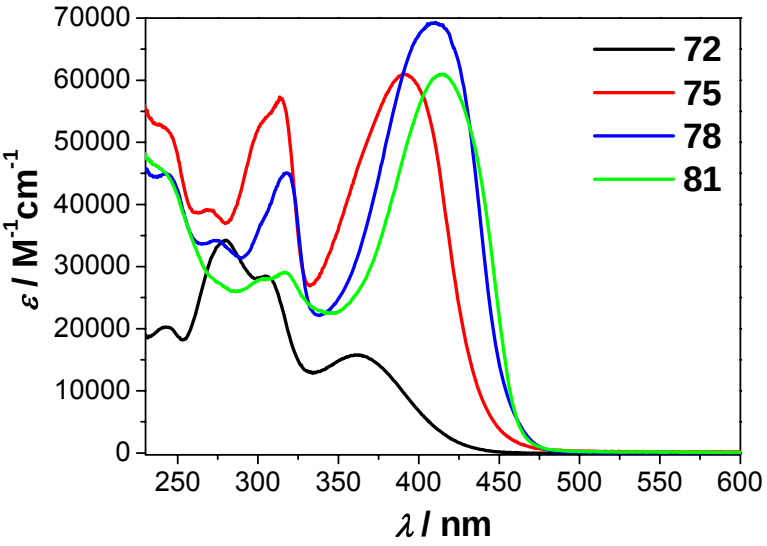

Fig. 8-11 UV/vis-spectra of compounds **72**, **75**, **78** and **81** in CH_2Cl_2

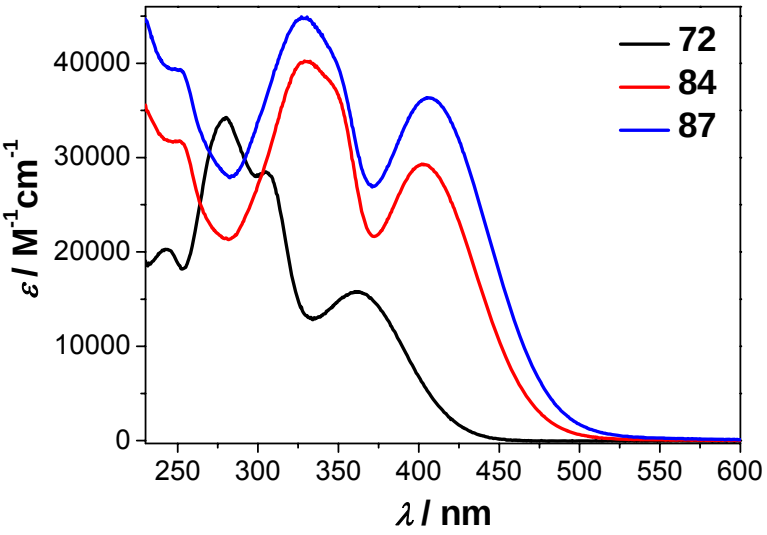

Fig. 8-12 UV/vis-spectra of compounds **72**, **84** and **87** in CH_2Cl_2

8.2.4 Impedance Measurements and Surface Coverage

As explained explained before the dilution of the redox active molecules with redox inactive dummy molecules for measuring the ET rates is very important (for monolayer preparation see chapter 5, 6.1 and 11.1.3; for surface coverage determination see chapter 6.1). The surface coverage and the ratio of the dummy molecules to the chromophores are

given for triarylamine **46** in **tab. 8-5**. Here the density of the chromophore decreases in the monolayer from 4.4 * 10^{-11} mol/cm^2 to 2.5 * 10^{-11} mol/cm^2 by increasing the amount of dummy molecules used for monolayer preparation. The overall concentration was 10^{-3} mol/l. One problem that occurs is that the composition of the solution for preparing mixed monolayers does not reflect the composition of the monolayer itself and that the formation of mixed SAMs strongly depends on the type of the solvent used for the experiments. Even for pure alkanethiol monolayers a prediction concerning the adsorption in different solvents is very difficult [234-236]. Also different dummy molecules to get well ordered monolayers were tested. But as described in literature [171] the use of tolane derivatives instead of alkanethiols does not have any effects on the formation of the monolayer or on the ET measurements.

Tab. 8-5 Surface coverage (Γ) and ratio of dummy to redox active molecules in mixed SAMs of **46**

Γ / mol/cm^2	ratio dummy : redox active molecules
2.5 * 10^{-11}	10 : 1
3.6 * 10^{-11}	7 : 1
4.4 * 10^{-11}	5 : 1

The CVs of the pure monolayers are shown in **fig. 8-13**. Although CVs of the diluted monolayers could be obtained, it was not possible to get reliable measurements from impedance spectroscopy due to the instability of the monolayers and therefore a very low and not evaluatable ratio of $I_{peak}/I_{background}$. An indiaction for the instability of the SAMs is that the current in the CV decreases by measuring several cycles. Even using different dummy molecules like tolane thiols [171] to stabilize and to get well ordered monolayers, was not successful. Changing the ration of tolane thiols to redox active molecules in solution for monolayer preparation yielded monolayers containing just pure tolane thiols because no redox process could be observed in the CVs. Also cyclodextrines which are known to make intercalation compounds with tolane derivatives to get redox active molecules which stand nearly perpendicular to the gold surface and which separate the chromophores to prevent redox processes between these molecules were tested, but no measurable monolayers could be obtained demonstrated by CV experiments. Undiluted monolayers resulted usable values. The peak separation in the CV of **52** is very small indicating that homogeneous, well ordered monolayers are formed [204]. The potential measured is relative to an Ag/AgCl-reference electrode and is not calibrated vs Fc / Fc$^+$.

The ratio of the redox potentials between **49**, **52** and **87** is comparable to the solutions of the same compounds investigated before by cyclic voltammetry. The unsymmetric shape of the CVs of **49** and **87** indicate that some defects, e. g. unordered areas, exist.

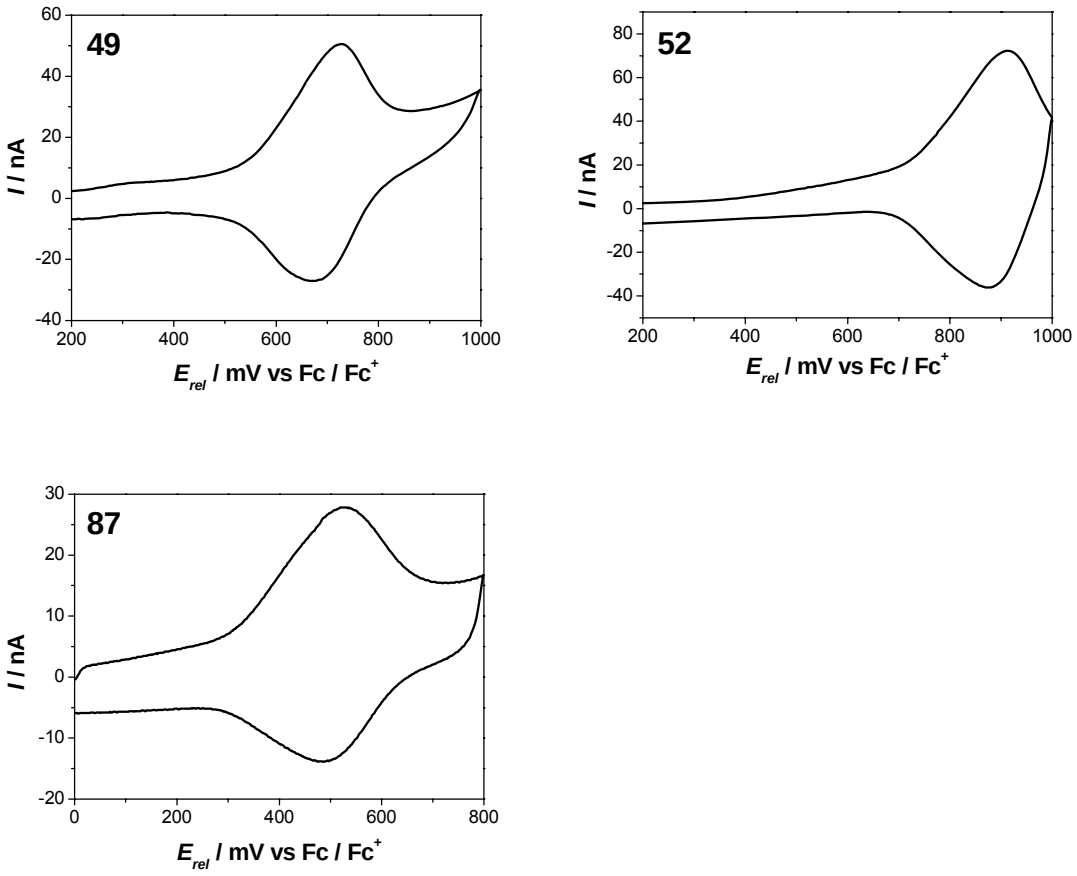

Fig. 8-13 Cyclic voltammograms for **49**, **52** and **87** as SAMs on spherical gold-electrodes. The measurements were carried out in MeCN / TBAHFP (0.2 M), scan rate: 50 mV/s

For only three compounds it was possible to measure the ET rate constants: For the phenothiazine compound **87** with two nitrile-substituted bridge units **(**n = 2**)** an ET rate of $k_{et} = (5.7 \pm 0.8) * 10^4\ s^{-1}$ (**fig. 8-14**, **tab. 8-6**) was measured. For the analogous triarylamine derivative with two nitrile substituted bridge units (**49,** n = 2) an ET rate of $k_{et} = (8.6 \pm 0.9) * 10^4\ s^{-1}$ and for its homologous compound **52** with n = 3 nearly the same rate constant of $k_{et} = (8.7 \pm 2.3) * 10^4\ s^{-1}$ was measured. These values were the average of up to eight independent measurements and were obtained for undiluted SAMs. The reason for using undiluted SAMs was that for diluted SAMs the values of the ET rate strongly depend on the composition of the mixed monolayers (see **fig. 8-16**). The somewhat higher rate constant for the triarylamine species (**49,** n = 2) compared to the phenothiazine derivative (**87,** n = 2) is again due to the higher reorganisation energy of phenothiazine (λ = 0.60 eV

in MeCN) compared to triarylamine-derivatives (about 0.50 eV in MeCN) (see chapter 5). The decreasing I_{peak} / $I_{background}$ ratio at low frequencies observed in the impedance spectra is caused, as observed for the saturated compounds **29**, **32** and **35**, by the instability of the monolayers during the redox process.

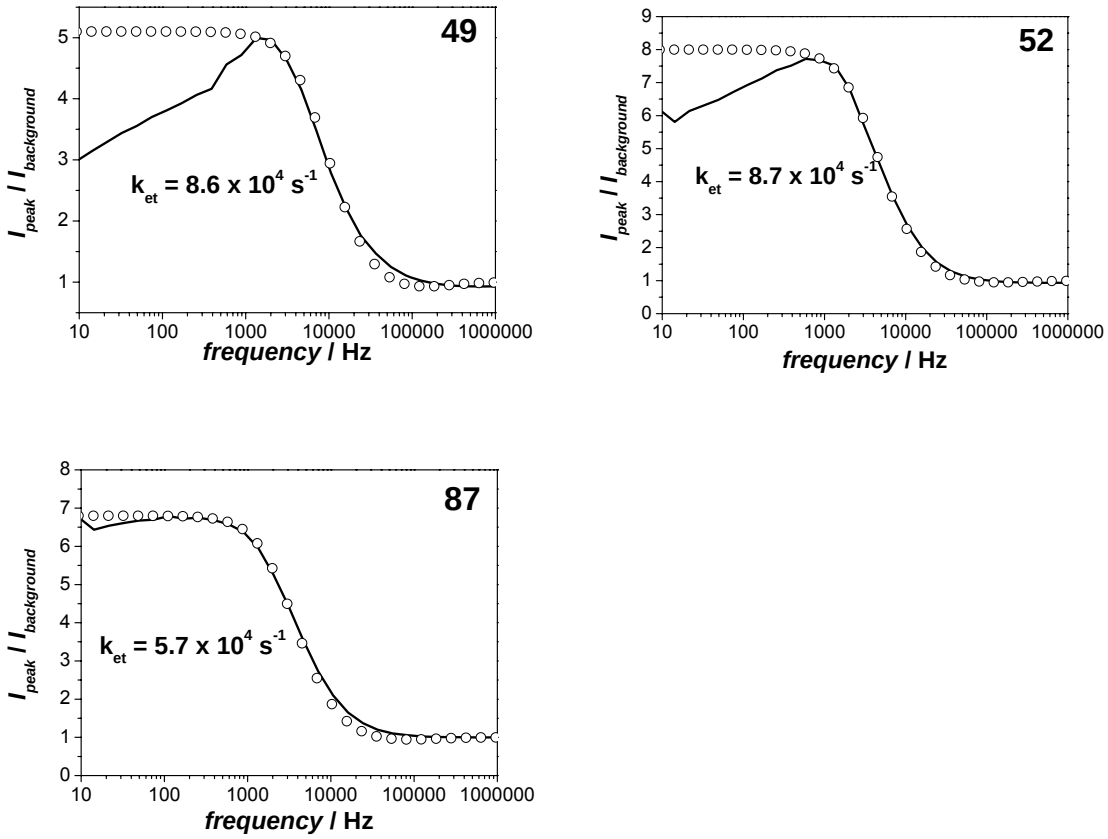

Fig. 8-14 Bode-plot for unsaturated triarylaminethiols **49** and **52** and phenothiazinethiol **87 (n = 2)** with two or three nitrile-substituted bridge units as SAM on a spherical gold-electrode (Bode-plot: —— measured curve, ○○○○ fitted curve).

All other compounds exhibit a rate constant which is too fast to be measurable. One reason is that the maximal rate constant which can be measured with the impedance set-up is limited by the cell constant, e. g. the product of uncompensated resistance R_u and the double layer capacity C_{dl}. If $\frac{1/(C_{dl} \cdot R_u)}{k_{et}}$ is larger than 1000 a reduction of $C_{dl} \cdot R_u$ does not make any difference for fitting the ET rate k_{et} and if $\frac{1/(C_{dl} \cdot R_u)}{k_{et}} < 1$ an enlargement of k_{et} causes no change. Thus for $1 < \frac{1/(C_{dl} \cdot R_u)}{k_{et}} < 1000$ $C_{dl} \cdot R_u$ has to be determined exactly

Tab. 8-6 ET rate (k_{et}), Surface coverage (Γ), electronic coupling factors (V), reorganisation energies (λ), double layer capacitance (C_{dl}), uncompensated resistance (R_u) and surface (A_{real}) for compounds **49**, **52** and **87**

	k_{et} / s^{-1}	Γ / mol/cm^2	V_{ab} / cm^{-1}	λ / eV [215]
49	$(8.6 \pm 0.9) * 10^4$	$(5.2 \pm 0.5) * 10^{-11}$	1.3 ± 0.3	0.51 (MeCN)
52	$(8.7 \pm 2.1) * 10^4$	$(8.7 \pm 0.6) * 10^{-11}$	1.3 ± 0.5	0.51 (MeCN)
87	$(5.7 \pm 0.8) * 10^4$	$(5.9 \pm 0.3) * 10^{-11}$	1.7 ± 0.4	0.60 (MeCN)

	C_{dl} / F	R_u / Ω	A_{real} / cm^2
49	$(4.2 \pm 0.6) * 10^{-8}$	118 ± 17	$(2.2 \pm 0.2) * 10^{-2}$
52	$(3.4 \pm 0.2) * 10^{-8}$	152 ± 32	$(1.8 \pm 0.1) * 10^{-2}$
87	$(3.9 \pm 0.6) * 10^{-8}$	200 ± 20	$(1.0 \pm 0.1) * 10^{-2}$

for a good fit of k_{et}. Even using microelectrodes to limit $C_{dl} \cdot R_u$ does not lead to the expected success. Another factor for these high ET rates are the oxidation potential of the chromophores. Comparison of the redox potentials of isolated triarylamines with two methoxy- or chloro-substituents and the permutations of chloro, methoxy and methyl for the third aryl [216] with the unsaturated triarylaminethiols discussed in this chapter underline this assumption. As for the methoxy- (**36**, **40**, **46**, **49** and **52**) and chloro- (**53**, **56**, **62**, **65**, **68** and **71**) substituted compounds the redox potentials of isolated triarylamines decrease by introducing an electron rich methoxy-substituent (comparable to propoxy-substituents of the bridge units in unsaturated triarylaminethiols **40**, **56**, **62**) instead of a methyl function or increase by using an electron withdrawing chloro-substituent (comparable to nitrile-substituents of the bridge units in unsaturated triarylaminethiols **46**, **49**, **52**, **65**, **68**, **71**) (for oxidation potential values see **tab. 8-3**). Therefore, if the oxidation potential of the terminal redox centre is too high (in **62**: $E_{1/2}^{ox,1}$ = 580 mV) and that of the bridge is too low (in **62**: $E_{1/2}^{ox,2}$ = 710 mV, comparable to alkoxy-substituted *p*-phenylene vinylene oligomers with $E_{1/2}^{ox,1}$ = 730 mV [237]) an oxidation of the bridge instead of the terminal redox centre is possible (**fig. 8-15, A**). Thus, the effective distance from the oxidised centre to the electrode is smaller than from the terminal redox centre to the electrode resulting in an ET rate which is too fast. Another possibility is that the chromophores do not have a perpendicular orientation to the surface but ly flat on the gold (**fig. 8-15**, **B**) or might even built up double layers due to van der Waals interactions and therefore limit the effective distance between the redox centre and the electrode.

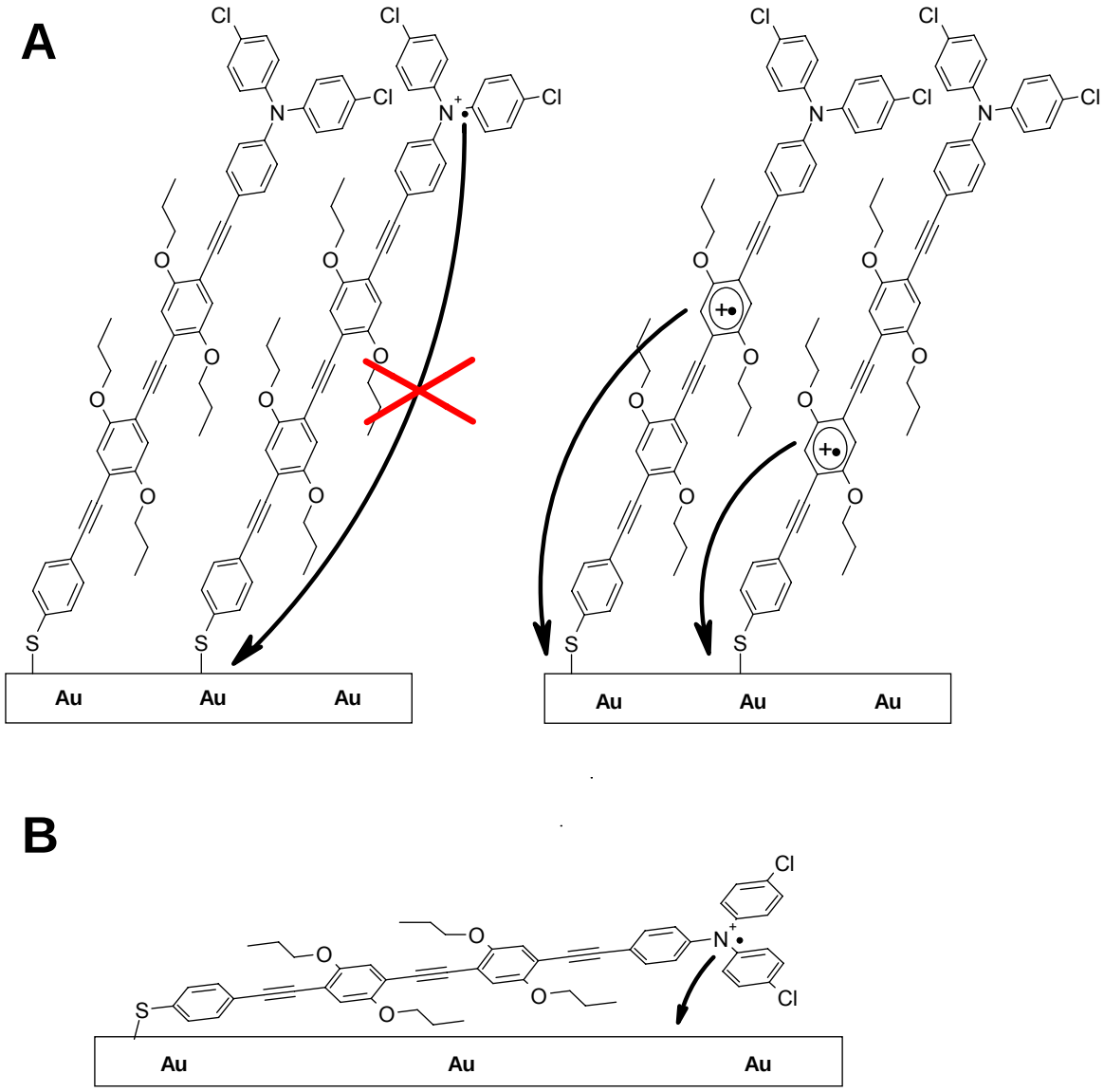

Fig. 8-15 Schematic structures for the explanation for high rate constants

The use of MeCN and *tetra*-butylammonium-*hexa*-fluorophosphate (TBAHFP) as electrolyte also causes problems because of very high uncompensated resistances and double layer capacitances with whichsoever it was not possible to fit the data. The potential window of aqueous solvent electrolytes is not wide enough for the measurement of the triarylamine and phenothiazine derivatives. Even the use of microelectrodes to circumvent these problems was not successful.

A further problem is the dilution of redox active molecules in mixed SAMS and the correlation with the measured ET rates. Although it is possible to control the amount of redox active thiols in mixed monolayers (see **tab. 8-5**), the ET rate and/or the cell constant strongly depends on the concentration of redox centres in the monolayer

(example: **fig. 8-16**). A higher dilution of the redox active component **49** with alkanethiols ($C_{10}H_{23}SH$) leads to higher ET rates (**fig. 8-16**, **A**). The ratio of $I_{Peak}/I_{Background}$ which is obtained from impedance measurements and is proportional to the amount of redox active molecules in mixed monolayers decreases with decreasing surface coverages Γ and rate constants k_{et} (**fig. 8-16**, **B**) indicating that the ET rate strongly depends on the structure of the SAMs.

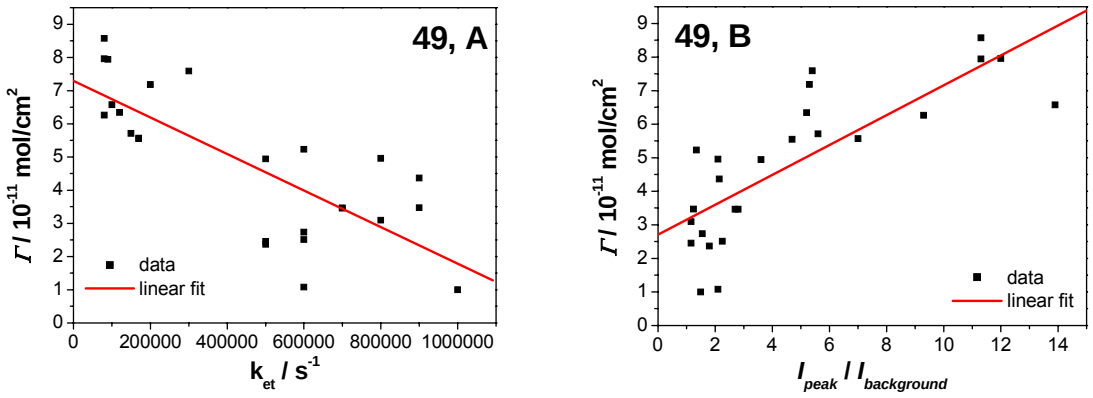

Fig. 8-16 Comparison of ET rates k_{et} and surface coverage Γ of **49** (n = 2) at different dilution with redox inactive alkanethiols. $I_{Peak}/I_{Background}$ represents the surface coverage of the monolayers and is proportional to the amount of redox active molecules in mixed monolayers

8.2.5 QCM-Measurements

To get more information about the pure monolayers of the chromophores and their density on gold surfaces, QCM (quartz crystal microbalance) measurements were carried out.

The QCM-measurements use the circumstance that mass changes on QCM-electrodes influence the oscillation frequency of the quartz crystal. *Sauerbrey* recognised the extremely sensitive nature of this technique and introduced an equation which combines the mass and frequency change and relies on a linear sensitivity factor C_f [238]:

$$\Delta f = -C_f \cdot \Delta m \qquad \textbf{equ. 8-1}$$

In this case Δf is the observed frequency change [Hz], Δm the change in mass per unit area [g/cm^2] and C_f the sensitivity factor for the crystal (56.6 Hzμg^{-1}cm^2 for a 5 MHz AT-cut quartz crystal at room temperature). The measurements can be performed in gas phase or in solution. The *Sauerbrey equation* itself is usable for uniform, rigid, thin-film

deposits [239]. More complex systems, e. g. viscoelastic ones, cannot be explained by the *Sauerbrey equation*. For a more detailed understanding see literature [240].

Before starting the investigation of the triarylamine- and phenothiazine-derivatives, the potential and accuracy of this method was tested using alkanethiol monolayers. **Fig. 8-17** shows the measurements for a $C_8H_{17}SH$ monolayer in gas phase and solution (for experimental setup see chapter 11.1.4).

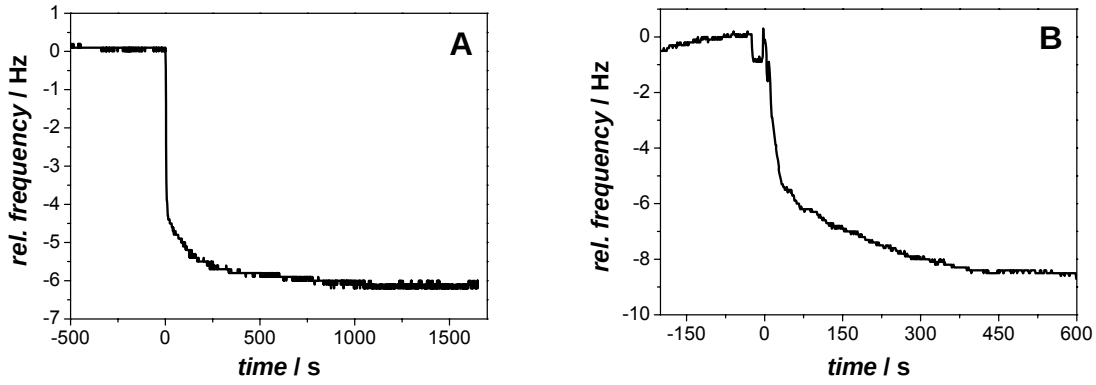

Fig. 8-17 QCM-measurements of a $C_8H_{17}SH$ monolayer in gas phase (**A**) and toluene solution (**B**)

The densitiy of the alkanethiol monolayer prepared from the gas phase is $\Gamma = 7.5 * 10^{-10}$ mol/cm^2 and corresponds very good with the values obtained from other experiments where a value of $\Gamma = 7.8 * 10^{-10}$ mol/cm^2 was obtained (**fig. 8-17**, **A**) [205]. The formation of the monolayer itself is very fast, within 1 min nearly 80% of the densiest packing is achieved, while in the following time the monolayer reaches its maximum packing and the ordering process takes place. The chemisorption rate depends on the concentration of the thiol both in gas phase or in solution and takes longer with decreasing concentration. These information are important if kinetic investigations concerning the ordering process or the formation of the monolayer are accomplished but not for determining the surface coverage itself. Nevertheless, independent of the concentration of the solution for monolayer preparation the same surface coverage (in case of a C_8-alkanethiol ~ 10^{-9} mol/cm^2) is obtained which only depends on the type of thiol. The C_8-alkanethiol in toluene solution shows a different absorption behaviour compared to the gas phase (**fig. 8-17**, **B**). After a rapid chemisorption of the thiol, where the monolayer reaches about 70% of the densiest packing, a long ordering process of the thiol occurs. At the end a packing of $\Gamma = 1.2 * 10^{-9}$ mol/cm^2 is achieved. The slightly higher monolayer density can be explained by either double-layer or solution effects. Aromatic compounds like a rigid tolane derivative (for structure see **tab. 8-7**, first row) have a slightly smaller packing of $\Gamma = 5.6 * 10^{-10}$ mol/cm^2

compared to alkane derivatives on account of the larger volume obtained by the aromatic system. The experimental determined value of Γ = 5.6 * 10^{-10} mol/cm^2 is in good agreement with surface coverages of the same compound calculated from AFM-measurements (Γ = 7.5 * 10^{-10} mol/cm^2) [241, 242] or from AM1-optimised structures (Γ = 6.9 * 10^{-10} mol/cm^2).

The measurements of the chromophores depicted in **tab. 8-7** were performed in toluene solution without stirring to prevent as litle perturbation to the quartz crystal as possible (for detailed experimental setup see chapter 11.1.4). The triarylaminealkanethiol **32** has a smaller surface coverage of Γ = 2.1 * 10^{-10} mol/cm^2 than the C_8-alkane thiol monolayers discussed before due to the large end group. The surface coverages for the unsaturated chromophores **49** and **87** (**fig. 8-18**) obtained by QCM measurements are larger than the values calculated from the CVs of spherical gold ball electrodes during impedance spectroscopy.

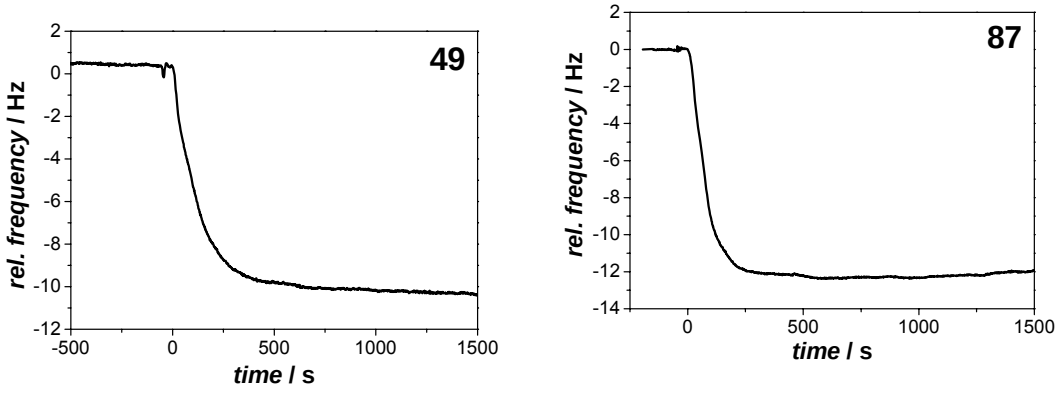

Fig. 8-18 QCM-measurements of pure monolayers of **49** and **87** in toluene solution

A problem is the instability of the monolayers in the oxidation and reduction process during cylic voltammetry and therefore in obtaining wrong surface coverages from the measured currents. For the chromophores **36**, **37**, **53** and **72** the surface coverage is in the range from Γ = 8.3 * 10^{-10} mol/cm^2 for **72** with the largest head group up to Γ = 2.8 * 10^{-9} mol/cm^2 for **53** (**tab. 8-7**). For chromophores with one bridge unit the surface coverage values decrease slightly from the chloro-substituted triarylamines **56** and **65** (surface coverage $\Gamma \sim$ 1.1 * 10^{-9} mol/cm^2), over the phenothiazine derivatives **75** and **84** (Γ = 4.5 * 10^{-10} mol/cm^2), to the methoxy-substituted triarylamine **40** (Γ = 1.9 * 10^{-10} mol/cm^2). Even here the chloro-substituted triarylamines **56** and **65** have the highest surface coverage from up to Γ = 1.2 * 10^{-9} mol/cm^2 down. Calculations depending on the surface coverage of the SAMs discussed here, using AM1-optimised structures and a

Tab. 8-7 Surface coverage values (Γ) determinde via QCM measurements and calculated values from from AF1-optimised structures for redox active thiols with unsaturated bridge units in [mol/cm^2]; calculated

Number of bridge units	n = 0	n = 1	n = 2
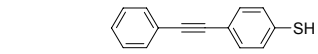	$5.6 * 10^{-10}$ ($6.9 * 10^{-10}$)		
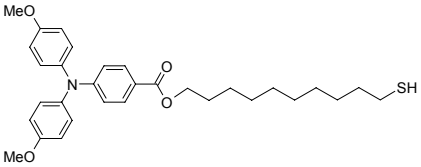	**32**: $2.1 * 10^{-10}$ ($2.0 * 10^{-10}$)		
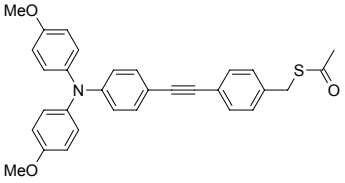	**37**: $9 * 10^{-10}$ ($2.9 * 10^{-10}$)		
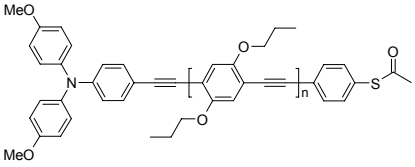	**36**: $1.2 * 10^{-9}$ ($2.4 * 10^{-10}$)	**40**: $1.9 * 10^{-10}$ ($1.3 * 10^{-10}$)	
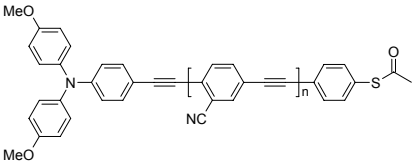		**46**: $4.8 * 10^{-10}$ ($2.5 * 10^{-10}$)	**49**: $2.8 * 10^{-10}$ ($1.7 * 10^{-10}$)
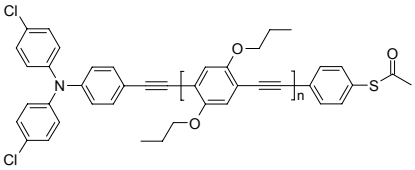	**53**: $2.8 * 10^{-9}$ ($2.8 * 10^{-10}$)	**56**: $1.1 * 10^{-9}$ ($1.3 * 10^{-10}$)	
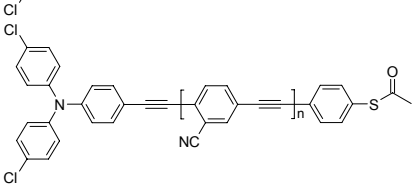		**65**: $1.2 * 10^{-9}$ ($2.0 * 10^{-10}$)	**68**: $3.3 * 10^{-9}$ ($1.9 * 10^{-10}$)
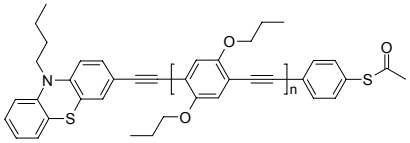	**72**: $8.3 * 10^{-10}$ ($2.3 * 10^{-10}$)	**75**: $4.5 * 10^{-10}$ ($1.3 * 10^{-10}$)	**78**: $7.3 * 10^{-10}$ ($1.7 * 10^{-10}$)
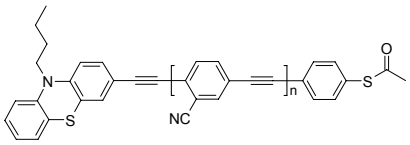		**84**: $4.5 * 10^{-10}$ ($2.4 * 10^{-10}$)	**87**: $3.2 * 10^{-10}$ ($2.6 * 10^{-10}$)

hexagonal arrangement for the SAMs on the surface show that the values are all in the region of $\Gamma = 1.3 * 10^{-10}$ mol/cm^2 for **40** to $\Gamma = 1.3 * 10^{-10}$ mol/cm^2 for **37**. These values are in contrast to the surface coverage e. g. of **36** (cal.: $\Gamma = 2.4 * 10^{-10}$ mol/cm^2) where the QCM measurements give a value which is five times larger ($\Gamma = 1.2 * 10^{-9}$ mol/cm^2). The influence of the redox centres or on the substituted bridge units in calculated structures on

the density of the surface is very small. One problem is that no investigations on the surface structures of triarylamine and phenothiazine SAMs using AFM or STM techniques were made until now and therefore no reliable values concerning the lattice of the monolayers could be achieved.

In conclusion the values do not show a clear direction, but the surface coverage itself depends more or less on the type of the redox centre and the space which is engaged by the end group and not on the propoxy- or nitrile-substituted spacer itself. The phenothiazine derivative **72** has the lowest surface coverage due to this effect, followed by the methoxy-substituted triarylamine **36** and the chloro-substituted chromophore **53**.

8.3 Discussion

A series of "molecular wires" consisting of methoxy- or chloro-substituted triarylamines and phenothiazines with different bridge units and bridge length between the redox centre and the anchor thiol function have been prepared in order to investigate their ET-behaviour.

Cyclic voltammetry and UV/vis-spectroscopy show that the oxidation potential and the energetic states could be controlled very well by the different redox centres and bridge units. The methoxy-substituted triarylamines **36** and **37** have the lowest oxidation potential, followed by the phenothiazine **72** and the chloro-substituted triarylamine **53**. To control the ET behaviour propoxy- or nitrile-substituted bridge units were investigated. An extension of the bridge length itself without substituents does not influence the oxidation potentials of the redox centres. In contrast introducing the electron rich propoxy-substituted bridge unit **23** and the electron withdrawing nitrile-substituted bridge unit **26** the oxidation potentials of the redox centres decreased. Here the influence of the propoxy groups was more remarkable resulting in a higher decrease of the oxidation potentials by introducing the first bridge unit than compared to the nitrile functions. Due to this behaviour it is possible to control the HOMO-LUMO-energies of the chromophores by using different substituted bridge units.

These observations are underlined by UV/vis-spectroscopy. The bathochromic shift of the absorption band of the triarylamine-function within a homologeous row (e. g. **36** (n = 0) > **46** (n = 1) > **49** (n = 2) > **52** (n = 3)**)** by raising the number of bridge units *n* can be explained by the increasing π-system, and therefore a reduction of the HOMO-LUMO-

energy difference of the transitions in the triarylamine or phenothiazine and the bridge units. This results in a lower excitation energy. Interesting is that this shift is larger for the nitrile-substituted bridge units with the same redox centre (e. g. **53** > **65** > **68** > **71**). These observations combined with the results obtained from cyclic voltammetry lead to the conclusion that the HOMO-LUMO-energies of the bridge units and the redox centres can be controlled.

As described for the saturated ferrocene- (chapter 6), phenothiazine- (chapter 7) and triarylaminealkanethiols (chapter 7) controlling the density of the redox active molecules within the mixed monolayers for measuring the ET rates is very important. In contrast to ferrocene compounds with phenylene and acetylene bridge units the ratio of dummy to redox active molecules for the preparation of the mixed monolayers was completely different. The ratio of the redox active molecules had to be increased up to 1 : 1 or more to get monolayers with redox active molecules. This is in contrast to the low concentration of the chromophores used for ferrocenethiol monolayers where the ratio of the redox active compound to the coadsorbate was up to 200 : 1 [203, 206, 210]. One reason for this behaviour is the use of different solvents for monolayer preparation. For ferrocenes, ethanolic solutions were used, where the solubility of the ferrocene is very low compared to the alkanethiols and therefore the affinity to gold rather high. Low concentrations of the chromophores compared to the coadsorbates had to be used to get sufficiently diluted monolayers. In case of the phenothiazine- or triarylamine-derivatives CH_2Cl_2 had to be used as solvent due to the very low solubility in ethanol. Because of this reasons for porphyrins investigated by *Lindsey et al.* a mixture of CH_2Cl_2 and ethanol was used [106, 173, 174]. The first possibility is that the solubility of the chromophores in CH_2Cl_2 is very high compared to ethanolic solutions and the affinity of the chromophores to adsorbate on gold might be smaller. Therefore higher concentrations of the redox active molecules compared to the dummy molecules had to be used. Secondly it is possible that these molecules built ordered stabile structures in solution. Thirdly the *van der Waals* interactions within the alkanethiols are stronger than between the chromophores and the coadsorbates so that high concentrations of the chromophore thiols yield measurable monolayers. Finally the density of the mixed monolayers itself could be controlled by using different concentrated solutions depending on the chromophore and the coadsorbate.

The surface coverage of pure monolayers were investigated by QCM-experiments. Compared to the density of pure alkanethiols ($7.8 * 10^{-10}$ mol/cm^2) the unsaturated triarylamine- (**36**, **37**, **53**) and phenothiazinethiols (**72**) are more densily packed. This

packing decreases slightly by introducing the bridge units. The phenothiazine derivatives have the lowest surface coverage in comparison with the homologous triarylamines due to the large end group and the space taken from it. The bridge units itself do not influence the packing density, it is mainly controlled by the redox centres. The higher surface coverage compared to the alkanethiols can be explained by compact packing due to stronger π-π-interactions between the redox centres and the bridge units of the chromophores or by the building of e. g. double layers. Comparable porphyrin monolayers on gold have a lower surface coverage at about 10^{-11} to 10^{-12} mol/cm^2 depending on the preparation time and the concentration of the solution used for the monolayers [106, 173, 174]. Here the low packing density is explained by the bulky nonpolar peripheral substituents on the porphyrin which even isolate the molecules electrically from each other. More information could be obtained by further examinations of the surface e. g. IRRAS- (infrared reflection absorption spectroscopy) experiments which are in progress at the moment.

The investigation of the ET rates of the above mentioned unsaturated triarylamine- and phenothiazinethiols was limited by the fast ET rates measured for these compounds. For the triarylamine- **49** and **52** and phenothiazinethiols **87** with nitrile-substituted bridge units reliable ET rates could be obtained. The ET rates are comparable with unsaturated ferrocenethiols with acetylene units as spacers [171, 210]. *Creager et al.* found for these ferrocene derivatives with two phenylacetylene bridge units that the ET rates were much faster, up to k_{et} = 5.0 * 10^5 s^{-1} [210]. But by using the ILIT-(indirect laser-induced temperature jump) technique to investigate the ET rates nearly the same value of about k_{et} = 6.4 * 10^4 s^{-1} was found [171]. On the other hand porphyrins show much slower ET rates [106, 173, 174].

In case of the propoxy-substituted triarylamine and phenothiazine chromophores the ET is limited by the uncompensated resistance (R_u) and the double layer capacitance (C_{dl}) and therefore a good fit could not be obtained. Several explanations exist for this behaviour. One is that the fast ET rates might be caused by an oxidation of the bridge unit itself due to their relatively high oxidation potential compared to the redox centre resulting in shortening of the bridge and higher ET rates. A second possibility is that the chromophores lie flat on the surface and here the distance between the redox centre and the electrode is shortened which results in higher ET rates at the end. Observations concerning the dilution of pure monolayers with dummy molecules and their effect on the ET rate underpin this fact. In pure monolayers the measured ET rates are low while they rise by increasing the dilution of the redox active chromophore with coadsorbates. The adsorption

geometry can change with coverage with the chromophores tilting to a more upright orientation as the surface becomes more crowded. Comparable observations depending on the influence of the dilution and of the adsorption geometry of the chromophores on the ET rates were made by *Lindsey et al.* in porphyrinthiol monolayers where the surface coverage was changed [106, 173-176]. Furthermore as theoretical predicted [193] and demonstrated in practice by *Ratner* and *Wasielewski et al.* using donor-acceptor substituted OPVs regimes exist wherein the distance dependence of the ET is very weak and the bridge molecules act as molecular wires [172] resulting in very high ET rates. Although the maximal distance between the redox centre and the electrode of 37 Å (e. g. for **52**) is in the range of the maximum distance of 40 Å in the OPVs where the molecular wire behaviour was observed, the triarylamine- or phenothiazine-moieties with acetylene spacers do not act as such molecular wires with very high ET rates. Another aspect is the conformational variability of the bridge and the resulting influence on the ET. *Creager et al.* investigated oligophenyleneethynelene (OPV) bridged ferrocenethiols by changing the conformation of the bridge using different substituted phenylene units [171]. For example in case of a ferrocene with three phenyleneethynelene units, the ET rate varied from $k_{et} = (6.4 \pm 0.4) * 10^4\ s^{-1}$ for unsubstituted bridge units up to $k_{et} = (2.3 \pm 0.2) * 10^6\ s^{-1}$ where one bridge unit is substituted by a methylene group [171]. Molecular orbital calculations showed that torsional variants of homologous OPE spacers have a great influence on V_{AB} and the β values and therefore on the ET rate itself. For the triarylamine and phenothiazine chromophores such a conformational influence on the ET rate is conceivable due to the space which is occupied by the propoxy- and nitrile-substituents of the bridge units. Because of the high ET rates observed for these compounds, they seem to be fully conjugated and all π-planes of the phenylene units should be nearly conincident. But no calculations on the structure of these molecules have been done until now to underline this assumption.

In addition the HOMO-LUMO-gap of the chromophores have a direct influence on the ET. The ET event can be seen as a movement of an electron from the LUMO of the donor to the LUMO of the acceptor (or the electrode) via the LUMO of the bridge. In general extending the bridge length in conjugated systems leads to a decrease in the HOMO-LUMO-gap [172]. Even the substituents on the bridge itself or the different redox centres influence the HOMO-LUMO-energies [243, 244]. By introducing NO_2- [243] or methoxy-groups [244] as substituents at the bridge, the LUMO-energies decrease and can be tuned by using different numbers of these substituents. *Wasielewski* and *Ratner et al.* found

that a normal superexchange mechanism takes place if the energy gap between the donor and bridge LUMOs is large enough [172]. In case of the highly substituted bridges of the triarylamine and phenothiazine chromophores in this work the HOMO-LUMO-gap gets smaller by increasing the bridge lenght and as depicted before the differences in the LUMO energies of the donor, bridge and electrode can be tuned by using propoxy- and nitrile-substituents and different redox centres. Due to this combination different HOMO-LUMO-energies of the molecules are received which might lead to different ET mechanisms. An indication for this predication is that for the nitrile-substituted compounds **49**, **52** and **87** ET rates were obtained, while for the propoxy-substituted ones no values could be measured.

In case of the nitrile-substituted thiols, the oxidation potential of the bridge units was high enough that the redox centres were oxidised and reliable ET rates could be measured. The fact that compound **49** shows almost the same rate constant independent of the length (n = 2 or n = 3) may indicate that a hopping process is operating for which a much weaker length dependence is expected than in the case of a superexchange.

Since there is practically no chance to extend the speed of the method for ET rates beyond approx. 10^5 s^{-1}, also using spectroelectrochemical methods or fast scan cyclic voltammetry did not lead to any succes due to the instability of the redox active monolayers, future work will be directed to the synthesis of analogous saturated compounds which will inherently show slower rate constants.

9 Bistriarylamine and Bisphenothiazine Chromophores – Robin/Day Class II Systems

9.1 Introduction

Electron transfer processes play an important role in biology and chemistry [188, 245, 246]. They take part in a lot of fundamental metabolic reactions like photosynthesis or respiration [247-251]. In natural photosynthetic systems the ET transport happens within reaction centres along a cascade of different redox centres. To mimic and investigate these ET processes a large number of different model compounds have been synthesised like basic donor-acceptor-molecules [252-261] up to supramolecular structures [262-270].

Another huge group are inorganic compounds [164, 271-276] including mixed valenced systems, which have been investigated regarding to their thermal or optical excitation behaviour. These derivatives normally show a characteristic IV-CT- (intervalence-charge-transfer) band which is attributed to the transition of an electron between the metal centres. However due to the weak absorption of these transitions and the overlap with other metal-ligand-charge-transfer-transitions (ML-CT or LM-CT) the analysis of these compounds is limited. Therefore the interest changed to organic molecules like bishydrazines [277-285], triarylamines [286-294], bis- and tris(perchlorotriphenylmethyl)radicals [295-298] and other derivatives [197, 299-302] within the last decade.

Especially triarylamines are in growing focus due to their broad application possibilities, e. g. as hole transportation layer in organic light-emitting diods (OLEDs) [303-312], in polymer batteries [313, 314], as photorefractive material for optical data storage [315-317] or as electrochromic windows [318, 319]. They are even successfully used for electrophotographic applications in photocopiers and laser printers [303-305, 320-325].

9.2 Marcus-Hush-Theory

One-dimensional IV-CT-compounds with two equivalent redox centres possess two degenerate ground states. Following *Marcus*, the potential energy of both diabatic states can be described by two parabolic potential energy surface (PES) [164, 272]. If the electronic interaction V_{AB} of these two diabatic ground states is larger than $V_{AB} >> k_B T$, two adiabatic states result, the ground and the excited state (**scheme 9-1**) [188]. Hereby the coupling of the nodal point of the diabatic PES is twice the magnitude of the coupling matrix element V_{AB}.

Knowing V_{AB} the adiabatic PES is obtained as energy eigenvalues E by solving the following secular equation, where the matrix elements V_{AA} and V_{BB}, which describe the energy of the compound in the diabatic ground state A and B, are approached by parabolic potentials:

$$\begin{vmatrix} V_{AA} - E & V_{AB} \\ V_{AB} & V_{BB} - E \end{vmatrix} = 0 \qquad \textbf{equ. 9-1}$$

with $V_{AA} = \langle \Psi_A | H | \Psi_A \rangle$, $V_{BB} = \langle \Psi_B | H | \Psi_B \rangle$ and $V_{AB} = \langle \Psi_A | H | \Psi_B \rangle$

To solve the problem in **equ. 9-1** *N. S. Hush* used equations which combine the adiabatic thermal and the optically induced ET (IV-CT). The coupling matrix element V_{AB} can be calculated using spectroscopic values (**equ. 9-2**) [165-167, 271, 326-330].

$$V_{AB} = \frac{\mu_{eg}}{er} \tilde{\nu}_{max} = \frac{0.09584}{er} \sqrt{\int \varepsilon(\tilde{\nu}) d\tilde{\nu} \cdot \tilde{\nu}_{max}} \qquad \textbf{equ. 9-2}$$

where μ_{eg} is the transition moment between the adiabatic ground and excited state, r the effective distance of the charge transfer, $\tilde{\nu}_{max}$ the energy for the optical transition and $\int \varepsilon(\tilde{\nu}) d\tilde{\nu}$ the integrated absorption band.

The effective distance of the charge transfer can either be calculted by using quantumchemical methods [330] or by estimating the direct distance between the redox centres. In the scope of the *Generalized Mulliken-Hush-Theory* [166-168] the diabatic dipole moment change er in **equ. 9-2** leads back to adiabatic magnitudes:

$$er \approx \Delta\mu_{AB} = \sqrt{\Delta\mu_{eg}^2 + 4\mu_{eg}^2} \qquad \textbf{equ. 9-3}$$

where $\Delta\mu_{eg}$ is the adiabatic dipole moment change.

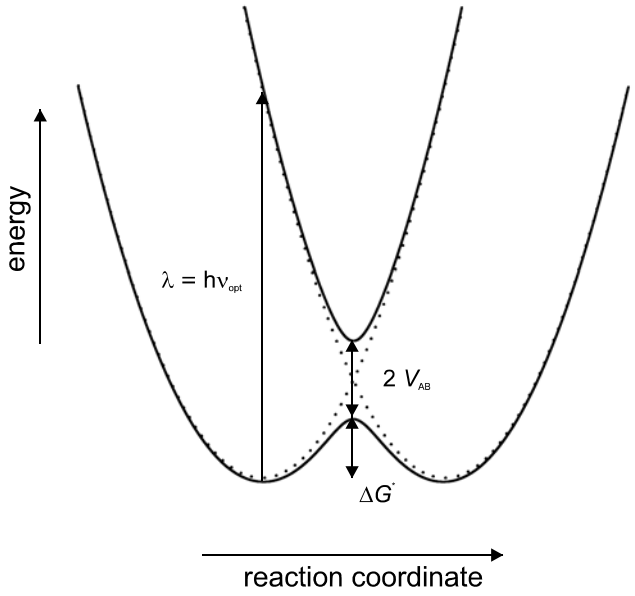

Scheme 9-1 Description of a symmetric mixed valence system according to *Mulliken* and *Hush* (line: adiabatic potentials, dotted line: diabatic potentials)

Depending on the magnitude of coupling the mixed valence compounds can be divided into three classes according to *Robin* and *Day* (**scheme 9-2**) [331, 332]. In class I systems the interaction of the redox centres is very small. Therefore, the redox centres can be considered as isolated systems. No coupling of the diabatic states appear, the thermal ET is forbidden and no IV-CT-band can be observed. However, an ET caused by tunnelling effects is possible.

In class III compounds the interaction of the redox centres is so strong that the characteristics of the system cannot be described by isolated states anymore, but have to be described by a new delocalised unit.

In compounds of Robin/Day class II an IV-CT transition can be observed. The coupling matrix element is large enough to provide a double minimum potential of the adiabatic PES of the ground state. Using two identical redox centre the maxima are degenerated. The IV-CT transition of compounds of Robin/Day class II between both degenerated ground states can be induced thermally or optically. A thermal ET takes place from the ground state PES over a transition state, if the coupling of the diabatic conditions are large enough ($V_{AB} >> k_bT$). Therefore tunnelling processes can be neglected. For this process the free energy of activation can be calculated by **equ. 9-4** [272, 333]:

$$\Delta G^{*} = \frac{\lambda}{4} - V_{AB} + \frac{V_{AB}^2}{\lambda} \qquad \textbf{equ. 9-4}$$

In the case of an optical ET a *Franck-Condon* transition is induced. By assuming a parabolic diabatic PES the sum of the inner and outer reorganisation energy by *Marcus* accords to the energy of the optical transition $\tilde{\nu}_{opt}$: $\tilde{\nu}_{opt} = \lambda$, $\lambda = \lambda_S + \lambda_V$.

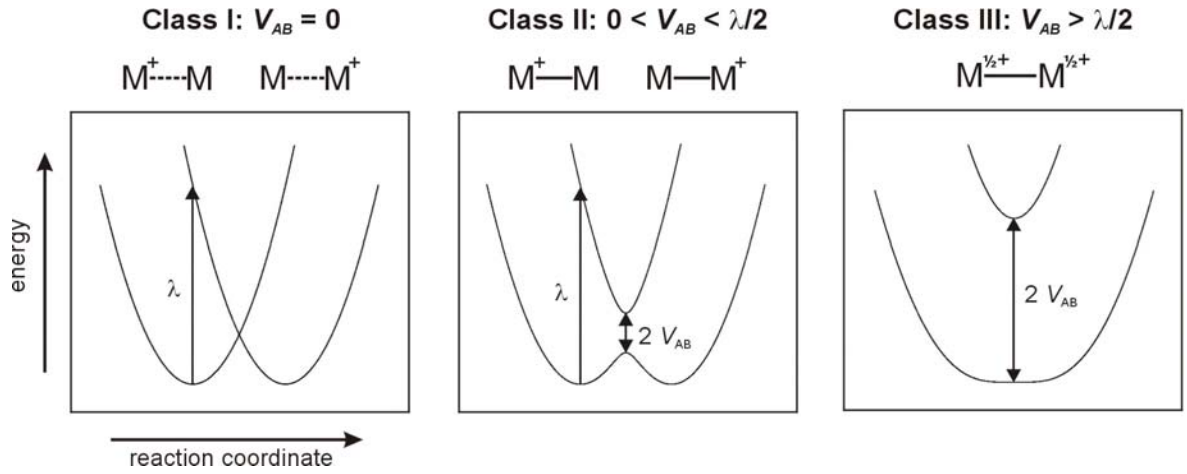

Scheme 9-2 Classification of the interaction of a one dimensional molecule with two redox centres M according to *Robin* and *Day*

The rate constant of the thermal ET in case of an adiabatic behaviour can be calculated by **equ. 9-5** [272]:

$$k_{et} = \nu_n \kappa e^{-\frac{\Delta G^*}{RT}} \qquad \textbf{equ. 9-5}$$

with ν_n as the effective nucleus frequency.

The value of the adiabatic factor κ is unity for a large coupling or can be calculated [164].

For the determination of the rate constant k_{et} it is important that enough higher vibrational modes are occupied. This precondition is fulfilled above a typical temperature ($2k_B T >> h\nu_n$) (high temperature limit, HTL). The effective nucleus frequency ν_n can be calculated using **equ. 9-6** to **9-8** [165]:

$$\tilde{\nu}_{\frac{1}{2}}(\mathrm{HTL}) = \sqrt{16 \ln 2 \cdot k_B T \cdot \lambda} \qquad \textbf{equ. 9-6}$$

$$\tilde{\nu}_{\frac{1}{2}} = g(\nu_n, T)\tilde{\nu}_{\frac{1}{2}}(\mathrm{HTL}) \qquad \textbf{equ. 9-7}$$

$$g(\nu_n, T) = \sqrt{\frac{h\nu_n}{2k_B T} \coth\left(\frac{h\nu_n}{2k_B T}\right)} \qquad \textbf{equ. 9-8}$$

where $\tilde{\nu}_{\frac{1}{2}}(\mathrm{HTL})$ is the theoretic band width at half hight of the IV-CT-absorption band at the HTL and $\tilde{\nu}_{\frac{1}{2}}$ the experimental band width at half hight of the IV-CT-band. The use of **equ. 9-8** is problematic as for compounds with the same effective nucleus frequencies different values for $g(\nu_n, T)$ can be found [282]. In the case of two degenerated redox centres λ can be replace by $\tilde{\nu}_{\max}$.

In principal by using the discussed model and with the assumption of a *Boltzmann*-distribution of the ground state energy level in systems with low coupling, *Gaussian*-like IV-CT-absorption bands are expected [274, 334, 335]. By an increasing coupling V_{AB} (transition from class II to class III) strong unsymmetric and very small IV-CT-bands can be observed with a off-peak decay at the lower energetic site of the absorption band (**scheme 9-3**) [275, 287]. An explanation can be found in the classical *Mulliken-Hush-theory* because in this case the energy of the transition with the smallest excitation energy is 2 V_{AB}. In theory a *Gaussian*-like absorption band is expected which is truncated at 2 V_{AB} [274, 275, 287, 335]. Nevertheless the absorption bands consist of an overlay of different Gaussian-like bands of the according vibration levels. Therefore the decay at 2 V_{AB} is continous and unsymmetric absorption bands are observed.

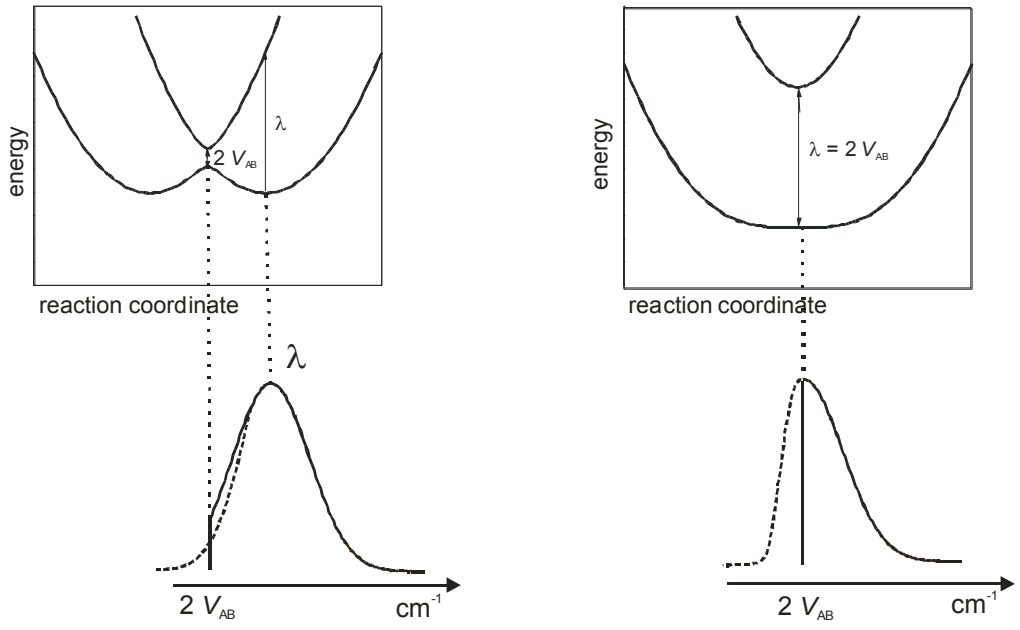

Scheme 9-3 Energy diagram for the adiabatic PES and the resulting absorption spectra for a compound of Robin/Day-class II (left) and for the border case between class II and III (right)

9.3 Homocoupled Bistriarylamine- and Bisphenothiazinediyns

A series of homocoupled bistriarylamine- (**88**, **89**) and bisphenothiazine-derivatives (**90**, **91**, **92**) were investigated according the ET behaviour in these organic mixed-valence systems (**fig. 9-1**). The chromophores have been obtained as side products during *Hagihara*-coupling reactions of the triarylamine or phenothiazine chromophores with anchor-functions **17** and **18** or bridge units **23** and **26** (see chapter 8.2.1). The slow reaction rate of the Pd-catalysed aryl-C-coupling and a side reaction, the Glaser-coupling reaction [336], are reasons for the obtained diynes. It is known that electron rich compounds have slower reaction times in Pd-catalysed reactions than comparable derivatives with electron withdrawing groups. This conclusion is reflected in our results because here the amount of the side product increases by using the propoxy-substituted electron rich bridge unit **23**, while faster reaction times and less or no homocoupled product could be observed by using

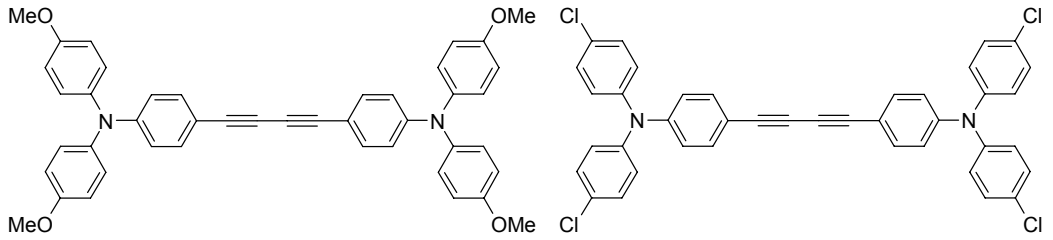

88 **89**

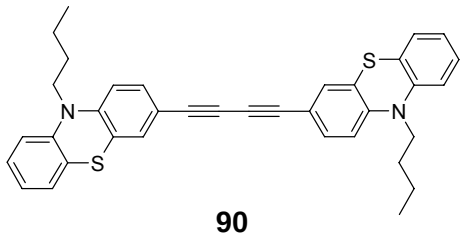

90

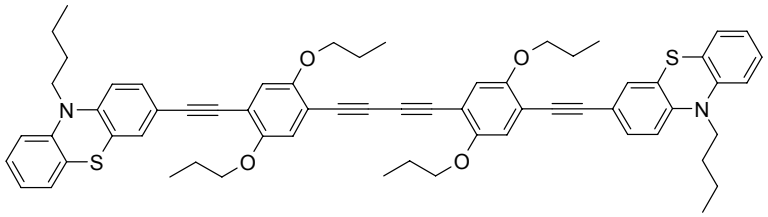

91

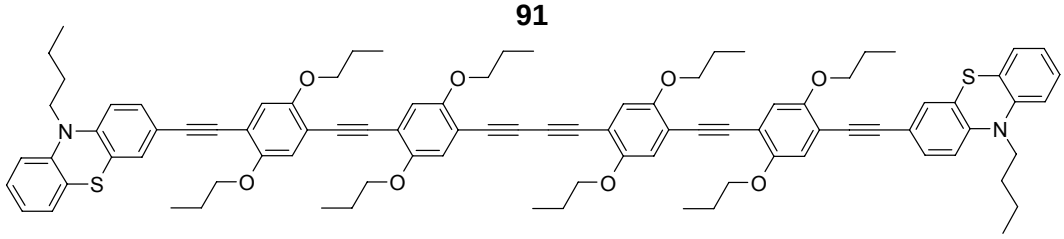

92

Fig. 9-1 Homocoupled bistriarylamine- and bisphenothiazinediynes with different bridge units

the nitrile-substituted bridge **26**. For the synthesis of comparable phenothiazine compounds (e. g. **90**) *Müller et al.* used nearly the same *Hagihara*-coupling reaction conditions [337].

9.4 Cyclic Voltammetry

The cyclic voltammograms for compounds **88** to **92** are depicted in **fig. 9-2**, the values in CH_2Cl_2 are given in **tab. 9-1**. Compounds **88** to **90** show two reversible oxidations of the nitrogen function with values of 280 mV for **88**, 620 mV for **89** and 320 mV for **90** for the first oxidation. The separation of the halfwave potentials are 90 mV for **88** and **90** and 100 mV for **89**. Due to the small interplay and therefore the overlay of the oxidation waves in the cyclic voltammogram the halfwave potentials were determined by digital simulation [338]. For **88** to **90** the second, irreversible oxidation of the nitrogen has almost the same value as for the triarylamine- (**36**, **53**) and phenothiazinethiols (**72**) (see chapter 6). As expected, the oxidation of the methoxy-subsituted bistriarylamine **88** appears at a lower potential than for the chloro-substituted bistriarylamine **89** due to its electron withdrawing functions. The bisphenothiazine-derivative **90** lies in between. For the bistriarylamine **88** nearly the same values have been obtained by *Lambert et al.* [287]. In case of **88** as for the other mixed-valence systems with equal distances between the two redox centres **89** and **90** the delocalisation is quite small. The first oxidation potential of **91** and **92** decreases compared to its homolgeous compound **90** due to the introduction of the electron rich bridge units. The large separation of the redox centres in **91** and **92** results in a very small peak separation (60 mV) which could not be fitted very well for **92**. There are two regions at higher potential where an irreversible oxidation process occurs. The first one at 880 - 1100 mV is caused by an irreversible oxidation of the propoxy-substituted bridge unit, the second at 1220 mV by a second oxidation of the phenothiazine unit. Bistriarylamine **92** shows almost the same behaviour as **91**, the irreversible oxidation of the bridge unit is shifted to smaller potential due to the increase of the electron density by introducing two more bridge units. In comparable alkoxy-substituted oligophenyleneacetylenes of the same bridge length nearly the same values for the peak separation were found and also an oxidation of the bridge unit was observed at higher potential [237].

The comproportionation constant K_C for the equilibrium

$$M + M^{2+} \rightleftharpoons 2\,M^{+}$$

can be calculated using the halfwave potentials of the first and second oxidation and **equ. 9-9**:

$$K_C = \frac{[M^+]^2}{[M][M^{2+}]} = \exp\left(\frac{\left(E_{1/2}^{ox,2} - E_{1/2}^{ox,1}\right)F}{RT}\right) \qquad \textbf{equ. 9-9}$$

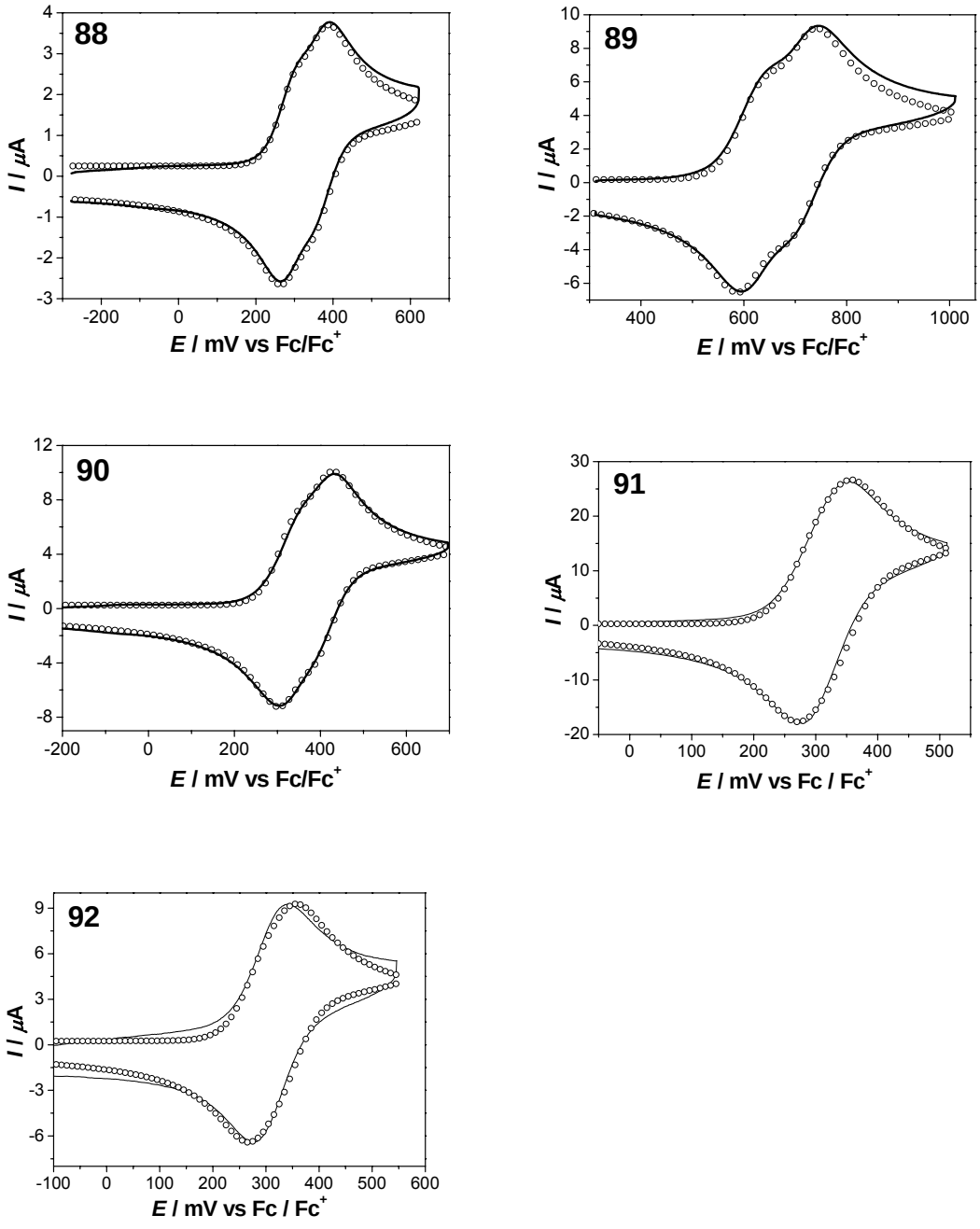

Fig. 9-2 Cyclic voltammograms of **88 - 92** in CH_2Cl_2 / TBAHFP (0.2 M), scan rate: v = 250mV/s; —— measurement, ○○○○ CV-simulation

Tab. 9-1 Halfwave potentials $E_{1/2}$ vs Fc / Fc^+ and comproportionation constants K_C for **88 - 92** in CH_2Cl_2 / TBAHFP (0.1 M), scan rate: v = 250 mV/s

	$E_{1/2}^{ox,1}$ / mV	$E_{1/2}^{ox,2}$ / mV	$E_{1/2}^{ox,3}$ / mV	$E_{1/2}^{ox,4}$ / mV	K_C
88	280	370			32.9
89	620	720			48.5
90	320	410			32.9
91	290	350	950[a]	1220[a]	10.3
92	270	330	770[a]	1350[a]	(10.3)

[a] irreversible process, peak potential

9.5 UV/vis/NIR-Spectroscopy of 88 – 91 and Corresponding Radical Cations and Dications

The UV/vis/NIR-spectra of the neutral compounds **88** to **92** in CH_2Cl_2 are depicted in **fig. 9-3**, the values are shown in **tab. 9-2**. All four chromophores have an intense absorption band at about 25000 cm^{-1}, in case of **91** this band is red shifted to 23900 cm^{-1}. Additional **89** has a shoulder at 25400 cm^{-1}. A second band system appears at 34200 cm^{-1} for the methoxy-substituted bistriarylamine **88** and is red shifted to 32100 cm^{-1} for the chloro-substituted compound **89**. In case of the bisphenothiazine derivatives **90** to **92** a band at 25500 cm^{-1} (for **90**) is visible which is caused by the bridge unit. By increasing the bridge length this absorption band increases monotonic in a homologous way. The band itself is slightly red shifted.

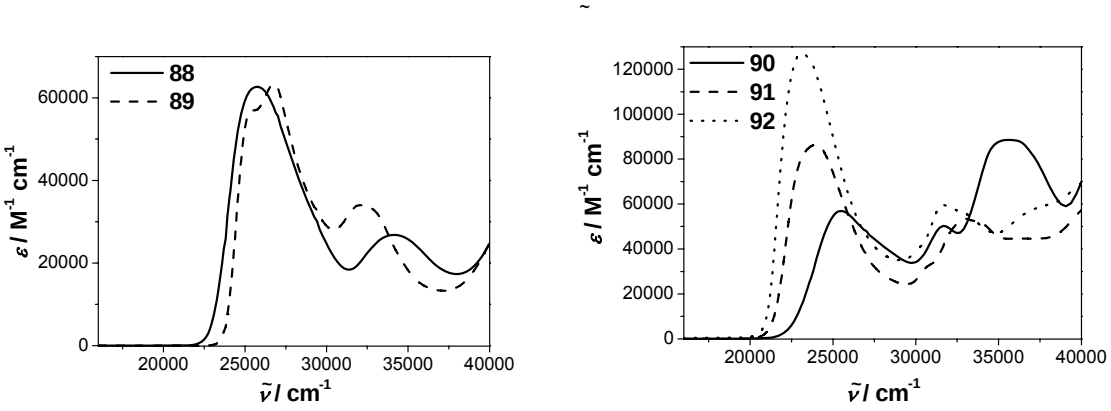

Fig. 9-3 UV/vis-spectra of **88** – **92** in CH_2Cl_2

Tab. 9-2 UV/vis-maxima of **88 - 92** in CH_2Cl_2

	$\tilde{\nu}_1$ / nm	ε_1 / $M^{-1}cm^{-1}$	$\tilde{\nu}_2$ / nm	ε_2 / $M^{-1}cm^{-1}$	$\tilde{\nu}_3$ / nm	ε_3 / $M^{-1}cm^{-1}$
88			25800	62600	34200	26800
89	25400 (sh)	56800	26700	63400	32100	34000
90	25500	56900	31600	50200	35500	88500
91	23900	86500	30900 (sh)	33000	33100	53300
92	23100	127200	31600	59600	33100 (sh)	55300

The oxidation of compounds **88** to **92** was performed in CH_2Cl_2 by a stepwise addition of a $SbCl_5$ solution in CH_2Cl_2 (see **fig. 9-4** for spectra). After each addition an UV/vis/NIR-spectrum was recorded. An increasing band at 6600 cm^{-1} for $\mathbf{88}^{1+}$ and at 8100 cm^{-1} for $\mathbf{90}^{1+}$ was observed which decreases by further oxidation to the diradical $\mathbf{88}^{2+}$ and $\mathbf{90}^{2+}$. These bands refer to an optically induced IV-CT transition. For the bistriarylamine $\mathbf{88}^{2+}$ an intensive absorption band at about 12800 cm^{-1} is visible which is typical for a π-π^*-transition in localised bistriarylaminecations [195, 339, 340].

The chloro-substituted derivative **89** shows a different behaviour. Upon oxidation three bands were visible at 4750 cm^{-1}, 10700 cm^{-1} and 17400 cm^{-1} whereof the first and the last one decrease, the second increases by further oxidation The spectra even show that **89** is not stable under these conditions. Also using of $NOBF_4$ as oxidant did not lead to a stable measurement. The band at 10700 cm^{-1} is again a π-π*-transition of the triarylamine whereas the band at 17400cm^{-1} belongs to a transition of the diyne bridge comparable to symmetric triarylamines with anthracene bridges [294]. The bisphenothiazines **91** and **92** are also instable under these conditions. The spectra indicate that the increasing band at 9200 cm^{-1} for **91** and 8600 cm^{-1} for **92** belong to the diradical cations $\mathbf{91}^{2+}$ and $\mathbf{92}^{2+}$ and not to an IV-CT-band. The band itself is shifted to higher energy from **90** to **91** (comparable to methoxy-subsituted bistriarylamines [287]) by introducing electron rich bridge units.

The radical cation spectra for compounds **88** and **90** were calculated by using the spectrum where the extinction of the IV-CT-band reaches its maximum and was corrected according to the comproportionation constant with **equ. 9-10**:

$$c_{M^+} = c_M^0 \frac{\sqrt{K_C}}{2+\sqrt{K_C}} \qquad \textbf{equ. 9-10}$$

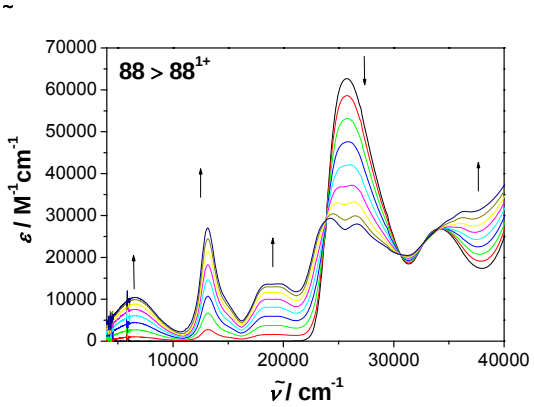
88 > 88^1+
ε / M^-1cm^-1
ν̃ / cm^-1

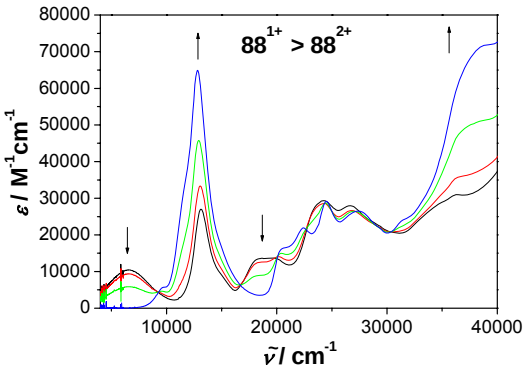
88^1+ > 88^2+
ε / M^-1cm^-1
ν̃ / cm^-1

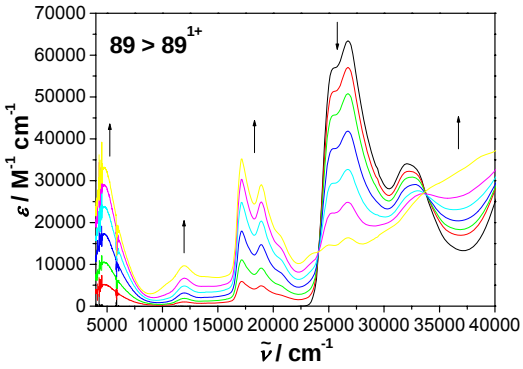
89 > 89^1+
ε / M^-1 cm^-1
ν̃ / cm^-1

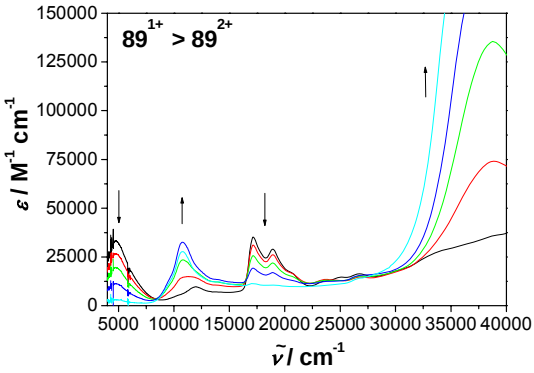
89^1+ > 89^2+
ε / M^-1 cm^-1
ν̃ / cm^-1

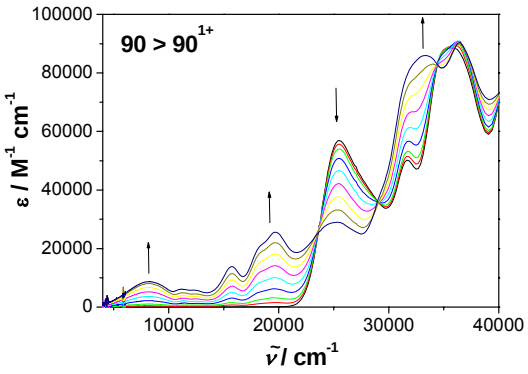
90 > 90^1+
ε / M^-1 cm^-1
ν̃ / cm^-1

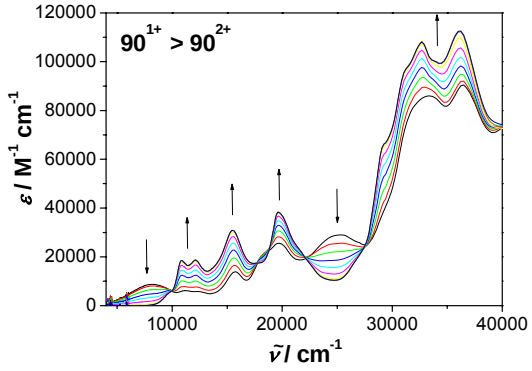
90^1+ > 90^2+
ε / M^-1 cm^-1
ν̃ / cm^-1

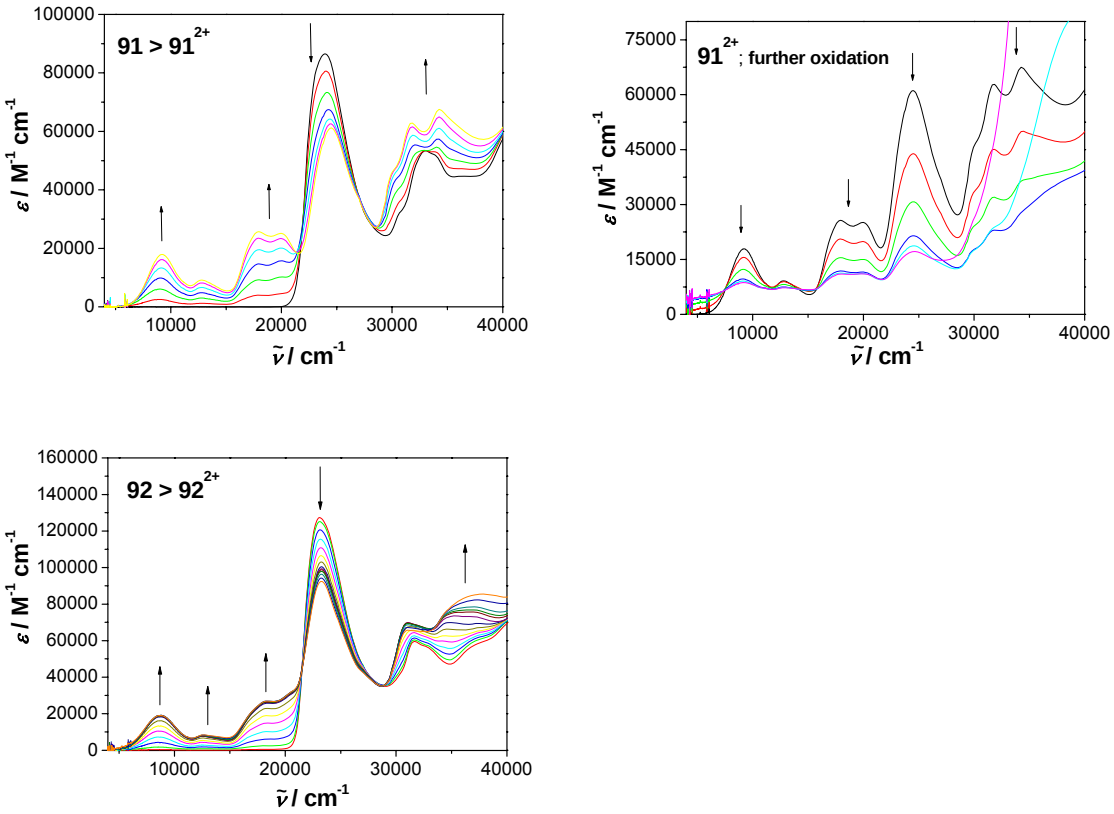

Fig. 9-4 UV/vis/NIR-spectra of compounds **88** – **92** in CH_2Cl_2 by the stepwise oxidation with $SbCl_5$ from e. g. **88** to **88**$^{1+}$ (left) and **88**$^{1+}$ to **88**$^{2+}$ (right)

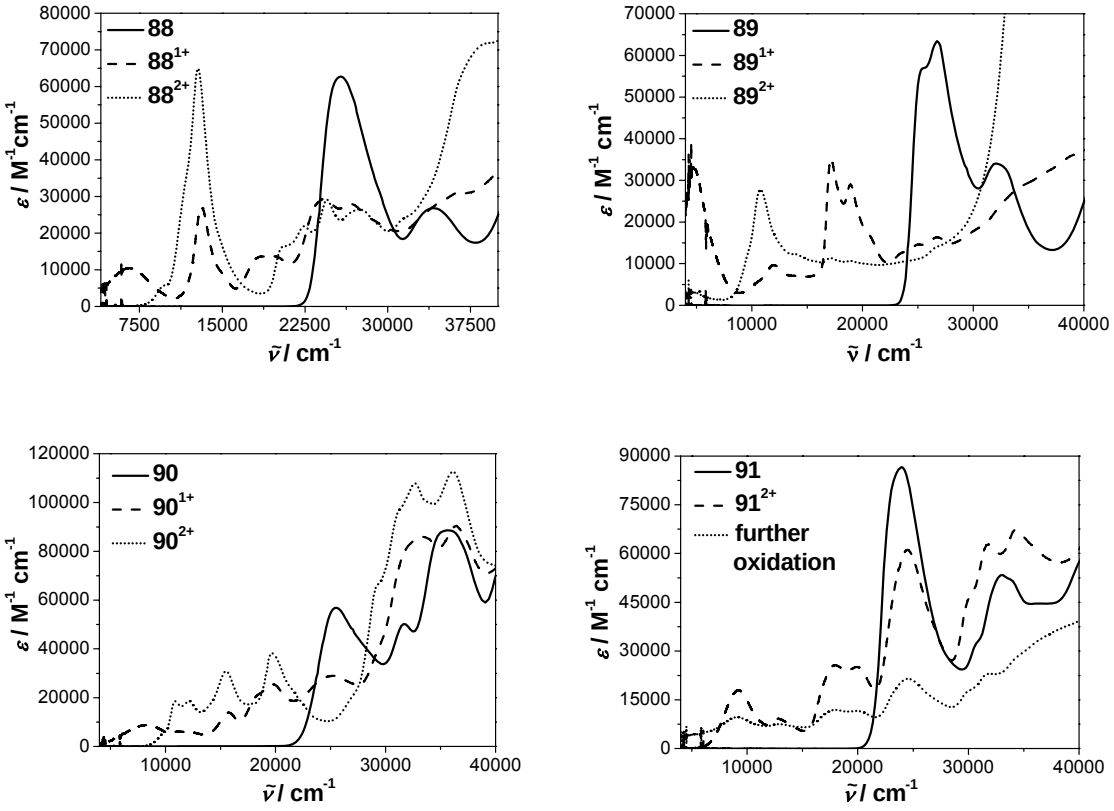

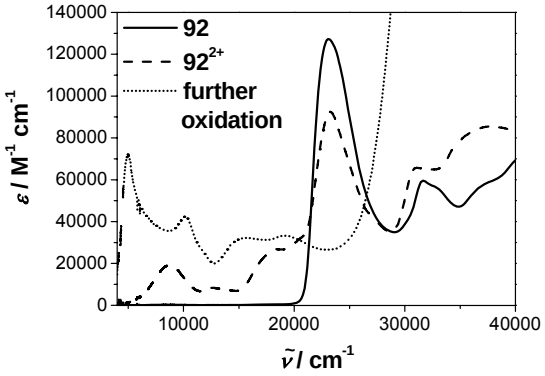

Fig. 9-5 UV/vis/NIR-spectra of chromophores **88** - **92** and the corresponding mono- and dications in CH_2Cl_2 generated by stepwise addition of $SbCl_5$

The bandwidth at half-hight of the bistriarylamine **88** and the bisphenothiazine **90** is slightly larger than the theoretical bandwidth at half-hight at the *high temperature level* (HTL) (**tab. 9-3**). The bands itself also show a symmetric shape. For chromophores **89** and **91** the values which were obtained are not very meaningful due to the fact that the observed bands do not belong to an IV-CT-transition (**fig. 9-5**).

Tab. 9-3 UV/vis/NIR-data for the IV-CT-bands of compounds $\mathbf{88^{1+}}$ to "$\mathbf{91^{2+}}$"

	$\tilde{\nu}_{abs}$ / cm^{-1} [a]	ε_{max} / M^{-1} cm^{-1} [b]	$\tilde{\nu}_{\frac{1}{2}}$ / cm^{-1} [c]	$\tilde{\nu}_{\frac{1}{2}}$(HTL) / cm^{-1} [c]	$\tilde{\nu}_{\frac{1}{2}}$ / $\tilde{\nu}_{\frac{1}{2}}$(HTL)
$\mathbf{88^{1+}}$	6600	14200	4190	3890	1.08
$\mathbf{89^{1+}}$	4750	40900	2480	3300	0.75
$\mathbf{90^{1+}}$	8100	11700	4450	4310	1.03
"$\mathbf{91^{2+}}$"	9010	18100	3210	4550	0.71

[a] ± 100 cm^{-1}; [b] ± 200 M^{-1} cm^{-1}; [c] ± 100 cm^{-1}

9.6 Analysis of IV-CT-Absorption Bands of 88^+ and 90^+

To determine the coupling matrix element V_{AB} the experimental IV-CT-bands of $\mathbf{88^{1+}}$ and $\mathbf{90^{1+}}$ have been fitted by one or two *Gaussian*-functions (**fig. 9-6**). After integration of these functions V_{AB} and ΔG^* have been calculated using **equ. 9-2** and **9-4**. The effective N-N-distance *r* was calculated using AM1-optimised structures (**88**: 15.2 Å; **91**: 15.1 Å; **90**: 15.0 Å; **92**: 28.8 Å).

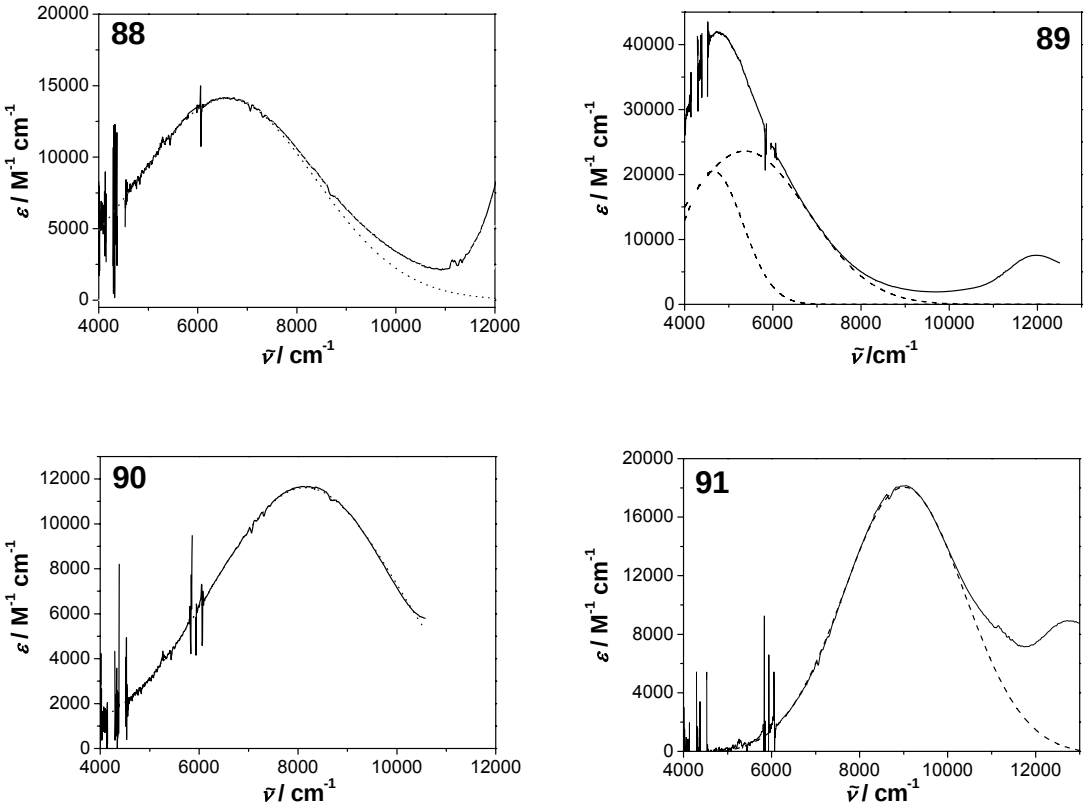

Fig. 9-6 IV-CT-absorption band of $\mathbf{88}^{1+}$ to $\mathbf{91}^{1+}$ (—) and *Gauss*-fits of these bands (····). UV/vis/NIR-spectra were recorded in CH_2Cl_2 using $SbCl_5$ as oxidant

As explained in chapter 9.5 for compounds $\mathbf{89}^{1+}$ and $\mathbf{91}^{2+}$ a different behaviour during oxidation was visible in the UV/vis/NIR spectra. The bands at lower energy do not belong to an IV-CT-transitions but to a transition of the positive charge from the bridge to the triarylamine in case of **89** and from the phenothiazine to the bridge in **91**. To include direct and bridge mediated coupling in the analysis these CT-bands have been investigated using a three-level approach (for a detailed description see ref. [294]) to determine V_{AB} instead of the two level model in case of $\mathbf{88}^{1+}$ and $\mathbf{90}^{1+}$. Using the three-level model no error values could be obtained.

In the homologeous compounds with diyne bridge units the electronic coupling decreases from 850 cm^{-1} for $\mathbf{88}^{1+}$ over 610 cm^{-1} for $\mathbf{90}^{1+}$ to 350 cm^{-1} for $\mathbf{89}^{1+}$ (**tab. 9-4**). As expected the activation energies show the same behaviour. The N-N-distance for these compounds is nearly the same. The lower electronic coupling of the bisphenothiazine $\mathbf{90}^{1+}$ compared to the bistriarylamine $\mathbf{88}^{1+}$ is due to the higher reorganisation energy of the phenothiazine unit which effects the activation energies. In case of $\mathbf{89}^{1+}$ the low electronic coupling is due to bridge coupling effects, where the charge is more localised at the bridge than at the destabilizing chloro-substituted triarylamine centres. This is, beside the bridge

elongation, also the reason for the low coupling of V_{AB} = 60 cm^{-1} in **91**. Despite this the coupling between the redox centres and the bridge is higher as expected and have values of $V_{Ab} = V_{Bb}$ = 1200 cm^{-1} for $\mathbf{89^{1+}}$ and of $V_{Ab} = V_{Bb}$ = 730 cm^{-1} for $\mathbf{92^{2+}}$ (b = bridge).

A simple criteria to refer compounds $\mathbf{88^{1+}}$ to $\mathbf{90^{1+}}$ to *Robin/Day*-class II or III is the quotient of $\frac{\tilde{\nu}_{abs}}{2V_{AB}}$, which has a value of >> 1 in localised systems and just slightly under one for delocalised ones. The value for $\mathbf{88^{1+}}$ is 3.88, 6.78 for $\mathbf{89^{1+}}$ and 6.64 for $\mathbf{90^{1+}}$. Taking this into account, compounds $\mathbf{88^{1+}}$ to $\mathbf{90^{1+}}$ are a crossing between compounds of *Robin/Day*-class II and III.

The ET rates have been determined using **equ. 9-5** assuming that the geometry of the neutral molecules **88** to **90** compared to the radicals $\mathbf{88^{1+}}$ to $\mathbf{90^{1+}}$ does not change remarkably (**tab. 9-4**). In the bistriarylamine derivatives $\mathbf{88^{1+}}$ and $\mathbf{89^{1+}}$ the ET is very fast and in the region of molecular vibrations. The clearly slower ET of the bisphenothiazine $\mathbf{90^{1+}}$ is caused by changing the butterfly geometry of the neutral subunit to the planar structure of the radical cation resulting in a higher reorganisation energy of the phenothiazine.

Tab. 9-4 Hush-analysis for the IV-CT-bands of compounds $\mathbf{88^{1+}}$ - $\mathbf{90^{1+}}$ and $\mathbf{91^{2+}}$

	λ / cm^{-1} [a]	μ_{eg} / D [b]	V_{AB} / cm^{-1}	ΔG^* / cm^{-1}	k_{th} / s^{-1}
$\mathbf{88^{1+}}$	6600	9.39	850 ± 20	900 ± 100	1.2 * 10^{11}
$\mathbf{89^{1+}}$	4750	15.1	350 ($V_{Ab} = V_{Bb}$ = 1200)	860	1.6 * 10^{12}
$\mathbf{90^{1+}}$	8100	5.44	610 ± 20	1470 ± 100	7.9 * 10^{9}
$\mathbf{91^{2+}}$	9010	7.98	60 ($V_{Ab} = V_{Bb}$ = 730)	2200	2.4* 10^{9}

[a] ± 100 cm^{-1}; [b] ± 0.2 D;

9.7 Discussion

Compounds **88** to **92** and their corresponding radical cations $\mathbf{88^{+}}$ to $\mathbf{92^{+}}$ should be investigated according to their electronic coupling V_{AB} and their belonging to mixed-valenced chromophores of *Robin/Day* class I - III using different redox centres and chain length of the spacers.

The results of the cyclic voltammetry measurements indicate that the interaction of the triarylamine or phenothiazine centres of compounds **88** to **90** are very small. This observation is also confirmed by the differences of half wave potentials between the first

and the second oxidation of about 90 to 100 mV and by comparable triarylamine- [287, 341, 342] or dihydrophenazinederivatives [197]. In the homologous row of bisphenothiazines **90** to **92** the half wave potentials decrease by increasing bridge length resulting in a peak separation for the first oxidation of ~ 60 mV indicating that the interaction of the redox centres becomes smaller.

The electronic coupling factors V_{AB} as the ET rates k_{th} drop from **88** over the bisphenothiazine **90** to **89**. Although the distance between the redox centres is equal the bisphenothiazine **90** possesses a higher reorganisation energy than the triarylamines which results in a smaller coupling and ET rates. Almost the same values were found for dihydrophenazine compounds with equal bisacetylene-bridges [197].

In case of $\mathbf{88}^{1+}$ and $\mathbf{90}^{1+}$ symmetric IV-CT-bands are observed. Comparison of the bandwidth at half-hight of the IV-CT-band and the theoretic bandwidth at half-hight at the *high temperature limit* shows that the quotient of $\frac{\tilde{\nu}_{\frac{1}{2}}}{\tilde{\nu}_{\frac{1}{2}}(\mathrm{HTL})}$ is about the value one for **88** and **90**. Additional the ratio of $\frac{\tilde{\nu}_{abs}}{2V_{AB}}$ indicate for compounds **88** and **90** that these derivatives are lying in between the transition of *Robin/Day* class II and III.

For compounds **89**, **91** and **92** another behaviour during oxidation was found. In case of $\mathbf{89}^{1+}$ an absorption band at 10700 cm^{-1} is observed referring to a transition of the dyine bridge which decreases upon further oxidation to $\mathbf{89}^{2+}$. The absorption band at 4750 cm^{-1} is caused by an optically induced hole transfer from the bridge to the triarylamines (**fig. 9-7**, **A**). Comparable observations were made by *Lambert et al.* or *Nelsen et al.* investigating methoxy- or chloro-substituted bistriarylamines with anthracene bridges [294] or diphenyl hydrazines [343]. Therefore a three-level model [294] had to be used to determine V_{AB} to include direct and bridge mediated coupling in the analysis of the CT-bands. For the phenothiazines **91** and **92** the absorption bands at 9200 cm^{-1} and 8600 cm^{-1} belong to the corresponding dications and are caused by optically induced charge transfer from the phenothiazine moieties to the bridge unit (**fig. 9-7**, **B**).

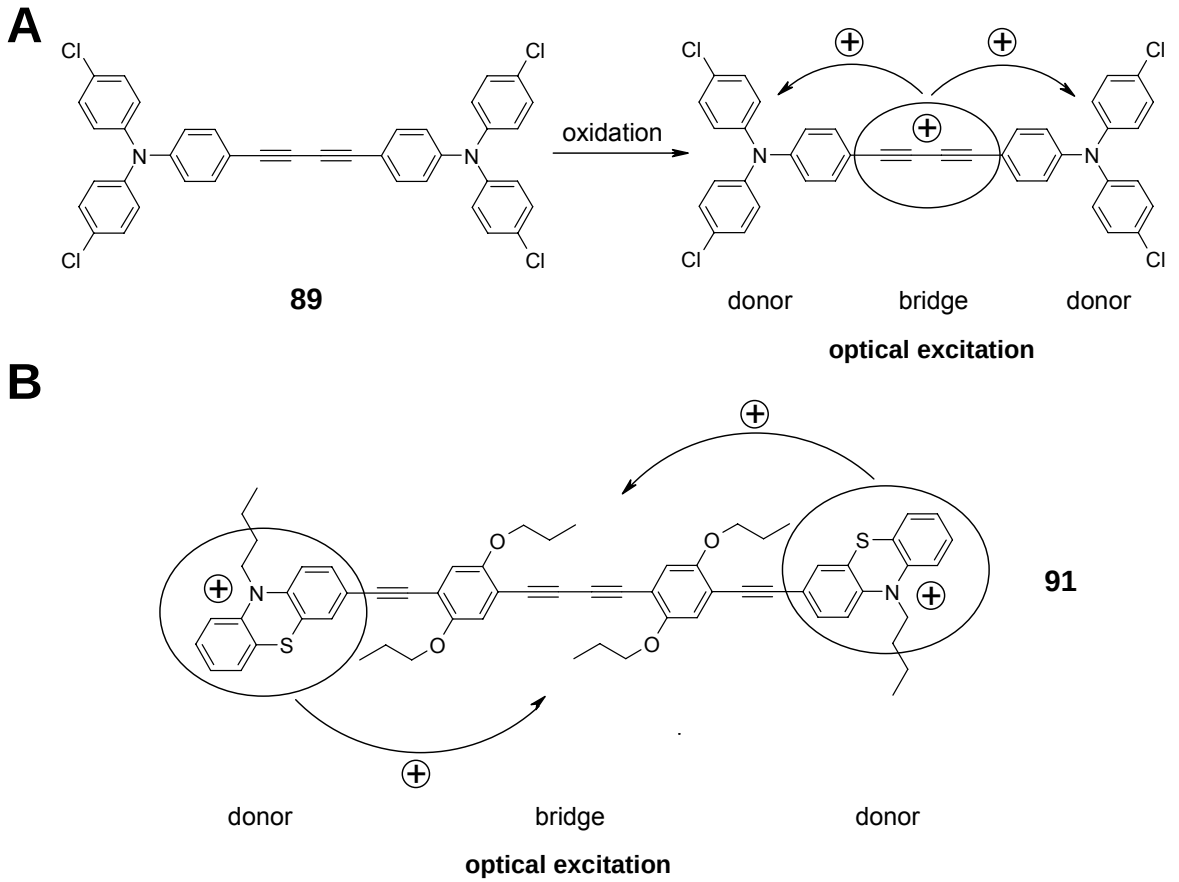

Fig. 9-7 Schematic structures to explain the absorption behaviour of compounds **89** (**A**) and **91**, **92** (**B**) by the stepwise oxidation with $SbCl_5$ during UV/vis investigations

10 Summary

In this work the influence of “active” bridge units on the electron transfer (ET) mechanism within organic donor-bridge-electrode arrays in self-assembled monolayers (SAMs) was studied by spectroscopic and electrochemical methods.

In the first part of this work ferrocenealkanethiols **1** – **3** and the ferrocenearylthiols **4**, **5** were investigated to get experience in the monolayer preparation for measuring ET rates.

Cyclic voltammetry of the monolayers indicates that homogeneously mixed monolayers containing redox active molecules and dummy molecules were formed. For the known ferrocenealkanethiols **1** – **3** the ET rates could be confirmed compared to the ones measured by *Creager et al.* [206]. As expected the ET rate decreases by increasing chain length of the alkane spacer from **2** to **3**. Changing the bonding between the redox centre and the alkane spacer with the same bridge lenght, e. g. by using a carboxy-group in case of **1**, does not influence the ET behaviour very strong. The aromatic ferrocenethiols **4** and **5** show very high ET rates due to the strong conjugated system although the distance between the redox centre and the electrode is comparable to the C_8-alkyl compound **2**. The electronic coupling factors all indicate a nonadiabatic ET between the redox centre and the electrode. As expected the electronic coupling factors increase with decreasing spacer length or with an enlarged conjugated system. To sum up, experience in monolayer preparation could be obtained, the measured ET rates for well known ferrocenealkane-compounds **1** - **3** could be verified and the information could be transferred to the conjugated systems **4** and **5**.

In the second part the triarylamine- **29**, **32** and the phenothiazinealkanethiol **35** have been examined relative to their ET behaviour in mixed monolayers.

The cyclic voltammograms of the diluted monolayers indicate that homogeneously formed monolayers are present. The ET rates of triarylamine- **29**, **32** and phenothiazinealkanethiols **35** are 10 to 100 times higher than compared to ferrocenealkanethiols with equal chain length[183, 206], whereas in a $[Ru(bpy)2(pp)]^+$-containing monolayer the same value was observed [177]. Almost two parameters influence the ET rate constant: the electronic coupling matrix element $|V_{ab}|$ and the reorganisation energy λ [209]. The ET rate in donor substituted alkanethiols is mainly influenced by the reorganisation energy λ [177] and even small changes have a dramatic effect on the observed

processes, therefore an increasing ET rate from the ferrocene (high reorganisation energy) over the phenothiazine **35** and the $[Ru(bpy)2(pp)]^+$ to the triarylamine chromophores **29** and **32** (low reorganisation energy) is observed. Furthermore the bonding between the redox centres and the alkane spacer plays an important role on the ET rate in case of the triarylamines **29** and **32** opposite to the assumption made by *Creager et al.* that the connection does not play any role. For the electron rich ether connected compound **29** the ET is not only dominated by the reorganisation energy but also by mesomeric effects where the positive charge of the electron rich derivative **29** is more located at the ether function so that the chain is formally shortend by one atom resulting in higher ET rates than compared to **32**.

In the third part of the thesis a series of "molecular wires" consisting of methoxy- or chloro-substituted triarylamines and phenothiazines with different bridge units and bridge length between the redox centre and the anchor thiol function have been prepared in order to investigate their ET-behaviour.

Cyclic voltammetry and UV/vis-spectroscopy show that the oxidation potential and the energetic states could be controlled very well by introducing different redox centres and bridge units resulting in a decreasing oxidation potential of the redox centres and a bathochromic shift of the absorption bands in the UV/vis-spectra. Also the densitiy of the chromophores in mixed monolayers could be controlled very well for only three compounds (**49**, **52** and **87**) with nitrile-substituted bridges reliable ET rates could be obtained. In these chromophores the ET rate decreases by increasing the density of the redox active molecules in the mixed monolayers indicating that the adsorption geometry changes with coverage with the chromophores tilting to a more upright orientation as the surface becomes more crowded. For all other compounds the measurements were limited by the fast ET rates. Conformational, as well as a very weak distance dependence of the ET resulting in very high ET rates [172] or unfavourable HOMO-LUMO energies of the donor, bridge and the electrode are reasons for this behaviour. The fact that compound **49** shows almost the same rate constant independent of the length (n = 2 or n = 3) may indicate that a hopping process is operating for which a much weaker length dependence is expected than in the case of a superexchange. Since there is practically no chance to extend the speed of the method for ET rates beyond approx. 10^5 s^{-1}, also using spectroelectrochemical methods or fast scan cyclic voltammetry did not lead to any success due to the instability of the

redox active monolayers, future work will be directed to the synthesis of analogous saturated compounds which will inherently show slower rate constants.

In the last part bistriarylamines and bisphenothiazines **88** - **92** and their corresponding radical cations or dications were investigated according to their electronic coupling V_{AB} and their belonging to mixed-valenced chromophores of *Robin/Day* class I - III using different redox centres and chain length of the spacers. The results of the cyclic voltammetry measurements show that the interaction of the triarylamine or phenothiazine centres of compounds **88** to **90** are very small while it decreases in the homologous row of the bisphenothiazines from **90** to **92** due to bridge extension. The values obtained by analyzing the IV-CT-bands of **88** and **90** indicate that these derivatives are lying in between the transition of *Robin/Day* class II and III. For compounds **89**, **91** and **92** a completely different behaviour during oxidation was found and no IV-CT-band could be observed. UV/vis-spectroscopy points out that in case of $\mathbf{89}^{1+}$ an optically induced charge-transfer from the bridge to the triarylamines takes place while the phenothiazines **91** and **92** are directly oxidised to dications and an optically induced charge-transfer from the phenothiazine moieties to the bridge unit is observed. To investigate V_{ab} for these compounds a three level model [294] was used to include direct and bridge mediated coupling in the analysis of the CT-bands.

11 Experimental Section

11.1 Apparatus and Methods

11.1.1 Analytical Methods

NMR Spectroscopy

- Bruker AC 250 FT-Spectrometer (^{1}H: 250.13 MHz, ^{13}C: 62.91 MHz)
- Bruker Avance 400 FT-Spectrometer (^{1}H: 400.1 MHz, ^{13}C: 100.6 MHz)
- Bruker Avance DMX 600 FT-Spectrometer (^{1}H: 600.13 MHz, ^{13}C: 150.92 MHz)

All ^{1}H- and ^{13}C-NMR spectra were recorded at 300 K unless otherwise indicated. The signal of the respective solvent was used as the internal reference and the chemical shifts are given in *ppm* (δ-scale) versus TMS. Multiplicities are denoted as *s* (singulet), *bs* (broad singulet), *d* (doublet), *dd* (doublet of doublets), *t* (triplet), *dt* (doublet of triplets), *q* (quartet), *qu* (quintet), *sex* (sextet), *m* (multiplet) and *sh* (shoulder). Coupling constants are given in *Hz*.

NMR-Spectroscopy data are quoted as follows: chemical shift (multiplicity, coupling constants, number of protons, assignment).

IR Spectroscopy

- Jasco 410 FT-IR Spectrometer

Absorption band maximums are given in cm^{-1} and intensities are denoted as *vs* (very strong), *s* (strong), *m* (medium), *w* (weak), *vw* (very weak).

Mass Spectroscopy

- Finnigan MAT 90
- Bruker Daltonik micrOTOF focus

Mass spectra were recorded at the Institute of Organic Chemistry, University of Würzburg. As otherwise described the samples for ESI-spectra were diluted with a solution of MeCN / CH_2Cl_2 (1 : 1). Mass spectroscopy data are quoted as follows: m/z (relative intensity, assignment).

Elemental Analysis

- Leco CHNS-932

The elemental analyses were performed at the Institute of Inorganic Chemistry, University of Würzburg.

Melting Points

All melting points were measured with a melting point apparatus by Dr. Tottoli from Büchi and are not corrected.

11.1.2 Spectroscopy

UV/vis/NIR Spectroscopy

- Jasco V-570 UV/vis/NIR spectrophotometer

All spectra were recorded in 1 cm quartz cells (Hellma) in solvents of spectroscopic grade unless otherwise indicated.
Modus of quotation: λ_{max} in nm (ε in l mol^{-1} cm^{-1}).

11.1.3 Electrochemistry

Cyclic Voltammetry

- Electrochemical Workstation BAS CV-50 W including software version 2.0
- Princeton Applied Research potentiostat/galvanostat model 283 including software Power Suite

Cyclic voltammograms were measured in a cylindrical glass cell using a three electrode setup consisting of a platinum disc electrode (∅ 3 mm) or a glassy carbon electrode (∅ 3 mm) (in case of all CV measurements thiol substituted compounds in solution) as the working electrode, a platinum coil as the counter electrode and a Ag/AgCl pseudoreference electrode. If possible, the ferrocene/ferrocenium redox couple was used as

an internal reference. All CV experiments were performed under inert gas (argon, dried with Sicapent® from Merck, traces of oxygen were removed with copperoxide catalyst R3-11 from BASF) and only purified and dried solvents were used[344, 345]. The test solutions were saturated with argon prior to the experiments. Unless otherwise indicated, tetrabutylammonium hexafluorophospate (TBAHFP) served as the electrolyte salt[344]. For measurements under thin layer conditions the working electrode was placed onto a mobile glass half ball[346].

Chemical Oxidation

- Jasco V-570 UV/vis/NIR spectrophotometer

For the chemical oxidation of triarylamine and phenothiazine compounds investigated in chapter 9 a $SbCl_5$ solution in CH_2Cl_2 was used. A 10^{-5} M (c_0) solution of the neutral derivative in CH_2Cl_2 in an UV-cuvette was prepared and the $SbCl_5$-solution in CH_2Cl_2 (concentration: ca. 50 c_0 – 100 c_0) was added dropwise with a microliter syringe. After each addition the UV-cuvette was shaked and an UV-spectrum of the formed solution was recorded.

Impedance Spectroscopy

- Princeton Applied Research potentiostat/galvanostat model 283 including software Power Suite
- Princeton Applied Research frequency response detector model 1025
- TTI synthesised arbitrary waveform generator TGA 1230 30 MHz
- Tektronix two channel digital real-time oscilloscope TDS 210

Electrochemical experiments were performed in a three-electrode configuration using a 0.2 M tetrabutylammonium hexafluorophospate (TBAHFP) electrolyte in MeCN or in case of the ferrocene compounds **1** – **5** an aqueous 1 M $HClO_4$ solution. An Ag/AgCl pseudoreference electrode and a platinum coil as the counter electrode were used and brought as near as possible to the working elektrode. The working electrode was positioned such that the freshly molten gold ball was immersed just below the surface of the electrolyte, with as little of the gold wire as possible exposed to the solution. All

experiments were performed under inert gas (argon, dried with Sicapent® from Merck, traces of oxygen removed with copperoxide catalyst R3-11 from BASF) and only purified and dried solvents were used. The samples were saturated with argon prior to the experiments.

Instrument settings for using programm "Power Suite":

Window PreScan Definition:	Measure Open Circuit Potential as Required	
Window Scan Definition:	Start frequency:	1 MHz
	End frequency:	100 mHz
	Number of points:	40 and activate "Logarithmic Point Space"
	AC-amplitude:	10 mV rms
	Data quality:	1
Window Advanced:	Fully automatic	

All other values have to be set as default.

Electrode and Monolayer Preparation

Gold electrodes for monolayer coating were prepared by melting the end of a clean gold wire (0.1 mm, Premion®, 99.998 %, Alfa Aesar) into a small spherical ball in a gas-air flame. The diameter of the spherical ball varied from one electrode to another, but was typically in the range of 0.3 – 0.4 mm. The gold ball electrodes were cleaned in a Piranha-solution for 1 min, rinsed with water (pro analysis, Merck) and CH_2Cl_2 (or just water in case of ferrocene compounds **1** – **5**) and blown dry in an argon stream. Afterwards the electrodes were immediately immersed in a coating solution to form the monolayer.

Coating solutions for preparing monolayers with thiol functions were always about 1mM total thiol in abs. CH_2Cl_2 (in case of ferrocene compounds **1** – **5** monolayer preparation was performed in abs. ethanol). Acetyl protected thiols were deprotected during monolayer preparation by using a coating solution containing 1 mM total thiol and 10 mM of abs. diethylamine in abs. CH_2Cl_2. Monolayer formation was allowed to proceed for not less than 18 h, after which the electrodes were rinsed with CH_2Cl_2 followed by MeCN prior to mounting in the electrochemical cell (for different strategies of SAM preparation see also chapter 5).

11.1.4 QCM Measurements

- Stanford Research Systems quartz crystal microbalance digital controller QCM 200 including software LabView™ 7 Express from National Instruments
- Stanford Research Systems 5 MHz crystal oscillator QCM 25 using a 5 MHz crystal (∅ 1 inch, gold / Cr, polished)

The quartz crystals were cleaned three times in a piranha solution (1 : 3, H_2O_2 (30%) : H_2SO_4, 3 min each) prior to use. The cleaned quartz crystals were washed with deionized water and blown dry in a gentle flow of nitrogen or dried at 100°C in drying stove. The solvents were purified, dried and degassed using standard procedures and stored under an inert gas atmosphere [347]. Measurements in gas phase or in solution were performed in a 100 ml beaker which was cooled to 20 °C ± 0.1 °C using an Ultra-Kryomat® model RUL-40. To cause as less perturbation to the quartz crystal as possible all samples were investigated without stirring the solution, otherwise no stable baseline could be obtained.

After establishing a stable QCM baseline a small volume of a high concentrated tempered thiol solution (or in case of gas phase measurements the pure thiol) was transferred to the QCM cell via syringe with as less perturbation to the system as possible. The concentration of the tempered thiol solution was about 0.05 mol/l, the end concentration of the measrued solution $1 * 10^{-3}$ mol/l.

It is important, also by using the flow cell, that the hole quartz crystal is wetted from the solution and that all air bubbles are removed from the surface of the quartz crystal. Solvents like CH_2Cl_2 or acetone cannot be used as solvents due to an uncontrollable swelling of the sealing rings of the QCM cell and the resulting strong influence on the frequency of the quartz crystal so that no stable baseline could be obtained.

11.1.5 Synthesis

All reactions were carried out in standard glass ware unless otherwise indicated. The chemicals were of standard quality (Fluka, Aldrich, Merck, Acros, Avocado, Chempur, Sigma, ABCR) and used without further purification. Reactions under inert gas

conditions (nitrogen, dried with Sicapent® from Merck, traces of oxygen removed with copperoxide catalyst R3-11 from BASF) were carried out in flame dried Schlenk vessels, the solvents were purified and dried by standard procedures and kept under inert gas atmosphere[347].

Chromatography

- silica gel for flash-chromatography (32 – 63 μm, Merck)
- aluminum oxide 90 neutral (63 – 200 μm, Macherey-Nagel), activity V

11.2 Synthesis

11.2.1 General Procedures

11.2.1.1 Hagihara-Coupling with $Pd(PPh_3)_2Cl_2$ / CuI / ^{i}PrEtN (GP1)

A mixture of the aryl halide (1.0 equivalents) and the alkyne (1.2 equivalents), $Pd(PPh_3)_2Cl_2$ (5 mol %), CuI (2.5 mol %) and $^{i}Pr_2EtN$ (2.2 equivalents) in dry THF were stirred under a nitrogen atmosphere at room temperature for 24 h. The solvent was removed in vacuo, the residue was redissolved in CH_2Cl_2 and washed with water. The organic layer was dried over $MgSO_4$ and the solvent was removed. The crude product was purified by column-chromatography (neutral aluminum oxide, activity V) or flash-chromatography (silica gel).

11.2.1.2 Hagihara-Coupling with $Pd(PPh_3)_2Cl_2$ / CuI (GP2) [223, 348]

A mixture of the alkyne (1.2 equivalents) and the aryl halide (1.0 equivalents), $Pd(PPh_3)_2Cl_2$ (4 - 10 mol %) and CuI (4 - 10 mol %) in dry Et_2NH were stirred under a nitrogen atmosphere at room temperature for 24 h. The solvent was removed in vacuo, the residue was redissolved in CH_2Cl_2 and washed with water. The organic layer was dried over $MgSO_4$ and the solvent was removed. The crude product was purified by column-chromatography (neutral aluminum oxide, activity V) or flash-chromatography (silica gel).

11.2.1.3 Palladium Catalysed Amination with $Pd_2(dba)_3 \cdot CHCl_3$ / $PtBu_3$ (GP3) [349, 350]

A mixture of the aryl halide (1.1 equivalents), aryl amine (1.0 equivalents), sodium-*tert*-butoxide (1.25 equivalents), $Pd_2(dba)_3 \cdot CHCl_3$ (0.5 – 2.0 mol % Pd) and P^tBu_3 (solution in hexane, 0.8 equivalents per Pd atom) in dry toluene were stirred under nitrogen atmosphere at 40 °C for 1 to 3 d. The solvent was reduced in vacuo, the residue was redissolved in CH_2Cl_2 and washed with water. The organic layer was dried over $MgSO_4$ and the solvent was removed. The crude product was purified by column-chromatography (neutral aluminum oxide, activity V) or flash-chromatography (silica gel).

11.2.1.4 Hagihara-Coupling with $Pd(C_6H_5CN)2Cl2$ / P^tBu_3 / CuI (GP4) [351]

The aryl halide (1.0 equivalents), the alkyne (1.1 – 1.25 equivalents), $Pd(C_6H_5CN)_2Cl_2$ (3 mol %) and CuI (2 mol %) were dissolved under a nitrogen atmosphere in dioxane. After addition of P^tBu_3 (solution in hexane, 6 mol %) and $^iPr_2NH$ (1.1 equivalents) the solution was stirred at room temperature for 1 – 3 d. The solvent was reduced in vacuo, the residue was redissolved in CH_2Cl_2 and washed with water. The organic layer was dried over $MgSO_4$ and the solvent was removed. The crude product was purified by column-chromatography (neutral aluminum oxide, activity V) or flash-chromatography (silica gel).

11.2.1.5 Deprotection of Trimethylsilyl Protected Alkines with K_2CO_3 (GP5) [352]

A mixture of the protected alkyne (1.0 equivalents) and K_2CO_3 (1.25 equivalents) in methanol was stirred under a nitrogen atmosphere at room temperature for 12 h. The solvent was removed in vacuo, the residue was redissolved CH_2Cl_2 and washed with water. The organic layer was dried over $MgSO_4$ and the solvent was removed. The crude product was purified by column-chromatography (neutral aluminum oxide, activity V) or flash-chromatography (silica gel).

11.2.1.6 Deprotection of Trimethylsilyl Protected Alkines with TBAF (GP6) [352]

The trimethylsilyl protected alkyne (1.0 equivalents) was dissolved in THF and TBAF in THF (1 M, 1.1 equivalents) was added. The solution was stirred at room temperature for 2 h. Afterwards water was added and the solution was extracted with CH_2Cl_2. The organic layers were combined, dried over $MgSO_4$ and the solvent was removed in vacuo. The product was used without further purification.

11.2.2 Synthesis of Triarylamine- and Phenothiazine-Precursors

11.2.2.1 (4-Bromophenyl)-bis-(4-methoxyphenyl)amine (6) [353]

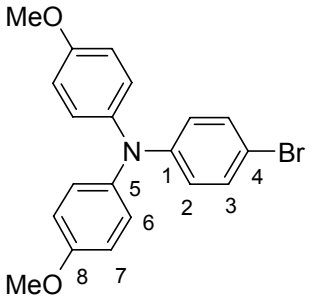

CA: [194416-45-0]

To a solution of 4-iodoanisol (14.3 g, 61.1 mmol) and 4-bromoaniline (5.00 g, 29.1 mmol) in dry toluene (20 ml) CuI (115 mg, 1.14 mmol), 1,10-phenanthroline (209 mg, 1.16 mmol) and powdered KOH (12.7 g, 226 mmol) were added under a nitrogen atmosphere. The suspension was refluxed for 24 h. The toluene was removed in vacuo, the residue was dissolved in water (150 ml) and extracted with CH_2Cl_2 (150 ml). The aqueous layer was again extracted with CH_2Cl_2 (2 x 150 ml). The combined organic phases were dried over $MgSO_4$ and the solvent was removed in vacuo. The crude product was purified by flash-chromatography (silica) with CH_2Cl_2 / PE (1 : 2) to obtain a colourless solid.

Formula: $C_{20}H_{18}BrNO_2$ (384.30).

Yield: 7.43 g (19.3 mmol, 66 %) of a colourless solid.

^{1}H-NMR (400 MHz, benzene–d_6, 300 K): δ / ppm = 7.16 (AA´, 2H, H-2 o. 3), 6.96 (AA´, 4H, H-6 o. 7), 6.75 (BB´, 2H, H-2 o. 3), 6.69 (BB´, 4H, H-6 o. 7), 3.29 (s, 6H, -OMe).

{^{1}H}^{13}C-NMR (101 MHz, benzene–d_6, 300 K): δ / ppm = 156.8 (quart.), 148.6 (quart.), 141.2 (quart.), 132.4 (CH), 127.1 (CH), 122.8 (CH), 115.4 (CH), 113.1 (quart.), 55.2 (CH_3).

Melting point (CH_2Cl_2 / PE): 95 – 97 °C.

11.2.2.2 Bis-(4-methoxyphenyl)-[4-(trimethylsilanylethynyl)phenyl]amine (7)

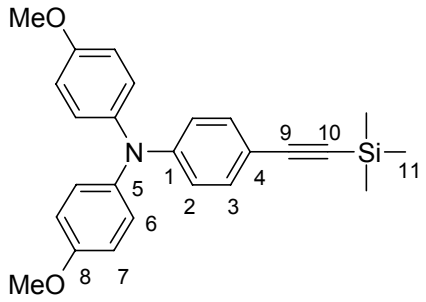

CA: [218608-72-1]

Synthesis according to GP 4:

Quantity:	(4-Bromophenyl)-bis-(4-methoxyphenyl)amine (**6**):		
		782 mg	2.13 mmol
	Ethynyltrimethylsilane:	272 mg	2.77 mmol
	$Pd(PhCN)_2Cl_2$:	23.8 mg	63.9 μmol
	CuI:	7.50 mg	42.5 μmol
	P^tBu_3 (0.33 M solution in hexane):	23.6 mg	128 μmol
	$^i Pr_2EtN$:	215 mg	2.13 mmol
	Dry dioxane:	7 ml	

The crude product was purified by flash-chromatography (silica) eluting with CH_2Cl_2 / PE (1 : 2) to obtain a yellow oil.

Formula: $C_{25}H_{27}NO_2Si$ (401.58).

Yield: 767 mg (1.91 mmol, 90 %) of a brown oil.

^{1}H-NMR (400 MHz, acetone–d_6, 300 K): δ / ppm = 7.23 (AA´, 2H, H-2 o. 3), 7.08 (AA´, 4H, H-6 o. 7), 6.94 (BB´, 4H, H-6 o. 7), 6.73 (BB´, 2H, H-2 o. 3), 3.79 (s, 6H, -OMe), 0.2 (s, 9H, H-11).

{^{1}H}^{13}C-NMR (101 MHz, acetone–d_6, 300 K): δ / ppm = 157.8 (quart.), 150.3 (quart.), 140.7 (quart.), 133.2 (CH), 128.1 (CH), 118.7 (CH), 115.6 (CH), 114.2 (quart.), 92.3 (quart.), 77.7 (quart.), 55.7 (CH_3), 0.2 (CH_3).

11.2.2.3 Bis-(4-methoxyphenyl)-[4-(ethynyl)phenyl]amine (8)

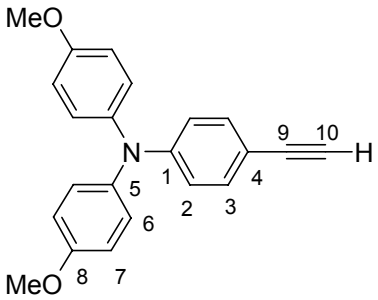

CA: [218608-73-2]

Synthesis according to GP5:

Quantity:	Bis-(4-methoxyphenyl)-[4-(trimethylsilanylethynyl)phenyl]amine (**7**):		
		800 mg	1.99 mmol
	K_2CO_3:	415 mg	3.00 mmol
	Dry MeOH:	15 ml	
	Dry CH_2Cl_2:	5 ml	

The crude product was purified by flash-chromatography (silica) eluting with CH_2Cl_2 / PE (1 : 2) to obtain a yellow oil.

Formula: $C_{22}H_{19}NO_2$ (329.30).

Yield: 596 mg (1.81 mmol, 90 %) of a colourless solid.

^{1}H-NMR (400 MHz, acetone–d_6, 300 K): δ / ppm = 7.25 (AA´, 2H, H-2 o. 3), 7.08 (AA´, 4H, H-6 o. 7), 6.93 (BB´, 4H, H-6 o. 7), 6.73 (BB´, 2H, H-2 o. 3), 3.79 (s, 6H, -OMe), 3.44 (s, 1H, H-10).

{^{1}H}^{13}C-NMR (101 MHz, acetone–d_6, 300 K): δ / ppm = 157.8 (quart.), 150.3 (quart.), 140.7 (quart.), 133.6 (CH), 128.4 (CH), 119.0 (CH), 115.8 (CH), 113.4 (quart.), 84.8 (quart.), 77.3 (quart.), 55.7 (CH_3).

Melting point (CH_2Cl_2 / PE): 85 – 87 °C.

11.2.2.4 4-(Bromophenyl)ethynyltrimethylsilane (9)

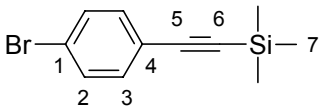

CA: [16116-78-2]

Synthesis according to GP2:

Quantity:	1-Bromo-4-iodobenzene:	2.80 g	9.90 mmol
	Ethynyltrimethylsilane:	982 mg	10.0 mmol
	$(PPh_3)_2PdCl_2$:	270 mg	390 μmol
	CuI:	74.0 mg	390 μmol
	Dry Et_2NH:	35 ml	

The residue was purified by flash-chromatographie (silica) eluting with PE to obtain a colourless solid.

Formula: $C_{11}H_{13}BrSi$ (253.19).

Yield: 2.33 g (9.20 mmol, 93 %) of a colourless solid.

^{1}H-NMR (400 MHz, $CDCl_3$, 300 K): δ / ppm = 7.42 (AA', 2H, H-2 o. 3), 7.31 (BB', 2H, H-2 o. 3), 0.25 (s, 9H, H-7).

{^{1}H}^{13}C-NMR (101 MHz, $CDCl_3$, 300 K): δ / ppm = 133.5 (CH), 131.6 (CH), 122.9 (quart.), 122.3 (quart.), 104.0 (quart.), 95.8 (quart.), 0.0 (CH_3).

Melting point (PE): 61 °C.

11.2.2.5 (4-Chlorophenyl)-(4-trimethylsilanylethynylphenyl)amine (10)

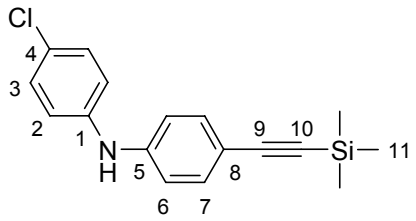

Synthesis according to GP3:

Quantity:	4-(Bromophenyl)ethynyltrimethylsilane (**9**):	4.72 g	18.6 mmol
	4-Chloroaniline:	2.85 g	22.3 mmol
	Sodium-*tert*-butoxide:	2.05 g	21.3 mmol
	$Pd_2(dba)_3 \cdot CHCl_3$:	98.0 mg	94.3 μmol
	P^tBu_3:	30.8 mg	152 μmol
	Dry toluene:	36 ml	

The residue was purified by flash-chromatographie (silica) eluting with CH_2Cl_2 / PE (1 : 3) to obtain a yellow solid.

Formula: $C_{17}H_{18}ClNSi$ (299.85).

Yield: 4.35 g (14.5 mmol, 78 %) of a yellow solid.

^{1}H-NMR (400 MHz, CD_2Cl_2, 300 K): δ / ppm = 7.34 (AA´, 2H), 7.25 (AA´, 2H), 7.05 (BB´, 2H), 6.95 (BB´, 2H), 5.91 (s, 1H, -NH), 0.23 (s, 9H, H-11)

{^{1}H}^{13}C-NMR (101 MHz, CD_2Cl_2, 300 K): δ / ppm = 143.8 (quart.), 141.1 (CH), 133.5 (CH), 129.7 (CH), 126.8 (CH), 120.5 (quart.), 116.7 (quart.), 115.3 (quart.), 105.7 (quart.), 92.8 (quart.), 0.1 (CH_3).

Melting point (CH_2Cl_2, PE): 102-103 °C.

11.2.2.6 Bis-(4-chlorophenyl)-(4-trimethylsilanylethynylphenyl)amine (11)

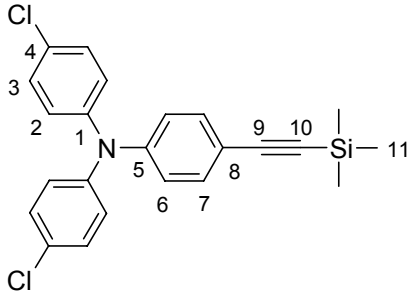

Synthesis according to GP3:

Quantity: (4-Chlorophenyl)-(4-trimethylsilanylethynylphenyl)amine (**10**):

	4.06 g	13.6 mmol
4-Chloro-1-iodobenzene:	3.87 g	16.3 mmol
Sodium-*tert*-butoxide:	1.56 g	16.2 mmol
$Pd_2(dba)_3 \cdot CHCl_3$:	70.0 mg	66.8 μmol
P^tBu_3:	22.0 mg	108 μmol
Dry toluene:	32 ml	

The residue was purified by flash-chromatographie (silica) eluting with CH_2Cl_2 / PE (1 : 4) to obtain a yellow solid.

The product was contaminated up to 5 % with an unknown compound which could not be removed by chromatography. The product was used without further purification.

Formula: $C_{23}H_{21}Cl_2NSi$ (410.42).

Yield: 3.52 g of a yellow solid.

^{1}H-NMR (400 MHz, CD_2Cl_2, 300 K): δ / ppm = 7.31 (AA', 2H, H-6 o. 7), 7.24 (AA', 4H, H-2 o. 3), 7.01 (BB', 4H, H-2 o. 3), 6.93 (BB', 2H, H-6 o. 7), 0.23 (s, 9H, H-11).

11.2.2.7 Bis-(4-chlorophenyl)-(4-ethynylphenyl)amine (12)

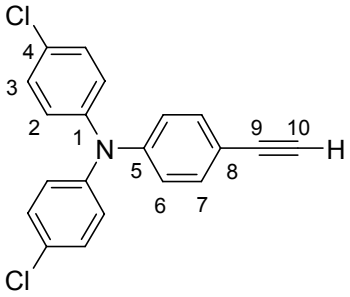

Synthesis according to GP5:

Quantity:	Bis-(4-chlorophenyl)-(4-trimethylsilanylethynylphenyl)amine (**11**):		
		3.30 g	9.76 mmol
	K_2CO_3:	2.38 g	17.2 mmol
	Dry MeOH:	47 ml	

The residue was purified by flash-chromatographie (silica) eluting with CH_2Cl_2 / PE (1 : 4) to obtain a yellow solid.
The product was contaminated up to 5 % with an unknown compound which could not be removed by chromatography. The product was used without further purification.

Formula: $C_{20}H_3Cl_2N$ (338.24).

Yield: 2.38 g of a yellow solid.

^{1}H-NMR (400 MHz, acetone–d_6, 300 K): δ / ppm = 7.35 (AA', 2H, H-6 o. 7), 7.25 (AA', 4H, H-2 o. 3), 7.02 (BB', 4H, H-2 o. 3), 6.95 (BB', 2H, H-6 o. 7), 3.10 (s, 1H, H-10).

11.2.2.8 10-Butylphenothiazine (13) [219]

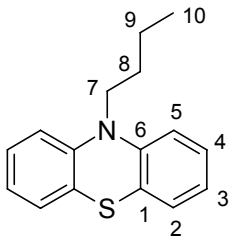

CA: [5909-56-8]

Phenothiazine (8.00 g, 40.1 mmol) was dissolved under a nitrogen atmosphere in dry DMSO (25 ml) and a sodium hydride suspenion (3.20 g, ~80 mmol NaH, 60% suspension in an oil) was slowly added. After complete addition the mixture was stirred for further 20 min and 1-iodobutane (7.85 g, 42.7 mmol) was added dropwise. The mixture was heated up to 60°C for 1 h, cooled down afterwards and water (100 ml) was slowly added to destroy excess amounts of sodium hydride. The aqueous solution was extracted with CH_2Cl_2 (3 x 80 ml), the organic layers were combined and extracted with water (2 x 100 ml) again. The organic layer was dried over $MgSO_4$ and the solvent was evaporated. The crude product was purified by flash-chromatography (silica) with CH_2Cl_2 / PE (1 : 5) to obtain a colourless oil.

Formula: $C_{16}H_{17}NS$ (255.38).

Yield: 9.73 g (38.1 mmol, 95 %) of a colourless oil.

^{1}H-NMR (400 MHz, acetone–d_6, 300 K): δ / ppm = 7.19-7.11 (4H, phenothiazine), 6.98-6.89 (4H, phenothiazine), 3.89 (t, 2H, H-7), 1.74 (p, 2H, H-8), 1.44 (st, 2H, H-9), 0.88 (t, 2H, H-10).

{^{1}H}^{13}C-NMR (101 MHz, acetone–d_6, 300 K): δ / ppm = 146.1 (quart.), 128.1 (CH), 127.9 (CH), 125.5 (quart.), 123.1 (CH), 116.5 (CH), 47.4 (CH_2), 29.4 (CH_2), 20.5 (CH_2), 14.0 (CH_3).

11.2.2.9 3-Bromo-10-butylphenothiazine (14) [354]

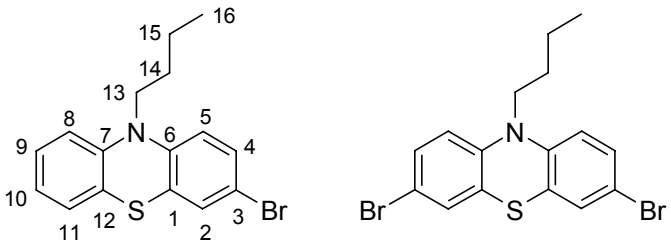

A solution of 10-butylphenothiazine (**13**) (2.00 g, 7.83 mmol) in benzene (18 ml) and EtOH (18 ml) was cooled to 0 °C and pyridinum bromide perbromide (3.00 g, 9.84 mmol; recrystalised from acetic acid) was added over 30 min. The deep brown solution was stirred over night and decolourises. The solution was extracted with water (50 ml) and the aqueous layer was extracted again with CH_2Cl_2 (3 x 30 ml). The combined organic layers were dried over $MgSO_4$ and the solvent was evaporated. The crude product was purified by flash-chromatography (silica) with PE to obtain a colourless oil.
A mixture of 3-bromo-10-butylphenothiazine and 3,6-dibromo-10-butylphenothiazine was obtained which could not be purified by column-chromatography and was used without further purification

Formula: $C_{16}H_{16}BrNS$ (334.28).

Yield: 9.73 g (38.1 mmol, 95 %) of a colourless oil.

^{1}H-NMR (400 MHz, acetone–d_6, 300 K): δ / ppm = 7.29 (dd, 1H, $^3J_{HH}$ = 8.3 Hz, $^4J_{HH}$ = 2.0 Hz, H-4), 7.21 (d, 1H, $^4J_{HH}$ = 1.9 Hz, H-2), 7.17 (ddd, 1H, $^3J_{HH}$ = 7.5 Hz, $^4J_{HH}$ = 1.5 Hz, H-9 o. 10), 7.10 (dd, 1H, $^3J_{HH}$ = 7.6 Hz, $^4J_{HH}$ = 1.5 Hz, H-8 o. 11), 6.97-6.90 (3H, H-5, H-9 o. 10, H-8 o. 11), 3.88 (t, 2H, H-13), 1.72 (p, 2H, H-14), 1.42 (st, 2H, H-15), 0.86 (t, 2H, H-16).

11.2.2.10 10-Butyl-3-(trimethylsilanylethynyl)phenothiazine (15)

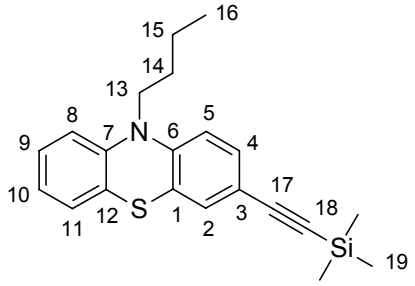

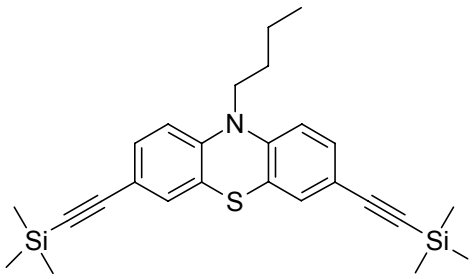

Synthesis according to GP4:

Quantity:	3-Bromo-10-butylphenothiazine (**14**):	3.00 g	8.97 mmol
	Ethynyltrimethylsilane:	3.87 g	16.3 mmol
	$Pd(PhCN)_2Cl_2$:	86.1 mg	220 μmol
	CuI:	28.4 mg	150 μmol
	P^tBu_3 (0.33 M solution in hexane):	88.9 mg	440 μmol
	Dry dioxane:	15 ml	

The crude product was purified by flash-chromatography (silica) eluting with PE > EtOAc / PE (1 : 20) to obtain a yellow oil.

A mixture of 10-butyl-3-(trimethylsilanylethynyl)phenothiazine (**15**) and 10-butyl-3,6-bis(trimethylsilanylethynyl)phenothiazine was obtained which could not be purified by column-chromatography and was used without further purification

Formula: $C_{25}H_{31}NSSi$ (351.59).

Yield: 9.73 g of a yellow oil.

^{1}H-NMR (400 MHz, acetone–d_6, 300 K): δ / ppm = 7.28 (dd, 1H, $^3J_{HH}$ = 8.5 Hz, $^4J_{HH}$ = 1.9 Hz, H-4), 7.21-7.17 (2H, phenothiazine), 7.08 (dd, 1H, $^3J_{HH}$ = 7.6 Hz, $^4J_{HH}$ = 1.4 Hz, H-8 o. 11), 7.04-6.93 (3H, phenothiazine), 3.95 (t, 2H, H-13), , 1.76 (q, 2H, H-14), 1.46 (st, 2H, H-15), 0.92 (t, 3H, H-16), 0.02 (s, 9H, H-19).

11.2.2.11 10-Butyl-3-ethynylphenothiazine (16)

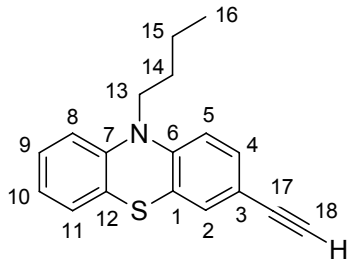

Synthesis according to GP5:

Quantity:	10-Butyl-3-(trimethylsilanylethynyl)phenothiazine (**15**):		
		880 mg	2.89 mmol
	K_2CO_3:	590 mg	4.33 mmol
	Dry MeOH:	15 ml	
	Dry CH_2Cl_2:	5 ml	

The crude product was purified by flash-chromatography (silica) with PE / CH_2Cl_2 (10 : 1) to obtain a yellow oil.

Formula: $C_{18}H_{17}NS$ (279.40).

Yield: 726 mg (2.60 mmol, 90 %) of a yellow oil.

^{1}H-NMR (400 MHz, acetone–d_6, 300 K): δ / ppm = 7.30 (dd, 1H, $^3J_{HH}$ = 8.5 Hz, $^4J_{HH}$ = 2.0 Hz, H-4), 7.23-7.20 (2H, phenothiazine), 7.13 (dd, 1H, $^3J_{HH}$ = 7.6 Hz, $^4J_{HH}$ = 1.4 Hz, H-8 o. 11), 7.05-6.94 (3H, phenothiazine), 3.95 (t, 2H, H-13), 3.57 (s, 1H, H-18), 1.76 (q, 2H, H-14), 1.46 (st, 2H, H-15), 0.92 (t, 3H, H-16).

{^{1}H}^{13}C-NMR (101 MHz, acetone–d_6, 300 K): δ / ppm = 146.8 (quart.), 145.6 (quart.), 132.2 (CH), 130.9 (CH), 128.5 (CH), 128.1 (CH), 125.3 (quart.), 124.7 (quart.), 123.7 (CH), 117.0 (quart.), 116.9 (CH), 116.4 (CH), 83.6 (CH), 78.8 (quart.), 47.6 (CH_2), 29.3 (CH_2), 20.5 (CH_2), 14.0 (CH_3).

11.2.3 Synthesis of Anchor-Functions

11.2.3.1 Thioacetic acid S-(4-iodophenyl) ester (17) [221]

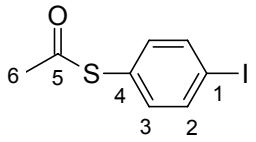

CA: [69746-43-6]

A solution of pipsyl chloride (1.51 g, 5.00 mmol) and dimethylacetamide (1.30 g, 15.0 mmol) in dry 1,2-dichloroethane (40 ml) was added dropwise to a suspension of zinc powder (1.13 g, 17.5 mmol) and dichlorodimethylsilane (2.12 ml, 17.5 mmol) in dry 1,2-dichloroethane (40 ml) under a nitrogen atmosphere during 30 min. The mixture was stirred for 1.5 h at 75°C. K_2CO_3 powder (380 mg, 2.75 mmol) was added when the zinc powder alomst disappeared and the mixture was stirred for another 30 min at 75°C. The mixture was cooled to room temperature, acetyle chloride (1.42 ml, 20.0 mmol) was added and the mixture was allowed to stir at room temperature overnight. The filtered solution was washed with brine and dried over $MgSO_4$. After filtration, the solvent was evaporated under reduced pressure. The crude product was purified by flash-chromatography (silica) with CH_2Cl_2 / PE (1 : 1) to obtain a colourless solid.

Formula: C_8H_7IOS (278.11).

Yield: 1.15 g (4.13 mmol, 83 %) of a colourless solid.

^{1}H-NMR (400 MHz, acetone–d_6, 300 K): δ / ppm = 7.83 (AA´, 2H, H-2 o. 3), 7.22 (BB´, 2H, H-2 o. 3), 2.42 (s, 3H, H-6).

{^{1}H}^{13}C-NMR (101 MHz, acetone–d_6, 300 K): δ / ppm = 192.8 (quart.), 139.2 (CH), 137.0 (CH), 129.3 (quart.), 96.0 (quart.), 30.0 (CH_3).

Melting point (CH_2Cl_2, PE): 55 °C.

11.2.3.2 1-(S-Acetylthiomethyl)-4-iodobenzene (18) [105]

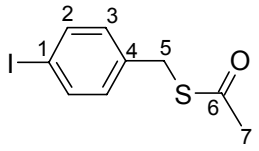

CA: [307537-93-5]

Potassium thioacetate (1.11 g, 9.69 mmol) was added to a solution of 1-(bromomethyl)-4-iodobenzene (2.40 g, 8.08 mmol) in dry *N,N*-dimethylacetamide (7.5 ml) under a nitrogen atmosphere. The mixture was stirred overnight at room temperature, poured into water (25 ml) and extracted with CH_2Cl_2 (3 x 25 ml). The organic phases were combined, dried over $NaSO_4$ and the solvent was evaporated. The crude product was purified by flash-chromatography (silica) eluting with CH_2Cl_2 / PE (1 : 3) to obtain a light yellow solid.

Formula: C_9H_9IOS (292.13).

Yield: 2.05 g (7.02 mmol, 87 % (99 %)) [105] of a light yellow solid.

^{1}H-NMR (400 MHz, $CDCl_3$, 300 K): δ / ppm = 7.61 (AA', 2 H, H-2 o. 3), 7.04 (BB', 2 H, H-2 o. 3), 4.04 (s, 2 H, H-5), 2.34 (s, 3 H, H-7).

{^{1}H}^{13}C-NMR (101 MHz, $CDCl_3$, 300 K): δ / ppm = 194.8 (quart.), 137.7 (CH), 137.5 (quart.), 130.8 (CH), 92.6 (quart.), 32.9 (CH_2), 30.3 (CH_3).

Melting point (CH_2Cl_2, PE): 45 °C (40 – 41 °C). [105]

11.2.4 Synthesis of Bridge-Units

11.2.4.1 1,4-Dipropoxybenzene (19) [355]

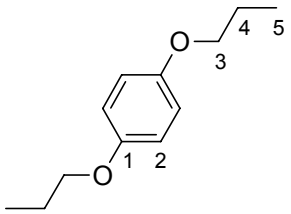

CA: [3898-41-7]

Hydroquinone (58.3 g, 530 mmol) was dissolved in dry and degassed EtOH (500 ml) under a nitrogen atmosphere. After addition of KOH (73.3 g, 1.31 mol), the solution was stirred under reflux for 20 min. 1-Bromopropane (91.1 g, 1.16 mol) was added to the light brown solution over 40 min, followed by stirring under reflux for 2 h. The solvent was evaporated and the residue was dissolved in CH_2Cl_2 (300 ml) and extracted with water (3 x 100 ml). The combined organic phases were washed with saturated $NaHCO_3$, dried with $MgSO_4$ and the solvent was removed in vacuo. The remaining solid was recrystallised from MeOH to obtain a colourless solid.

Formula: $C_{12}H_{18}O_2$ (194.28).

Yield: 101 g (519 mmol, 98 %, lit.: 85 %) [355] of a colourless solid.

^{1}H-NMR (400 MHz, $CDCl_3$, 300 K): δ / ppm = 6.82 (s, 4H, H-2), 3.87 (t, 4H, H-3), 1.78 (s, 4H, H-4), 1.02 (t, 6H, H-5).

{^{1}H}^{13}C-NMR (101 MHz, Aceton–d_6, 300 K): δ / ppm = 153.4 (C-1), 115.6 (C-2), 70.3 (C-3), 22.8 (C-4), 10.6 (C-5).

Melting point (MeOH): 49 °C.

11.2.4.2 1-Bromo-2,5-dipropoxybenzene (20) [355]

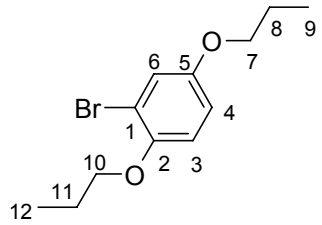

CA: [216306-43-3]

1,4-Dipropoxybenzene (**19**) (32.7 g, 170 mmol) and sodium acetate (13.3 g, 165 mmol) were dissolved in acetic acid (100 ml). At 0°C, bromine (26.9 g, 168 mmol) was slowly added to the solution over 2.5 h. After stirring for 12 h at room temperature, the mixture was poured into water (750 ml). After extraction with CH_2Cl_2 (4 x 100 ml), the organic phases were neutralised with saturated $NaHCO_3$ and dried with $MgSO_4$. The solvent was evaporated and the remaining brown oil was distilled twice under vacuum (0.5 mbar) to obtain a light yellow oil.

Formula: $C_{12}H_{17}BrO_2$ (273.17).

Yield: 29.8 g (109 mmol, 65 %, lit.: 76 %) [355] of a light yellow oil.

^{1}H-NMR (400 MHz, $CDCl_3$, 300 K): δ / ppm = 7.12 (d, 1H, $^4J_{HH}$ = 2. Hz, H-6), 6.82 (d, 1H, $^3J_{HH}$ = 8. Hz, H-3), 6.78 (dd, 1H, $^3J_{HH}$ = 8.7 Hz, $^4J_{HH}$ = 2.8 Hz, H-4), 3.91 (t, 2H, H-7 o. 11), 3.89 (t, 2H, H-7 o. 8), 1.87-1.73 (4H, H-8, 11), 1.08-1.00 (6H, H-9, 12).

{^{1}H}^{13}C-NMR (101 MHz, $CDCl_3$, 300 K): δ / ppm = 153.7 (quart.), 149.9 (quart.), 119.6 (CH), 114.8 (CH), 114.5 (CH), 112.9 (quart.), 71.8 (CH_2), 70.4 (CH_2), 22.8 (CH_2), 22.7 (CH_2), 10.7 (CH_3), 10.6 (CH_3).

11.2.4.3 1-Bromo-4-iodo-2,5-dipropoxybenzene (21) [355]

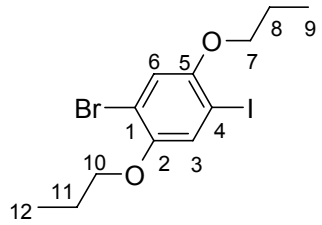

CA: [216306-45-5]

1-Bromo-2,5-dipropoxybenzene (**20**) (22.5 g, 85.0 mmol) was dissolved in acetic acid (55 ml) and CCl_4 (14 ml). To this solution were added iodine (20.7 g, 80.0 mmol), conc. H_2SO_4 (7 ml), water (3.5 ml) and finally potassium iodate (7.25 g, 35.0 mmol). The mixture was stirred for 5 h under reflux. To remove excess iodine $Na_2S_2O_3$ was added until the violet colour of the iodine disappeared. The mixture was poured into ice / water (500 ml) and was extracted with CH_2Cl_2 (3 x 100 ml). The organic phase was neutralised with a saturated $NaHCO_3$-solution and dried over $MgSO_4$. The solvent was evaporated and the residue was recrystallised from MeOH to obtain a colourless solid.

Formula: $C_{12}H_{16}BrIO_2$ (399.07).

Yield: 24.3 g (60.8 mmol, 76 %, lit.: 77 %) [355] of a colourless solid.

^{1}H-NMR (400 MHz, $CDCl_3$, 300 K): δ / ppm = 7.28 (s, 1H, H-3), 6.98 (s, 1H, H-6), 3.93-3.88 (4H, H-7,10), 1.86-1.77 (4H, H-8,11), 1.09-1.03 (6H, H-9,12).

{^{1}H}^{13}C-NMR (101 MHz, $CDCl_3$, 300 K): δ / ppm = 152.7 (quart.), 150.6 (quart.), 124.5 (CH), 117.2 (CH), 112.7 (quart.), 84.9 (quart.), 71.9 (CH_2), 71.8 (CH_2), 22.71 (CH_2), 22.68 (CH_2), 10.8 (CH_3), 10.6 (CH_3).

Melting point (MeOH): 77 °C.

11.2.4.4 1-Bromo-2,5-dipropoxy-4-trimethylsilylethynylbenzene (22)

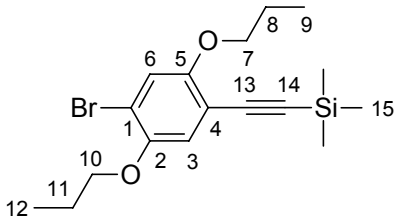

CA: [406721-40-2]

Synthesis according to GP2:

Quantity:	Ethynyltrimethylsilane:	491 mg	5.00 mmol
	1-Bromo-4-iodo-2,5-dipropoxybenzene (**21**):		
		2.00 g	5.01 mmol
	$(PPh_3)_2PdCl_2$:	105 mg	150 μmol
	CuI:	57.0 mg	300 μmol
	Dry Et_2NH:	10 ml	

The crude product was purified by flash-chromatography (silica) eluting with CH_2Cl_2 / PE (1 : 2) to obtain a colourless solid.

Formula: $C_{17}H_{25}BrO_2Si$ (369.38).

Yield: 1.55 g (4.20 mmol, 84 %) of a colourless solid.

^{1}H-NMR (400 MHz, $CDCl_3$, 300 K): δ / ppm = 7.04 (s, 1H, H-6), 6.93 (s, 1H, H-3), 3.93-3.89 (4H, H-7,10), 1.84-1.78 (4H, H-8,11), 1.09-1.03 (6H, H-9,12), 0.25 (s, 9H, H-15).

{^{1}H}^{13}C-NMR (101 MHz, acetone–d_6, 300 K): δ / ppm = 154.9 (quart.), 149.5 (quart.), 118.3 (CH), 118.1 (CH), 113.7 (quart.), 112.7 (quart.), 100.8 (quart.), 99.4 (quart.), 71.7 (CH_2), 71.5 (CH_2), 22.8 (CH_2), 22.7 (CH_2), 10.7 (CH_3), 10.6 (CH_3), 0.1 (CH_3).

Melting point (CH_2Cl_2, PE): 64 °C.

11.2.4.5 1-Iodo-2,5-dipropoxy-4-trimethylsilanylethynylbenzene (23) [231]

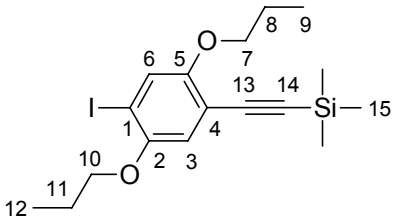

CA: [221292-49-5]

A solution of 1-bromo-2,5-dipropoxy-4-trimethylsilyethynylbenzene (**22**) (1.00 g, 2.70 mmol) in dry THF (15 ml) was cooled to -78 °C under a nitrogen atmosphere and a solution of ^{n}BuLi (1.6 M in hexane, 3.20 mmol, 2.00 ml) was added at such a rate that the internal temperature did not exceed -80 °C. This cold solution was added via a cannula to a solution of iodine (786 mg, 3.10 mmol) in dry THF (10 ml) at -60 °C. After addition, the cooling bath was removed and the reaction mixture was stirred for 30 min. After disscolouring by adding saturated an aqueous $Na_2S_2O_3$-solution, the water phase was extracted with Et_2O (3 x 50 ml) and the combined organic phases were dried over $MgSO_4$. The solvent was removed and the crude product was purified by flash-chromatography (silica) eluting with Et_2O / PE (2 : 98) to obtain a colourless solid.

Formula: $C_{17}H_{25}IO_2Si$ (416.38).

Yield: 989 mg (2.38 mmol, 88 %, lit.: 86 %) [231] of a colourless solid.

^{1}H-NMR (400 MHz, $CDCl_3$, 300 K): δ / ppm = 7.27 (s, 1H, H-6), 6.83 (s, 1H, H-3), 3.93-3.89 (4H, H-7,10), 1.84-1.78 (4H, H-8,11), 1.09-1.04 (6H, H-9,12), 0.25 (s, 9H, H-15).

{^{1}H}^{13}C-NMR (101 MHz, acetone–d_6, 300 K): δ / ppm = 155.1 (quart.), 151.9 (quart.), 124.2 (CH), 116.3 (CH), 113.7 (quart.), 101.0 (quart.), 99.5 (quart.), 88.0 (quart.), 71.7 (CH_2), 71.5 (CH_2), 22.8 (CH_2), 22.7 (CH_2), 10.9 (CH_3), 10.7 (CH_3), 0.0 (CH_3).

Melting point (MeOH): 46 °C.

11.2.4.6 2-Cyano-4-iodoaniline (24) [232]

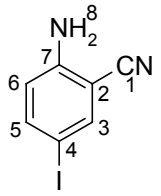

CA: [132131-24-9]

2-Cyanoaniline (25.0 g, 210 mmol) was dissolved in a mixture of water (625 ml) and conc. HCl (37 %, 60 ml) and the solution was cooled to 20 °C. A solution of iodine monochloride (34.7 g, 214 mmol) in a mixture of water (125 ml) and conc. HCl (37%, 35 ml) was cooled to 5°C and was added rapidly to the cyanoaniline mixture at 20°C. The solution was stirred for 2 h while a brown solid precipitated. The product was filtered and washed with cold water (4 x 100 ml). The crude product was recrystallised from EtOH to obtain a brown solid.

Formula: $C_7H_5N_2I$ (224.03 g/mol).

Yield: 38.3 g (0.16 mol, 74%, lit.: 81%) [232] of a brown solid.

^{1}H-NMR (400 MHz, $CDCl_3$, 300 K): δ / ppm = 7.65 (dd, $^4J_{HH}$ = 2.1 Hz, $^5J_{HH}$ = 0.3 Hz, 1 H, H-3), 7.56 (dd, $^3J_{HH}$ = 8.7 Hz, $^4J_{HH}$ = 2.1 Hz, 1 H, H-5), 7.53 (dd, $^3J_{HH}$ = 8.7 Hz, $^5J_{HH}$ = 0.3 Hz, 1 H, H-6), 4.44 (s, 2 H, H-8).

{^{1}H}^{13}C-NMR (101 MHz, $CDCl_3$, 300 K): δ / ppm = 149.2 (quart.), 142.6 (CH), 140.1 (CH), 117.2 (CH), 116.2 (quart.), 98.4 (quart.), 77.1 (quart.).

Melting point (EtOH): 86 °C, lit.: 85-87 °C. [232]

11.2.4.7 2-Amino-5-trimethylsilylethynylbenzonitrile (25) [233]

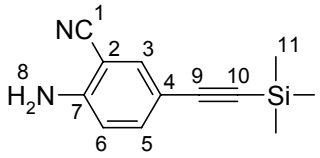

CA: [518342-60-4]

Synthesis according to GP2:

Quantity:	2-Cyano-4-iodoaniline (**24**):	20.0 g	82.0 mmol
	Ethynyltrimethylsilane:	9.27 g	94.4 mmol
	$Pd(PPh_3)_2Cl_2$:	1.15 g	1.64 mmol
	CuI:	160 mg	82.0 mmol
	Dry Et_2NH:	25 ml	

Water (75 ml) was added and the solution was extracted with Et_2O (4 x 75 ml). The combined organic phases were washed with aqueous NH_4Cl (2 M, 2 x 40 ml, brine (50 ml) and dried over $NaSO_4$. The product was used without further purification.

Formula: $C_{12}H_{14}N_2Si$ (214.34 g/mol).

Yield: 17.4 g (81.2 mmol, 99 %, lit.: 91% [Hwang, 2002 #505; Hwang, 2002 #222]) of a brown solid.

^{1}H-NMR (400 MHz, $CDCl_3$, 300 K): δ / ppm = 7.52 (dd, $^4J_{HH}$ = 2.0 Hz, $^5J_{HH}$ = 0.5 Hz, 1 H, H-3), 7.40 (dd, $^3J_{HH}$ = 8.6 Hz, $^4J_{HH}$ = 2.0 Hz, 1 H, H-5), 6.66 (dd, $^3J_{HH}$ = 8.6 Hz, $^5J_{HH}$ = 0.5 Hz, 1 H, H-6), 4.54 (s, 2 H, H-8), 0.23 (s, 9 H, H-11).

{^{1}H}^{13}C-NMR (101 MHz, $CDCl_3$, 300 K): δ / ppm = 149.3 (quart.), 137.6 (CH), 136.2 (CH), 116.8 (quart.), 115.1 (CH), 113.1 (quart.), 103.4 (quart.), 96.2 (quart.), 93.6 (quart.), 0.1 (CH_3).

Melting point (Et_2O): 126 - 127°C (dest.).

11.2.4.8 2-Iodo-5-trimethylsilylethynylbenzonitrile (26) [233]

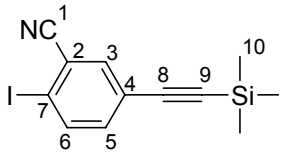

CA: [518342-65-9]

Boron trifluoride etherate (35.3 ml, 280 mmol) was cooled to -25 °C and a solution of 2-amino-5-trimethylsilylethynylbenzonitrile (**25**) (15.0 g, 70.0 mmol) in dry Et_2O (70 ml) was added dropwise over a period of 5 min, followed by adding a solution of *t*butylnitrite (29.2 ml, 245 mmol) in dry Et_2O (50 ml) over 30 min. The chilled mixture was stirred an additional 10 min and the cold bath was allowed to warm to 5°C over 20 min. Et_2O (40 ml, 0 °C) was added and the solution was stirred in an ice-bath for 15 min. The solid was collected by filtration, washed with cold Et_2O (2 x 40 ml, 0 °C) and briefly dried in air to give the diazonium salt. The solid was dissolved in dry MeCN (80 ml) and then added dropwise to a solution of sodium iodide (11.7 g, 78.1 mmol) and iodine (1.78 g, 7.01 mmol) in dry MeCN (80 ml). The mixture was stirred at room temperature for 1 h, then an aqueous solution of $Na_2S_2O_3$ (2 M, 25 ml) and water (75 ml) were added. The mixture was extracted with CH_2Cl_2 (3 x 100 ml) and the combined organic phases were dried over Na_2SO_4. The crude product was purified by flash-chromatography (silica) eluting with EtOAc / PE (5 : 95) to obtain a red oil.

Formula: $C_{12}H_{12}INSi$ (325.22 g/mol).

Yield: 7.71 g (23.7 mmol, 34 %, lit.: 70 %) [233] of a red oil.

^{1}H-NMR (400 MHz, $CDCl_3$, 300 K): δ / ppm = 7.86 (dd, $^3J_{HH}$ = 8.3 Hz, $^5J_{HH}$ = 0.5 Hz, 1 H, H-6), 7.66 (dd, $^4J_{HH}$ = 2.1 Hz, $^5J_{HH}$ = 0.5 Hz, 1 H, H-3), 7.31 (dd, $^3J_{HH}$ = 8.3 Hz, $^4J_{HH}$ = 2.1 Hz, 1 H, H-5), 0.25 (s, 9 H, H-10).

{^{1}H}^{13}C-NMR: (101 MHz, $CDCl_3$, 300 K): δ / ppm = 139.7 (CH), 137.2 (CH), 136.5 (CH), 124.3 (quart.), 121.1 (quart.), 118.7 (quart.), 101.6 (quart.), 99.1 (quart.), 98.0 (quart.), -0.2 (CH_3).

11.2.5 Synthesis of Thioacetic acid S-(11-{4-[bis-(4-methoxyphenyl)amino]-phenoxy}-undecyl) ester (29)

11.2.5.1 11-(4-Iodophenoxy)-1-undecanol (27) [356]

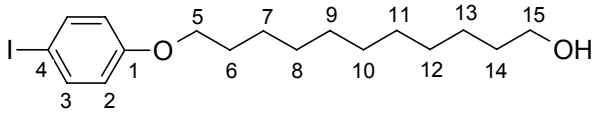

To a solution of 4-iodophenol (2.20 g, 10.0 mmol) in dry EtOH (100 ml) a solution of KOH (720 mg, 12.8 mmol) in dry EtOH (20 ml) was added under a nitrogen atmosphere. After refluxing the mixture for 1 h a solution of 11-bromo-1-undecanol (2.50 g, 10.0 mmol) in dry EtOH (5 ml) was added dropwise over a period of 10 min to the reaction mixture and the resulting solution was refluxed for 18 h. As the solution cooled, it became cloudy with a KBr precipitate. The solvent was removed, water (100 ml) was added and the resulting solution was extracted with CH_2Cl_2 (3 x 100 ml). The organic phases were dried over $MgSO_4$ and the solvent was evaporated. The product was obtained by flash-chromatography (silica) eluting with EtOAc / PE (1 : 2) as a colourless solid.

Formula: $C_{17}H_{27}IO_2$ (390.30).

Yield: 2.85 g (7.31 mmol, 73 %) of a colourless solid.

^{1}H-NMR (400 MHz, benzene-d_6, 300 K): δ / ppm = 7.38 (AA', 2H, H-2 o. 3), 6.50 (BB', 2H, H-2 o. 3), 3.60 (t, 2H, H-5 o. 15), 2.30 (t, 2H, H-5 o. 15), 1.59-1.43 (4H, H-6, 14), 1.35-1.18 (14H, H-7-13).

{^{1}H}^{13}C-NMR (101 MHz, benzene-d_6, 300 K): δ / ppm = 159.5 (quart.), 138.4 (CH), 117.2 (CH), 82.8 (quart.), 50.1 (CH_2), 30.2 (CH_2), 29.9 (CH_2), 29.85 (CH_2), 29.81 (CH_2), 29.7 (CH_2), 29.6 (CH_2), 29.3 (CH_2), 29.1 (CH_2), 26.3 (CH_2).

11.2.5.2 Thioacetic acid S-[11-(4-iodophenoxy)undecyl] ester (28) [357]

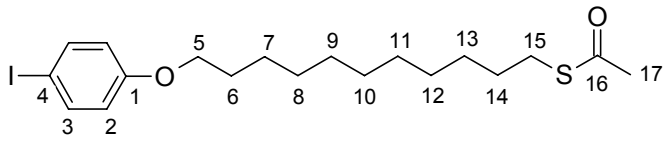

A mixture of diisopropyl azodicarboxylate (1.04 g, 5.12 mmol) and triphenylphosphine (0.67 g, 2.56 mmol) in dry THF (30 ml) was stirred for 1 h under nitrogen atmosphere at 0 °C. A solution of 11-(4-iodophenoxy)-1-undecanol (**27**) (1.00 g, 2.56 mmol) in dry THF (20 ml) was slowly added and the mixture was stirred at 20 °C for 1 h. Thioacetic acid (195 mg, 2.56 mg) was added and the reaction mixture was stirred for a further 18 h. After evaporation of the solvent the residue was purified by flash-chromatography (silica) eluting the product with CH_2Cl_2 / PE (1 : 4) as a light yellow oil.

Formula: $C_{19}H_{29}IO_2S$ (448.41).

Yield: 515 mg (1.15 mmol, 45 %) of a light yellow oil.

^{1}H-NMR (400 MHz, benzene-d_6, 300 K): δ / ppm = 7.40 (AA', 2H, H-2 o. 3), 6.42 (BB', 2H, H-2 o. 3), 3.47 (t, 2H, H-5 o. 15), 2.80 (t, 2H, H-5 o. 15), 1.90 (s, 3H, H-17), 1.57-1.45 (4H, H-6, 14), 1.31-1.21 (14H, H-7-13).

{^{1}H}^{13}C-NMR (101 MHz, benzene-d_6, 300 K): δ / ppm = 194.3 (C-16), 159.5 (quart.), 138.6 (CH), 117.2 (CH), 82.7 (quart.), 68.0 (CH_3), 30.3 (CH_3), 30.2 (CH_2), 30.1 (CH_2), 29.92 (CH_2), 29.87 (CH_2), 29.8 (CH_2), 29.7 (CH_2), 29.5 (CH_2), 29.3 (CH_2), 29.1 (CH_2), 26.3 (CH_2).

Melting point (CH_2Cl_2, PE): 43 °C.

11.2.5.3 Thioacetic acid S-(11-{4-[bis-(4-methoxyphenyl)amino]phenoxy}-undecyl) ester (29)

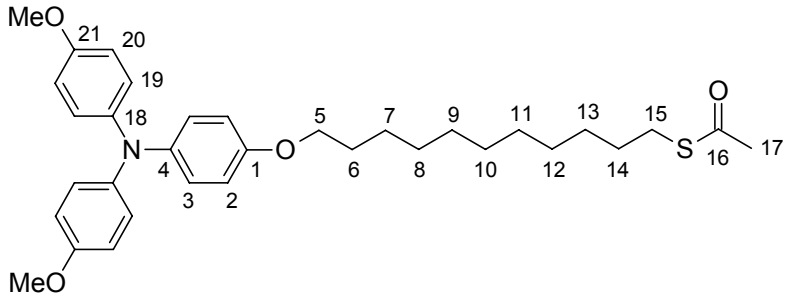

A solution of bis(4-methoxyphenyl)amine (146 mg, 0.64 mmol), thioacetic acid S-[11-(4-iodophenoxy)undecyl] ester (**28**) (290 mg, 0.64 mmol), sodium-*tert*-butanolate (44.1 mg, 0.64 mmol), $Pd_2(dba)_3$*$CHCl_3$ (33.1 mg, 32.0 μmol) and DPPF (26.6 mg, 48.0 μmol) in dry toluene (7 ml) was heated up to 40°C for 20 h under nitrogen atmosphere. The solvent was evaporated, CH_2Cl_2 (50 ml) was added and the solution was extracted with water (50 ml). The aqueous layer was extracted once again with CH_2Cl_2 (2 x 75 ml), the organic phases were dried over $MgSO_4$ and the solvent was removed. The residue was cleaned by flash-chromatography (silica) eluting with CH_2Cl_2 / PE (1 : 2) to get a yellow oil.

Formula: $C_{33}H_{43}NO_4S$ (549.77).

Yield: 102 mg (185 μmol, 29 %) of a yellow oil.

^{1}H-NMR (400 MHz, acetone-d_6, 300 K): δ / ppm = 6.93 (6H, H-2 o. 3, H-19 o. 20), 6.84 (6H, H-2 o. 3, H-19 o. 20), 3.96 (t, 2H, H-5), 3.76 (s, 6H, -OMe), 2.86 (t, 2H, H-15), 2.29 (s, 3H, H-17), 1.76 (s, 2H, H-6 o. 14), 1.56 (s, 2H, H-6 o. 14), 1.48-1.32 (14H, H-7-13).

{^{1}H}^{13}C-NMR (101 MHz, acetone-d_6, 300 K): δ / ppm = 195.4 (quart.), 156.2 (quart.), 155.7 (quart.), 143.4 (quart.), 142.8 (quart.), 125.62 (CH), 125.59 (CH), 116.0 (CH), 115.4 (CH), 68.5 (CH_2), 68.4 (CH_2), 55.5 (CH_3), 30.31 (CH_3), 30.2 (CH_2), 29.9 (CH_2), 29.93 (CH_2), 29.87 (CH_2), 29.6 (CH_2), 29.19 (CH_2), 29.15 (CH_2), 26.5 (CH_2).

EI-MS (high resolution, PI): calc. m/z = 549.29073
found m/z = 549.29072 Δ = 0.02 ppm

11.2.6 Synthesis of 4-[Bis-(4-methoxyphenyl)amino]benzoic acid-10-mercaptodecyl ester (32)

11.2.6.1 4-[Bis(4-methoxyphenyl)amino]benzoic acid (30)

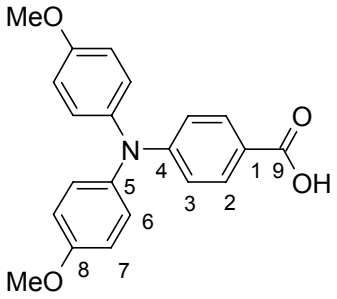

CA: [704914-80-7]

To a solution of bis(4-methoxyphenyl)-(4-bromophenyl)amine (**6**) (1.33 g, 3.46 mmol) in dry THF (30 ml) ^{t}BuLi (7.68 mmol of a 1.6 M solution in hexane) was added under an atmosphere of nitrogen. Afterwards carbon dioxid (dried over conc. H_2SO_4) was discharged through the solution at -78 °C meanwhile the reaction mixture came up to room temperature. Water (50 ml) was added and the solution was extracted with CH_2Cl_2 (3 x 100 ml). The organic phase was dried over $MgSO_4$ and the solvent was removed in vacuo. The yellow residue was solved in less CH_2Cl_2 and dropped in MeOH to get a yellow precipitate.

Formula: $C_{21}H_{19}NO_4$ (349.39).

Yield: 0.98 g (2.80 mmol, 81 %) of a yellow solid.

^{1}H-NMR (400 MHz, acetone–d_6, 300 K): δ / ppm = 7.66 (AA´, 2H, H-2 o. 3), 7.04 (AA´, 4H, H-6 o. 7), 6.83 (BB´, 4H, H-6 o. 7), 6.61 (BB´, 2H, H-2 o. 3), 3.67 (s, 6H, -OMe).

{^{1}H}^{13}C-NMR (101 MHz, acetone–d_6, 300 K): δ / ppm = 167.6 (quart.), 158.3 (quart.), 153.9 (quart.), 140.2 (quart.), 131.8 (CH), 129.0 (CH), 121.2 (quart.), 117.1 (CH), 115.9 (CH), 55.7 (CH_3).

11.2.6.2 4-[Bis-(4-methoxyphenyl)amino]benzoic acid-10-bromodecyl ester (31) [357]

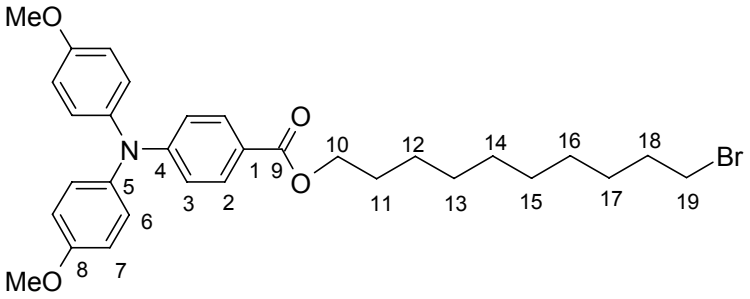

To a suspension of 4-[bis(4-methoxyphenyl)amino]benzoic acid (**30**) (200 mg, 0.52 mmol) in dry CH_2Cl_2 (5 ml) dicyclohexylcarbodiimide (166 mg, 0.81 mmol) was added and the mixture was stirred for 10 min at 0°C under nitrogen atmosphere. 10-bromo-1-decanol (155 mg, 0.65 mmol) and 4-(dimethylamino)pyridine (18.7 mg, 0.15 mmol) were added, and the mixtures was stirred at room temperature for 24 h. The solution was filtered and the filtrate was evaporated. The product was obtained by flash-chromatography (silica) eluting with CH_2Cl_2 / PE (1 : 2) as a yellow oil.

Formula: $C_{31}H_{38}BrNO_4$ (568.56).

Yield: 174 mg (0.31 mmol, 59 %) of a yellow oil.

^{1}H-NMR (400 MHz, acetone–d_6, 300 K): δ / ppm = 7.79 (AA´, 2H, H-2 o. 3), 7.16 (AA´, 4H, H-6 o. 7), 6.97 (BB´, 4H, H-6 o. 7), 6.76 (BB´, 2H, H-2 o. 3), 4.23 (t, 2H, H-10), 3.82 (s, 6H, -OMe), 3.48 (t, 2H, H-10), 1.87-1.70 (4H, H-11,19), 1.50-1.33 (14H, H-12-18).

{^{1}H}^{13}C-NMR (101 MHz, acetone–d_6, 300 K): δ / ppm = 206.5 (quart.), 166.9 (quart.), 158.6 (quart.), 154.2 (quart.), 140.5 (quart.), 131.8 (CH), 129.3 (CH), 117.5 (CH), 116.3 (CH), 65.2 (CH_2), 56.1 (CH_3), 35.1 (CH_2), 34.0 (CH_2),

29.8 (CH_2), 29.7 (CH_2), 29.6 (CH_2), 29.5 (CH_2), 29.1 (CH_2), 28.9 (CH_2), 27.1 (CH_2).

11.2.6.3 4-[Bis-(4-methoxyphenyl)amino]benzoic acid-10-mercaptodecyl ester (32) [357]

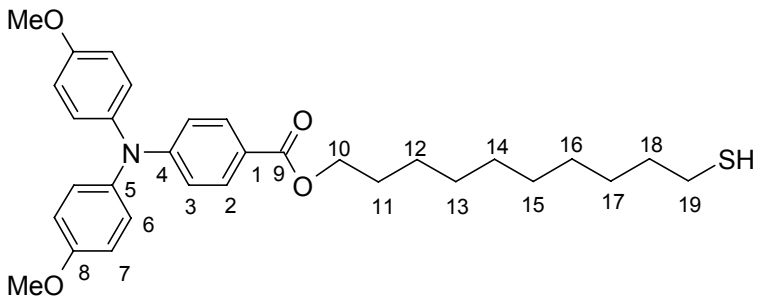

A solution of 4-[bis-(4-methoxyphenyl)amino]benzoic acid-10-bromodecyl ester (**31**) (150 mg, 0.26 mmol) and thiourea (60.9 mg, 0.80 mmol) in dry ethanol (30 ml) was stirred at reflux under nitrogen for 24 h. After the solution was cooled to room temperature the solvent was removed and an aqueous potassium hydroxide solution (1 M, 15 ml) was added to the residue. The mixture was stirred at reflux for 24 h. After the mixture was cooled to room temperature it was extracted with diethyl ether (3 x 50 ml), the combined organic layers were dried over $MgSO_4$ and the solvent was evaporated. Flash-chromatography (silica) of the residue eluting with CH_2Cl_2 / PE (2 : 1) > DCM / MeOH (9 : 1) afforded the product as a yellow oil.

Formula: $C_{31}H_{39}NO_4S$ (521.72).

Yield: 48.8 mg (93.6 μmol, 36 %) of a yellow oil.

^{1}H-NMR (400 MHz, CD_2Cl_2, 300 K): δ / ppm = 7.75 (AA´, 2H, H-2 o. 3), 7.09 (AA´, 4H, H-6 o. 7), 6.88 (BB´, 4H, H-6 o. 7), 6.77 (BB´, 2H, H-2 o. 3), 4.21 (t, 2H, H-10), 3.79 (s, 6H, -OMe), 2.67 (t, 2H, H-20), 1.75-1.64 (4H, H-11,19), 1.50-1.33 (14H, H-12-18).

{^{1}H}^{13}C-NMR (101 MHz, CD_2Cl_2, 300 K): δ / ppm = 166.7 (quart.), 157.5 (quart.), 153.1 (quart.), 139.8 (quart.), 130.9 (CH), 128.2 (CH), 121.0 (quart.),

117.2 (CH), 115.3 (CH), 64.8 (CH_2), 55.8 (CH_3), 39.5 (CH_2), 33.2 (CH_2), 29.84 (CH_2), 29.80 (CH_2), 29.64 (CH_2), 29.59 (CH_2), 29.56 (CH_2), 29.2 (CH_2), 28.9 (CH_2).

IR (KBr): $\tilde{\nu}$ / cm^{-1} = 3292 (vw), 2927 (m, C-H), 2860 (m, C-H), 1705 (m), 1597 (m), 1505 (s), 1270 (s), 1241 (s), 1173 (s), 1030 (m), 829 (m), 767 (m), 575 (w).

ESI-MS (M^+; high resolution): calc. m/z = 521.25998
found m/z = 521.26043 Δ = 0.86 ppm

11.2.7 Synthesis of 3-(10-Sulfanyl-1-decyloxycarbonyl)-10-butyl-phenothiazine (35)

11.2.7.1 10-Butylphenothiazine-3-carboxylic acid (33) [358]

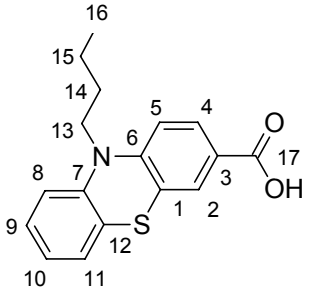

CA: [461384-98-5]

3-Bromo-10-butylphenothiazine (**14**) (2.00 g, 5.98 mmol) was dissolved in dry ether (40 ml) under an atmosphere of nitrogen. Slow addition of ^{n}BuLi (12.0 mmol of a 1.6 M solution in hexane) was carried out at -78 °C and the mixture was stirred for another 50 min at -25°C while a colourless solid precipitated. Afterwards carbon dioxed (dried over conc. H_2SO_4) was discharged through the solution at -78 °C meanwhile the reaction mixture came up to room temperature. Water (50 ml) was added, the solution was acidified with H_2SO_4 (20 %, 20 ml) and was extracted with CH_2Cl_2 (3 x 100 ml). The organic phase

was dried over $MgSO_4$ and the solvent was removed in vacuo. Recrystallisation of the residue from toluene / acetone (5 : 1) gave a yellow solid.

Formula: $C_{17}H_{17}NO_2S$ (299.39).

Yield: 1.62 g (5.41 mmol, 90 %) of a yellow solid.

^{1}H-NMR (400 MHz, acetone–d_6, 300 K): δ / ppm = 7.86 (dd, 1H, $^3J_{HH}$ = 8.6 Hz, $^4J_{HH}$ = 2.0 Hz, H-4), 7.73 (d, 1H, $^4J_{HH}$ = 1.9 Hz, H-2), 7.17 (ddd, 1H, $^3J_{HH}$ = 8.7 Hz, $^4J_{HH}$ = 1.6 Hz, H-9 o. 10), 7.10 (dd, 1H, $^3J_{HH}$ = 7.6 Hz, $^4J_{HH}$ = 1.5 Hz, H-8 o. 11), 7.11-7.07 (2H, H-5, H-8 o. 11), 6.99 (ddd, 1H, $^3J_{HH}$ = 7.60 Hz, $^4J_{HH}$ = 1.16 Hz, H-9 o. 10), 4.02 (t, 2H, H-13), 1.80 (qu, 2H, H-14), 1.49 (sex, 2H, H-15), 0.93 (t, 2H, H-16).

{^{1}H}^{13}C-NMR (101 MHz, acetone–d_6, 300 K): δ / ppm = 206.1 (C-17), 150.4 (quart.), 145.1 (quart.), 130.5 (CH), 129.2 (CH), 128.6 (CH), 128.1 (CH), 125.3 (quart.), 125.0 (quart.), 124.7 (quart.), 124.1 (CH), 117.1 (CH), 116.0 (CH), 47.8 (C-13), 29.4 (C-14), 20.6 (C-15), 14.0 (C-16).

Melting point (toluene, acetone): 138 °C.

11.2.7.2 3-(10-Bromo-1-decyloxycarbonyl)-10-butylphenothiazine (34) [357]

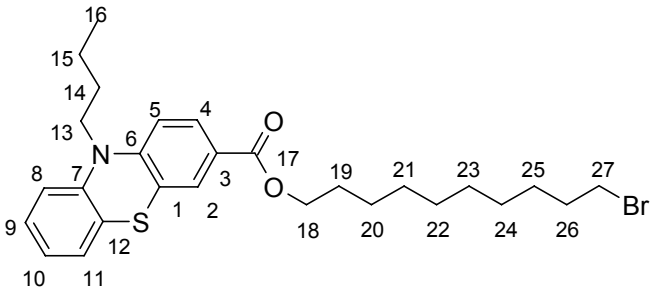

To a suspension of 10-butylphenothiazine-3-carboxylic acid (**33**) (500 mg, 1.67 mmol) in dry CH_2Cl_2 (15 ml) dicyclohexylcarbodiimide (528 mg, 2.56 mmol) was added and the mixture was stirred at 0°C under nitrogen for 10 min. 10-Bromo-1-decanol (493 mg, 2.07 mmol) and 4-(dimethylamino)pyridine (55.5 mg, 0.49 mmol) were added, and the mixture

was stirred at room temperature for 24 h. The solution was filtered and the filtrate was evaporated. The product was obtained by flash-chromatography of the residue (silica) eluting with CH_2Cl_2 / PE (1 : 2 > 2 : 1) as a yellow oil.

Formula: $C_{27}H_{36}BrNO_2S$ (518.56).

Yield: 650 mg (1.25 mmol, 75 %) of a yellow oil.

^{1}H-NMR (400 MHz, acetone–d_6, 300 K): δ / ppm = 7.86 (dd, 1H, $^3J_{HH}$ = 8.6 Hz, $^4J_{HH}$ = 2.0 Hz, H-4), 7.73 (d, 1H, $^4J_{HH}$ = 1.9 Hz, H-2), 7.17 (ddd, 1H, $^3J_{HH}$ = 8.7 Hz, $^4J_{HH}$ = 1.6 Hz, H-9 o. 10), 7.10 (dd, 1H, $^3J_{HH}$ = 7.6 Hz, $^4J_{HH}$ = 1.5 Hz, H-8 o. 11), 7.11-7.07 (2H, H-5, H-8 o. 11), 6.99 (ddd, 1H, $^3J_{HH}$ = 7.6 Hz, $^4J_{HH}$ = 1.2 Hz, H-9 o. 10), 4.29 (t, 2H, H-18), 4.02 (t, 2H, H-13), 3.49 (t, 2H, H-27), 1.87-1.74 (6H, H-15, 19, 26), 1.50-1.35 (12H, H-20-25), 0.94 (t, 3H, H-16).

{^{1}H}^{13}C-NMR (101 MHz, acetone–d_6, 300 K): δ / ppm = 165.9 (C-17), 150.4 (quart.), 145.0 (quart.), 130.1 (CH), 128.8 (CH), 128.6 (CH), 128.1 (CH), 125.3 (quart.), 125.0 (quart.), 124.6 (quart.), 124.1 (CH), 117.2 (CH), 116.0 (CH), 65.4 (CH_2), 47.8 (CH_2), 34.8 (CH_2), 33.6 (CH_2), 30.2 (CH_2), 29.9 (CH_2), 29.6 (2 x CH_2), 29.5 (CH_2), 29.4 (CH_2), 28.9 (CH_2), 26.8 (CH_2), 20.5 (CH_2), 14.0 (CH_3).

11.2.7.3 3-(10-Sulfanyl-1-decyloxycarbonyl)-10-butyl-phenothiazine (35) [357]

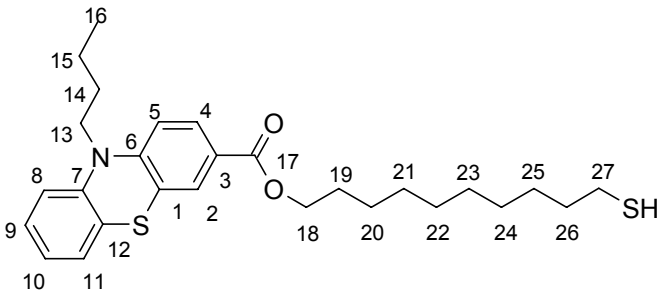

A solution of 3-(10-bromo-1-decyloxycarbonyl)-10-butylphenothiazine (**34**) (420 mg, 0.81 mmol) and thiourea (190 mg, 2.50 mmol) in dry ethanol (30 ml) was stirred at reflux under

nitrogen for 24 h. After the solution was cooled to room temperature the solvent was removed, an aqueous potassium hydroxide solution (1 M, 15 ml) was added, and the mixture was stirred at reflux for 24 h. After the mixture was cooled to room temperature it was extracted with diethyl ether (3 x 50 ml), the combined extracts were dried ($MgSO_4$), and the solvent was evaporated. Flash-chromatography of the residue (silica) eluting with CH_2Cl_2 / PE (2 : 1) afforded the product as a yellow oil.

Formula: $C_{27}H_{37}NO_2S_2$ (471.73).

Yield: 340 mg (720 μmol, 89 %) of a yellow oil.

^{1}H-NMR (400 MHz, acetone–d_6, 300 K): δ / ppm = 7.86 (dd, 1H, $^3J_{HH}$ = 8.6 Hz, $^4J_{HH}$ = 2.0 Hz, H-4), 7.7 (d, 1H, $^4J_{HH}$ = 1.9 Hz, H-2), 7.17 (ddd, 1H, $^3J_{HH}$ = 8.7 Hz, $^4J_{HH}$ = 1.6 Hz, H-9 o. 10), 7.10 (dd, 1H, $^3J_{HH}$ = 7.6 Hz, $^4J_{HH}$ = 1.5 Hz, H-8 o. 11), 7.11-7.07 (2H, H-5, H-8 o. 11), 6.99 (ddd, 1H, $^3J_{HH}$ = 7.6 Hz, $^4J_{HH}$ = 1.2 Hz, H-9 o. 10), 4.26 (t, 2H, H-18), 4.02 (t, 2H, H-13), 2.70 (t, 2H, H-27), 1.87-1.74 (6H, H-15, 19, 26), 1.50-1.35 (12H, H-20-25), 0.92 (t, 3H, H-16).

{^{1}H}^{13}C-NMR (101 MHz, acetone–d_6, 300 K): δ / ppm = 165.9 (C-17), 150.4 (quart.), 145.0 (quart.), 130.1 (CH), 128.8 (CH), 128.6 (CH), 128.1 (CH), 125.3 (quart.), 125.0 (quart.), 124.6 (quart.), 124.1 (CH), 117.1 (CH), 116.0 (CH), 65.4 (CH_2), 47.8 (CH_2), 39.5 (CH_2), 30.2 (CH_2), 30.1 (CH_2), 29.9 (CH_2), 29.6 (3 x CH_2), 29.5 (CH_2), 28.9 (CH_2), 26.8 (CH_2), 20.6 (CH_2), 14.0 (CH_3).

EI-MS (high resolution, PI): calc. m/z = 471.22602
found m/z = 471.22601 Δ = 0.02 ppm

11.2.8 Synthesis of Thioacetic acid S-(4-{4-[bis-(4-methoxyphenyl)amino]-phenyl-ethynyl}phenyl) ester (36)

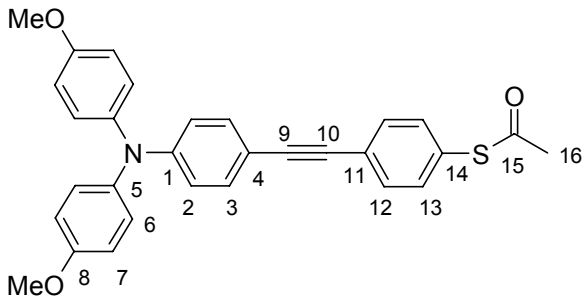

Synthesis according to GP1:

Quantity: Bis-(4-methoxyphenyl)-[4-(ethynyl)phenyl]amine (**8**):

	400 mg	562 μmol
Thioacetic acid S-(4-iodophenyl) ester (**17**):	589 mg	2.30 mmol
$(PPh_3)_2PdCl_2$:	48.2 mg	68.5 μmol
CuI:	13.1 mg	68.5 μmol
$^iPr_2EtN$:	336 mg	3.31 mmol
Dry THF:	15 ml	

The crude product was purified by flash-chromatography (silica) eluting with CH_2Cl_2 / PE (1 : 2 > 2 : 1 > 4 : 1) to obtain a yellow oil.

Formula: $C_{30}H_{25}NO_3S$ (479.60).

Yield: 690 mg (1.43 mmol, 63 %) of a yellow solid.

^{1}H-NMR (400 MHz, acetone–d_6, 300 K): δ / ppm = 7.55 (AA′, 2H, H-12 o. 13), 7.43 (BB′, 2H, H-12 o. 13), 7.34 (AA′, 2H, H-2 o. 3), 7.12 (AA′, 4H, H-6 o. 7), 6.95 (BB′, 2H, H-6 o. 7), 6.79 (BB′, 2H, H-2 o. 3), 3.81 (s, 6H, -OMe), 2.43 (s, 3H, H-16).

{^{1}H}^{13}C-NMR (101 MHz, acetone–d_6, 300 K): δ / ppm = 193.2 (quart.), 157.9 (quart.), 140.6 (quart.), 135.3 (CH), 134.1 (quart.), 133.3 (CH), 132.5 (CH), 128.9

(quart.), 128.5 (CH), 125.8 (quart.), 119.0 (CH), 115.8 (CH), 113.7 (quart.), 92.7 (quart.), 87.9 (quart.), 55.5 (CH_3), 30.3 (CH_3).

IR (KBr): $\tilde{\nu}$ / cm^{-1} = 3060 (vw, C-H-aryl), 2928 (vw, C-H), 2846 (vw, C-H), 2207 (w, C≡C), 1707 (m), 1602 (m), 1505 (s), 1240 (s), 1110 (m), 1032 (m), 825 (s), 718 (w), 613 (w), 575 (w).

EI-MS (high resolution, PI): calc. m/z = 479.15497
found m/z = 479.15505 Δ = 0.17 ppm

11.2.9 [4-(S-Acetylthiomethyl)ethynylphenyl]-bis(4-methoxyphenyl)amine (37)

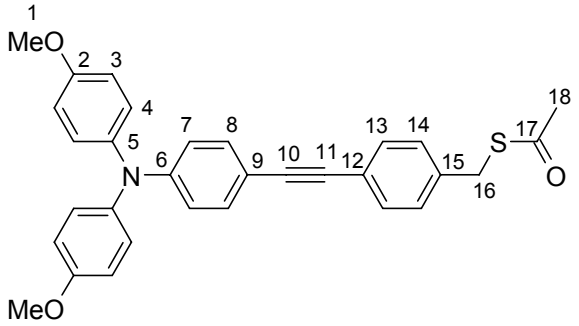

Synthesis according to GP1:

Quantity:			
	1-(S-Acetylthiomethyl)-4-iodobenzene (**18**):	500 mg	1.71 mmol
	(4-Ethynylphenyl)-bis(4-methoxyphenyl)amine (**8**):		
		297 mg	900 μmol
	$Pd(PPh_3)_2Cl_2$:	25.9 mg	51.0 μmol
	CuI:	8.92 mg	46.8 μmol
	$^{i}Pr_2EtN$:	330 μl	2.46 mmol
	Dry THF:	5 ml	

The crude product was purified by column-chromatography (aluminum oxide neutral, activity V) eluting with EtOAc / PE (1 : 29 > 1 : 25) to obtain a yellow solid.

Formula: $C_{31}H_{27}NO_3S$ (493.62 g/mol).

Yield: 110 mg (0.22 mmol, 25 %) of a yellow solid.

^{1}H-NMR (400 MHz, Aceton-d_6, 300 K): δ / ppm = 7.42 (AA', 2 H), 7.35-7.29 (4 H), 7.11 (AA', 4 H, H-3 o. 4), 6.94 (BB', 4 H, H-3 o. 4), 6.78 (BB', 2 H, H-7 o. 8), 4.14 (s, 2 H, H-16), 3.80 (s, 6 H, H-1), 2.34 (s, 3 H, H-18).

{^{1}H}^{13}C-NMR (101 MHz, Aceton-d_6, 300 K): δ / ppm = 194.9 (quart.), 157.8 (quart.), 150.2 (quart.), 140.8 (quart.), 139.2 (quart.), 133.2 (CH), 132.2 (CH), 129.9 (CH), 128.4 (CH), 123.5 (quart.), 119.2 (CH), 115.8 (CH), 114.2 (quart.), 91.1 (quart.), 88.4 (quart.), 55.8 (-OMe), 33.4 (CH_2), 30.0 (CH_3).

IR (KBr): $\tilde{\nu}$ / cm^{-1} = 3030 (vw, C-H-aryl), 2929 (w, C-H), 2832 (w, C-H), 2208 (w, C≡C), 1690 (m), 1597 (m), 1506 (s), 1240 (s), 1132 (m), 1033 (m), 827 (m), 624 (w), 576 (w).

EI-MS (high resolution, PI): calc. m/z = 493.17062
found m/z = 493.17104 Δ = 0.85 ppm

11.2.10 Synthesis of Thioacetic acid S-[4-(4-{4-[bis-(4-methoxyphenyl)amino]-phenylethynyl}-2,5-dipropoxy-phenylethynyl)-phenyl] ester (40)

11.2.10.1 {4-[2,5-Dipropoxy-4-(trimethylsilylethynyl)phenylethynyl]phenyl}-bis-(4-methoxyphenyl)amine (38)

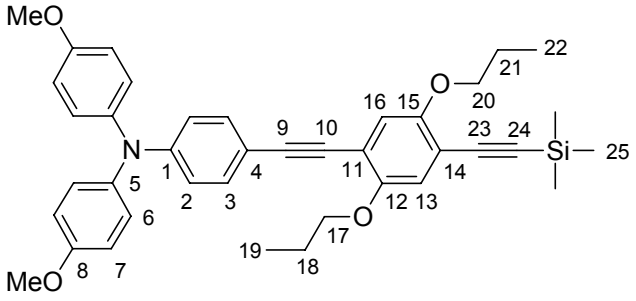

Synthesis according to GP2:

Quantity:	Bis-(4-methoxyphenyl)-[4-(ethynyl)phenyl]amine (**8**):		
		1.50 g	5.04 mmol
	(4-Iodo-2,5-dipropoxyphenylethynyl)trimethylsilane (**23**):		
		2.84 g	6.83 mmol
	$(PPh_3)_2PdCl_2$:	383 mg	546 μmol
	CuI:	103 mg	546 μmol
	Dry Et_2NH:	10 ml	

The crude product was purified by column-chromatography (aluminum oxide, act. V) eluting with CH_2Cl_2 / PE (1 : 9 > 2 : 8 > 4 : 6) to obtain a yellow solid.

Formula: $C_{39}H_{43}NO_4Si$ (617.87).

Yield: 400 mg (647 μmol, 13 %) of a yellow solid.

^{1}H-NMR (400 MHz, CD_2Cl_2, 300 K): δ / ppm = 7.28 (AA´, 2H, H-2 o. 3), 7.08 (AA´, 4H, H-6 o. 7), 6.94 (s, 1H, H-13 o. 16), 6.92 (s, 1H, H-13 o. 16), 6.87 (BB´, 4H, H-6 o. 7), 6.80 (BB´, 2H, H-2 o. 3), 3.95-3.92 (4H, H-17, 20), 3.79 (s, 6H, -OMe), 1.86-1.77 (4H, H-18, 21), 1.09-1.05 (6H, H-19, 22), 0.25 (s, 9H, H-25).

{^{1}H}^{13}C-NMR (101 MHz, CD_2Cl_2, 300 K): δ / ppm = 157.0 (quart.), 154.6 (quart.), 153.6 (quart.), 149.5 (quart.), 140.4 (quart.), 132.6 (CH), 127.7 (CH), 119.0 (CH), 117.6 (CH), 117.2 (CH), 115.4 (quart.), 115.2 (CH), 114.0 (quart.), 113.5 (quart.), 101.7 (quart.), 100.1 (quart.), 96.0 (quart.), 84.9 (quart.), 71.5 (2 x CH_2), 55.8 (CH_3), 23.12 (CH_2), 23.11 (CH_2), 10.70 (CH_3), 10.67 (CH_3), 0.0 (CH_3).

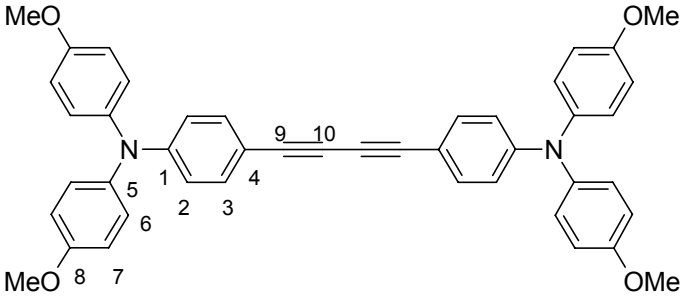

Formula: $C_{44}H_{36}N_2O_4$ (656.78).

Yield: 80.0 mg (122 μmol, 19 %) of a yellow solid.

^{1}H-NMR (400 MHz, C_6D_6, 300 K): δ / ppm = 7.34 (AA', 4H, H-2 o. 3), 6.94 (AA', 8H, H-6 o. 7), 6.79 (BB', 4H, H-2 o. 3), 6.67 (BB', 8H, H-6 o. 7), 3.28 (s, 12H, -OMe).

{^{1}H}^{13}C-NMR (101 MHz, C_6D_6, 300 K): δ / ppm = 157.1 (quart.), 149.8 (quart.), 140.4 (quart.), 133.9 (CH), 127.6 (CH), 119.4 (CH), 115.3 (CH), 113.3 (quart.), 82.9 (quart.), 55.0 (CH_3).

ESI-MS (high resolution, PI): calc. m/z = 656.26696
found m/z = 656.26626 Δ = 1.06 ppm

11.2.10.2 {4-[2,5-Dipropoxy-4-(ethynyl)phenylethynyl]phenyl}-bis-(4-methoxyphenyl)amine (39)

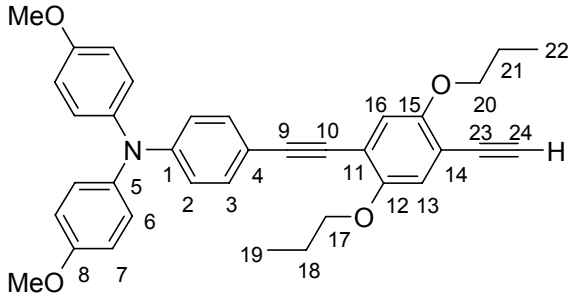

Synthesis according to GP5:

Quantity:			
	{4-[2,5-Dipropoxy-4-(trimethylsilylethynyl)phenylethynyl]phenyl}-bis-(4-methoxyphenyl)amine (**38**):	500 mg	810 μmol
	K_2CO_3:	167 mg	1.21 mmol
	Dry MeOH:	10 ml	
	Dry CH_2Cl_2:	5 ml	

The crude product was purified by flash-chromatography (silica) eluting with CH_2Cl_2 / PE (1 : 2 > 1 : 1 > 2 : 1) to obtain a yellow solid.

Formula: $C_{36}H_{35}NO_4$ (545.68).

Yield: 353 mg (648 μmol, 80 %) of a yellow solid.

^{1}H-NMR (400 MHz, C_6D_6, 300 K): δ / ppm = 7.58 (AA´, 2H, H-2 o. 3), 7.01-6.98 (5H, H-6 o. 7, H-13 o. 16), 6.96 (BB´, 2H, H-2 o. 3), 6.89 (s, 1H, H-13 o. 16), 6.69 (BB', 4H, H-6 o. 7), 3.44 (q, 4H, H-17, 20), 3.29 (s, 6H, -OMe), 2.31 (s, 1H, H-24), 1.62-1.51 (4H, H-18, 21), 0.95 (t, 3H, H-19 o. 22), 0.87 (t, 3H, H-19 o. 22).

{^{1}H}^{13}C-NMR (101 MHz, C_6D_6, 300 K): δ / ppm = 157.0 (quart.), 155.7 (quart.), 154.0 (quart.), 149.5 (quart.), 140.6 (quart.), 133.0 (CH), 127.5 (CH), 119.8 (CH), 117.9 (CH), 116.9 (CH), 116.5 (quart.), 115.3 (CH), 115.2 (quart.), 112.4 (quart.), 97.1 (quart.), 86.0 (quart.), 80.7 (quart.), 80.3 (quart.), 70.7 (CH_2), 70.6 (CH_2), 55.0 (CH_3), 23.0 (CH_2), 22.8 (CH_2), 10.8 (CH_3), 10.7 (CH_3).

11.2.10.3 Thioacetic acid S-[4-(4-{4-[bis-(4-methoxyphenyl)amino]phenyl-ethynyl}-2,5-dipropoxy-phenylethynyl)-phenyl] ester (40)

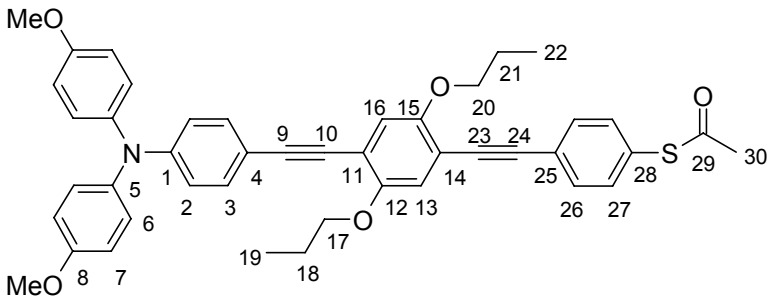

Synthesis according to GP1:

Quantity:	{4-[2,5-Dipropoxy-4-(ethynyl)phenylethynyl]phenyl}-bis-(4-methoxyphenyl)-amine (**39**):	130 mg	238 μmol
	Thioacetic acid S-(4-iodophenyl) ester (**17**):	66.2 mg	238 μmol

$(PPh_3)_2PdCl_2$:	14.2 mg	20.0 μmol
CuI:	3.70 mg	20.0 μmol
$^{i}Pr_2EtN$:	31.2 mg	240 μmol
Dry THF:	4 ml	

The crude product was purified by flash-chromatography (silica) eluting with CH_2Cl_2 / PE (1 : 4 > 1 : 2 > 4 : 1) to obtain a yellow solid.

Formula: $C_{44}H_{45}NO_5S$ (695.89).

Yield: 73.1 mg (105 μmol, 44 %) of a yellow solid.

^{1}H-NMR (400 MHz, CD_2Cl_2, 300 K): δ / ppm = 7.54-7.47 (4H, H-26, 27), 7.30 (AA´, 2H, H-2 o. 3), 7.08 (AA´, 4H, H-6 o. 7), 7.00 (s, 1H, H-13 o. 16), 6.99 (s, 1H, H-13 o. 16), 6.87 (BB´, 4H, H-6 o. 7), 6.82 (BB´, 2H, H-2 o. 3), 4.01-3.95 (4H, H-17, 20), 3.79 (s, 6H, -OMe), 2.42 (s, 3H, H-30), 1.88-1.82 (4H, H-18, 21), 1.11-1.06 (6H, H-19, 22).

{^{1}H}^{13}C-NMR (101 MHz, CD_2Cl_2, 300 K): δ / ppm = 196.2 (quart.), 157.1 (quart.), 155.5 (quart.), 154.1 (quart.), 153.6 (quart.), 149.6 (quart.), 149.5 (quart.), 140.3 (quart.), 132.7 (CH), 127.7 (CH), 119.0 (CH), 118.0 (CH), 117.3 (CH), 117.0 (CH), 116.8 (CH), 116.4 (quart.), 115.3 (CH), 115.2 (quart.), 111.7 (quart.), 96.9 (quart.), 87.6 (quart.), 80.1 (quart.), 79.1 (quart.), 71.49 (CH_2), 71.43 (CH_2), 55.8 (CH_3), 31.2 (CH_3), 23.13 (CH_2), 23.09 (CH_2), 10.73 (CH_3), 10.71 (CH_3).

Elemental analysis:

calc.:	C: 75.95 %	H: 5.94 %	N: 2.01 %	S: 4.61 %
found:	C: 76.07 %	H: 6.21 %	N: 2.17 %	S: 2.24 %

11.2.11 Attempted Synthesis of Thioacetic acid S-{4-[4-(4-{4-[bis-(4-methoxyphenyl)amino]-phenylethynyl}-2,5-dipropoxy-phenylethynyl)-2,5-dipropoxy-phenylethynyl]-phenyl} ester (43)

11.2.11.1 {4-[4-(2,5-Dipropoxy-4-(trimethylsilanylethynyl)phenylethynyl)-2,5-dipropoxy-phenylethynyl]phenyl}-bis-(4-methoxyphenyl)amine (41)

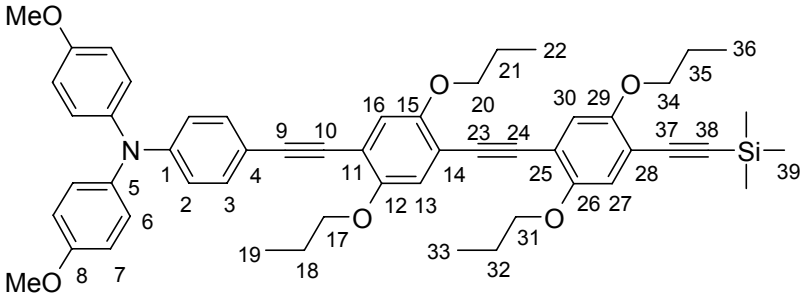

Synthesis according to GP2:

Quantity:	{4-[2,5-Dipropoxy-4-(ethynyl)phenylethynyl]phenyl}-bis-(4-methoxyphenyl)-amine (**39**):	1.00 g	1.83 mmol
	(4-Iodo-2,5-dipropoxyphenylethynyl)trimethylsilane (**23**):	1.15 g	2.75 mmol
	$(PPh_3)_2PdCl_2$:	84.3 mg	220 μmol
	CuI:	22.9 mg	220 μmol
	Dry Et_2NH:	5 ml	

The crude product was purified by column-chromatography (aluminum oxide, act. V) eluting with CH_2Cl_2 / PE (1 : 9 > 2 : 8 > 4 : 6) to obtain a yellow solid.

Formula: $C_{53}H_{59}NO_6Si$ (834.12).

Yield: 777 mg (932 μmol, 51 %) of a yellow solid.

^{1}H-NMR (400 MHz, CD_2Cl_2, 300 K): δ / ppm = 7.32 (AA´, 2H, H-2 o. 3), 7.10 (AA´, 4H, H-6 o. 7), 7.02 (s, 1H), 7.01 (s, 1H), 7.00 (s, 1H), 6.97 (s, 1H), 6.88 (BB´, 4H, H-6 o. 7), 6.83 (BB´, 2H, H-2 o. 3), 4.02-3.94 (8H, H-17, 20, 31, 34), 3.79 (s, 6H, -OMe), 1.89-1.82 (8H, H-18, 21, 32, 35), 1.11-1.07 (12H, H-19, 22, 33, 36), 0.25 (s, 9H, H-25).

{^{1}H}^{13}C-NMR (101 MHz, CD_2Cl_2, 300 K): δ / ppm = 157.0 (quart.), 154.5 (quart.), 153.9 (quart.), 153.74 (quart.), 153.71 (quart.), 149.5 (quart.), 140.4 (quart.), 132.7 (CH), 127.7 (CH), 119.0 (CH), 117.7 (CH), 117.6 (CH), 117.5 (CH), 117.2 (CH), 115.3 (quart.), 115.2 (CH), 114.9 (quart.), 114.2 (quart.), 114.1 (quart.), 113.7 (quart.), 101.6 (quart.), 100.4 (quart.), 96.2 (quart.), 92.0 (quart.), 91.5 (quart.), 85.0 (quart.), 71.53 (CH_2), 71.52 (CH_2), 71.47 (CH_2), 71.46 (CH_2), 55.8 (CH_3), 23.14 (CH_2), 23.12 (CH_2), 23.08 (2 x CH_2), 10.72 (3 x CH_3), 10.69 (CH_3), 0.0 (CH_3).

11.2.11.2 {4-[4-(4-Ethynyl-2,5-dipropoxy-phenylethynyl)-2,5-dipropoxy-phenylethynyl]-phenyl}-bis-(4-methoxyphenyl)amine (42)

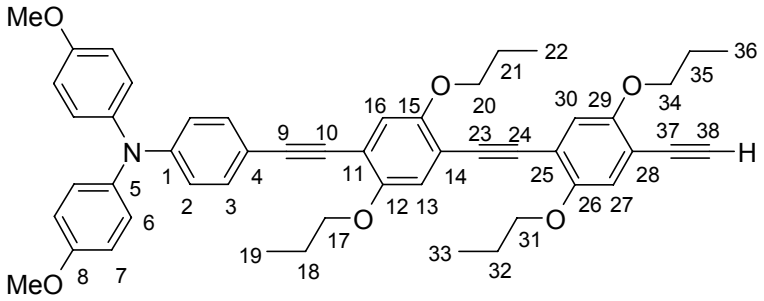

Synthesis according to GP6:

Quantity: {4-[4-(2,5-Dipropoxy-4-(trimethylsilanylethynyl)phenylethynyl)-2,5-dipropoxy-phenylethynyl] phenyl}-bis-(4-methoxyphenyl)amine (**41**):

	630 mg	755 μmol
TBAF (1 M solution in THF):	221 mg	846 μmol
THF:	6 ml	

Formula: $C_{50}H_{51}NO_6$ (761.94).

Yield: 549 mg (720 μmol, 95 %) of a yellow solid.

^{1}H-NMR (400 MHz, C_6D_6, 300 K): δ / ppm = 7.34 (AA´, 2H, H-2 o. 3), 7.15 (AA´, 4H, H-6 o. 7), 7.04 (s, 2H), 7.03 (s, 1H), 7.02 (s, 1H), 6.87 (BB´, 4H, H-6 o. 7), 6.82

(BB´, 2H, H-2 o. 3), 4.03-3.95 (8H, H-17, 20, 31, 34), 3.90 (s, 1H, H-38), 3.83 (s, 6H, -OMe), 1.91-1.83 (8H, H-18, 21, 32, 35), 1.13-1.07 (12H, H-19, 22, 33, 36).

{^{1}H}^{13}C-NMR (101 MHz, C_6D_6, 300 K): δ / ppm = 157.0 (quart.), 154.5 (quart.), 153.9 (quart.), 153.8 (quart.), 153.7 (quart.), 149.5 (quart.), 140.3 (quart.), 132.7 (CH), 127.7 (CH), 119.0 (CH), 117.7 (CH), 117.6 (CH), 117.5 (CH), 117.2 (CH), 115.3 (quart.), 115.2 (CH), 114.9 (quart.), 114.2 (quart.), 114.1 (quart.), 113.6 (quart.), 101.6 (quart.), 100.4 (quart.), 96.2 (quart.), 92.0 (quart.), 91.5 (quart.), 85.0 (quart.), 71.6 (CH_2), 71.51 (CH_2), 71.47 (CH_2), 71.45 (CH_2), 55.8 (CH_3), 23.13 (CH_2), 23.11 (CH_2), 23.07 (2 x CH_2), 10.74 (3 x CH_3), 10.70 (CH_3).

11.2.11.3 Thioacetic acid S-{4-[4-(4-{4-[bis-(4-methoxyphenyl)amino]phenylethynyl}-2,5-dipropoxy-phenylethynyl)-2,5-dipropoxy-phenylethynyl]phenyl} ester (43)

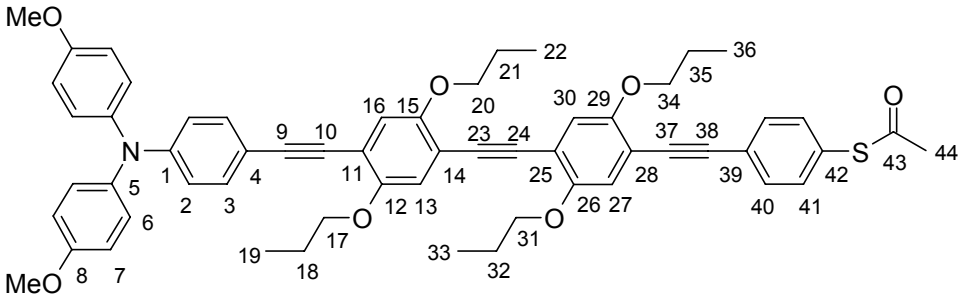

Synthesis according to GP1:

Quantity: {4-[4-(4-Ethynyl-2,5-dipropoxy-phenylethynyl)-2,5-dipropoxy-phenyl-ethynyl]-phenyl}-bis-(4-methoxyphenyl)amine (**42**):

	590 mg	774 μmol
Thioacetic acid S-(4-iodophenyl) ester (**17**):	527 mg	1.90 mmol
$(PPh_3)_2PdCl_2$:	32.6 mg	46.5 μmol
CuI:	8.80 mg	46.5 μmol
^{i}Pr$_2$EtN:	200 mg	1.50 mmol
Dry THF:	4 ml	

The crude product was purified by column-chromatography on aluminum oxide (neutral, activity V) eluting with CH_2Cl_2 / PE (1 : 9 > 2 : 8 > 4 : 6) to obtain an orange solid.
The homo-coupled side product could be isolated.

11.2.12 Synthesis of Thioacetic acid S-[4-(4-{4-[bis-(4-methoxyphenyl)amino]-phenylethynyl}-3-cyanophenylethynyl)phenyl] ester (46)

11.2.12.1 2-{4-[Bis-(4-methoxyphenyl)amino]phenylethynyl}-5-trimethylsilanyl-ethynylbenzonitrile (44)

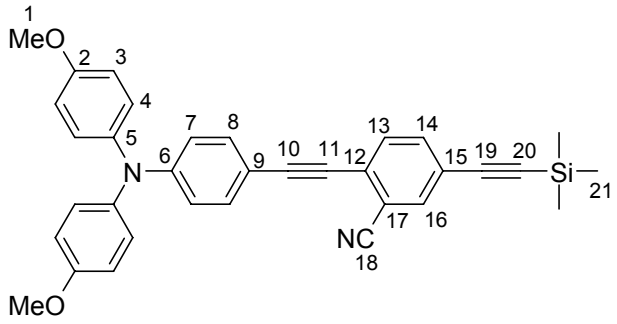

Synthesis according to GP2:

Quantity:	(4-Ethynylphenyl)-bis(4-methoxyphenyl)amine (**8**):		
		2.00 g	6.07 mmol
	2-Iodo-5-trimethylsilanylethynylbenzonitrile (**26**):		
		2.72 g	8.36 mmol
	$Pd(PPh_3)_2Cl_2$:	480 mg	680 μmol
	CuI:	135 mg	710 μmol
	Dry Et_2NH:	11 ml	

The crude product was purified by column-chromatography (aluminum oxide neutral, activity V) eluting with EtOAc / PE (2 : 98) to obtain a yellow solid.

Formula: $C_{34}H_{30}N_2O_2Si$ (526.71 g/mol).

Yield: 2.00 g (3.80 mmol, 63 %) of a yellow solid.

^{1}H-NMR (400 MHz, acetone-d_6, 299 K): δ / ppm = 7.86 (dd, $^{4}J_{HH}$ = 1.7 Hz, $^{5}J_{HH}$ = 0.6 Hz, 1H, H-16), 7.72 (dd, $^{3}J_{HH}$ = 8.2 Hz, $^{4}J_{HH}$ = 1.7 Hz, 1H, H-14), 7.65 (dd, $^{3}J_{HH}$ = 8.2 Hz, $^{5}J_{HH}$ = 0.6 Hz, 1H, H-13), 7.39 (AA', 2H, H-7 o. 8), 7.15 (AA', 4H, H-3 o. 4), 6.96 (BB', 4H, H-3 o. 4), 6.80 (BB', 2H, H-7 o. 8), 3.81 (s, 6H, H-1), 0.26 (s, 9H, H-21).

{^{1}H}^{13}C-NMR (101 MHz, acetone-d_6, 299 K): δ / ppm = 157.3 (quart.), 150.4 (quart.), 140.0 (quart.), 136.5 (CH), 136.4 (CH), 133.5 (CH), 132.6 (CH), 128.5 (CH), 127.6 (quart.), 123.2 (quart.), 118.3 (CH), 117.3 (quart.), 115.3 (quart.), 115.2 (CH), 111.9 (quart.), 102.6 (quart.), 99.4 (quart.), 99.0 (quart.), 85.1 (quart.), 55.5 (CH_3), -0.2 (CH_3).

11.2.12.2 2-{4-[Bis-(4-methoxyphenyl)amino]phenylethynyl}-5-ethynylbenzonitrile (45)

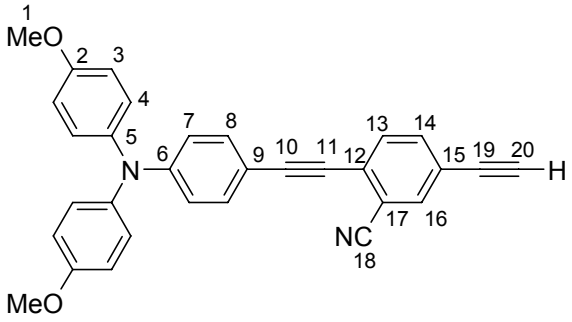

Synthesis according to GP6:

Quantity:			
	2-{4-[Bis-(4-methoxyphenyl)amino]phenylethynyl}-5-trimethylsilyl-ethynyl-benzonitrile (**44**):	2.00 g	4.18 mmol
	TBAF (1 M solution in THF):	4.51 ml	4.51 mmol
	THF:	20 ml	

Formula: $C_{31}H_{22}N_2O_2$ (454.53 g/mol).

Yield: 1.88 g (4.14 mmol, 99 %) of a brown solid.

^{1}H-NMR (400 MHz, acetone-d_6, 299 K): δ / ppm = 7.91 (dd, $^{4}J_{HH}$ = 1.7 Hz, $^{5}J_{HH}$ = 0.5 Hz, 1H, H-16), 7.76 (dd, $^{3}J_{HH}$ = 8.2 Hz, $^{4}J_{HH}$ = 1.7, 1H, H-14), 7.67 (dd, $^{3}J_{HH}$ =

8.2 Hz, $^5J_{HH}$ = 0.5 Hz, 1H, H-13), 7.39 (AA', 2H, H-7 o. 8), 7.14 (AA', 4H, H-3 o. 4), 6.95 (BB', 4H, H-3 o. 4), 6.80 (BB', 2H, H-7 o. 8), 3.96 (s, 1H, H-21), 3.80 (s, 6H, H-1).

{^{1}H}^{13}C-NMR (101 MHz, acetone-d_6, 299 K): δ / ppm = 157.3 (quart.), 150.5 (quart.), 140.0 (quart.), 136.3 (CH), 136.0 (CH), 133.3 (CH), 132.1 (CH), 128.2 (quart.), 127.9 (CH), 122.0 (quart.), 118.5 (CH), 117.2 (quart.), 115.4 (quart.), 115.2 (CH), 111.8 (quart.), 99.6 (quart.), 85.0 (quart.), 81.5 (quart.), 80.9 (CH), 55.8 (CH_3).

11.2.12.3 Thioacetic acid S-[4-(4-{4-[bis-(4-methoxyphenyl)amino]phenylethynyl}-3-cyanophenylethynyl)phenyl] ester (46)

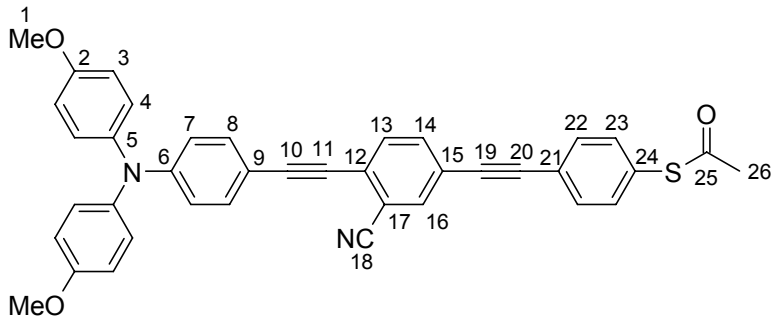

Synthesis according to GP1:

Quantity:			
	2-{4-[Bis-(4-methoxyphenyl)amino]phenylethynyl}-5-ethynylbenzonitrile (**45**):	300 mg	660 μmol
	Thioacetic acid S-(4-iodophenyl) ester (**17**):	348 mg	1.25 mmol
	CuI:	7.09 mg	37.2 μmol
	$Pd(PPh_3)_2Cl_2$:	26.2 mg	37.2 μmol
	$^i Pr_2NEt$:	250 μml	1.39 mmol
	Dry THF:	4.0 ml	

The crude product was purified by column-chromatography (aluminum oxide neutral, activity V) eluting with EtOAc / PE (10 : 1) to obtain a yellow solid.

Formula: $C_{39}H_{28}N_2O_3S$ (604.72 g/mol).

Yield: 56.0 mg (92.6 μmol, 14 %) of a yellow solid.

^{1}H-NMR (600 MHz, acetone-d_6, 299K): δ / ppm = 8.01 (dd, $^4J_{HH}$ = 1.8 Hz, $^5J_{HH}$ = 0.6 Hz, 1H, H-16), 7.85 (dd, $^3J_{HH}$ = 8.3 Hz, $^4J_{HH}$ = 1.8 Hz, 1H, H-14), 7.72 (dd, $^3J_{HH}$ = 8.3 Hz, $^5J_{HH}$ = 0.6, 1H, H-13), 7.66 (AA', 2H, H-22 o.23), 7.51 (BB', 2H, H-22 o. 23), 7.41 (AA', 2H, H-7 o. 8), 7.15 (AA', 4H, H-3 o. 4), 6.97 (BB', 4H, H-3 o. 4), 6.80 (BB', 2H, H-7 o. 8), 3.81 (s, 6H, H-1), 2.45 (s, 3H, H-26).

{^{1}H}^{13}C-NMR (151 MHz, acetone-d_6, 299 K): δ / ppm = 192.9 (quart.), 158.1 (quart.), 151.2 (quart.), 140.2 (quart.), 139.2 (quart.), 136.3 (CH), 136.3 (CH), 135.4 (CH), 133.8 (CH), 133.0 (CH), 132.9 (CH), 130.6 (quart.), 128.7 (CH), 128.0 (quart.), 124.0 (quart.), 123.6 (quart.), 118.5 (CH), 117.5 (quart.), 115.9 (CH), 112.1 (quart.), 99.9 (quart.), 92.6 (quart.), 89.3 (quart.), 85.5 (quart.), 55.8 (CH_3), 30.3 (CH_3).

IR (KBr): $\tilde{\nu}$ / cm^{-1} = 3050 (vw, C-H-aryl), 2929 (vw, C-H), 2856 (vw, C-H), 2199 (m, C≡C), 1704 (w), 1589 (w), 1504 (s), 1287 (w), 1240 (s), 1149 (w), 1032 (w), 826 (m), 617 (w), 576 (w).

ESI-MS (high resolution): calc. m/z = 608.18206
found m/z = 608.18284 Δ = 1.29 ppm

11.2.13 Synthesis of Thioacetic acid S-{4-[4-(4-{4-[bis-(4-methoxyphenyl)-amino]phenylethynyl}-3-cyanophenyl-ethynyl)-3-cyanophenyl-ethynyl]phenyl} ester (49)

11.2.13.1 {4-[4-(2-Cyano-4-(trimethylsilanylethynyl)phenylethynyl)-2-cyano-phenylethynyl]phenyl}-bis-(4-methoxyphenyl)amine (47)

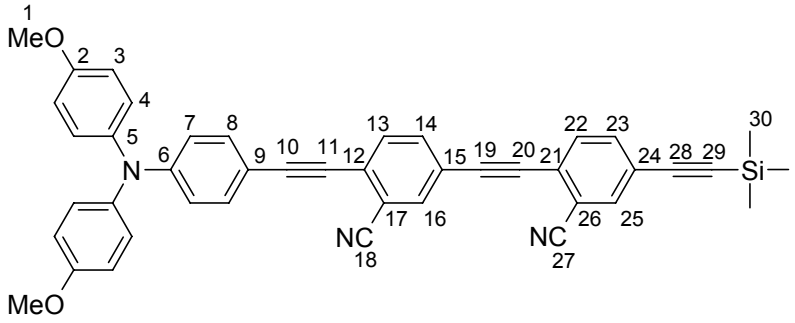

Synthesis according to GP2:

Quantity:	2-{4-[Bis-(4-methoxyphenyl)amino]phenylethynyl}-5-ethynylbenzonitrile (**45**):	1.90 g	4.18 mmol
	2-Iodo-5-trimethylsilanylethynylbenzonitrile (**26**):	1.87 g	5.75 mmol
	$Pd(PPh_3)_2Cl_2$:	332 mg	473 μmol
	CuI:	103 mg	541 μmol
	Dry Et_2NH:	8 ml	

The crude product was purified by flash-chromatography (silica) eluting with PE / EtOAc (90 : 10 > 85 : 15 > 80 : 20 > 74 : 25 > 50 : 50) to obtain a yellow solid.

Formula: $C_{43}H_{30}N_3O_2Si$ (648.81 g/mol).

Yield: 1.51 g (2.32 mmol, 55 %) of a yellow solid.

^{1}H-NMR (400 MHz, $CDCl_3$, 299 K): δ / ppm = 7.83 (dd, $^4J_{HH}$ = 1.7 Hz, $^5J_{HH}$ = 0.6 Hz, 1H, H-16 o. 25), 7.76 (dd, $^4J_{HH}$ = 1.6 Hz, $^5J_{HH}$ = 0.6 Hz, 1H, H-16 o. 25), 7.72 (dd, $^3J_{HH}$ = 8.2 Hz, $^4J_{HH}$ = 1.7 Hz, 1H, H-14 o. 23), 7.64 (dd, $^3J_{HH}$ = 8.2 Hz, $^4J_{HH}$ = 1.6 Hz, 1H, H-14 o. 23), 7.58 – 7.54 (2H, H-13 u. 22), 7.39 (AA', 2H,

H-7 o. 8), 7.09 (AA', 4H, H-3 o. 4), 6.89 – 6.82 (6H, H-3 o. 4 u. H-7 o. 8), 3.81 (s, 6H, H-1), 0.27 (s, 9H, H-30).

{^{1}H}^{13}C-NMR (151 MHz, acetone-d_6, 299 K): δ / ppm = 157.3 (quart.), 150.5 (quart.), 139.9 (quart.), 136.2 (CH), 136.0 (CH), 135.9 (CH), 135.8 (CH), 133.3 (CH), 132.6 (CH), 132.2 (CH), 128.6 (quart.), 128.0 (CH), 125.8 (quart.), 124.8 (quart.), 121.7 (quart.), 118.5 (CH), 117.2 (quart.), 116.9 (quart.), 116.1 (quart.), 115.6 (quart.), 115.2 (CH), 111.8 (quart.), 102.2 (quart.), 100.3 (quart.), 100.0 (quart.), 95.1 (quart.), 88.9 (quart.), 85.2 (quart.), 55.8 (CH_3), -0.3 (CH_3).

11.2.13.2 {4-[4-(2-Cyano-4-(ethynyl)phenylethynyl)-2-cyano-phenylethynyl]phenyl}-bis-(4-methoxyphenyl)amine (48)

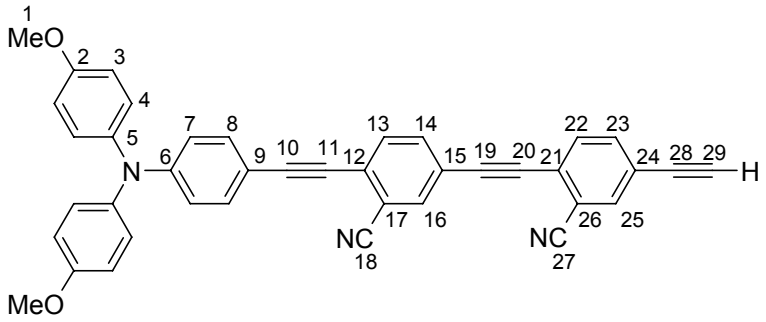

Synthesis according to GP6:

Quantity: {4-[4-(2-Cyano-4-(trimethylsilanylethynyl)phenylethynyl)-2-cyano-phenylethynyl]phenyl}-bis-(4-methoxyphenyl)amine (**47**):

	1.40 g	2.14 mmol
TBAF (1 M solution in THF):	2.58 ml	2.58 mmol
THF:	15 ml	

Formula: $C_{40}H_{22}N_2O_2$ (562.63 g/mol).

Yield: 1.22 g (2.10 mmol, 98 %) of a brown solid.

^{1}H-NMR (400 MHz, $CDCl_3$, 299 K): δ / ppm = 7.83 (dd, $^4J_{HH}$ = 1.7 Hz, $^5J_{HH}$ = 0.6 Hz, 1H, H-16 o. 25), 7.78 (dd, $^4J_{HH}$ = 1.6 Hz, $^5J_{HH}$ = 0.6 Hz, 1H, H-16 o. 25), 7.73 (dd, $^3J_{HH}$ = 8.2 Hz, $^4J_{HH}$ = 1.7 Hz, 1H, H-14 o. 23), 7.67 (dd, $^3J_{HH}$ = 8.1 Hz, $^4J_{HH}$ = 1.6 Hz, 1H, H-14 o. 23), 7.58 (dd, $^3J_{HH}$ = 8.1 Hz, $^5J_{HH}$ = 0.6 Hz, 1H, H-13 o. 22), 7.56 (dd, $^3J_{HH}$ = 8.2 Hz, $^5J_{HH}$ = 0.6 Hz, 1H, H-13 o. 22), 7.39 (AA', 2H, H-7 o. 8), 7.09 (AA', 4H, H-3 o. 4), 6.89 – 6.81 (BB' u. BB', 4H u. 2 H, H-3 o. 4 u. H-7 o. 8), 3.81 (s, 6H, H-1), 3.30 (s, 1H, H-29).

{^{1}H}^{13}C-NMR (151 MHz, acetone-d_6, 299 K): δ / ppm = 159.7 (quart.), 150.5 (quart.), 139.9 (quart.), 136.4 (CH), 136.2 (CH), 136.0 (CH), 135.8 (CH), 133.4 (CH), 132.7 (CH), 132.2 (CH), 128.7 (quart.), 128.0 (CH), 126.4 (quart.), 123.7 (quart.), 121.6 (quart.), 118.5 (CH), 117.2 (quart.), 116.8 (quart.), 116.2 (quart.), 115.6 (quart.), 115.3 (CH), 111.7 (quart.), 100.4 (quart.), 95.3 (quart.), 88.7 (quart.), 85.2 (quart.), 81.8 (CH), 81.2 (quart.), 59.5 (CH_3).

11.2.13.3 Thioacetic acid S-{4-[4-(4-{4-[bis-(4-methoxyphenyl)amino]phenylethynyl}-3-cyanophenyl-ethynyl)-3-cyanophenylethynyl]phenyl} ester (49)

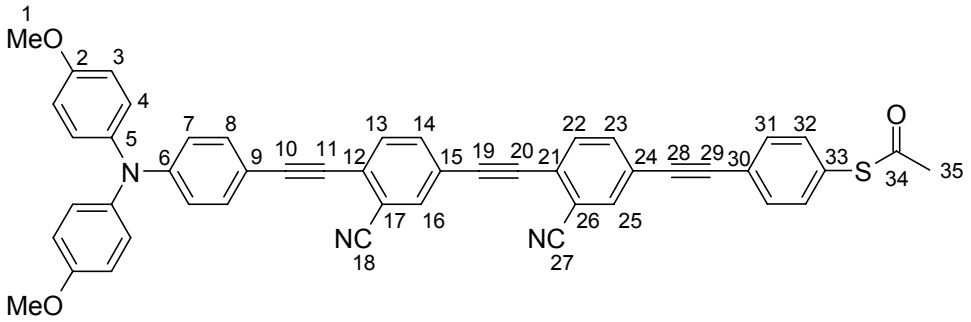

Synthesis according to GP1:

Quantity:			
	{4-[4-(2-Cyano-4-(ethynyl)phenylethynyl)-2-cyano-phenylethynyl]-phenyl}-bis-(4-methoxyphenyl)amine (**48**):	304 mg	520 μmol
	Thioacetic acid S-(4-iodophenyl) ester (**17**):	357 mg	1.28 mmol
	CuI:	5.62 mg	29.5 μmol
	$Pd(PPh_3)_2Cl_2$:	20.6 mg	29.3 μmol
	$^i Pr_2NEt$:	190 μl	1.06 μmol

Dry THF: 2.0 ml

The crude product was purified by flash-chromatography (silica) eluting with PE / EtOAc / CH_2Cl_2 (75 : 20 : 5 > 65 : 20 : 15) to obtain a yellow solid.

Formula: $C_{48}H_{28}N_3O_3S$ (729.84 g/mol).

Yield: 60.0 mg (82.2 μmol, 16 %) of a yellow solid.

^{1}H-NMR (600 MHz, CD_2Cl_2, 299 K): δ / ppm = 7.87 (dd, $^4J_{HH}$ = 1.7 Hz, $^5J_{HH}$ = 0.5 Hz, 1H, H-16 o. 25), 7.86 (dd, $^4J_{HH}$ = 1.7 Hz, $^5J_{HH}$ = 0.5 Hz, 1H, H-16 o. 25), 7.76 (dd, $^3J_{HH}$ = 8.1 Hz, $^4J_{HH}$ = 1.7 Hz, 1H, H-14 o. 23), 7.75 (dd, $^3J_{HH}$ = 8.1 Hz, $^4J_{HH}$ = 1.7 Hz, 1H, H-14 o. 23), 7.66 (dd, $^3J_{HH}$ = 8.1 Hz, $^5J_{HH}$ = 0.5 Hz, 1H, H-13 o. 22), 7.61 (dd, $^3J_{HH}$ = 8.1 Hz, $^5J_{HH}$ = 0.5 Hz, 1H, H-13 o. 22), 7.60 (AA', 2H, H-31 o. 32), 7.44 (BB', 2H, H-31 o. 32), 7.38 (AA', 2H, H-7 o. 8), 7.10 (AA', 4H, H-2 o. 3), 6.88 (BB', 4H, H-2 o. 3), 6.82 (BB', 2H, H-7 o. 8), 3.80 (s, 6H, H-1), 2.43 (s, 3H, H-35).

{^{1}H}^{13}C-NMR (151 MHz, CD_2Cl_2, 299 K): δ / ppm = 193.1 (quart.), 157.0 (quart.), 150.2 (quart.), 139.6 (quart.), 135.7 (CH), 135.6 (CH), 135.5 (CH), 135.4 (CH), 134.5 (CH), 133.0 (CH), 132.3(CH), 132.5 (CH), 131.89 (CH), 129.7 (quart.), 128.3 (quart.), 127.7 (CH), 125.5 (quart.), 124.3 (quart.), 123.2 (quart.), 121.4 (quart.), 118.2 (CH), 116.9 (quart.), 116.6 (quart.), 115.9 (quart.), 115.3 (quart.), 114.9 (CH), 111.4 (quart.), 100.0 (quart.), 94.9 (quart.), 92.7 (quart.), 88.6 (quart.), 88.3 (quart.), 84.9 (quart.), 55.5 (CH_3), 30.2 (CH_3).

ESI-MS (high resolution, PI): calc. m/z = 729.20861
found m/z = 729.20888 Δ = 0.37 ppm

11.2.14 Synthesis of Thioacetic acid S-(4-{4-[4-(4-{4-[bis-(4-methoxyphenyl)amino]phenylethynyl}-3-cyanophenylethynyl)-3-cyanophenylethynyl]-3-cyanophenylethynyl}phenyl) ester (52)

11.2.14.1 {4-[4-(4-(2-Cyano-4-(trimethylsilanylethynyl)phenylethynyl)-2-cyanophenyl-ethynyl)-2-cyanophenylethynyl]phenyl}-bis-(4-methoxyphenyl)amine (50)

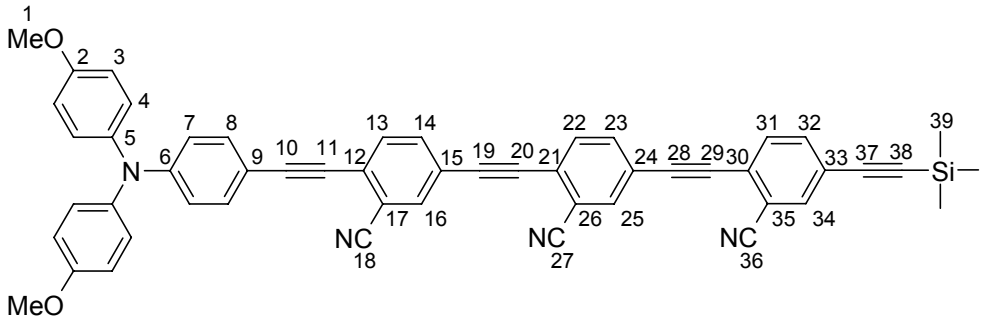

Synthesis according to GP2:

Quantity:	{4-[4-(2-Cyano-4-(ethynyl)phenylethynyl)-2-cyano-phenylethynyl]-phenyl}-bis-(4-methoxyphenyl)amine (**48**):	900 mg	1.55 mmol
	2-Iodo-5-trimethylsilanylethynylbenzonitrile (**26**):	700 mg	2.13 mmol
	$Pd(PPh_3)_2Cl_2$:	120 mg	171 μmol
	CuI:	34.0 mg	179 μmol
	Dry Et_2NH:	1 ml	
	Dry THF:	3 ml	

Because of solubility problems THF was added to the reaction mixture.

The crude product was purified by column-chromatography (aluminum oxide neutral, activity V) eluting with PE / CH_2Cl_2 (50 : 50) to obtain a yellow solid.

Formula: $C_{52}H_{33}N_4O_2Si$ (773.94 g/mol).

Yield: 110 mg (0.14 mmol, 9 %) of a yellow solid.

^{1}H-NMR (600 MHz, CD_2Cl_2, 299 K): δ / ppm = 7.91 (d, $^4J_{HH}$ = 1.4 Hz, 1H, H-16 o. 25 o. 34), 7.87 (d, $^4J_{HH}$ = 1.6 Hz, 1H, H-16 o. 25 o. 34), 7.81 (dd, $^3J_{HH}$ = 8.1 Hz, $^4J_{HH}$ = 1.6 Hz, 1H, H- 14 o. 23 o. 32), 7.78 – 7.75 (2H), 7.68 (d, $^3J_{HH}$ = 8.1 Hz,

1H, H-13 o. 22 o. 31), 7.66 (dd, $^3J_{HH}$ = 8.1 Hz, $^4J_{HH}$ = 1.6 Hz, 1H, H-14 o. 23 o. 32), 7.63 – 7.58 (2H), 7.38 (AA', 2H, H-7 o. 8), 7.10 (AA', 4H, H-3 o. 4), 6.88 (BB', 4H, H-3 o.4), 6.82 (BB', 2H, H-7 o. 8), 3.80 (s, 6H, H-1), 0.27 (s, 9H, H-39).

{^{1}H}^{13}C-NMR (151 MHz, CD_2Cl_2, 299 K): δ / ppm = 157.0 (quart.), 150.2 (quart.), 139.6 (quart.), 135.9 (CH), 135.7 (CH), 135.7 (CH), 135.6 (CH), 135.6 (CH), 135.5 (CH), 133.0 (CH), 132.6 (CH), 132.4 (CH), 131.9 (CH), 128.4 (quart.), 127.7 (CH), 126.4 (quart.), 125.2 (quart.), 124.7 (quart.), 123.1 (quart.), 121.3 (quart.), 118.1 (CH), 116.8 (quart.), 116.6 (quart.), 116.5 (quart.), 116.1 (quart.), 115.9 (quart.), 115.3 (quart.), 114.9 (CH), 111.4 (quart.), 101.8 (quart.), 100.1 (quart.), 99.9 (quart.), 95.4 (quart.), 94.3 (quart.), 89.3 (quart.), 88.5 (quart.), 85.0 (quart.), 55.5 (CH_3), -0.6 (CH_3).

11.2.14.2 {4-[4-(4-(2-Cyano-4-(ethynyl)phenylethynyl)-2-cyanophenylethynyl)-2-cyanophenylethynyl]phenyl}-bis-(4-methoxyphenyl)amine (51)

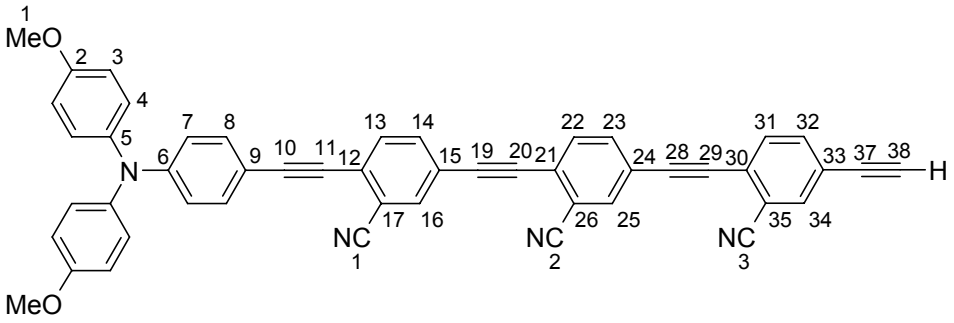

Synthesis according to GP6:

Quantity:			
	{4-[4-(4-(2-Cyano-4-(trimethylsilanylethynyl)phenylethynyl)-2-cyano-phenylethynyl)-2-cyanophenylethynyl]phenyl}-bis-(4-methoxyphenyl)-amine (**50**):	100 mg	129 μmol
	TBAF (1 M solution in THF):	160 μl	160 μmol
	Dry THF:	1.0 ml	
	Dry CH_2Cl_2:	1.5 ml	

Because of solubility problems CH_2Cl_2 was added to the reaction mixture.

Formula: $C_{49}H_{25}N_4O_2$ (701.76 g/mol).

Yield: 90.5 mg (128 mmol, 99 %) of an orange solid.

^{1}H-NMR (600 MHz, CD_2Cl_2, 299 K): δ / ppm = 7.92 (dd, $^4J_{HH}$ = 1.6 Hz, $^5J_{HH}$ = 0.4 Hz, 1H, H-16 o. 25 o. 34), 7.88 (dd, $^4J_{HH}$ = 1.6 Hz, $^5J_{HH}$ = 0.4 Hz, 1H, H-16 o. 25 o. 34), 7.83 – 7.81 (2H), 7.77 (dd, $^3J_{HH}$ = 8.3 Hz, $^4J_{HH}$ = 1.6 Hz, 1H, H-14 o. 23 o. 32), 7.71 (dd, $^3J_{HH}$ = 8.1 Hz, $^4J_{HH}$ = 1.6 Hz, 1H, H-14 o. 23 o. 32), 7.69 (dd, $^3J_{HH}$ = 8.1 Hz, $^5J_{HH}$ = 0.4 Hz, 1H, H-13 o. 22 o. 31), 7.64 (dd, $^3J_{HH}$ = 8.1 Hz, $^5J_{HH}$ = 0.4 Hz, 1H, H-13 o. 22 o. 31), 7.61 (dd, $^3J_{HH}$ = 8.3 Hz, $^5J_{HH}$ = 0.4 Hz, 1H, H-13 o. 22 o. 31), 7.38 (AA', 2H, H-7 o. 8), 7.10 (AA', 4H, H-3 o. 4), 6.88 (BB', 4H, H-3 o.4), 6.82 (BB', 2H, H-7 o. 8), 3.80 (s, 6H, H-1), 3.39 (s, 1H, H-38).

{^{1}H}^{13}C-NMR (151 MHz, CD_2Cl_2, 299 K): δ / ppm = 157.0 (quart.), 150.2 (quart.), 139.6 (quart.), 136.1 (CH), 135.9 (CH), 135.8 (CH), 135.7 (CH), 135.7 (CH), 135.5 (CH), 133.0 (CH), 132.6 (CH), 132.5 (CH), 131.9 (CH), 129.7 (CH), 128.4 (quart.), 127.7 (CH), 126.5 (quart.), 125.8 (quart.), 123.6 (quart.), 123.0 (quart.), 121.3 (quart.), 118.1 (CH), 116.8 (quart.), 116.5 (quart.), 116.1 (quart.), 116.0 (quart.), 115.3 (quart.), 114.9 (CH), 111.4 (quart.), 100.1 (quart.), 95.5 (quart.), 94.5 (quart.), 89.1 (quart.), 88.5 (quart.), 84.9 (quart.), 81.6 (quart.), 80.8 (quart.), 55.5 (CH_3).

11.2.14.3 Thioacetic acid S-(4-{4-[4-(4-{4-[bis-(4-methoxyphenyl)amino]phenylethynyl}-3-cyanophenylethynyl)-3-cyanophenylethynyl]-3-cyanophenylethynyl}phenyl) ester (52)

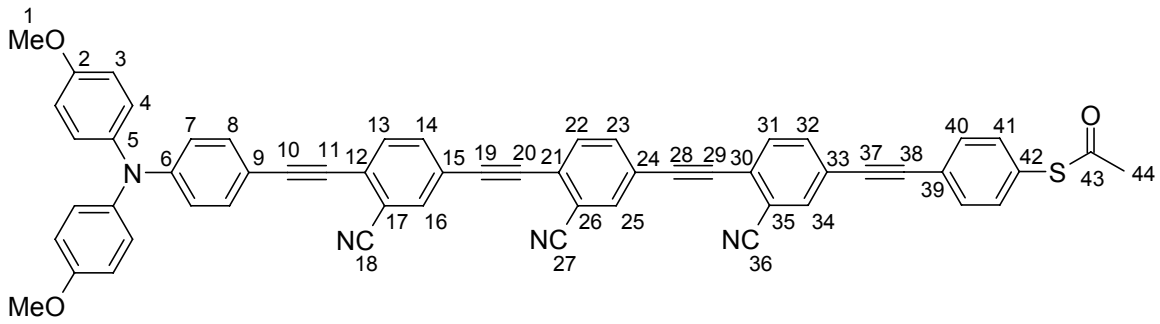

Synthesis according to GP1:

Quantity: {4-[4-(4-(2-Cyano-4-(ethynyl)phenylethynyl)-2-cyanophenylethynyl)-2-cyanophenylethynyl]phenyl}-bis-(4-methoxyphenyl)amine (**51**):

	53.0 mg	75.2 μmol
Thioacetic acid S-(4-iodophenyl) ester (**17**):	60.7 mg	218 μmol
CuI:	1.44 mg	7.56 μmol
$Pd(PPh_3)_2Cl_2$:	6.16 mg	8.78 μmol
$^{i}Pr_2EtN$:	30 μl	
Dry THF:	0.38 ml	
Dry toluene:	0.40 ml	

Because of solubility problems toluene was added to the reaction mixture.
The crude product was purified by column-chromatography (aluminum oxide neutral, activity V) eluting with PE / CH_2Cl_2 (7 : 3 > 5 : 5) to obtain a yellow solid.

Formula: $C_{57}H_{34}N_4O_3S$ (854.96 g/mol).

Yield: 6.50 mg (7.60 μmol, 10 %).

^{1}H-NMR (400 MHz, CD_2Cl_2, 300 K): δ / ppm = 7.92 (dd, $^4J_{HH}$ = 1.6 Hz, $^5J_{HH}$ = 0.4 Hz, 1H, H-16 o. 25 o. 34), 7.87 (dd, $^4J_{HH}$ = 1.6 Hz, $^5J_{HH}$ = 0.4 Hz, 1H, H-16 o. 25 o. 34), 7.83 – 7.81 (2 H), 7.78 (dd, $^3J_{HH}$ = 8.3 Hz, $^4J_{HH}$ = 1.6 Hz, 1H, H-14 o. 23 o. 32), 7.70 (dd, $^3J_{HH}$ = 8.1 Hz, $^4J_{HH}$ = 1.6 Hz, 1H, H-14 o. 23 o. 32),

7.68 (dd, $^3J_{HH}$ = 8.1 Hz, $^5J_{HH}$ = 0.4 Hz, 1H, H-13 o. 22 o. 31), 7.64 (dd, $^3J_{HH}$ = 8.1 Hz, $^5J_{HH}$ = 0.4 Hz, 1H, H-13 o. 22 o. 31), 7.61 (3H, H-13 o. 22 o. 31, 40 o. 41), 7.44 (BB', 2Hm H-40 o. 41), 7.37 (AA', 2H, H-7 o. 8), 7.10 (AA', 4H, H-3 o. 4), 6.88 (BB', 4H, H-3 o.4), 6.82 (BB', 2H, H-7 o. 8), 3.80 (s, 6H, H-1), 2.42 (s, 3H, H-44).

{^{1}H}^{13}C-NMR (101 MHz, CD_2Cl_2, 300 K): δ / ppm = 192.4 (quart.), 157.3 (quart.), 150.2 (quart.), 139.9 (CH), 139.6 (quart.), 138.9 (CH), 137.1 (quart.), 136.8 (quart.) 136.1 (CH), 136.0 (CH), 135.9 (CH), 135.8 (CH), 133.4 (CH), 132.9 (CH), 132.81 (CH), 132.75 (CH), 132.6 (CH), 132.23 (CH), 132.15 (CH), 128.4 (quart.), 127.8 (CH), 126.5 (quart.), 125.8 (quart.), 123.6 (quart.), 123.0 (quart.), 121.3 (quart.), 118.3 (CH), 116.8 (quart.), 116.5 (quart.), 116.1 (quart.), 116.0 (quart.), 115.3 (quart.), 115.1 (CH), 111.4 (quart.), 100.1 (quart.), 95.5 (quart.), 94.5 (quart.), 89.1 (quart.), 88.5 (quart.), 84.9 (quart.), 81.6 (quart.), 80.8 (quart.), 55.5 (CH_3), 25.1 (CH_3).

ESI-MS (high resolution, PI): calc. m/z = 854.23516
found m/z = 854.23345 Δ = 2.00 ppm

11.2.15 Synthesis of Thioacetic acid S-(4-{4-[bis-(4-chlorophenyl)amino]-phenylethynyl}phenyl) ester (53)

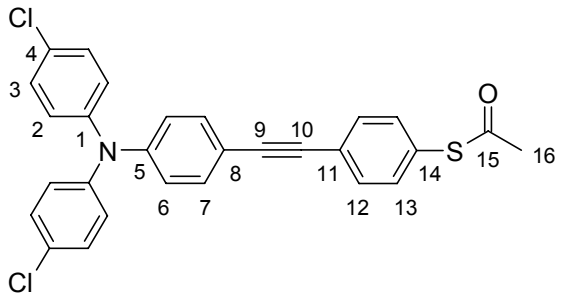

Synthesis according to GP1:

Quantity: Bis-(4-chlorophenyl)-(4-ethynylphenyl)amine (**12**):
500 mg 1.48 mmol

Thioacetic acid S-(4-iodophenyl) ester (**17**):	617 mg	2.22 mmol
$(PPh_3)_2PdCl_2$:	105 mg	150 μmol
CuI:	28.6 mg	150 μmol
$^{i}Pr_2EtN$:	232 mg	1.80 mmol
Dry THF:	10 ml	

The residue was cleaned by flash-chromatography (silica) eluting with CH_2Cl_2 / PE (1 : 6 > 1 : 4 > 1 : 2 > 2 : 1) to obtain a yellow solid.

Formula: $C_{28}H_{19}Cl_2NOS$ (488.44).

Yield: 420 mg (0.86 mmol, 58 %) of a yellow oil.

^{1}H-NMR (400 MHz, acetone–d_6, 300 K): δ / ppm = 7.59 (AA', 2H), 7.49-7.45 (4H), 7.37 (AA', 4H, H-2 o. 3), 7.13 (BB', 4H, H-2 o. 3), 7.05 (BB', 2H), 2.44 (s, 3H, H-16).

{^{1}H}^{13}C-NMR (101 MHz, acetone–d_6, 300 K): δ / ppm = 193.1 (quart.), 148.5 (quart.), 146.6 (quart.), 135.3 (CH), 133.8 (CH), 132.7 (CH), 130.6 (CH), 130.2 (quart.), 129.4 (quart.), 127.2 (CH), 125.3 (quart.), 123.6 (CH), 117.5 (quart.), 91.8 (quart.), 88.9 (quart.), 29.4 (CH_3).

EI-MS (high resolution, PI): calc. m/z = 487.05589

found m/z = 487.05560 Δ = 0.59 ppm

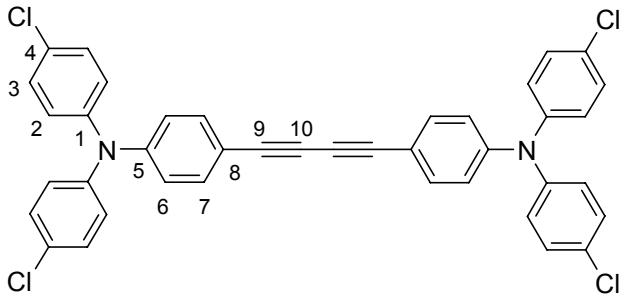

Formula: $C_{40}H_{24}Cl_2N_2$ (674.46).

Yield: 110 mg (0.16 mmol, 22 %) of a yellow solid.

^{1}H-NMR (400 MHz, CD_2Cl_2, 300 K): δ / ppm = 7.37 (AA', 4H, H-6 o. 7), 7.26 (AA', 8H, H-2 o. 3), 7.04 (BB', 8H, H-2 o. 3), 6.94 (AA', 4H, H-2 o. 3).

{^{1}H}^{13}C-NMR (101 MHz, CD_2Cl_2, 300 K): δ / ppm = 148.5 (quart.), 145.8 (quart.), 134.2 (CH), 130.2 (CH), 129.7 (quart.), 126.8 (CH), 122.7 (CH), 115.7 (quart.), 82.3 (quart.), 74.3 (quart.).

Elemental analysis: calc.: C: 71.23 % H: 3.59 % N: 4.15 %
found: C: 71.07 % H: 4.09 % N: 3.99 %

11.2.16 Synthesis of Thioacetic acid S-[4-(4-{4-[bis-(4-chlorophenyl)amino]-phenylethynyl}-2,5-dipropoxyphenylethynyl)phenyl] ester (56)

11.2.16.1 Bis-(4-chlorophenyl)-[4-(2,5-dipropoxy-4-trimethylsilanylethynyl-phenylethynyl)phenyl]amine (54)

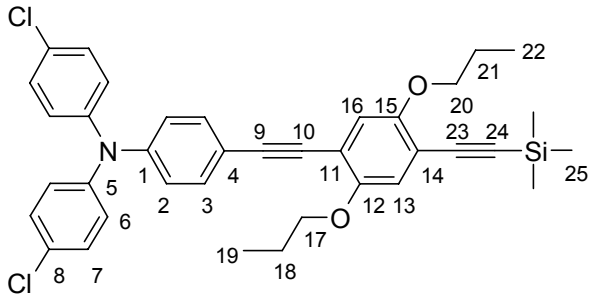

Synthesis according to GP2:

Quantity:	Bis-(4-chlorophenyl)-(4-ethynylphenyl)amine (**12**):		
		750 mg	2.20 mmol
	(4-Iodo-2,5-dipropoxyphenylethynyl)trimethylsilane (**23**):		
		1.19 g	2.86 mmol
	$(Ph_3P)_2PdCl_2$:	42.0 mg	110 μmol
	CuI:	420 mg	220 μmol
	Dry Et_2NH:	10 ml	

The crude product was purified by column chromatography on silica eluting with CH_2Cl_2 / PE (1 : 8) to obtain an orange solid.

Formula: $C_{37}H_{37}Cl_2O_2NSi$ (626.68).

Yield: 1.20 g (2.54 mmol, 88 %) of an orange solid.

^{1}H-NMR (400 MHz, acetone-d_6, 300 K): δ = 7.45 (AA´, 2H, H-2 o. H-3), 7.37 (AA´, 4H, H-6 o. H-7), 7.13 (BB´, 4H, H-6 o. H-7), 7.05 (BB´, 2H, H-2 o. H-3), 7.06 (s, 1H, H-16), 7.00 (s, 1H, H-13), 3.97 (4H, H-17, 20), 1.83 (4H, H-18, 21), 1.09 (6H, H-19, 21), 0.25 (s, 9H, H-25).

{^{1}H}^{13}C-NMR (101 MHz, acetone-d_6, 300 K): δ = 155.2 (quart.), 154.4 (quart.), 148.2 (quart.), 146.6 (quart.), 133.5 (CH), 130.5 (CH), 129.4 (quart.), 127.1 (C-6 o. 7), 123.7 (CH), 118.3 (quart), 117.9 (CH), 117.7 (CH), 115.5 (quart.), 114.6 (quart), 102.3 (quart.), 100.2 (quart.), 95.6 (quart.), 86.4 (quart.), 71.63 (CH_2), 71.61 (CH_2), 23.47 (CH_2), 23.46 (CH_2), 10.90 (CH_2), 10.88 (CH_2), 0.0 (CH_3).

11.2.16.2 Bis-(4-chlorophenyl)-[4-(2,5-dipropoxy-4-ethynylphenylethynyl)phenyl]amine (55)

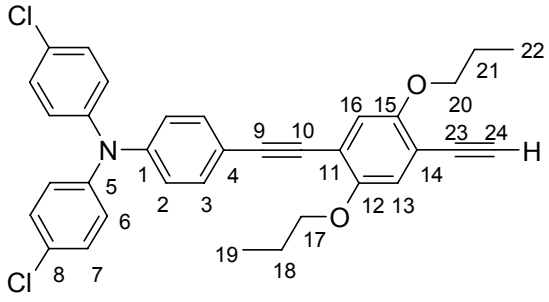

Synthesis according to GP5:

Quantity:	Bis-(4-chlorophenyl)-[4-(2,5-dipropoxy-4-trimethylsilanylethynyl-phenylethynyl)phenyl]amine (**54**):	1.03 g	2.18 mmol
	K_2CO_3 :	377 mg	2.72 mmol

Dry MeOH:	10 ml
Dry CH_2Cl_2:	10 ml

The crude product was purified by column-chromatography on silica eluting with CH_2Cl_2 / PE (1 : 8) to obtain an orange solid.

Formula: $C_{34}H_{29}Cl_2O_2N$ (554.49).

Yield: 0.42 g (0.88 mmol, 40 %) of a yellow solid.

^{1}H-NMR (400 MHz, acetone-d_6, 300 K): δ = 7.46 (AA´, 2H, H-2 o. H-3), 7.38 (AA´, 4H, H-6 o. H-7), 7.15 (BB´, 4H, H-6 o. H-7), 7.08 (BB´, 2H, H-2 o. H-3), 7.07 (s, 1H, H-16), 7.05 (s, 1H, H-13), 4.05 (4H, H-17, 20), 3.80 (s, 1H, H-24), 1.80 (4H, H-18, 21), 1.05 (6H, H-19, 22).

{^{1}H}^{13}C-NMR (101 MHz, acetone-d_6, 300 K): δ = 155.2 (quart.), 154.4 (quart.), 148.3 (quart.), 146.7 (quart.), 133.5 (CH), 130.5 (CH), 129.4 (quart.), 127.1 (CH), 123.7 (CH), 118.6 (quart), 118.3 (CH), 117.5 (CH), 115.6 (quart.), 113.7 (quart), 95.5 (quart.), 86.3 (quart.), 84.3 (quart.), 80.7 (quart.), 71.64 (CH_2), 71.57 (CH_2), 23.4 (CH_2), 23.3 (CH_2), 10.9 (CH_2), 10.8 (CH_2).

Melting point: 53 °C (CH_2Cl_2 / PE).

11.2.16.3 Thioacetic acid S-[4-(4-{4-[bis-(4-chlorophenyl)amino]phenyl-ethynyl}-2,5-dipropoxyphenylethynyl)phenyl] ester (56)

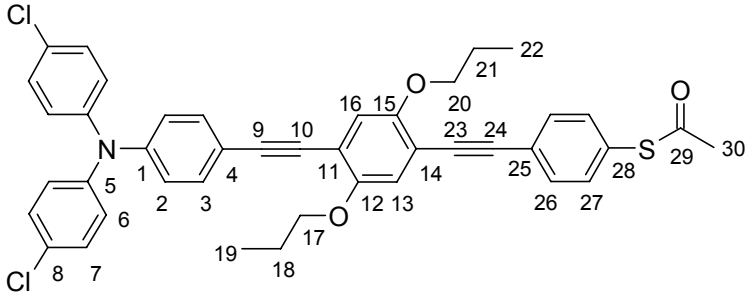

Synthesis according to GP4:

Quantity:	*N,N*-Di(4-chlorphenyl)-*N*-[4-(2,5-dipropoxy-4-ethinylphenyl)-ethinylphenyl]amin (**55**):	250 mg	520 μmol
	Thioacetic acid S-(4-iodophenyl) ester (**17**):	160 mg	580 μmol
	$Pd(C_6H_5CN)_2Cl_2$:	6.18 mg	15.7 μmol
	CuI:	1.06 mg	5.20 μmol
	P^{t}Bu:	2.70 mg	31.3 μmol
	^{i}PrNH:	58.0 mg	0.58 mmol
	Dry dioxane:	1 ml	
	Dry THF:	1 ml	

The crude product was purified by column-chromatography (aluminum oxide neutral, activity V) eluting with CH_2Cl_2 / PE (1 : 4) to obtain a yellow oil.

Formula: $C_{42}H_{35}Cl_2O_3NS$ (704.68).

Yield: 250 mg (355 μmol, 49 %) of a yellow oil.

^{1}H-NMR (400 MHz, acetone-d_6, 300 K): δ = 7.60 (AA´, 2H), 7.50-7.45 (4H), 7.37 (AA´, 4H, H-6 o. 7), 7.15-7.12 (6H, H-6 o. 7, H-13, 16), 7.06 (BB´, 2H), 4.07-4.04 (4H, H-17, 20), 2.79-2.76 (4H, H-18, 21), 2.44 (s, 3H, H-30), 1.13-1.09 (6H, H-19, 22).

{^{1}H}^{13}C-NMR (101 MHz, acetone-d_6, 300 K): δ = 195.6 (C-29), 157.3 (quart.), 157.0 (quart.), 150.8 (quart.), 149.2 (quart.), 137.9 (CH), 136.0 (CH), 135.2 (CH), 133.1 (CH), 132.2 (quart.), 131.9 (quart.), 129.7 (CH), 127.9 (quart.), 126.2 (CH), 120.8 (quart.), 120.3 (CH), 120.1 (CH), 118.2 (quart.), 116.7 (quart.), 98.3 (quart.), 97.0 (quart.), 91.2 (quart.), 89.0 (quart.), 74.2 (CH_2), 29.6 (CH_3), 26.0 (CH_2), 13.42 (CH_2), 13.40 (CH_2).

IR (KBr): $\tilde{\nu}$ / cm^{-1} = 3041 (vw, C-H-aryl), 2962 (w, C-H), 2933 (w, C-H), 2202 (vw, CC), 1709 (w), 1589 (w), 1487 (s), 1313 (m), 1271 (m), 1091 (m), 1012 (w), 825 (m), 614 (w), 525 (w).

ESI-MS (high resolution, M-Na$^+$): calc. m/z = 703.17147
found m/z = 703.17205 Δ = 0.82 ppm

Elemental analysis: calc.: C: 71.58 % H: 5.01 % N: 1.99 % S: 4.55 %
found: C: 70.34 % H: 5.02 % N: 1.97 % S: 4.41 %

11.2.17 Attempted Synthesis of Thioacetic acid S-{4-[4-(4-{4-[bis-(4-chlorophenyl)amino]-phenylethynyl}-2,5-dipropoxyphenylethynyl)-2,5-dipropoxyphenylethynyl]phenyl} ester (59)

11.2.17.1 Bis-(4-chlorophenyl)-{4-[4-(2,5-dipropoxy-4-trimethylsilanylethynyl-phenylethynyl)-2,5-dipropoxyphenylethynyl]phenyl}-amine (57)

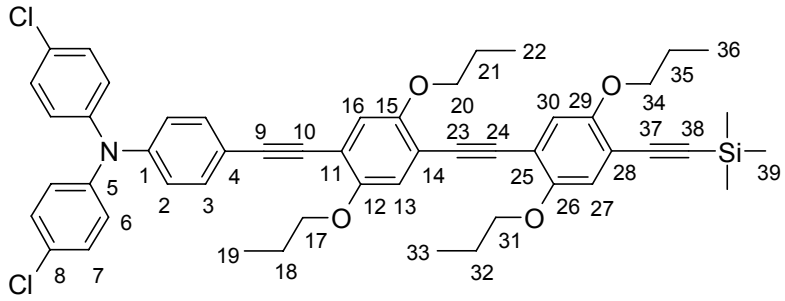

Synthesis according to GP2:

Quantity:	Bis-(4-chlorophenyl)-[4-(4-ethynyl-2,5-dipropoxyphenylethynyl)phenyl]-amine (**55**):	1.29 g	2.06 mmol
	(4-Iodo-2,5-dipropoxyphenylethynyl)trimethylsilane (**23**):	1.11 g	2.67 mmol
	$(PPh_3)_2PdCl_2$:	135 mg	210 μmol
	CuI:	35.0 mg	350 μmol
	Dry Et_2NH:	10 ml	

The crude product was purified by column-chromatography (aluminum oxide neutral, activity V) eluting with CH_2Cl_2 / PE (1 : 9 > 1 : 4 > 2 : 3 > 3 : 2) to obtain a yellow solid.

Formula: $C_{51}H_{53}Cl_2NO_4Si$ (842.98).

Yield: 950 mg (1.13 mmol, 55 %) of a yellow solid.

^{1}H-NMR (400 MHz, CD_2Cl_2, 300 K): δ / ppm = 7.39 (AA´, 2H, H-2 o. 3), 7.25 (AA', 4 H, H-6 o. 7), 7.05 (BB´, 4H, H-6 o. 7), 7.00-6.98 (5H, H-2 o. 3, 13, 27, 30), 6.94 (s, 1H, H-16), 4.01-3.93 (8H, H-17, 20, 31, 34), 1.87-1.79 (8H, H-18, 21, 32, 35), 1.10-1.05 (12H, H-19, 22, 33, 36), 0.25 (s, 9H, H-39).

{^{1}H}^{13}C-NMR (101 MHz, CD_2Cl_2, 300 K): δ / ppm = 154.5 (quart.), 153.87 (quart.), 153.86 (quart.), 153.7 (quart.), 147.6 (quart.), 145.9 (quart.), 133.0 (CH), 129.9 (CH), 129.1 (quart.), 126.4 (CH), 123.1 (CH), 117.69 (CH), 117.64 (CH), 117.61 (CH), 117.5 (CH), 117.3 (quart.), 114.8 (quart.), 114.7 (quart.), 114.3 (quart.), 114.2 (quart.), 101.5 (quart.), 100.5 (quart.), 95.2 (quart.), 91.9 (quart.), 91.6 (quart.), 86.0 (quart.), 71.55 (CH_2), 71.53 (CH_2), 71.47 (CH_2), 71.45 (CH_2), 23.11 (CH_2), 23.10 (CH_2), 23.06 (2 x CH_2), 10.69 (3 x CH_3), 10.65 (CH_3), 0.0 (CH_3).

11.2.17.2 Bis-(4-chlorophenyl)-{4-[4-(2,5-dipropoxy-4-ethynylphenyl-ethynyl)-2,5-dipropoxyphenylethynyl]phenyl}amine (58)

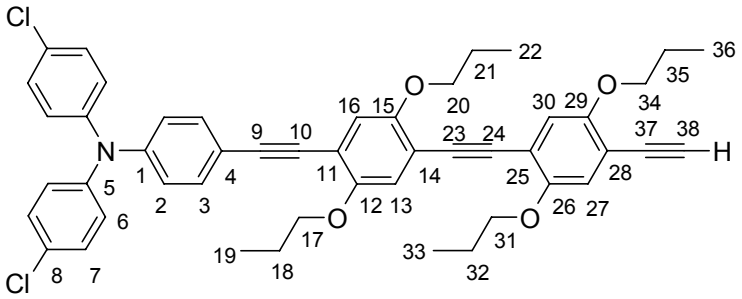

Synthesis according to GP6:

Quantity: Bis-(4-chlorophenyl)-{4-[4-(2,5-dipropoxy-4-trimethylsilanyl-ethynyl-phenylethynyl)-2,5-dipropoxyphenylethynyl]phenyl}amine (**57**):

	900 mg	1.07 mmol
TBAF (1 M solution in THF):	303 mg	1.16 mmol
THF:	10 ml	

Formula: $C_{48}H_{45}Cl_2NO_4$ (770.80).

Yield: 710 mg (920 μmol, 86 %) of a yellow solid.

^{1}H-NMR (400 MHz, CD_2Cl_2, 300 K): δ / ppm = 7.39 (AA´, 2H, H-2 o. 3), 7.26 (AA', 4H, H-6 o. 7), 7.04 (BB´, 4H, H-6 o. 7), 7.00-6.98 (6H, H-2 o. 3, 13, 16, 27, 30), 4.02-3.94 (8H, H-17, 20, 31, 34), 3.38 (s, 1H, H-38), 1.87-1.79 (8H, H-18, 21, 32, 35), 1.10-1.03 (12H, H-19, 22, 33, 36).

{^{1}H}^{13}C-NMR (101 MHz, CD_2Cl_2, 300 K): δ / ppm = 154.5 (quart.), 153.9 (quart.), 153.86 (quart.), 153.6 (quart.), 147.6 (quart.), 145.9 (quart.), 133.0 (CH), 129.9 (CH), 129.1 (quart.), 126.4 (CH), 123.1 (CH), 118.3 (CH), 117.59 (quart.), 117.48 (CH), 117.36 (CH), 117.26 (CH), 115.2 (quart.), 114.7 (quart.), 114.1 (quart.), 113.0 (quart.), 95.2 (quart.), 91.9 (quart.), 91.5 (quart.), 86.0 (CH), 82.6 (quart.), 80.3 (quart.), 71.58 (CH_2), 71.53 (CH_2), 71.44 (CH_2), 71.40 (CH_2), 23.11 (CH_2), 23.07 (CH_2), 23.04 (CH_2), 22.96 (CH_2), 10.70 (3 x CH_3), 10.57 (CH_3).

11.2.17.3 Synthesis of Thioacetic acid S-{4-[4-(4-{4-[bis-(4-chlorophenyl)amino]phenyl-ethynyl}-2,5-dipropoxyphenylethynyl)-2,5-dipropoxy-phenylethynyl]phenyl} ester (59)

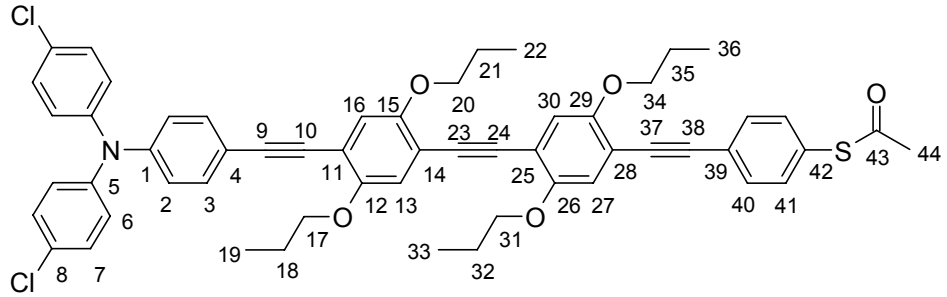

Synthesis according to GP1:

Quantity: Bis-(4-chlorophenyl)-{4-[4-(2,5-dipropoxy-4-ethynylphenyl-ethynyl)-2,5-dipropoxyphenylethynyl]phenyl}amine (**58**):

30.0 mg 32.6 μmol

Thioacetic acid S-(4-iodophenyl) ester (**17**):	22.6 mg	81.5 μmol
$(PPh_3)_2PdCl_2$:	2.80 mg	4.70 μmol
CuI:	760 μg	4.70 μmol
$^{i}Pr_2EtN$:	4.26 mg	33.0 μmol
Dry THF:	1.5 ml	

The crude product was purified by column-chromatography on aluminum oxide (neutral, activity V) eluting with CH_2Cl_2 / PE (1 : 4 > 1 : 1) to obtain a yellow solid.
No product could be isolated.

11.2.18 Synthesis of Thioacetic acid S-(4-{4-[4-(4-{4-[bis-(4-chlorophenyl)-amino]phenylethynyl}-2,5-dipropoxy-phenylethynyl)-2,5-dipropoxy-phenylethynyl]-2,5-dipropoxyphenylethynyl}phenyl) ester (62)

11.2.18.1 Bis-(4-chlorophenyl)-(4-{4-[4-(2,5-dipropoxy-4-trimethylsilanylethynyl-phenylethynyl)-2,5-dipropoxyphenylethynyl]-2,5-dipropoxyphenylethynyl}-phenyl)amine (60)

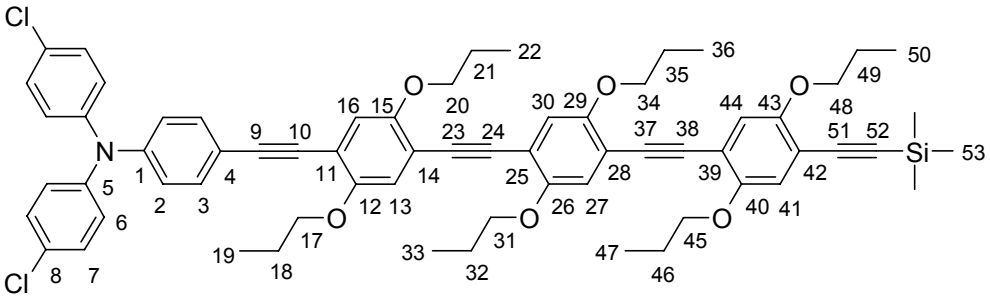

Synthesis according to GP2:

Quantity: Bis-(4-chlorophenyl)-{4-[4-(2,5-dipropoxy-4-ethynylphenyl-ethynyl)-2,5-dipropoxyphenylethynyl]phenyl}amine (**58**):

	900 mg	1.17 mmol

(4-Iodo-2,5-dipropoxyphenylethynyl)trimethylsilane (**23**):

	630 mg	1.52 mmol
$(PPh_3)_2PdCl_2$:	40.0 mg	57.0 μmol
CuI:	10.9 mg	57.0 μmol
Dry Et_2NH:	7.6 ml	

The crude product was purified by column-chromatography (aluminum oxide neutral, activity V) eluting with EtOAc / PE (2 : 98 > 4 : 96 > 8 : 92 > 15 : 85) to obtain a yellow solid.

Formula: $C_{65}H_{69}Cl_2NO_6Si$ (1059.27).

Yield: 700 mg (0.66 mmol, 57 %) of a yellow solid.

^{1}H-NMR (600 MHz, CD_2Cl_2, 300 K): δ / ppm = 7.40 (AA´, 2H, H-2 o. 3), 7.26 (AA', 4H, H-6 o. 7), 7.04 (BB´, 4H, H-6 o. 7), 7.03-6.99 (7H, H-2 o. 3, 13, 27, 30, 41, 44), 6.95 (s, 1H, H-16), 4.03-3.93 (12H, H-17, 20, 31, 34, 45, 48), 1.88-1.80 (12H, H-18, 21, 32, 35, 46, 49), 1.10-1.06 (18H, H-19, 22, 33, 36, 47, 50), 0.26 (s, 9H, H-39).

{^{1}H}^{13}C-NMR (150 MHz, CD_2Cl_2, 300 K): δ / ppm = 154.4 (quart.), 153.83 (quart.), 153.82 (quart.), 153.77 (quart.), 153.75 (quart.), 153.67 (quart.), 147.8 (quart.), 145.9 (quart.), 133.0 (CH), 129.9 (CH), 129.1 (quart.), 126.3 (CH), 123.1 (CH), 117.59 (CH), 117.55 (quart., CH), 117.51 (CH), 117.49 (CH), 117.4 (CH), 117.2 (CH), 114.67 (quart.), 114.58 (quart.), 114.54 (quart.), 114.42 (quart.), 114.20 (quart.), 114.14 (quart.), 101.5 (quart.), 100.5 (quart.), 95.2 (quart.), 91.9 (quart.), 91.8 (quart.), 91.74 (quart.), 91.71 (quart.), 86.0 (quart.), 71.48 (CH_2), 71.45 (3 x CH_2), 71.39 (CH_2), 71.38 (CH_2), 23.09 (CH_2), 23.06 (CH_2), 23.05 (CH_2), 23.02 (3 x CH_2), 10.69 (2 x CH_3), 10.68 (CH_3), 10.67 (CH_3), 10.66 (CH_3), 10.64 (CH_3), 0.0 (CH_3).

11.2.18.2 Bis-(4-chlorophenyl)-(4-{4-[4-(2,5-dipropoxy-4-ethynylphenyl-ethynyl)-2,5-dipropoxyphenylethynyl]-2,5-dipropoxyphenyl-ethynyl}phenyl)amine (61)

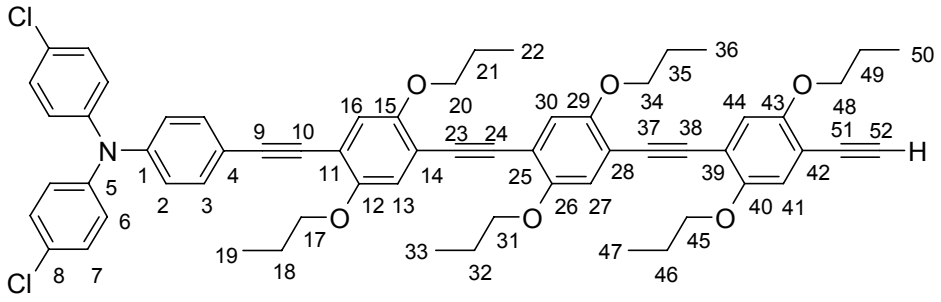

Synthesis according to GP6:

Quantity: Bis-(4-chlorophenyl)-(4-{4-[4-(2,5-dipropoxy-4-trimethylsilanylethynyl-phenylethynyl)-2,5-dipropoxyphenylethynyl]-2,5-dipropoxyphenylethynyl}-phenyl)amine (**60**): 670 mg 630 μmol

TBAF (1 M solution in THF): 178 mg 680 μmol

THF: 5.8 ml

Formula: $C_{62}H_{61}Cl_2NO_6$ (987.09).

Yield: 610 mg (618 μmol, 98 %) of a yellow solid.

^{1}H-NMR (600 MHz, CD_2Cl_2, 300 K): δ / ppm = 7.41 (AA´, 2H, H-2 o. 3), 7.26 (AA', 4H, H-6 o. 7), 7.04 (BB´, 4H, H-6 o. 7), 7.03-6.99 (8H, H-2 o. 3, 13, 16, 27, 30, 41, 44), 4.02-3.95 (10H, H-17, 20, 31, 34, 45 o. 48), 3.69-3.67 (2H, H-17, 20, 31, 34, 45 o. 48), 3.39 (s, 1H, H-52), 1.88-1.80 (12H, H-18, 21, 32, 35, 46, 49), 1.10-1.06 (18H, H-19, 22, 33, 36, 47, 50).

{^{1}H}^{13}C-NMR (150 MHz, CD_2Cl_2, 300 K): δ / ppm = 154.5 (quart.), 153.83 (quart.), 153.82 (quart.), 153.79 (quart.), 153.75 (quart.), 153.6 (quart.), 147.6 (quart.), 145.9 (quart.), 133.0 (CH), 129.9 (CH), 129.0 (quart.), 126.3 (CH), 123.1 (CH), 118.2 (CH), 117.54 (quart.), 117.51 (CH), 117.48 (CH), 117.38 (CH), 117.31 (CH), 117.17 (CH), 115.1 (quart.), 114.61 (quart.), 114.59 (quart.), 114.3 (quart.), 114.1 (quart.), 112.9 (quart.), 95.2 (quart.), 91.94 (quart.), 91.85 (quart.), 91.7 (quart.), 91.6 (quart.), 96.0

(quart.), 82.6 (quart.), 80.3 (CH), 71.51 (CH_2), 71.48 (CH_2), 71.46 (CH_2), 71.44 (CH_2), 71.38 (CH_2), 71.33 (CH_2), 23.09 (CH_2), 23.05 (CH_2), 23.02 (3 x CH_2), 22.9 (CH_2), 10.69 (2 x CH_3), 10.67 (3 x CH_3), 10.56 (CH_3).

11.2.18.3 Thioacetic acid S-(4-{4-[4-(4-{4-[bis-(4-chlorophenyl)amino]-phenylethynyl}-2,5-dipropoxy-phenylethynyl)-2,5-dipropoxy-phenylethynyl]-2,5-dipropoxy-phenylethynyl}phenyl) ester (62)

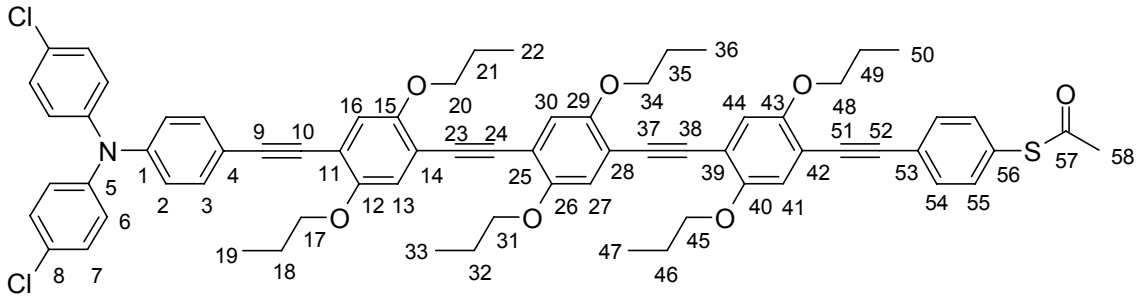

Synthesis according to GP1:

Quantity: Bis-(4-chlorophenyl)-(4-{4-[4-(2,5-dipropoxy-4-ethynylphenylethynyl)-2,5-dipropoxyphenylethynyl]-2,5-dipropoxyphenylethynyl}phenyl)amine (**61**):

	300 mg	304 μmol
Thioacetic acid S-(4-iodophenyl) ester (**17**):	195 mg	700 μmol
$(PPh_3)_2PdCl_2$:	21.0 mg	30.0 μmol
CuI:	5.70 mg	30.0 μmol
$^{i}Pr_2EtN$:	44.5 mg	350 μmol
Dry THF:	3 ml	

The crude product was purified by column-chromatography on aluminum oxide (neutral, activity V) eluting with EtOAc / PE (2 : 98 > 5 : 95 > 10 : 90) to obtain a yellow solid.

Formula: $C_{70}H_{67}Cl_2NO_7S$ (1137.28).

Yield: 63.1 mg (55.5 μmol, 18 %) of a yellow solid.

^{1}H-NMR (400 MHz, CD_2Cl_2, 300 K): δ / ppm = 7.57 (AA´, 2H, H-54 o. 55), 7.43-7.39 (4H, H-2 o. 3, H-54 o. 55), 7.26 (AA', 4 H, H-6 o. 7), 7.06-6.98 (12H, H-2 o. 3, H-6 o. 7, H-13, 16, 27, 30, 41, 44), 4.04-3.97 (12H, H-17, 20, 31, 34, 45, 48), 2.42 (s, 3H, H-58), 1.89-1.83 (12H, H-18, 21, 32, 35, 46, 49), 1.12-1.08 (18H, H-19, 22, 33, 36, 47, 50).

{^{1}H}^{13}C-NMR (101 MHz, CD_2Cl_2, 300 K): δ / ppm = 193.7 (quart.), 154.2 (quart.), 153.89 (quart.), 153.88 (quart.), 153.85 (quart.), 153.84 (quart.), 153.82 (quart.), 147.6 (quart.), 145.9 (quart.), 134.8 (CH), 133.0 (CH), 132.3 (CH), 129.9 (CH), 129.0 (quart.), 128.8 (quart.), 126.4 (CH), 125.0 (quart.), 123.1 (CH), 117.61 (2 x CH), 117.59 (quart.), 117.47 (3 x CH), 117.2 (CH), 114.9 (quart.), 114.7 (2 x quart.), 114.5 (quart.), 114.2 (quart.), 113.9 (quart.), 95.2 (quart.), 94.3 (quart.), 92.02 (quart.), 91.96 (quart.), 91.82 (quart.), 91.78 (quart.), 88.1 (quart.), 86.0 (quart.), 71.57 (CH_2), 71.55 (CH_2), 71.53 (2 x CH_2), 71.48 (CH_2), 71.45 (CH_2), 30.5 (CH_3), 23.11 (CH_2), 23.07 (2 x CH_2), 23.06 (3 x CH_2), 10.71 (4 x CH_3), 10.69 (2 x CH_3).

ESI-MS (high resolution, M-Na$^+$): calc. m/z = 1158.39075
found m/z = 1158.39022 Δ = 0.46 ppm

11.2.19 Synthesis of Thioacetic acid S-[4-(4-{4-[bis-(4-chlorophenyl)amino]-phenylethynyl}-3-cyano-phenylethynyl)phenyl] ester (65)

11.2.19.1 2-{4-[Bis-(4-chlorophenyl)amino]phenylethynyl}-5-trimethylsilanylethynyl-benzonitrile (63)

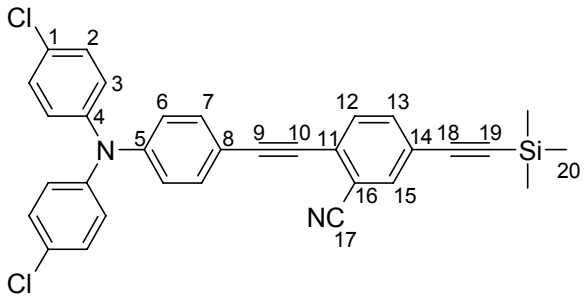

Synthesis according to GP2:

Quantity:	Bis-(4-chlorophenyl)-(4-ethynylphenyl)amine (**12**):		
		2.00 g	5.91 mmol
	2-Iodo-5-(trimethylsilanylethynyl)benzonitrile (**26**):		
		2.89 g	8.87 mmol
	$(PPh_3)_2PdCl_2$:	415 mg	591 μmol
	CuI:	113 mg	593 μmol
	Dry Et_2NH:	10 ml	

The crude product was purified by column-chromatography on aluminum oxide (neutral, activity V) eluting with DCM / PE (1 : 20 > 1 : 10 > 1 : 7) to obtain a yellow solid.

Formula: $C_{32}H_{24}Cl_2N_2Si$ (535.54 g/mol).

Yield: 1.39 g (2.60 mmol, 44 %) of a yellow solid.

^{1}H-NMR (600 MHz, CD_2Cl_2, 299 K): δ / ppm = 7.73 (dd, $^4J_{HH}$ = 1.6 Hz, $^5J_{HH}$ = 0.5 Hz, 1H, H-15), 7.61 (dd, $^3J_{HH}$ = 8.2 Hz, $^4J_{HH}$ = 1.7 Hz, 1H, H-13), 7.54 (dd, $^3J_{HH}$ = 8.2 Hz, $^5J_{HH}$ = 0.5 Hz, 1H, H-12), 7.46 (AA', 2H, H-6 o. 7), 7.27 (AA', 4H, H-2 o. 3), 7.05 (BB', 4H, H-2 o. 3), 7.00 (BB', 2H, H-6 o. 7), 0.26 (s, 9H, H-20).

{^{1}H}^{13}C-NMR (151 MHz, CD_2Cl_2, 299 K): δ / ppm = 148.6 (quart.), 145.6 (quart.), 136.0 (CH), 135.8 (CH), 133.5 (CH), 132.2 (CH), 130.0 (CH), 129.4 (quart.), 127.1 (quart.), 126.7 (CH), 123.6 (quart.), 122.5 (CH), 117.2 (quart.), 115.6 (quart.), 115.4 (quart.), 102.4 (quart.), 99.2 (quart.), 98.2 (quart.), 85.7 (quart.), -0.5 (CH_3).

11.2.19.2 2-{4-[Bis-(4-chlorophenyl)amino]phenylethynyl}-5-ethynyl-benzonitrile (64)

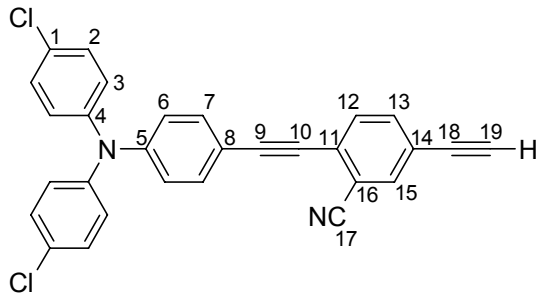

Synthesis according to GP6:

Quantity:	2-{4-[Bis-(4-chlorophenyl)amino]phenylethynyl}-5-trimethylsilanyl-ethynyl-benzonitrile (**63**):	1.39 g	2.60 mmol
	TBAF (1 M solution in THF):	2.81 ml	2.81 mmol
	Dry THF:	12 ml	

Formula: $C_{29}H_{16}Cl_2N_2$ (463.37 g/mol).

Yield: 1.19 g (2.57 mmol, 99 %) of a yellow solid.

^{1}H-NMR (400 MHz, CD_2Cl_2, 299 K): δ / ppm = 7.77 (d, $^4J_{HH}$ = 1.5 Hz, 1H, H-15), 7.65 (dd, $^3J_{HH}$ = 8.2 Hz, $^4J_{HH}$ = 1.6, 1H, H-13), 7.57 (dd, $^3J_{HH}$ = 8.1 Hz, $^5J_{HH}$ = 0.4 Hz, 1H, H-12), 7.47 (AA', 2H, H-6 o. 7), 7.28 (AA', 4H, H-2 o. 3), 7.06 (BB', 4H, H-2 o. 3), 7.00 (BB', 2H, H-6 o. 7), 3.34 (s, 1H, H-19).

{^{1}H}^{13}C-NMR (101 MHz, $CDCl_3$, 299 K): δ / ppm = 148.7 (quart.), 145.7 (quart.), 136.3 (CH), 136.1 (CH), 133.6 (CH), 132.3 (CH), 130.0 (CH), 129.5 (quart.), 127.7 (quart.), 126.7 (CH), 122.5 (CH), 117.1 (quart.), 115.7 (quart.), 115.4 (quart.), 98.4 (quart.), 85.5 (quart.), 82.3 (CH), 81.4 (quart.), 81.1 (quart.).

11.2.19.3 Thioacetic acid S-[4-(4-{4-[bis-(4-chlorophenyl)amino]phenylethynyl}-3-cyano-phenylethynyl)phenyl] ester (65)

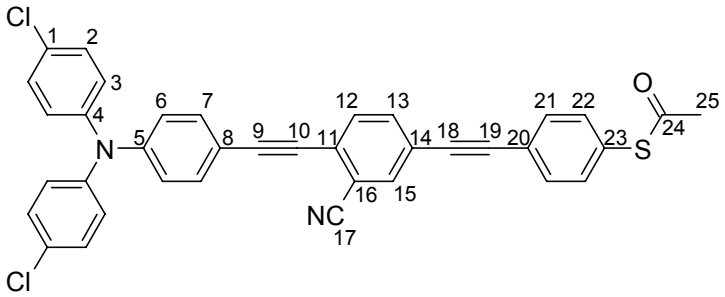

Synthesis according to GP1:

Quantity:	2-{4-[Bis-(4-chlorophenyl)amino]phenylethynyl}-5-ethynyl-benzonitrile (**64**):	300 mg	647 μmol
	Thioacetic acid S-(4-iodophenyl) ester (**17**):	360 mg	1.29 mmol
	$(PPh_3)_2PdCl_2$:	45.0 mg	63.8 μmol
	CuI:	12.0 mg	63.8 μmol
	Dry $^{i}Pr_2NEt$:	0.13 ml	720 μmol
	Dry THF:	6.4 ml	

The crude product was purified by column-chromatography on aluminum oxide (neutral, activity V) eluting with DCM / PE (1 : 4 > 1 : 3 > 1 : 1) to obtain a yellow solid.

Formula: $C_{37}H_{22}Cl_2N_2OS$ (613.55 g/mol).

Yield: 55.0 mg (89.6 μmol, 14 %) of a yellow solid.

^{1}H-NMR (400 MHz, $CDCl_3$, 299K): δ / ppm = 7.80 (dd, $^{4}J_{HH}$ = 1.6 Hz, $^{5}J_{HH}$ = 0.5 Hz, 1H, H-15), 7.67 (dd, $^{3}J_{HH}$ = 8.2 Hz, $^{4}J_{HH}$ = 1.8 Hz, 1H, H-13), 7.57 (dd, $^{3}J_{HH}$ = 8.1 Hz, $^{5}J_{HH}$ = 0.4, 1H, H-12), 7.56 (AA', 2H, H-21 o.22), 7.47 (AA', 2H, H-6 o. 7), 7.43 (BB', 2H, H-21 o. 22), 7.26 (AA', 4H, H-2 o. 3), 7.04 (BB', 4H, H-2 o. 3), 6.99 (BB', 2H, H-6 o. 7), 2.45 (s, 3 H, H-25).

{^{1}H}^{13}C-NMR (101 MHz, $CDCl_3$, 299 K): δ / ppm = 193.3 (quart.), 148.3 (quart.), 145.4 (quart.), 135.6 (CH), 135.3 (CH), 134.4 (CH), 133.5 (CH), 132.4 (CH),

132.0 (CH), 129.9 (CH), 129.4 (quart.), 129.3 (quart.), 127.1 (quart.), 126.3 (CH), 123.5 (quart.), 123.2 (quart.), 122.3 (CH), 117.0 (quart.), 115.6 (quart.), 115.4 (quart.), 98.5 (quart.), 92.5 (quart.), 88.7 (quart.), 85.6 (quart.), 30.5 (CH_3).

Elemental analysis: calc.: C: 72.43 % H: 3.61 % N: 4.57 % S: 5.23 %
found: C: 72.54 % H: 3.78 % N: 4.89 % S: 4.45 %

11.2.20 Synthesis of Thioacetic acid S-{4-[4-(4-{4-[bis-(4-chlorophenyl)-amino]-phenyl-ethynyl}-3-cyano-phenylethynyl)-3-cyanophenylethynyl]phenyl} ester (68)

11.2.20.1 Bis-(4-chlorophenyl)-{4-[4-(2-cyano-4-(trimethylsilanylethynyl)phenyl-ethynyl)-2-cyano-phenylethynyl]phenyl}amine (66)

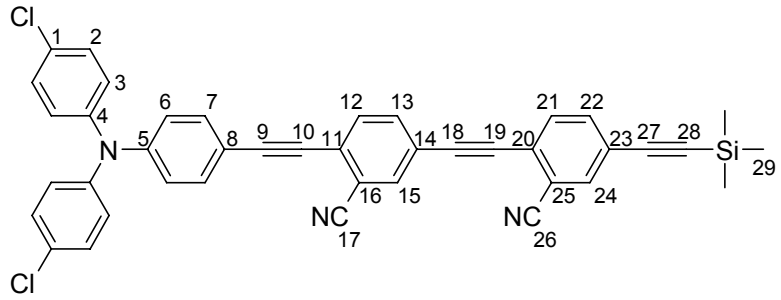

Synthesis according to GP2:

Quantity:		
2-{4-[Bis-(4-chlorophenyl)amino]phenylethynyl}-5-ethynyl-benzonitrile (**64**):	850 mg	1.83 mmol
2-Iodo-5-(trimethylsilanylethynyl)benzonitrile (**26**):	890 mg	2.75 mol
$(PPh_3)_2PdCl_2$:	129 mg	183 μmol
CuI:	35.0 mg	183 μmol
Dry Et_2NH:	5 ml	

The crude product was purified by column-chromatography on aluminum oxide (neutral, activity V) eluting with DCM / PE (1 : 5 > 1 : 4 > 1 : 2 > 2 : 1) to obtain a yellow solid.

Formula: $C_{41}H_{27}Cl_2N_3Si$ (660.66 g/mol).

Yield: 0.87 g (1.32 mmol, 44 %) of a yellow solid.

^{1}H-NMR (400 MHz, CD_2Cl_2, 299 K): δ / ppm = 7.87 (dd, $^4J_{HH}$ = 1.6 Hz, $^5J_{HH}$ = 0.5 Hz, 1H, H-15 o. 24), 7.77 – 7.75 (2H, H-13 o. 22, H-15 o. 24), 7.66 – 7.58 (3H, H-12 u. H-21 u. H-13 o. 22), 7.47 (AA', 2H, H-6 o. 7), 7.27 (AA', 4H, H-2, 3), 7.05 (BB', 4H, H-2 o. 3), 7.00 (BB', 2H, H-6 o. 7), 0.25 (s, 9 H, H-29).

{^{1}H}^{13}C-NMR (101 MHz, CD_2Cl_2, 299 K): δ / ppm = 148.7 (quart.), 145.6 (quart.), 136.1 (CH), 136.0 (CH), 135.9 (CH), 135.8 (CH), 133.6 (CH), 132.7 (CH), 132.4 (CH), 130.0 (CH), 129.5 (quart.), 128.1 (quart.), 126.7 (CH), 125.7 (quart.), 124.9 (quart.), 122.4 (CH), 122.2 (quart.), 117.1 (quart.), 116.9 (quart.), 116.1 (quart.), 115.9 (quart.), 115.3 (quart.), 102.2 (quart.), 100.1 (quart.), 99.0 (quart.), 94.9 (quart.), 89.0 (quart.), 85.8 (quart.), -0.3 (CH_3).

11.2.20.2 Bis-(4-chlorophenyl)-{4-[4-(2-cyano-4-(ethynyl)phenylethynyl)-2-cyano-phenylethynyl]phenyl}amine (67)

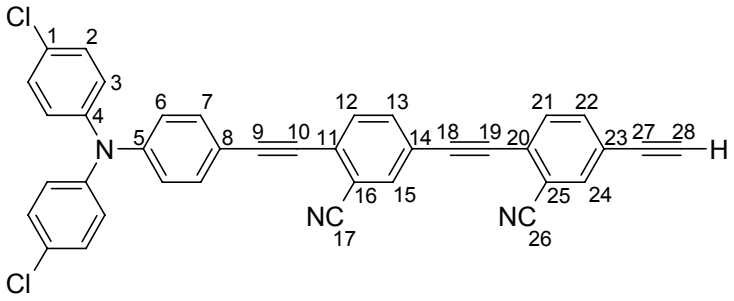

Synthesis according to GP6:

Quantity: Bis-(4-chlorophenyl)-{4-[4-(2-cyano-4-(trimethylsilanylethynyl)phenyl-ethynyl)-2-cyano-phenylethynyl]phenyl}amine (**66**):

	800 mg	1.21 mmol
TBAF (1 M solution in THF):	1.31 ml	1.31 mmol
Dry THF:	7 ml	

Formula: $C_{38}H_{19}Cl_2N_3$ (588.48 g/mol).

Yield: 0.70 g (1.19 mmol, 98 %) of a yellow solid.

^{1}H-NMR (400 MHz, $CDCl_3$, 299 K): δ / ppm = 7.86 (dd, $^4J_{HH}$ = 1.5 Hz, $^5J_{HH}$ = 0.3 Hz, 1H, H-15 o. 24), 7.79 (d, $^4J_{HH}$ = 1.4 Hz, 1H, H-15 o. 24), 7.75 (dd, $^3J_{HH}$ = 8.2 Hz, $^4J_{HH}$ = 1.6 Hz, 1H, H-13 o. 22), 7.68 (dd, $^3J_{HH}$ = 8.2 Hz, $^4J_{HH}$ = 1.6 Hz, 1H, H-13 o. 22), 7.60 – 7.58 (2H, H-12, 21), 7.47 (AA', 2H, H-6 o. 7), 7.25 (AA', 4H, H-2 o. 3), 7.04 (BB' 4H, H-2 o. 3), 6.99 (BB', 2H, H-6 o. 7), 3.31 (s, 1H, H-28).

{^{1}H}^{13}C-NMR (101 MHz, $CDCl_3$, 299 K): δ / ppm = 148.5 (quart.), 145.3 (quart.), 136.2 (CH), 136.0 (CH), 135.8 (CH), 135.7 (CH), 133.5 (CH), 132.4 (CH), 132.1 (CH), 129.9 (CH), 129.5 (quart.), 128.2 (quart.), 126.4 (CH), 126.2 (quart.), 123.7 (quart.), 122.2 (CH), 121.9 (quart.), 116.8 (quart.), 116.6 (quart.), 116.1 (quart.), 115.8 (quart.), 115.2 (quart.), 99.3 (quart.), 95.2 (quart.), 88.7 (quart.), 85.6 (quart.), 81.9 (CH), 81.0 (quart.).

11.2.20.3 Thioacetic acid S-{4-[4-(4-{4-[bis-(4-chlorophenyl)amino]-phenyl-ethynyl}-3-cyano-phenylethynyl)-3-cyanophenylethynyl]phenyl} ester (68)

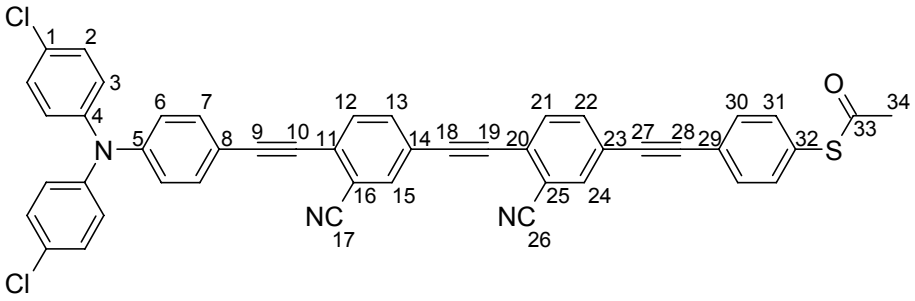

Synthesis according to GP1:

Quantity:			
	Bis-(4-chlorophenyl)-{4-[4-(2-cyano-4-(ethynyl)phenylethynyl)-2-cyanophenyl-ethynyl]phenyl}amine (**67**):	300 mg	510 μmol
	Thioacetic acid S-(4-iodophenyl) ester (**17**):	326 mg	1.17 mmol
	$(PPh_3)_2PdCl_2$:	45.0 mg	50.0 μmol

CuI:	9.58 mg	50.0 μmol
Dry $^{i}Pr_2NEt$:	0.10 ml	
Dry THF:	5.0 ml	

The crude product was purified by column-chromatography on aluminum oxide (neutral, activity V) eluting with DCM / PE (1 : 2) to obtain a yellow solid.

Formula: $C_{46}H_{25}Cl_2N_3OS$ (738.68 g/mol).

Yield: 50.0 mg (68.0 μmol, 13 %) of a yellow solid.

^{1}H-NMR (400 MHz, CD_2Cl_2, 299 K): δ / ppm = 7.89 (dd, $^{4}J_{HH}$ = 1.7 Hz, $^{5}J_{HH}$ = 0.4 Hz, 1H, H-15 o. 24), 7.87 (dd, $^{4}J_{HH}$ = 1.7 Hz, $^{5}J_{HH}$ = 0.4 Hz, 1H, H-15 o. 24), 7.79 (dd, $^{3}J_{HH}$ = 8.2 Hz, $^{4}J_{HH}$ = 1.8 Hz, 1H, H-13 o. 22), 7.76 (dd, $^{3}J_{HH}$ = 8.2 Hz, $^{4}J_{HH}$ = 1.7 Hz, 1H, H-13 o. 22), 7.66 (dd, $^{3}J_{HH}$ = 8.2 Hz, $^{5}J_{HH}$ = 0.5 Hz, 1H, H-12 o. 21), 7.63 (dd, $^{3}J_{HH}$ = 8.2 Hz, $^{5}J_{HH}$ = 0.5 Hz, 1H, H-12 o. 21), 7.60 (AA', 2H, H-30 o. 31), 7.49 (AA', 2H, H-6 o. 7), 7.45 (BB', 2H, H-30 o. 31), 7.28 (AA', 4H, H-2 o. 3), 7.06 (BB', 4H, H-2 o. 3), 7.01 (BB', 2H, H-6 o. 7), 2.43 (s, 3H, H-34).

{^{1}H}^{13}C-NMR (101 MHz, CD_2Cl_2, 299 K): δ / ppm = 193.4 (quart.), 148.8 (quart.), 145.6 (quart.), 136.0 (CH), 135.91 (CH), 135.87 (CH), 135.70 (CH), 134.8 (CH), 133.6 (CH), 132.8 (CH), 132.6 (CH), 132.5 (CH), 130.0 (CH), 129.5 (quart.), 128.2 (quart.), 126.74 (CH), 126.68 (quart.), 125.8 (quart.), 124.7 (quart.), 123.5 (quart.), 122.5 (CH), 122.3 (quart.), 117.1 (quart.), 116.9 (quart.), 116.3 (quart.), 116.0 (quart.), 115.3 (quart.), 99.1 (quart.), 95.1 (quart.), 93.1 (quart.), 89.2 (quart.), 88.6 (quart.), 85.8 (quart.), 31.0 (CH_3).

ESI-MS ($M\text{-}H^+$; high resolution): calc. m/z = 738.11736
found m/z = 738.11530 Δ = 2.79 ppm

11.2.21 Synthesis of Thioacetic acid S-(4-{4-[4-(4-{4-[bis-(4-chlorophenyl)-amino]phenylethynyl}-3-cyano-phenylethynyl)-3-cyanophenylethynyl]-3-cyano-phenylethynyl}phenyl) ester (71)

11.2.21.1 Bis-(4-chlorophenyl)-{4-[4-(4-(2-cyano-4-(trimethylsilanylethynyl)phenyl-ethynyl)-2-cyanophenyl-ethynyl)-2-cyanophenylethynyl]phenyl}amine (69)

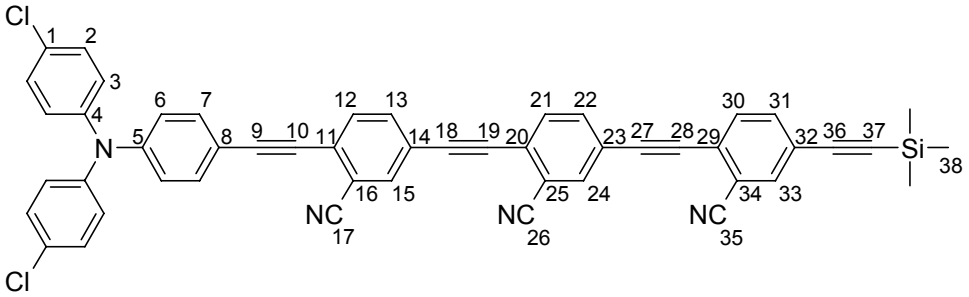

Synthesis according to GP2:

Quantity:	Bis-(4-chlorophenyl)-{4-[4-(2-cyano-4-(ethynyl)phenylethynyl)-2-cyano-phenyl-ethynyl]phenyl}amine (**67**):	400 mg	680 μmol
	2-Iodo-5-(trimethylsilanylethynyl)benzonitrile (**26**):	442 mg	1.36 mmol
	$(PPh_3)_2PdCl_2$:	48.0 mg	68.0 μmol
	CuI:	12.9 mg	68.0 μmol
	Dry Et_2NH:	0.35 ml	1.94 mmol
	Dry THF:	1.8 ml	

Because of solubility problems of **67** in Et_2NH THF was added to the reaction mixture. The crude product was purified by column-chromatography on aluminum oxide (neutral, activity V) eluting with DCM / PE (1 : 4 > 1 : 3) to obtain a yellow solid.

Formula: $C_{50}H_{30}Cl_2N_4Si$ (785.79 g/mol).

Yield: 160 mg (204 μmol, 30 %) of a yellow solid.

^{1}H-NMR (600 MHz, CD_2Cl_2, 299 K): δ / ppm = 7.91 (dd, $^4J_{HH}$ = 1.7 Hz, $^5J_{HH}$ = 0.6 Hz, 1H, H-15 o. 24 o. 33), 7.89 (dd, $^4J_{HH}$ = 1.7 Hz, $^5J_{HH}$ = 0.6 Hz, 1H, H-15 o. 24 o. 33), 7.82 (dd, $^3J_{HH}$ = 8.2 Hz, $^4J_{HH}$ = 1.7 Hz, 1H, H- 13 o. 22 o. 31), 7.79 (dd,

$^{3}J_{HH}$ = 8.2 Hz, $^{4}J_{HH}$ = 1.7 Hz, 1H, H- 13 o. 22 o. 31), 7.77 (dd, $^{4}J_{HH}$ = 1.7 Hz, $^{5}J_{HH}$ = 0.6 Hz, 1H, H-15 o. 24 o. 33), 7.69 (d, $^{3}J_{HH}$ = 8.1 Hz, $^{4}J_{HH}$ = 0.5 Hz, 1H, H-12 o. 21 o. 30), 7.66 (dd, $^{3}J_{HH}$ = 8.2 Hz, $^{4}J_{HH}$ = 1.6 Hz, 1H, H-13 o. 22 o. 31), 7.64 (dd, $^{3}J_{HH}$ = 8.1 Hz, $^{4}J_{HH}$ = 0.5 Hz, 1H, H-12 o. 21 o. 30), 7.62 (dd, $^{3}J_{HH}$ = 8.2 Hz, $^{4}J_{HH}$ = 0.5 Hz, 1H, H-12 o. 21 o. 30), 7.49 (AA', 2H, H-6 o. 7), 7.28 (AA', 4H, H-2 o. 3), 7.07 (BB', 4H, H-2 o. 3), 7.01 (BB', 2H, H-6 o. 7), 0.26 (s, 9H, H-38).

{^{1}H}^{13}C-NMR (150 MHz, CD_2Cl_2, 299 K): δ / ppm = 148.8 (quart.), 145.6 (quart.), 136.16 (CH), 136.05 (CH), 136.03 (CH), 135.96 (CH), 135.92 (CH), 135.89 (CH), 133.6 (CH), 132.9 (CH), 132.7 (CH), 132.4 (CH), 130.0 (CH), 129.5 (quart.), 128.2 (quart.), 126.7 (CH), 126.6 (quart.), 125.5 (quart.), 125.1 (quart.), 123.5 (quart.), 122.4 (CH), 122.1 (quart.), 117.04 (quart.), 116.85 (quart.), 116.75 (quart.), 116.43 (quart.), 116.20 (quart.), 115.9 (quart.), 115.2 (quart.), 102.1 (quart.), 100.2 (quart.), 99.1 (quart.), 95.6 (quart.), 94.6 (quart.), 89.6 (quart.), 89.2 (quart.), 85.8 (quart.), -0.3 (CH_3).

11.2.21.2 Bis-(4-chlorophenyl)-{4-[4-(4-(2-cyano-4-(ethynyl)phenylethynyl)-2-cyano-phenyl-ethynyl)-2-cyanophenylethynyl]phenyl}amine (70)

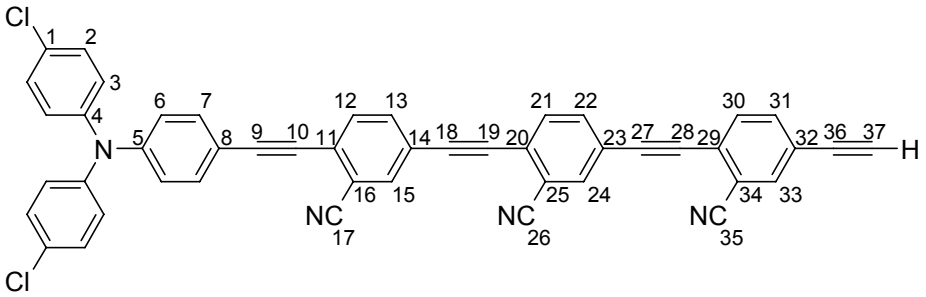

Synthesis according to GP6:

Quantity: Bis-(4-chlorophenyl)-{4-[4-(4-(2-cyano-4-(trimethylsilanylethynyl)-phenyl-ethynyl)-2-cyanophenyl-ethynyl)-2-cyanophenylethynyl]-phenyl}amine (**69**): 136 mg 173 μmol

TBAF (1 M solution in THF): 190 μl 187 μmol

Dry THF: 1.6 ml

Formula: $C_{47}H_{22}Cl_2N_4$ (713.61 g/mol).

Yield: 121 mg (169 μmol, 98 %) of a yellow solid.

^{1}H-NMR (400 MHz, CD_2Cl_2, 300 K): δ / ppm = 7.93 (d, $^4J_{HH}$ = 1.3 Hz, 1H, H-15 o. 24 o. 33), 7.90 (d, $^4J_{HH}$ = 1.3 Hz, 1H, H-15 o. 24 o. 33), 7.84 – 7.78 (3H, 2 x H- 13 o. 22 o. 31; H-15 o. 24 o. 33), 7.72 – 7.62 (4H, H- 13 o. 22 o. 31; H-12, 21, 30), 7.49 (AA', 2H, H-6 o. 7), 7.28 (AA', 4H, H-2 o. 3), 7.06 (BB', 4H, H-2 o. 3), 7.01 (BB', 2H, H-6 o. 7), 3.39 (s, 1H, H-37).

{^{1}H}^{13}C-NMR (101 MHz, CD_2Cl_2, 300 K): δ / ppm = 148.8 (quart.), 145.6 (quart.), 136.41 (CH), 136.24 (CH), 136.08 (CH), 136.04 (CH), 135.99 (CH), 135.89 (CH), 133.6 (CH), 132.9 (CH), 132.8 (CH), 132.3 (quart.), 132.4 (CH), 130.0 (CH), 129.5 (quart.), 128.2 (quart.), 126.7 (CH), 126.1 (quart.), 123.9 (quart.), 123.4 (quart.), 122.4 (CH), 122.1 (quart.), 117.04 (quart.), 116.76 (quart.), 116.74 (quart.), 116.45 (quart.), 116.30 (quart.), 115.9 (quart.), 115.2 (quart.), 99.1 (quart.), 95.6 (quart.), 94.7 (quart.), 89.4 (quart.), 89.0 (quart.), 85.8 (quart.), 81.9 (CH), 81.1 (quart.).

11.2.21.3 Thioacetic acid S-(4-{4-[4-(4-{4-[bis-(4-chlorophenyl)amino]-phenylethynyl}-3-cyano-phenylethynyl)-3-cyanophenylethynyl]-3-cyano-phenylethynyl}phenyl) ester (71)

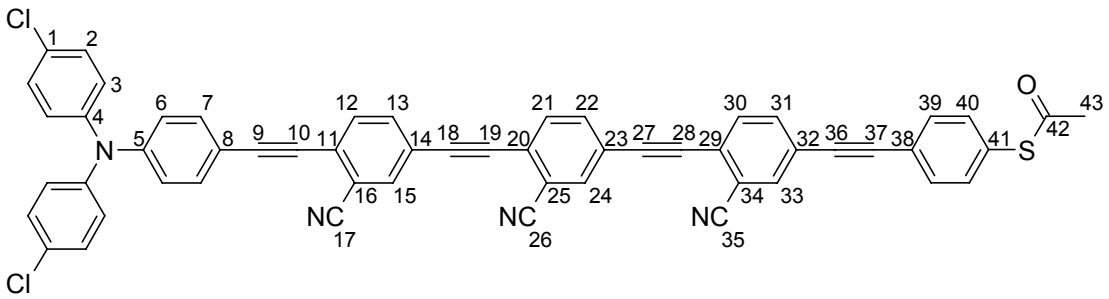

Synthesis according to GP1:

Quantity: Bis-(4-chlorophenyl)-{4-[4-(4-(2-cyano-4-(ethynyl)phenylethynyl)-2-cyano-phenyl-ethynyl)-2-cyanophenylethynyl]phenyl}amine (**70**):

	140 mg	196 μmol
Thioacetic acid S-(4-iodophenyl) ester (**17**):	109 mg	392 mmol
$(PPh_3)_2PdCl_2$:	14.0 mg	19.6 μmol
CuI:	3.74 mg	19.6 μmol
Dry $^{i}Pr_2NEt$:	40.0 μl	
Dry THF:	2 ml	

The crude product was purified by column-chromatography on aluminum oxide (neutral, activity V) eluting with DCM / PE (1 : 3 > 1 : 1) to obtain a yellow solid.

Formula: $C_{55}H_{28}Cl_2N_4OS$ (863.81 g/mol).

Yield: 8.00 mg (9.26 μmol, 5 %) of a yellow solid.

^{1}H-NMR (400 MHz, CD_2Cl_2, 300 K): δ / ppm = 7.93 (dd, $^{4}J_{HH}$ = 1.6 Hz, $^{5}J_{HH}$ = 0.6 Hz, 1H, H-15 o. 24 o. 33), 7.90 (dd, $^{4}J_{HH}$ = 1.6 Hz, $^{5}J_{HH}$ = 0.7 Hz, 1H, H-15 o. 24 o. 33), 7.87 (dd, $^{4}J_{HH}$ = 1.6 Hz, $^{5}J_{HH}$ = 0.6 Hz, 1H, H-15 o. 24 o. 33), 7.83 (dd, $^{3}J_{HH}$ = 8.1 Hz, $^{4}J_{HH}$ = 1.6 Hz, 1H, H- 13 o. 22 o. 31), 7.79 (dd, $^{3}J_{HH}$ = 8.1 Hz, $^{4}J_{HH}$ = 1.6 Hz, 1H, H- 13 o. 22 o. 31), 7.76 (dd, $^{3}J_{HH}$ = 8.1 Hz, $^{4}J_{HH}$ = 1.6 Hz, 1H, H-13 o. 22 o. 31), 7.70 – 7.63 (3H, H-12, 21, 30), 7.60 (AA', 2H, H-39 o. 40), 7.49 (AA', 2H, H-6 o. 7), 7.44 (BB', 2H, H-39 o. 40), 7.28 (AA', 4H, H-2 o. 3), 7.06 (BB', 4H, H-2 o. 3), 7.01 (BB', 2H, H-6 o. 7), 2.43 (s, 3H, H-43).

{^{1}H}^{13}C-NMR (101 MHz, CD_2Cl_2, 300 K): δ / ppm = 193.4 (quart.), 148.8 (quart.), 145.6 (quart.), 136.09 (CH), 136.06 (CH), 136.00 (CH), 135.91 (CH), 135.73 (CH), 134.8 (CH), 133.6 (CH), 132.93 (CH), 132.86 (CH), 132.6 (CH), 132.5 (CH), 132.4 (quart.), 132.3 (CH), 130.08 (quart.), 130.04 (CH), 129.9 (quart.), 129.5 (quart.), 128.9 (quart.), 128.8 (quart.), 128.3 (quart.), 126.7 (CH), 126.2 (quart.), 125.6 (quart.), 123.54 (quart.), 123.51 (quart.), 122.5 (CH), 117.06 (quart.), 116.77 (quart.), 116.48 (quart.), 116.41 (quart.), 115.9 (quart.), 115.3 (quart.), 99.2 (quart.), 95.6 (quart.),

94.7 (quart.), 93.3 (quart.), 89.1 (quart.), 88.6 (quart.), 85.8 (quart.), 30.5 (CH_3).

ESI-MS (high resolution, PI): calc. m/z = 862.13608
found m/z = 862.13696 Δ = 1.02 ppm

11.2.22 Synthesis of Thioacetic acid S-[4-(10-butylphenothiazin-3-ylethynyl)phenyl] ester (72)

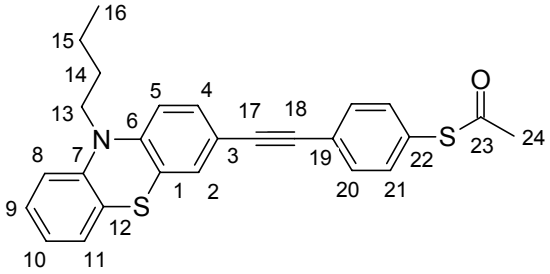

Synthesis according to GP1:

Quantity:			
	10-Butyl-3-ethynylphenothiazine (**16**):	530 mg	1.90 mmol
	Thioacetic acid S-(4-iodophenyl) ester (**17**):	723 mg	2.60 mmol
	$(PPh_3)_2PdCl_2$:	133 mg	190 μmol
	CuI:	36.0 mg	190 μmol
	$^{i}Pr_2EtN$:	243 mg	1.90 mmol
	Dry THF:	7 ml	

The crude product was purified by column-chromatography (aluminum oxide neutral, activity V) with PE / CH_2Cl_2 (10 : 1) to obtain a light yellow solid.

Formula: $C_{26}H_{23}NO_2S$ (429.63).

Yield: 450 mg (1.05 mm, 55 %) of a light yellow solid.

^{1}H-NMR (400 MHz, acetone–d_6, 300 K): δ / ppm = 7.58 (AA`, 2H, H-20 o. 21), 7.45 (BB', 2H, H-20 o. 21), 7.39 (dd, 1H, $^3J_{HH}$ = 8.4 Hz, $^4J_{HH}$ = 1.9 Hz, H-4), 7.30

(d, 1H, $^4J_{HH}$ = 1.9 Hz, H-2), 7.22 (ddd, 1H, $^3J_{HH}$ = 8.2 Hz, $^4J_{HH}$ = 1.5 Hz, H-9 o. 10), 7.15 (dd, 1H, $^3J_{HH}$ = 7.7 Hz, $^4J_{HH}$ = 1.5 Hz, H-8 o. 11), 7.06 (dd, 1H, $^3J_{HH}$ = 8.2 Hz, $^4J_{HH}$ =1.0 Hz, H-4), 7.05 (d, 1H, $^3J_{HH}$ = 8.5 Hz, H-5), 6.98 (ddd, 1H, $^3J_{HH}$ = 7.5 Hz, $^4J_{HH}$ = 1.2 Hz, H-9 o. 10), 3.99 (t, 2H, H-13), 2.43 (s, 3H, H-24), 1.78 (p, 2H, H-14), 1.48 (st, 2H, H-15), 0.93 (t, 2H, H-16).

{^{1}H}^{13}C-NMR (101 MHz, acetone–d_6, 300 K): δ / ppm = 193.1 (quart.), 146.8 (quart.), 145.5 (quart.), 135.3 (CH), 132.7 (CH), 131.9 (CH), 130.6 (CH), 129.4 (quart.), 128.5 (CH), 128.1 (CH), 125.7 (quart.), 125.3 (quart.), 124.7 (quart.), 123.8 (CH), 117.3 (quart.), 117.0 (CH), 116.6 (CH), 91.3 (quart.), 89.1 (quart.), 47.7 (CH_2), 20.6 (CH_2), 30.3 (CH_3), 29.6 (CH_2), 14.0 (CH_3).

EI-MS (high resolution, PI): calc. m/z = 429.12156

found m/z = 429.12182 Δ = 0.61 ppm

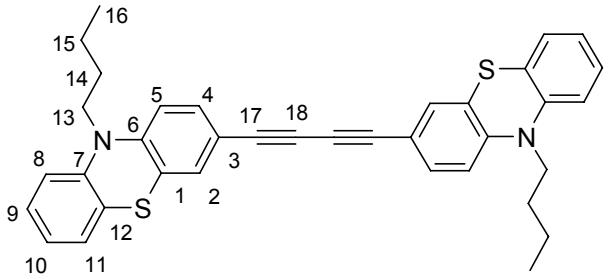

Formula: $C_{36}H_{32}N_2S_2$ (556.78).

Yield: 95.8 mg (172 μmol, 19 %) of a yellow solid.

^{1}H-NMR (400 MHz, acetone-d_6, 300 K): δ / ppm = 7.38 (dd, 1H, $^3J_{HH}$ = 8.5 Hz, $^4J_{HH}$ = 2.0 Hz, H-4), 7.29 (d, 1H, $^4J_{HH}$ = 2.0 Hz, H-2), 7.22 (ddd, 1H, $^3J_{HH}$ = 8.1 Hz, $^4J_{HH}$ = 1.5 Hz, H-9 o. 10), 7.14 (dd, 1H, $^3J_{HH}$ = 7.7 Hz, $^4J_{HH}$ = 1.5 Hz, H-8 o. 11), 7.06 (dd, 1H, $^3J_{HH}$ = 8.2 Hz, $^4J_{HH}$ =0.9 Hz, H-4), 7.04 (d, 1H, $^3J_{HH}$ = 8.6 Hz, H-5), 6.98 (ddd, 1H, $^3J_{HH}$ = 7.6 Hz, $^4J_{HH}$ = 1.3 Hz, H-9 o. 10), 3.99 (t, 2H, H-13), 1.78 (p, 2H, H-14), 1.48 (st, 2H, H-15), 0.91 (t, 2H, H-16).

{^{1}H}^{13}C-NMR (101 MHz, acetone-d_6, 300 K): δ / ppm = 147.5 (quart.), 145.3 (quart.), 132.9 (CH), 131.2 (CH), 128.6 (CH), 128.1 (CH), 125.7 (quart.), 124.5 (quart.), 124.0 (CH), 117.0 (CH), 116.6 (CH), 115.9 (quart.), 82.0 (quart.), 74.6 (quart.), 47.7 (CH_2), 29.2 (CH_2), 20.6 (CH_2), 14.0 (CH_3).

ESI-MS (high resolution, PI): calc. m/z = 556.20014
found m/z = 556.19946 Δ = 1.23 ppm

11.2.23 Synthesis of Thioacetic acid S-{4-[4-(10-butylphenothiazin-3-ylethynyl)-2,5-dipropoxyphenylethynyl]-phenyl} ester (75)

11.2.23.1 10-Butyl-3-[2,5-dipropoxy-4-(trimethylsilanylethynyl)phenylethynyl]-phenothiazine (73)

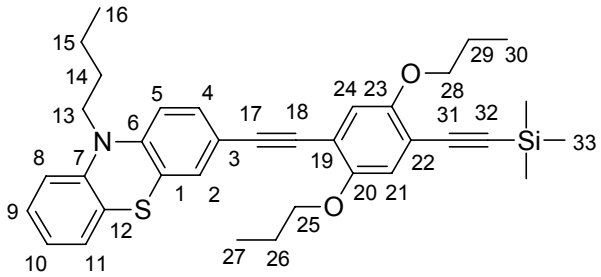

Synthesis according to GP2:

Quantity:	10-Butyl-3-ethynylphenothiazine (**16**):	293 mg	1.05 mmol
	1-Iodo-2,5-dipropoxy-4-trimethylsilanylethynylbenzene (**23**):	400 mg	960 μmol
	$(PPh_3)_2PdCl_2$:	36.8 mg	57.6 μmol
	CuI:	16.5 mg	86.5 μmol
	Dry Et_2NH:	8 ml	

The crude product was purified by flash-chromatography (silica) eluting with PE > CH_2Cl_2 / PE (1: 10 > 1 : 8 > 1 : 6) to obtain a yellow oil.

Formula: $C_{35}H_{41}NO_2SSi$ (567.87).

Yield: 333 mg (586 μmol, 61 %) of a yellow oil.

^{1}H-NMR (400 MHz, acetone–d_6, 300 K): δ / ppm = = 7.35 (dd, 1H, $^3J_{HH}$ = 8.44 Hz, $^4J_{HH}$ = 2.00 Hz, phenothiazine), 7.25-7.20 (2H, phenothiazine), 7.15 (dd, 1H, $^3J_{HH}$ = 7.56 Hz, $^4J_{HH}$ = 1.36 Hz, phenothiazine), 70.7-7.04 (3H), 6.99 (s, 1H, H-21 o. 24), 6.96 (dd, 1H, $^3J_{HH}$ = 7.44 Hz, $^4J_{HH}$ = 1.00 Hz, phenothiazine), 3.99-3.97 (6H, H-13, 25, 28), 1.90-1.75 (6H, H-14, 26, 29), 1.49 (st, 2H, H-15), 1.12-1.07 (6H, H-27, 30), 0.93 (t, 3H, H-16), 0.24 (s, 9H, H-33).

{^{1}H}^{13}C-NMR (101 MHz, acetone–d_6, 300 K): δ / ppm = 155.2 (quart.), 154.3 (quart.), 146.6 (quart.), 145.5 (quart.), 131.7 (CH), 130.3 (CH), 128.5 (CH), 128.1 (CH), 125.7 (quart.), 124.7 (quart.), 123.8 (CH), 118.1 (quart.), 117.9 (CH), 117.7 (CH), 116.9 (CH), 116.6 (CH), 115.5 (quart.), 114.6 (quart.), 102.3 (quart.), 100.2 (quart.), 95.0 (quart.), 86.7 (quart.), 71.63 (CH_2), 71.61 (CH_2), 47.7 (CH_2), 26.9 (CH_2), 23.5 (2 x CH_2), 20.6 (CH_2), 14.0 (CH_3), 10.90 (CH_3), 10.87 (CH_3), 0.0 (CH_3).

11.2.23.2 10-Butyl-3-[2,5-dipropoxy-4-(ethynyl)phenylethynyl]phenothiazine (74)

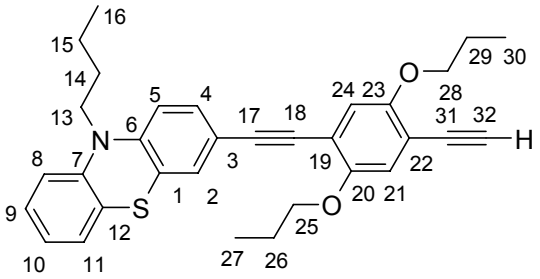

Synthesis according to GP5:

Quantity:			
	10-Butyl-3-[2,5-dipropoxy-4-(trimethylsilanylethynyl)phenylethynyl]-phenothiazine (**73**):	3.00 g	5.28 mmol
	K_2CO_3:	1.29 mg	9.33 mmol
	Dry MeOH:	20 ml	
	Dry CH_2Cl_2:	20 ml	

The crude product was purified by flash-chromatography (silica) eluting with CH_2Cl_2 / PE (1: 3) to obtain a yellow oil.

Formula: $C_{32}H_{33}NO_2S$ (495.69).

Yield: 2.30 mg (4.64 mmol, 88 %) of a yellow oil.

^{1}H-NMR (400 MHz, acetone–d_6, 300 K): δ / ppm = 7.35 (dd, 1H, $^3J_{HH}$ = 8.6 Hz, $^4J_{HH}$ = 2.0 Hz, H-4), 7.25 (d, 1H, $^4J_{HH}$ = 1.9 Hz, H-2), 7.22 (ddd, 1H, , $^3J_{HH}$ = 8.3 Hz, $^4J_{HH}$ = 1.4 Hz, H-9 o. 10), 7.15 (dd, 1H, $^3J_{HH}$ = 7.6 Hz, $^4J_{HH}$ = 1.4 Hz, H-8 o. 11), 7.07-7.04 (4H, H-5, 21, 24, H-8 o. 11), 6.97 (ddd, 1H, $^3J_{HH}$ = 7.5 Hz, $^4J_{HH}$ = 1.00 Hz, H-9 o. 10), 4.04-3.97 (6H, H-13, 25, 28), 3.84 (s, 1H, H-32), 1.90-1.75 (6H, H-14, 26, 29), 1.49 (st, 2H, H-15), 1.12-1.07 (6H, H-27, 30), 0.93 (t, 3H, H-16).

{^{1}H}^{13}C-NMR (101 MHz, acetone–d_6, 300 K): δ / ppm = 155.1 (quart.), 154.3 (quart.), 146.6 (quart.), 145.5 (quart.), 131.7 (CH), 130.4 (CH), 128.5 (CH), 128.1 (CH), 125.7 (quart.), 124.7 (quart.), 123.8 (CH), 118.6 (CH), 118.0 (quart.), 117.5 (CH), 116.9 (CH), 116.6 (CH), 115.5 (quart.), 113.7 (quart.), 94.9 (quart.), 86.5 (quart.), 84.2 (quart.), 80.7 (quart.), 71.7 (CH_2), 71.6 (CH_2), 47.7 (CH_2), 26.9 (CH_2), 23.5 (CH_2), 23.4 (CH_2), 20.6 (CH_2), 14.0 (CH_3), 10.9 (CH_3), 10.8 (CH_3).

11.2.23.3 Thioacetic acid S-{4-[4-(10-butylphenothiazin-3-ylethynyl)-2,5-dipropoxyphenylethynyl]-phenyl} ester (75)

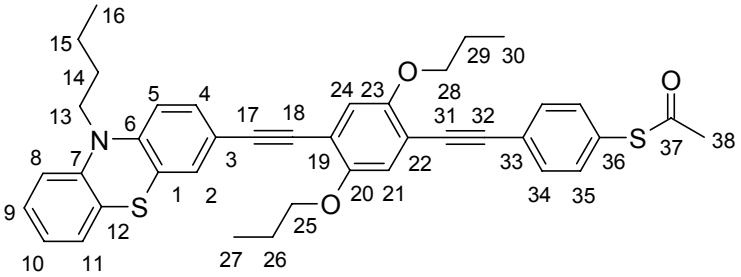

Synthesis according to GP1:

Quantity:	10-Butyl-3-[2,5-dipropoxy-4-(ethynyl)phenylethynyl]phenothiazine (**74**):	600 mg	1.21 mmol
	Thioacetic acid S-(4-iodophenyl) ester (**17**):	500 mg	1.80 mmol
	$(PPh_3)_2PdCl_2$:	84.9 mg	121 μmol
	CuI:	23.0 mg	121 μmol
	$^{i}Pr_2EtN$:	194 mg	1.50 mmol
	Dry THF:	10 ml	

The crude product was purified by flash-chromatography (silica) eluting with CH_2Cl_2 / PE (1: 4 > 1 : 2 > 2 : 1) to obtain a yellow oil.

Formula: $C_{40}H_{39}NO_3S_2$ (645.89).

Yield: 430 mg (666 μmol, 55 %) of a yellow oil.

^{1}H-NMR (400 MHz, acetone–d_6, 300 K): δ / ppm = 7.61 (AA', 2H, H-34 o. 35), 7.49 (BB', 2H, H-34 o. 35), 7.37 (dd, 1H, $^3J_{HH}$ = 8.32 Hz, $^4J_{HH}$ = 1.88 Hz, H-4),), 7.27 (d, 1H, $^4J_{HH}$ = 1.92 Hz, H-2), 7.23 (ddd, 1H, $^3J_{HH}$ = 8.72 Hz, $^4J_{HH}$ = 1.52 Hz, H-9 o. 10), 7.16 (dd, 1H, $^3J_{HH}$ = 7.72 Hz, $^4J_{HH}$ = 1.52 Hz, H-8 o. 11), 7.14-7.12 (2H, H-2, H-8 o. 10), 7.08 (s, 1H, H-21 o. 24), 7.05 (s, 1H, H-21 o. 24), 6.98 (dt, 1H, $^3J_{HH}$ = 8.56 Hz, $^4J_{HH}$ = 1.12 Hz, H-9 o. 10), 4.08-4.04 (4H, H-25, 28), 4.00 (t, 2H, H-13), 1.90-1.76 (6H, H-14, 26, 29), 1.50 (st, 2H, H-15), 1.14-1.10 (6H, H-27, 30), 0.94 (t, 2H, H-16).

{^{1}H}^{13}C-NMR (101 MHz, acetone–d_6, 300 K): δ / ppm = 193.5 (C-37), 155.2 (quart.), 154.8 (quart.), 147.0 (quart.), 145.9 (quart.), 135.8 (CH), 133.1 (CH), 132.1 (CH), 130.7 (CH), 130.0 (quart.), 128.9 (CH), 128.5 (CH), 126.0 (quart.), 125.8 (quart.), 125.0 (quart.), 124.2 (CH), 118.4 (quart.), 118.2 (CH), 117.9 (CH), 117.3 (CH), 117.0 (CH), 116.0 (quart.), 114.5 (quart.), 95.6 (quart.), 94.9 (quart.), 89.0 (quart.), 87.1 (quart.), 72.05 (CH_2), 72.02 (CH_2), 48.0 (CH_2), 30.0 (CH_3), 29.4 (CH_2), (23.84 (CH_2), 23.82 (CH_2), 20.94 (CH_2), 14.4 (CH_3), 11.29 (CH_3), 11.27 (CH_3).

EI-MS: 645 (100%, M^+).

EI-MS (high resolution, PI): calc. m/z = 645.2372

found m/z = 645.2371 Δ = 0.2 ppm

11.2.24 Synthesis of Thioacetic acid S-(4-{4-[4-(10-butylphenothiazin-3-ylethynyl)-2,5-dipropoxyphenylethynyl]-2,5-dipropoxyphenylethynyl}phenyl) ester (78)

11.2.24.1 10-Butyl-3-{4-[2,5-dipropoxy-4-(trimethylsilanylethynyl)-phenylethynyl]-2,5-dipropoxy-phenylethynyl}phenothiazine (76)

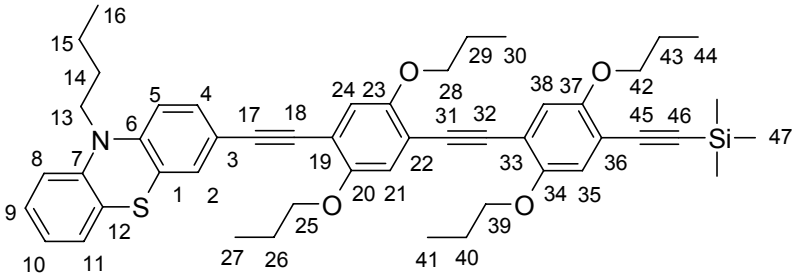

Synthesis according to GP2:

Quantity: 10-Butyl-3-[2,5-dipropoxy-4-(ethynyl)phenylethynyl]phenothiazine (**74**):

1.50 g 2.75 mmol

1-Iodo-2,5-dipropoxy-4-trimethylsilanylethynylbenzene (**23**):

1.48 g 3.57 mmol

$(PPh_3)_2PdCl_2$: 193 mg 275 μmol

CuI: 52.4 mg 275 μmol

Dry Et_2NH: 10 ml

The crude product was purified by flash-chromatography (silica) eluting with CH_2Cl_2 / PE (1: 2 > 1 : 1 > 2 : 1) to obtain a yellow solid.

Formula: $C_{49}H_{57}NO_4SSi$ (784.15).

Yield: 1.50 g (1.91 mmol, 69 %) of a yellow solid.

^{1}H-NMR (400 MHz, C_6D_6, 300 K): δ / ppm = 7.53 (d, 1H, $^4J_{HH}$ = 1.9 Hz, H-2), 7.44 (dd, 1H, $^3J_{HH}$ = 8.4 Hz, $^4J_{HH}$ = 1.9 Hz, H-4), 7.19 (s, 1H, H-21 o. 24 o. 35 o. 38), 7.14 (s, 1H, H-21 o. 24 o. 35 o. 38), 7.11 (s, 1H, H-21 o. 24 o. 35 o. 38), 7.05 (s, 1H, H-21 o. 24 o. 35 o. 38), 6.98 (dd, 1H, $^3J_{HH}$ = 7.6 Hz, $^4J_{HH}$ = 1.4 Hz, H-8 o. 11), 6.90 (ddd, 1H, $^3J_{HH}$ = 7.3 Hz, $^4J_{HH}$ = 1.5 Hz, H-9 o. 10), 6.67 (ddd, 1H, $^3J_{HH}$ = 7.5 Hz, $^4J_{HH}$ = 1.2 Hz, H-9 o. 10), 7.53 (dd, 1H, $^3J_{HH}$ = 8.2 Hz, $^4J_{HH}$ =0.9 Hz, H-4), 6.42 (d, 1H, $^3J_{HH}$ = 8.6 Hz, H-5), 3.62-3.58 (4H, H-25, 28 o. H-39, 42), 3.55-3.49 (4H, H-25, 28 o. H-39, 42), 3.34 (t, 2H, H-13), 1.66-1.53 (8H, H-26, 29, 40, 43), 1.43 (qt, 2H, H-14), 1.15 (st, 2H, H-15), 0.96-0.86 (12H, H-27, 30, 41, 44), 0.70 (t, 3H, H-16), 0.30 (s, 9H, H-47).

{^{1}H}^{13}C-NMR (101 MHz, C_6D_6, 300 K): δ / ppm = 154.9 (quart.), 154.3 (quart.), 154.2 (quart.), 154.0 (quart.), 145.9 (quart.), 145.1 (quart.), 131.0 (CH), 130.7 (CH), 127.9 (CH), 127.4 (CH), 125.8 (quart.), 128.1 (quart.), 123.0 (CH), 118.2 (quart.), 118.0 (CH), 117.7 (CH), 117.6 (CH), 117.5 (CH), 115.9 (CH), 115.6 (CH), 115.5 (quart.), 115.1 (quart.), 114.8 (quart.), 114.5 (quart.), 102.7 (quart.), 100.0 (quart.), 95.1 (quart.), 92.7 (quart.), 92.3 (quart.), 87.1 (quart.), 70.9 (CH_2), 70.79 (CH_2), 70.78 (CH_2), 70.6 (CH_2), 47.2 (CH_2), 29.01 (CH_2), 23.00 (CH_2), 22.96 (2 x CH_2), 22.90 (CH_2), 20.2 (CH_2), 13.8 (CH_3), 10.69 (2 x CH_3), 10.65 (2 x CH_3), 0.2 (CH_3).

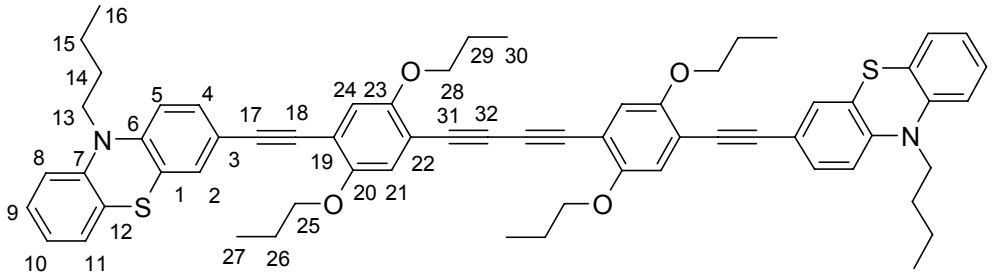

Formula: $C_{64}H_{64}N_2O_4S_2$ (989.36).

Yield: 280 mg (283 μmol, 20 %) of a yellow solid.

^{1}H-NMR (400 MHz, C_6D_6, 300 K): δ / ppm = 7.52 (d, 2H, $^4J_{HH}$ = 1.9 Hz, H-2), 7.43 (dd, 2H, $^3J_{HH}$ = 8.3 Hz, $^4J_{HH}$ = 1.9 Hz, H-4),), 7.00 (s, 2H, H-21 o. 24), 6.97 (dd,

2H, $^3J_{HH}$ = 7.6 Hz, $^4J_{HH}$ = 1.5 Hz, H-8 o. 11), 6.92-6.88 (4H, $^3J_{HH}$ = 7.5 Hz, $^4J_{HH}$ = 1.5 Hz, H-9 o. 10, H-21 o. 24), 6.67 (ddd, 2H, $^3J_{HH}$ = 7.5 Hz, $^4J_{HH}$ = 1.1 Hz, H-9 o. 10),7.16 (dd, 2H, $^3J_{HH}$ = 8.2 Hz, $^4J_{HH}$ = 0.9 Hz, H-8 o. 11), 6.41 (d, 2H, $^3J_{HH}$ = 8.6 Hz, H-5), 7.12 (s, 2H, H-21 o. 24), 3.50-3.44 (8H, H-25, 28), 3.33 (t, 4H, H-13), 1.62-1.52 (8H, H-26, 29), 1.43 (qt, 4H, H-14), 1.15 (st, 4H, H-15), 0.95 (t, 3H, H-27 o. 30), 0.89 (t, 3H, H-27 o. 30), 0.70 (t, 3H, H-16).

{^{1}H}^{13}C-NMR (101 MHz, C_6D_6, 300 K): δ / ppm = 155.7 (quart)., 154.0 (quart)., 145.9 (quart)., 145.1 (quart)., 131.0 (CH), 130.7 (CH), 127.8 (CH), 127.4 (CH), 125.8 (quart)., 125.1 (quart)., 123.1 (CH), 118.1 (quart)., 117.9 (CH), 117.0 (CH), 116.0 (quart)., 115.9 (CH), 115.6 (CH), 112.8 (quart)., 95.7 (quart)., 87.0 (quart)., 80.7 (quart)., 80.3 (quart)., 70.8 (CH_2), 70.7 (CH_2), 47.2 (CH_2), 29.1 (CH_2), 22.9 (CH_2), 22.8 (CH_2), 20.2 (CH_2), 13.8 (CH_3), 10.72 (CH_3), 10.67 (CH_3).

Elemental analysis: calc.: C: 77.70 % H: 6.52 % N: 2.83 % S: 6.48 %
found: C: 78.04 % H: 6.90 % N: 2.86 % S: 6.38 %

11.2.24.2 10-Butyl-3-{4-[2,5-dipropoxy-4-(ethynyl)phenylethynyl]-2,5-dipropoxy-phenylethynyl}phenothiazine (77)

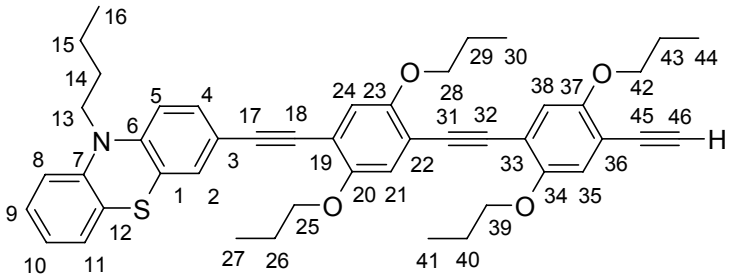

Synthesis according to GP5:

Quantity: 10-Butyl-3-{4-[2,5-dipropoxy-4-(trimethylsilanylethynyl)phenylethynyl]-2,5-dipropoxy-phenylethynyl}phenothiazine (**76**):

1.82 g 2.32 mmol

K_2CO_3:	566 mg	4.10 mmol
Dry MeOH:	10 ml	
Dry CH_2Cl_2:	10 ml	

The crude product was purified by flash-chromatography (silica) eluting with CH_2Cl_2 / PE (1: 2 > 1 : 1) to obtain a yellow solid.

Formula: $C_{46}H_{49}NO_4S$ (711.97).

Yield: 1.10 g (1.54 mmol, 66 %) of a yellow solid.

^{1}H-NMR (400 MHz, CD_2Cl_2, 300 K): δ / ppm = 7.32 (dd, 1H, $^3J_{HH}$ = 8.5 Hz, $^4J_{HH}$ = 1.9 Hz, H-4), 7.26 (d, 1H, $^4J_{HH}$ = 1.9 Hz, H-2), 7.17 (ddd, 1H, $^3J_{HH}$ = 7.6 Hz, $^4J_{HH}$ = 1.3 Hz, H-9 o. 10), 7.12 (dd, 1H, $^3J_{HH}$ = 7.72 Hz, $^4J_{HH}$ = 1.52 Hz, H-8 o. 11), 7.01-6.99 (4H, H-21, 24, 35, 38), 6.95-6.89 (2H, H-8 o. 11, H-9 o. 10), 6.85 (d, 1H, H-5), 4.04-3.95 (8H, H-25, 28, 39, 42), 3.85 (t, 3H, H-13), 3.38 (s, 1H, H-46), 1.90-1.77 (10H, H-14, 26, 29, 40, 43), 1.49 (st, 2H, H-15), 1.14-1.05 (12H, H-27, 30, 41, 44), 0.95 (t, 3H, H-16).

{^{1}H}^{13}C-NMR (101 MHz, CD_2Cl_2, 300 K): δ / ppm = 154.5 (quart.), 153.9 (quart.), 153.8 (quart.), 153.6 (quart.), 145.9 (quart.), 145.0 (quart.), 131.1 (CH), 130.2 (CH), 127.8 (CH), 127.7 (CH), 125.2 (quart.), 124.4 (quart.), 123.1 (CH), 118.3 (CH), 117.5 (CH), 117.4 (CH), 117.4 (sh, quart.), 117.3 (CH), 116.0 (CH), 115.6 (CH), 115.2 (quart.), 114.8 (quart.), 114.0 (quart.), 112.9 (quart.), 94.7 (quart.), 91.9 (quart.), 91.4 (quart.), 86.2 (quart.), 82.6 (quart.), 80.3 (C-46), 71.59 (CH_2), 71.53 (CH_2), 71.48 (CH_2), 71.40 (CH_2), 47.6 (C-13), 26.3 (C-14), 23.11 (CH_2), 23.06 (CH_2), 23.04 (CH_2), 22.96 (CH_2), 20.45 (C-15), 13.9 (C-16), 10.71 (CH_3), 10.69 (CH_3), 10.68 (CH_3), 10.57 (CH_3).

11.2.24.3 Thioacetic acid S-(4-{4-[4-(10-butylphenothiazin-3-ylethynyl)-2,5-dipropoxy-phenylethynyl]-2,5-dipropoxyphenylethynyl}phenyl) ester (78)

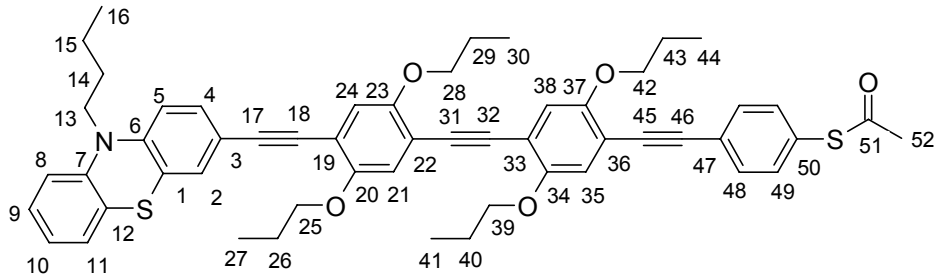

Synthesis according to GP1:

Quantity:			
	10-Butyl-3-{4-[2,5-dipropoxy-4-(ethynyl)phenylethynyl]-2,5-dipropoxy-phenylethynyl}phenothiazine (**77**):	400 mg	562 μmol
	Thioacetic acid S-(4-iodophenyl) ester (**17**):	281 mg	1.02 mmol
	$(PPh_3)_2PdCl_2$:	99.5 mg	56.2 μmol
	CuI:	10.7 mg	56.2 μmol
	$^{i}Pr_2EtN$:	76.3 mg	600 μmol
	Dry THF:	9 ml	

The crude product was purified by flash-chromatography (silica) eluting with CH_2Cl_2 / PE (1: 2 > 1 : 1 > 2 : 1) to obtain a yellow solid.

Formula: $C_{54}H_{55}NO_5S_2$ (862.17).

Yield: 50 mg (58.0 μmol, 10 %) of a yellow solid.

^{1}H-NMR (400 MHz, acetone-d_6, 300 K): δ / ppm = 7.61 (AA', 2H, H-48 o. 49), 7.49 (BB', 2H, H-48 o. 49), 7.36 (dd, 1H, $^3J_{HH}$ = 8.5 Hz, $^4J_{HH}$ = 2.0 Hz, H-4), 7.27 (d, 1H, $^4J_{HH}$ = 1.9 Hz, H-2), 7.22 (ddd, 1H, $^3J_{HH}$ = 7.5 Hz, $^4J_{HH}$ = 1.3 Hz, H-9 o. 10), 7.16 (dd, 1H, $^3J_{HH}$ = 7.6 Hz, $^4J_{HH}$ = 1.5 Hz, H-8 o. 11), 7.16 (s, 1H, H-21 o. 24 o. 35 o. 38), 7.11 (2H, H-21 o. 24 o. 35 o. 38), 7.09 (2H, H-21 o. 24 o. 35 o. 38), 7.07-7.05 (2H, H-5, H-8 o. 11), 6.98 (ddd, 1H, $^3J_{HH}$ = 7.5 Hz, $^4J_{HH}$ = 1.0 Hz, H-9 o. 10), 4.09-4.02 (8H, H-25, 28, 39, 42), 3.99 (t, 3H, H-13), 2.45 (s,

1H, H-52), 1.89-1.77 (10H, H-14, 26, 29, 40, 43), 1.49 (st, 2H, H-15), 1.14-1.09 (12H, H-27, 30, 41, 44), 0.94 (t, 3H, H-16).

{^{1}H}^{13}C-NMR (101 MHz, acetone-d_6, 300 K): δ / ppm = 193.0 (quart.), 154.7 (quart.), 154.5 (quart.), 154.44 (quart.), 124.42 (quart.), 146.5 (quart.), 145.5 (quart.), 135.4 (CH), 132.7 (CH), 131.7 (CH), 130.4 (CH), 129.7 (quart.), 128.5 (CH), 128.1 (CH), 125.7 (quart.), 125.3 (quart.), 124.7 (quart.), 123.7 (CH), 118.08 (quart.), 118.01 (CH), 117.85 (CH), 117.79 (2 x CH), 116.9 (CH), 116.6 (CH), 115.7 (quart.), 115.3 (quart.), 114.9 (quart.), 114.5 (quart.), 95.1 (quart.), 94.6 (quart.), 92.6 (quart.), 92.2 (quart.), 88.6 (quart.), 86.8 (quart.), 71.77 (CH_2), 71.74 (CH_2), 71.62 (2 x CH_2), 47.6 (CH_2), 30.3 (CH_3), 29.6 (CH_2), 23.46 (CH_2), 23.43 (3 x CH_2), 20.6 (CH_2), 14.0 (CH_3), 10.94 (2 x CH_3), 10.93 (CH_3), 10.90 (CH_3).

ESI-MS (high resolution, PI): calc. m/z = 861.35216
found m/z = 861.35049 Δ = 1.9 ppm

11.2.25 Synthesis of Thioacetic acid S-[4-(4-{4-[4-(10-butylphenothiazin-3-ylethynyl)-2,5-dipropoxy-phenylethynyl]-2,5-dipropoxyphenylethynyl}-2,5-dipropoxyphenylethynyl)phenyl] ester (81)

11.2.25.1 10-Butyl-3-{4-[4-(2,5-dipropoxy-4-(trimethylsilanylethynyl)-phenylethynyl)-2,5-dipropoxyphenylethynyl]-2,5-dipropoxy-phenylethynyl}phenothiazine (79)

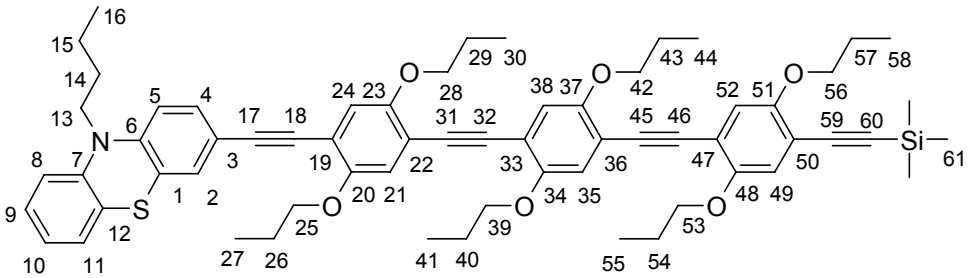

Synthesis according to GP2:

Quantity: 10-Butyl-3-{4-[2,5-dipropoxy-4-(ethynyl)phenylethynyl]-2,5-dipropoxy-phenylethynyl}phenothiazine (**77**): 680 mg 960 μmol

1-Iodo-2,5-dipropoxy-4-trimethylsilanylethynylbenzene (**23**):

	620 mg	1.50 mmol
$(PPh_3)_2PdCl_2$:	35.0 mg	50.0 μmol
CuI:	9.50 mg	50.0 μmol
Dry Et_2NH:	8 ml	

The crude product was purified by flash-chromatography (aluminum oxide neutral, activity V) eluting with EtOAc / PE (2 : 98 > 5 : 95 > 20 : 80) to obtain a yellow solid.

Formula: $C_{63}H_{73}NO_6SSi$ (1000.43).

Yield: 270 mg (270 μmol, 28 %) of a yellow solid.

^{1}H-NMR (400 MHz, CD_2Cl_2, 300 K): δ / ppm = 7.32 (dd, 1H, $^3J_{HH}$ = 8.3 Hz, $^4J_{HH}$ = 1.9 Hz, H-4), 7.26 (d, 1H, $^4J_{HH}$ = 1.9 Hz, H-2), 7.17 (ddd, 1H, $^3J_{HH}$ = 7.6 Hz, $^4J_{HH}$ = 1.3 Hz, H-9 o. 10), 7.12 (dd, 1H, $^3J_{HH}$ = 7.6 Hz, $^4J_{HH}$ = 1.5 Hz, H-8 o. 11), 7.03 (s, 1H), 7.02 (s, 1H), 7.01 (s, 1H), 7.00 (s, 1H), 6.99 (s, 1H), 6.95-6.89 (3H), 6.85 (d, 1H, $^3J_{HH}$ = 8.3 Hz, H-5), 4.02-3.93 (12H, H-25, 28, 39, 42, 53, 56), 3.87 (t, 3H, H-13), 1.91-1.76 (14H, H-14, 26, 29, 40, 43, 54, 56), 1.49 (st, 2H, H-15), 1.12-1.05 (18H, H-27, 30, 41, 44, 55, 58), 0.95 (t, 3H, H-16), 0.26 (s, 9H, H-61).

{^{1}H}^{13}C-NMR (101 MHz, CD_2Cl_2, 300 K): δ / ppm = 154.5 (quart.), 153.87 (quart.), 153.82 (2 x quart.), 153.80 (quart.), 153.7 (quart.), 145.7 (quart.), 145.0 (quart.), 131.1 (CH), 130.2 (CH), 127.8 (CH), 127.7 (CH), 125.2 (quart.), 124.4 (quart.), 123.1 (CH), 117.69 (CH), 117.64 (CH), 117.61 (CH), 117.58 (CH), 117.50 (CH), 117.37 (quart.), 117.26 (CH), 116.0 (CH), 115.6 (CH), 114.76 (quart.), 114.68 (quart.), 114.65 (quart.), 114.47 (quart.), 114.27 (quart.), 114.61 (quart.), 101.5 (quart.), 100.5 (quart.), 94.7 (quart.), 91.97 (quart.), 91.86 (quart.), 91.73 (2 x quart.), 86.2 (quart.), 71.53 (4 x CH_2), 71.49 (CH_2), 71.47 (CH_2), 47.6 (CH_2), 29.3 (CH_2), 23.12 (CH_2), 23.09 (CH_2), 23.06 (4 x CH_2), 20.5 (CH_2), 13.9 (CH_3), 10.71 (CH_3), 10.69 (4 x CH_3), 10.66 (CH_3), 0.0 (CH_3).

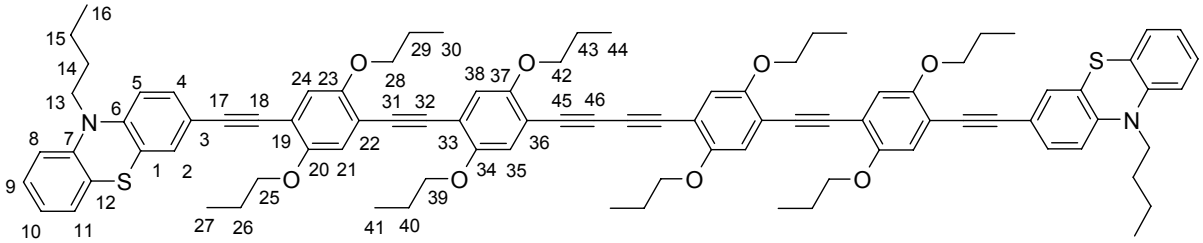

Formula: $C_{92}H_{96}N_2O_8S_2$ (1421.92).

Yield: 194 mg (136 μmol, 28 %) of a yellow solid.

^{1}H-NMR (400 MHz, CD_2Cl_2, 300 K): δ / ppm = 7.32 (dd, 2H, $^3J_{HH}$ = 8.3 Hz, $^4J_{HH}$ = 1.9 Hz, H-4), 7.26 (d, 2H, $^4J_{HH}$ = 1.9 Hz, H-2), 7.17 (ddd, 2H, $^3J_{HH}$ = 7.6 Hz, $^4J_{HH}$ = 1.3 Hz, H-9 o. 10), 7.12 (dd, 2H, $^3J_{HH}$ = 7.6 Hz, $^4J_{HH}$ = 1.5 Hz, H-8 o. 11), 7.02-7.00 (4H, H-21, 24, 35, 38), 6.94 (ddd, 2H), 6.90 (dd, 2H), 6.85 (d, 1H, $^3J_{HH}$ = 8.3 Hz, H-5), 4.01-3.97 (16H, H-25, 28, 39, 42), 3.87 (t, 4H, H-13), 1.90-1.76 (20H, H-14, 26, 29, 40, 43), 1.47 (st, 4H, H-15), 1.12-1.06 (24H, H-27, 30, 41, 44), 0.95 (t, 6H, H-16).

{^{1}H}^{13}C-NMR (101 MHz, CD_2Cl_2, 300 K): δ / ppm = 155.4 (quart.), 153.9 (quart.), 153.8 (quart.), 153.6 (quart.), 146.0 (quart.), 145.0 (quart.), 131.1 (CH), 130.2 (CH), 127.8 (CH), 127.7 (CH), 125.1 (quart.), 124.4 (quart.), 123.1 (CH), 118.1 (CH), 117.5 (CH), 117.3 (quart.), 117.2 (2 x CH), 116.0 (CH), 115.9 (quart.), 115.6 (CH), 114.9 (quart.), 114.0 (quart.), 112.5 (quart.), 94.2 (quart.), 92.7 (quart.), 91.5 (quart.), 86.2 (quart.), 80.1 (quart.), 79.3 (quart.), 71.56 (CH_2), 71.53 (CH_2), 71.49 (2 x CH_2), 47.6 (CH_2), 29.3 (CH_2), 23.11 (CH_2), 23.07 (CH_2), 23.02 (CH_2), 22.95 (CH_2), 20.5 (CH_2), 13.9 (CH_3), 10.71 (2 x CH_3), 10.68 (CH_3), 10.60 (CH_3).

ESI-MS (M^+; high resolution): calc. m/z = 1420.66026
found m/z = 1420.65869 Δ = 1.11 ppm

11.2.25.2 10-Butyl-3-{4-[4-(2,5-dipropoxy-4-(ethynyl)phenylethynyl)-2,5-dipropoxyphenylethynyl]-2,5-dipropoxy-phenylethynyl}phenothiazine (80)

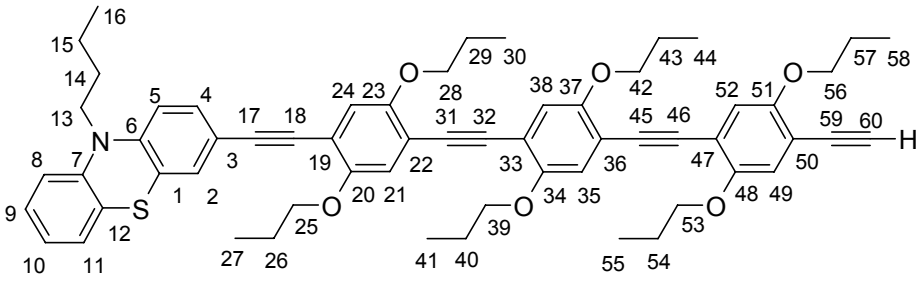

Synthesis according to GP6:

Quantity:

10-Butyl-3-{4-[4-(2,5-dipropoxy-4-(trimethylsilanylethynyl)-phenylethynyl)-2,5-dipropoxyphenylethynyl]-2,5-dipropoxy-phenylethynyl}phenothiazine (**79**):	250 mg	250 μmol
TBAF (1 M solution in THF):	70.6 mg	270 μmol
THF:	7 ml	

Formula: $C_{60}H_{65}NO_6S$ (928.25).

Yield: 225 mg (242 μmol, 97 %) of a yellow solid.

^{1}H-NMR (400 MHz, CD_2Cl_2, 300 K): δ / ppm = 7.32 (dd, 1H, $^3J_{HH}$ = 8.3 Hz, $^4J_{HH}$ = 1.9 Hz, H-4), 7.26 (d, 1H, $^4J_{HH}$ = 1.9 Hz, H-2), 7.17 (ddd, 1H, $^3J_{HH}$ = 7.6 Hz, $^4J_{HH}$ = 1.3 Hz, H-9 o. 10), 7.12 (dd, 1H, $^3J_{HH}$ = 7.6 Hz, $^4J_{HH}$ = 1.5 Hz, H-8 o. 11), 7.032 (s, 1H), 7.027 (s, 1H), 7.018 (s, 1H), 7.011 (s, 1H), 7.006 (s, 1H), 6.997 (s, 1H), 6.93 (ddd, 1H, $^3J_{HH}$ = 7.5 Hz, $^4J_{HH}$ = 1.2 Hz, H-9 o. 10), 6.90 (dd, 1H, $^3J_{HH}$ = 8.6 Hz, $^4J_{HH}$ = 1.4, H-8 o. 11), 6.85 (d, 1H, $^3J_{HH}$ = 8.5 Hz, H-5), 4.02-3.95 (12H, H-25, 28, 39, 42, 53, 56), 3.87 (t, 3H, H-13), 1.89-1.75 (14H, H-14, 26, 29, 40, 43, 54, 56), 1.45 (st, 2H, H-15), 1.12-1.03 (18H, H-27, 30, 41, 44, 55, 58), 0.95 (t, 3H, H-16).

{^{1}H}^{13}C-NMR (101 MHz, CD_2Cl_2, 300 K): δ / ppm = 154.5 (quart.), 153.87 (quart.), 153.86 (quart.), 153.82 (quart.), 153.80 (quart.), 153.7 (quart.), 145.9 (quart.), 145.0 (quart.), 131.1 (CH), 130.2 (CH), 127.8 (CH), 127.7 (CH),

125.1 (quart.), 124.4 (quart.), 123.1 (CH), 118.3 (CH), 117.61 (CH), 117.57 (CH), 117.50 (CH), 117.37 (quart., CH), 117.26 (CH), 116.0 (CH), 115.6 (CH), 115.2 (quart.), 114.71 (quart.), 114.69 (quart.), 114.4 (quart.), 114.1 (quart.), 113.0 (quart.), 94.7 (quart.), 91.98 (quart.), 91.88 (quart.), 91.7 (quart.), 91.6 (quart.), 86.2 (quart.), 82.6 (quart.), 80.3 (quart.), 71.59 (CH_2), 71.54 (2 x CH_2), 71.51 (CH_2), 71.49 (CH_2), 71.40 (CH_2), 47.6 (CH_2), 29.3 (CH_2), 23.12 (CH_2), 23.07 (CH_2), 23.05 (3 x CH_2), 22.96 (CH_2), 20.5 (CH_2), 13.9 (CH_3), 10.71 (2 x CH_3), 10.68 (3 x CH_3), 10.57 (CH_3).

11.2.25.3 Thioacetic acid S-[4-(4-{4-[4-(10-butylphenothiazin-3-ylethynyl)-2,5-dipropoxy-phenylethynyl]-2,5-dipropoxyphenylethynyl}-2,5-dipropoxyphenylethynyl)phenyl] ester (81)

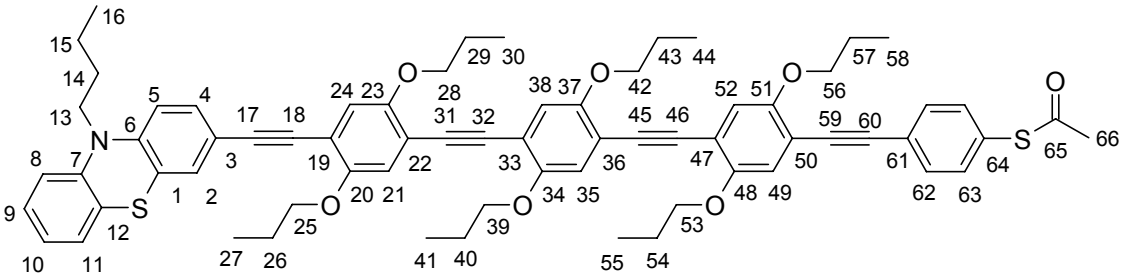

Synthesis according to GP1:

Quantity: 10-Butyl-3-{4-[4-(2,5-dipropoxy-4-(ethynyl)phenylethynyl)-2,5-dipropoxyphenylethynyl]-2,5-dipropoxy-phenylethynyl}phenothiazine (**80**):

	220 mg	237 μmol
Thioacetic acid S-(4-iodophenyl) ester (**17**):	131 mg	474 μmol
$(PPh_3)_2PdCl_2$:	8.42 mg	12.0 μmol
CuI:	2.28 mg	12.0 μmol
$^{i}Pr_2EtN$:	34.3 mg	270 μmol
Dry THF:	5 ml	

The crude product was purified by flash-chromatography (aluminum oxide neutral, activity V) eluting with DCM / PE (2 : 98 > 5 : 95 > 20 : 80 > 40 : 60) to obtain a yellow solid.

Formula: $C_{68}H_{71}NO_7S_2$ (1078.45).

Yield: 25.3 mg (23.5 μmol, 10 %) of a yellow solid.

^{1}H-NMR (400 MHz, CD_2Cl_2, 300 K): δ / ppm = 7.57 (AA´, 2H, H-62 o. 63), 7.42 (BB´, 2H, H-62 o. 63), 7.32 (dd, 1H, $^3J_{HH}$ = 8.3 Hz, $^4J_{HH}$ = 1.9 Hz, H-4), 7.26 (d, 1H, $^4J_{HH}$ = 1.9 Hz, H-2), 7.17 (ddd, 1H, $^3J_{HH}$ = 7.6 Hz, $^4J_{HH}$ = 1.3 Hz, H-9 o. 10), 7.11 (dd, 1H, $^3J_{HH}$ = 7.6 Hz, $^4J_{HH}$ = 1.5 Hz, H-8 o. 11), 7.032 (s, 1H), 7.027 (s, 1H), 7.018 (s, 1H), 7.06-7.00 (6H, H-21, 24, 35, 38, 49, 52), 6.96-6.98 (2H, H-9 o. 10, H-8 o. 11), 6.85 (d, 1H, $^3J_{HH}$ = 8.5 Hz, H-5), 4.04-3.98 (12H, H-25, 28, 39, 42, 53, 56), 3.87 (t, 3H, H-13), 2.43 (s, 3H, H-66), 1.88-1.75 (14H, H-14, 26, 29, 40, 43, 54, 56), 1.46 (st, 2H, H-15), 1.13-1.03 (18H, H-27, 30, 41, 44, 55, 58), 0.95 (t, 3H, H-16).

{^{1}H}^{13}C-NMR (101 MHz, CD_2Cl_2, 300 K): δ / ppm = 194.2 (quart.), 154.5 (quart.), 153.87 (quart.), 153.86 (quart.), 153.82 (quart.), 153.80 (quart.), 153.7 (quart.), 145.9 (quart.), 145.0 (quart.), 131.2 (CH), 131.0 (CH), 130.5 (CH), 129.6 (CH), 129.2 (CH), 127.3 (quart.), 127.1 (CH), 126.1 (quart.), 125.1 (quart.), 124.4 (quart.), 122.5 (CH), 121.9 (CH), 120.9 (CH), 117.59 (CH), 117.50 (CH), 117.39 (quart., CH), 117.23 (CH), 116.2 (CH), 115.4 (CH), 115.2 (quart.), 114.71 (quart.), 114.69 (quart.), 114.4 (quart.), 114.1 (quart.), 113.0 (quart.), 94.7 (quart.), 91.98 (quart.), 91.88 (quart.), 91.7 (quart.), 91.6 (quart.), 86.2 (quart.), 82.6 (quart.), 80.3 (quart.), 71.93 (3 x CH_2), 71.89 (CH_2), 71.75 (CH_2), 71.69 (CH_2), 47.0 (CH_2), 29.5 (CH_3), 28.7 (CH_2), 22.56 (CH_2), 22.52 (2 x CH_2), 22.50 (3 x CH_2), 19.9 (CH_2), 13.3 (CH_3), 10.22 (CH_3), 10.15 (CH_3), 10.11 (CH_3), 10.09 (3 x CH_3).

ESI-MS (high resolution): calc. m/z = 1077.46719
found m/z = 1077.46714 Δ = 0.05 ppm

11.2.26 Synthesis of Thioacetic acid S-{4-[4-(10-butylphenothiazin-3-ylethynyl)-3-cyano-phenylethynyl]phenyl} ester (84)

11.2.26.1 2-(10-Butylphenothiazin-3-ylethynyl)-5-trimethylsilanylethynyl-benzonitrile (82)

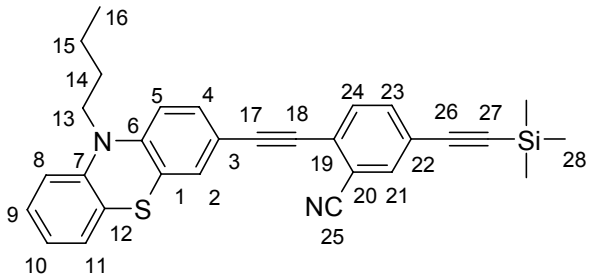

Synthesis according to GP2:

Quantity:	10-Butyl-3-ethynylphenothiazin (**16**):	1.20 g	4.30 mmol
	2-Iodo-5-(trimethylsilanylethynyl)benzonitrile (**26**):		
		2.07 g	6.36 mmol
	$(PPh_3)_2PdCl_2$:	365 mg	520 μmol
	CuI:	99.0 mg	520 μmol
	Dry Et_2NH:	4 ml	

The crude product was purified by column-chromatography (aluminum oxide neutral, activity V) eluting with CH_2Cl_2 / PE (5 : 95) to obtain a yellow oil.

Formula: $C_{30}H_{28}N_2SSi$ (476.72).

Yield: 1.21 g (2.54 mmol, 59 %) of a yellow oil.

^{1}H-NMR (400 MHz, $CDCl_3$, 300 K): δ / ppm = 7.71 (dd, 1H, $^4J_{HH}$ = 1.6 Hz, $^5J_{HH}$ = 0.5 Hz, H-21), 7.58 (dd, 1H, $^3J_{HH}$ = 8.2 Hz, $^4J_{HH}$ = 1.6 Hz, H-23), 7.49 (dd, 1H, $^3J_{HH}$ = 8.2 Hz, $^5J_{HH}$ = 0.5 Hz, H-24), 7.38 (dd, 1H, $^3J_{HH}$ = 8.5 Hz, $^4J_{HH}$ = 2.0 Hz, H-4), 7.25 (d, 1H, $^4J_{HH}$ = 1.9 Hz, H-2), 7.15 (ddd, 1H, $^3J_{HH}$ = 7.5 Hz, $^4J_{HH}$ = 1.5 Hz, H-9 o. 10), 7.11 (dd, 1H, $^3J_{HH}$ = 7.4 Hz, $^4J_{HH}$ = 1.5 Hz, H-8 o. 11), 6.93 (ddd, 1H, $^3J_{HH}$ = 7.5 Hz, $^4J_{HH}$ = 1.1 Hz, H-9 o. 10), 6.86 (dd, 1H, $^3J_{HH}$ = 9.0 Hz,

$^4J_{HH}$ = 0.9 Hz, H-8 o. 11), 6.80 (d, 1H, $^3J_{HH}$ = 8.5 Hz, H-5), 3.85 (t, 2H, H-13), 1.78 (qt, 2H, H-14), 1.45 (st, 2H, H-15), 0.94 (t, 3H, H-16), 0.26 (s, 9H, H-28).

{^{1}H}^{13}C-NMR (101 MHz, $CDCl_3$, 300 K): δ / ppm = 146.6 (quart.), 144.5 (quart.), 135.9 (CH), 135.5 (CH), 131.8 (CH), 131.7 (CH), 130.6 (CH), 127.7 (CH), 127.5 (CH), 127.1 (quart.), 125.1 (quart.), 124.2 (quart.), 123.3 (quart.), 123.1 (CH), 117.0 (quart.), 115.8 (CH), 115.5 (quart.), 115.3 (quart.), 115.2 (CH), 102.4 (quart.), 99.0 (quart.), 98.0 (quart.), 85.8 (quart.), 47.5 (CH_2), 29.0 (CH_2), 20.2 (CH_2), 13.9 (CH_3), -0.1 (CH_3).

11.2.26.2 2-(10-Butylphenothiazin-3-ylethynyl)-5-ethynylbenzonitrile (83)

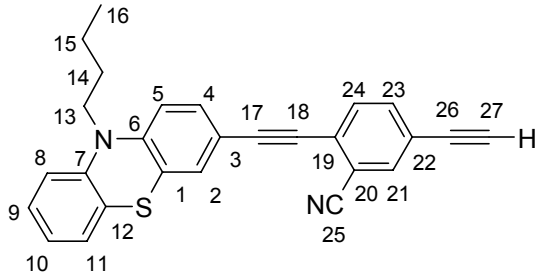

Synthesis according to GP6:

Quantity:			
	2-(10-Butylphenothiazin-3-ylethynyl)-5-trimethylsilanylethynyl-benzonitrile (**82**):	1.20 g	2.51 mmol
	TBAF (1 M solution in THF):	732 mg	2.80 mmol
	THF:	7 ml	

Formula: $C_{27}H_{20}N_2S$ (404.53).

Yield: 0.98 g (2.42 mmol, 96 %) of a yellow oil.

^{1}H-NMR (400 MHz, CD_2Cl_2, 300 K): δ / ppm = 7.74 (d, 1H, $^4J_{HH}$ = 1.6 Hz, H-21), 7.61 (dd, 1H, $^3J_{HH}$ = 8.2 Hz, $^4J_{HH}$ = 1.6 Hz, H-23), 7.52 (dd, 1H, $^3J_{HH}$ = 8.2 Hz, $^5J_{HH}$ = 0.5 Hz, H-24), 7.39 (dd, 1H, $^3J_{HH}$ = 8.5 Hz, $^4J_{HH}$ = 2.0 Hz, H-4), 7.33 (d, 1H, $^4J_{HH}$ = 1.9 Hz, H-2), 7.15 (ddd, 1H, $^3J_{HH}$ = 7.5 Hz, $^4J_{HH}$ = 1.5 Hz, H-9 o. 10),

7.11 (dd, 1H, $^3J_{HH}$ = 7.4 Hz, $^4J_{HH}$ = 1.5 Hz, H-8 o. 11), 6.93 (ddd, 1H, $^3J_{HH}$ = 7.5 Hz, $^4J_{HH}$ = 1.1 Hz, H-9 o. 10), 6.86 (dd, 1H, $^3J_{HH}$ = 9.0 Hz, $^4J_{HH}$ = 0.9 Hz, H-8 o. 11), 6.81 (d, 1H, $^3J_{HH}$ = 8.5 Hz, H-5), 3.86 (t, 2H, H-13), 3.25 (s, 1H, H-28), 1.78 (qt, 2H, H-14), 1.47 (st, 2H, H-15), 0.94 (t, 3H, H-16).

{^{1}H}^{13}C-NMR (101 MHz, CD_2Cl_2, 300 K): δ / ppm = 146.7 (quart.), 144.5 (quart.), 136.1 (CH), 135.7 (CH), 131.9 (CH), 131.7 (CH), 130.6 (CH), 127.7 (CH, quart.), 127.5 (CH), 125.2 (quart.), 124.2 (quart.), 123.1 (CH), 122.3 (quart.), 116.9 (quart.), 115.8 (CH), 115.5 (quart.), 115.4 (quart.), 115.2 (CH), 98.2 (quart.), 85.7 (quart.), 81.4 (quart.), 81.1 (quart.), 47.5 (CH_2), 29.0 (CH_2), 20.3 (CH_2), 13.9 (CH_3).

11.2.26.3 Thioacetic acid S-{4-[4-(10-butylphenothiazin-3-ylethynyl)-3-cyano-phenylethynyl]phenyl} ester (84)

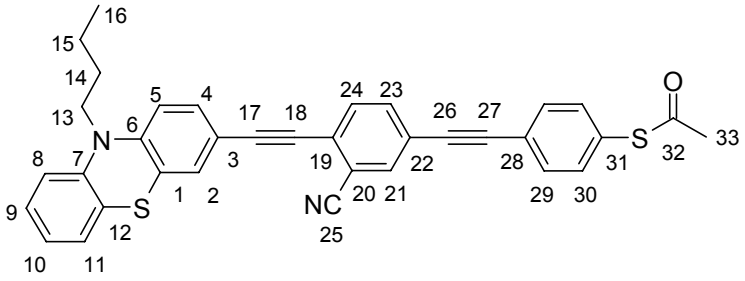

Synthesis according to GP1:

Quantity:			
	2-(10-Butylphenothiazin-3-ylethynyl)-5-ethynylbenzonitrile (**83**):	170 mg	420 μmol
	Thioacetic acid S-(4-iodophenyl) ester (**17**):	230 mg	830 μmol
	$(PPh_3)_2PdCl_2$:	14.3 mg	20.4 μmol
	CuI:	3.90 mg	20.4 μmol
	^{i}Pr$_2$EtN:	55.6 mg	430 μmol
	Dry THF:	4 ml	

The crude product was purified by column-chromatography (aluminum oxide neutral, activity V) eluting with CH_2Cl_2 / PE (1 : 9 > 2 : 8 > 4 : 6) to obtain a red solid.

Formula: $C_{35}H_{36}N_2OS_2$ (554.73).

Yield: 68.0 mg (123 μmol, 29 %) of a red solid.

^{1}H-NMR (400 MHz, CD_2Cl_2, 300 K): δ / ppm = 7.79 (d, 1H, $^4J_{HH}$ = 1.6 Hz, H-21), 7.67 (dd, 1H, $^3J_{HH}$ = 8.2 Hz, $^4J_{HH}$ = 1.7 Hz, H-23), 7.57 (d, 1H, $^3J_{HH}$ = 8.3 Hz, H-24), 7.54-7.48 (4H, H-29, 30), 7.40 (dd, 1H, $^3J_{HH}$ = 8.5 Hz, $^4J_{HH}$ = 2.0 Hz, H-4), 7.33 (d, 1H, $^4J_{HH}$ = 1.9 Hz, H-2), 7.17 (ddd, 1H, $^3J_{HH}$ = 7.5 Hz, $^4J_{HH}$ = 1.4 Hz, H-9 o. 10), 7.11 (dd, 1H, $^3J_{HH}$ = 7.6 Hz, $^4J_{HH}$ = 1.5 Hz, H-8 o. 11), 6.94 (ddd, 1H, $^3J_{HH}$ = 7.5 Hz, $^4J_{HH}$ = 1.0 Hz, H-9 o. 10), 6.90 (d, 1H, $^3J_{HH}$ = 8.2 Hz, H-8 o. 11), 6.86 (d, 1H, $^3J_{HH}$ = 8.6 Hz, H-5), 3.87 (t, 2H, H-13), 1.78 (qt, 2H, H-14), 1.52 (s, 3H, H-33), 1.46 (st, 2H, H-15), 0.94 (t, 3H, H-16).

{^{1}H}^{13}C-NMR (101 MHz, CD_2Cl_2, 300 K): δ / ppm = 193.4 (quart.), 146.9 (quart.), 144.7 (quart.), 138.3 (quart.), 135.7 (CH), 135.4 (CH), 132.7 (CH, quart.), 132.3 (CH), 131.8 (CH), 130.6 (CH), 127.8 (CH), 127.7 (CH), 127.5 (CH, quart.), 127.0 (quart.), 125.3 (quart.), 124.2 (quart.), 123.5 (quart.), 123.3 (CH), 117.2 (quart.), 116.1 (CH), 115.7 (quart.), 115.60 (quart.), 115.57 (CH), 97.9 (quart.), 92.6 (quart.), 88.4 (quart.), 86.2 (quart.), 47.7 (CH_2), 29.4 (CH_3), 29.2 (CH_2), 20.4 (CH_2), 13.9 (CH_3).

ESI-MS (high resolution, PI): calc. m/z = 554.14865
found m/z = 554.14787 Δ = 1.4 ppm

Elemental analysis: calc.: C: 75.78 % H: 4.72 % N: 5.05 % S: 11.56 %
found: C: 76.95 % H: 4.87 % N: 5.44 % S: 11.90 %

11.2.27 Synthesis of Thioacetic acid S-(4-{4-[4-(10-butylphenothiazin-3-ylethynyl)-3-cyanophenylethynyl]-3-cyanophenylethynyl}phenyl) ester (87)

11.2.27.1 3-[2-Cyano-4-(2-cyano-4-trimethylsilylethinyl-phenyl)ethinylphenyl]ethinyl-10-butylphenothiazin (85)

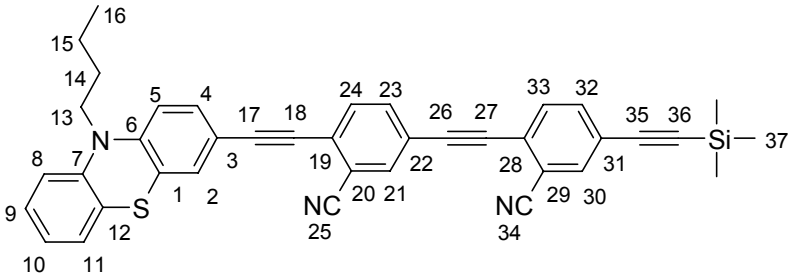

Synthesis according to GP2:

Quantity:	2-(10-Butylphenothiazin-3-ylethynyl)-5-ethynylbenzonitrile (**83**):		
		800 mg	1.98 mmol
	2-Iodo-5-(trimethylsilanylethynyl)benzonitrile (**26**):		
		900 mg	2.76 mmol
	$(PPh_3)_2PdCl_2$:	156 mg	223 μmol
	CuI:	44.0 mg	223 μmol
	Dry Et_2NH:	5 ml	

The crude product was purified by column-chromatography (aluminum oxide neutral, activity V) eluting with CH_2Cl_2 / PE (1 : 5) to obtain an orange solid.

Formula: $C_{39}H_{31}N_3SSi$ (601.85).

Yield: 410 mg (681 μmol, 34 %) of an orange solid.

^{1}H-NMR (400 MHz, CD_2Cl_2, 300 K): δ / ppm = 7.88 (d, 1H, $^4J_{HH}$ = 1.3 Hz, H-21 o. 30), 7.81 (d, 1H, $^4J_{HH}$ = 1.4 Hz, H-21 o. 30), 7.77 (dd, 1H, $^3J_{HH}$ = 8.2 Hz, $^4J_{HH}$ = 1.8 Hz, H-23 o. 32), 7.70 (dd, 1H, $^3J_{HH}$ = 8.1 Hz, $^4J_{HH}$ = 1.6 Hz, H-23 o. 32), 7.63 (d, 1H, $^3J_{HH}$ = 8.2 Hz, H-24 o. 33), 7.61 (d, 1H, $^3J_{HH}$ = 8.2 Hz, H-24 o. 33), 7.42 (dd, 1H, $^3J_{HH}$ = 8.3 Hz, $^4J_{HH}$ = 1.9 Hz, H-4), 7.33 (d, 1H, $^4J_{HH}$ = 2.0 Hz, H-2),

7.17 (ddd, 1H, $^3J_{HH}$ = 7.3 Hz, $^4J_{HH}$ = 1.5 Hz, H-9 o. 10), 7.11 (dd, 1H, $^3J_{HH}$ = 7.6 Hz, $^4J_{HH}$ = 1.3 Hz, H-8 o. 11), 6.96 – 6.90 (2H, H-9 o. 10, H-8 o. 11), 6.87 (d, 1H, $^3J_{HH}$ = 8.6 Hz, H-5), 3.88 (t, 2H, H-13), 1.76 (qt, 2H, H-14), 1.47 (st, 2H, H-15), 0.94 (t, 3H, H-16), 0.26 (s, 9H, H-28).

{^{1}H}^{13}C-NMR (101 MHz, CD_2Cl_2, 300 K): δ / ppm = 147.1 (quart.), 144.7 (quart.), 136.2 (CH, quart.), 136.0 (CH), 135.9 (CH), 135.8 (CH), 132.7 (CH), 132.4 (CH), 131.9 (CH), 131.8 (CH), 128.1 (quart.), 127.9 (CH), 127.7 (CH), 125.8 (quart.), 125.3 (quart.), 124.9 (quart.), 124.2 (quart.), 123.3 (CH), 122.2 (quart.), 117.1 (quart.), 116.9 (quart.), 116.2 (CH), 115.9 (quart.), 115.6 (CH), 115.5 (quart.), 102.2 (quart.), 100.1 (quart.), 98.6 (quart.), 95.0 (quart.), 98.1 (quart.), 86.1 (quart.), 47.7 (CH_2), 29.2 (CH_2), 20.4 (CH_2), 13.9 (CH_3), -0.3 (CH_3).

11.2.27.2 3-[2-Cyano-4-(2-cyano-4-ethinylphenyl)ethinylphenyl]ethinyl-10-butylphenothiazin (86)

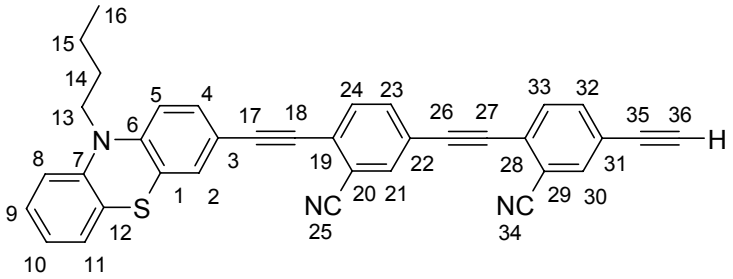

Synthesis according to GP6:

Quantity:			
	3-[2-Cyano-4-(2-cyano-4-trimethylsilylethinylphenyl)ethinylphenyl]ethinyl-10-butylphenothiazin (**85**):	387 mg	643 μmol
	TBAF (1 M solution in THF):	182 mg	694 μmol
	THF:	6 ml	

Formula: $C_{36}H_{23}N_3S$ (529.67).

Yield: 330 mg (623 μmol, 97 %) of a yellow solid.

^{1}H-NMR (400 MHz, $CDCl_3$, 300 K): δ / ppm = 7.75 (d, 1H, $^4J_{HH}$ = 1.5 Hz, H-21 o. 30), 7.69 (d, 1H, $^4J_{HH}$ = 1.4 Hz, H-21 o. 30), 7.64 (dd, 1H, $^3J_{HH}$ = 8.1 Hz, $^4J_{HH}$ = 1.7 Hz, H-23 o. 32), 7.58 (dd, 1H, $^3J_{HH}$ = 8.1 Hz, $^4J_{HH}$ = 1.6 Hz, H-23 o. 32), 7.49 (d, 1H, $^3J_{HH}$ = 8.2 Hz, H-24 o. 33), 7.47 (d, 1H, $^3J_{HH}$ = 8.2 Hz, H-24 o. 33), 7.29 (dd, 1H, $^3J_{HH}$ = 8.3 Hz, $^4J_{HH}$ = 1.9 Hz, H-4), 7.24 (d, 1H, $^4J_{HH}$ = 1.9 Hz, H-2), 7.05 (ddd, 1H, $^3J_{HH}$ = 7.3 Hz, $^4J_{HH}$ = 1.5 Hz, H-9 o. 10), 7.01 (dd, 1H, $^3J_{HH}$ = 7.6 Hz, $^4J_{HH}$ = 1.4 Hz, H-8 o. 11), 6.83 (ddd, 1H, $^3J_{HH}$ = 7.5 Hz, $^4J_{HH}$ = 1.4 Hz, H-9 o. 10), 6.76 (d, 1H, $^3J_{HH}$ = 8.2 Hz, H-8 o. 11), 6.87 (d, 1H, $^3J_{HH}$ = 8.6 Hz, H-5), 3.76 (t, 2H, H-13), 3.18 (s, 1H, H-36), 1.71 (qt, 2H, H-14), 1.35 (st, 2H, H-15), 0.85 (t, 3H, H-16).

{^{1}H}^{13}C-NMR (101 MHz, $CDCl_3$, 300 K): δ / ppm = 146.9 (quart.), 144.5 (quart.), 136.2 (CH, quart.), 135.9 (CH), 135.8 (CH), 135.6 (CH), 132.4 (CH), 132.1 (CH), 131.8 (CH), 130.7 (CH), 128.2 (quart.), 127.7 (CH), 127.6 (CH), 126.1 (quart.), 125.2 (quart.), 124.2 (quart.), 124.1 (quart.), 123.1 (CH), 121.8 (quart.), 116.9 (quart.), 116.5 (quart.), 115.8 (CH), 115.7 (quart.), 115.3 (quart.), 115.2 (CH), 100.7 (quart.), 100.4 (quart.), 98.9 (quart.), 92.2 (quart.), 88.5 (quart.), 85.9 (quart.), 47.5 (CH_2), 29.0 (CH_2), 20.3 (CH_2), 13.9 (CH_3).

11.2.27.3 Thioacetic acid S-(4-{4-[4-(10-butylphenothiazin-3-ylethynyl)-3-cyanophenylethynyl]-3-cyanophenylethynyl}phenyl) ester (87)

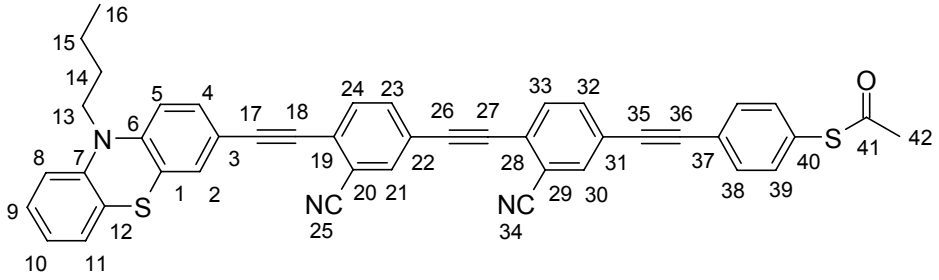

Synthesis according to GP1:

Quantity:	3-[2-Cyano-4-(2-cyano-4-ethinylphenyl)ethinylphenyl]ethinyl-10-butylphenothiazin (**86**):	300 mg	566 μmol
	Thioacetic acid S-(4-iodophenyl) ester (**17**):	387 mg	1.39 mmol

$(PPh_3)_2PdCl_2$:	24.0 mg	34.0 μmol
CuI:	6.50 mg	34.0 μmol
$^{i}Pr_2EtN$:	77.4 mg	600 μmol
Dry THF:	4 ml	

The crude product was purified by column-chromatography (aluminum oxide neutral, activity V) eluting with CH_2Cl_2 / PE (1 : 9 > 2 : 8 > 4 : 6) to obtain red solid.

Formula: $C_{44}H_{29}N_3OS_2$ (679.87).

Yield: 275 mg (404 μmol, 71 %) of a red solid.

^{1}H-NMR (400 MHz, CD_2Cl_2, 300 K): δ / ppm = 7.88 (d, 1H, $^4J_{HH}$ = 1.5 Hz, $^5J_{HH}$ = 0.5 Hz, H-21 o. 30), 7.86 (d, 1H, $^4J_{HH}$ = 1.6 Hz, $^5J_{HH}$ = 0.5 Hz, H-21 o. 30), 7.78 (dd, 1H, $^3J_{HH}$ = 8.1 Hz, $^4J_{HH}$ = 1.6 Hz, H-23 o. 32), 7.75 (dd, 1H, $^3J_{HH}$ = 8.2 Hz, $^4J_{HH}$ = 1.8 Hz, H-23 o. 32), 7.66 (d, 1H, $^3J_{HH}$ = 8.2 Hz, H-24 o. 33), 7.62 (d, 1H, $^3J_{HH}$ = 8.2 Hz, H-24 o. 33), 7.60 (AA´, 2H, H-38 o. 39), 7.45 (BB´, 2H. H-38 o. 39), 7.40 (dd, 1H, $^3J_{HH}$ = 12.6 Hz, $^4J_{HH}$ = 2.5 Hz, H-4), 7.34 (d, 1H, $^4J_{HH}$ = 1.9 Hz, H-2), 7.09 (ddd, 1H, $^3J_{HH}$ = 8.1 Hz, $^4J_{HH}$ = 1.6 Hz, H-9 o. 10), 7.11 (dd, 1H, $^3J_{HH}$ = 7.7 Hz, $^4J_{HH}$ = 1.5 Hz, H-8 o. 11), 6.94 (ddd, 1H, $^3J_{HH}$ = 7.5 Hz, $^4J_{HH}$ = 1.2 Hz, H-9 o. 10), 6.76 (dd, 1H, $^3J_{HH}$ = 8.3 Hz, $^4J_{HH}$ = 0.8 Hz, H-8 o. 11), 6.87 (d, 1H, $^3J_{HH}$ = 8.6 Hz, H-5), 3.88 (t, 2H, H-13), 2.43 (s, 1H, H-42), 1.78 (qt, 2H, H-14), 1.45 (st, 2H, H-15), 0.95 (t, 3H, H-16).

{^{1}H}^{13}C-NMR (101 MHz, CD_2Cl_2, 300 K): δ / ppm = 193.3 (quart.), 147.1 (quart.), 144.7 (quart.), 136.0 (CH), 135.89 (CH), 135.84 (CH), 135.7 (CH), 134.8 (CH), 132.8 (CH), 132.6 (CH), 132.4 (CH), 131.9 (CH), 130.6 (CH), 130.0 (quart.), 128.1 (quart.), 127.8 (CH), 127.7 (CH), 125.8 (quart.), 125.3 (quart.), 124.7 (quart.), 124.2 (quart.), 123.5 (quart.), 123.3 (CH), 122.2 (quart.), 117.1 (quart.), 116.9 (quart.), 116.3 (quart.), 116.1 (CH), 115.9 (quart.), 115.6 (CH), 115.5 (quart.), 98.6 (quart.), 95.1 (quart.), 93.1 (quart.), 89.1 (quart.), 88.6 (quart.), 86.2 (quart.), 47.7 (CH_2), 30.5 (CH_3), 29.2 (CH_2), 20.4 (CH_2), 13.9 (CH_3).

ESI-MS ($M\text{-}H^+$; high resolution): calc. m/z = 680.18303

found m/z = 680.18215 Δ = 1.29 ppm

12 Literature

[1] A. Ulman, *An Introduction to Ultrathin Organic Films: From Langmuir-Blodgett to Self-Assembly*, Academic Press, Boston, **1991**.

[2] H. O. Finklea, in *J. Electroanal. Chem., Vol. 19* (Eds.: A. J. Bard, I. Rubinstein), Marcel Dekker, New York, **1996**.

[3] A. Ulman, *Chem. Rev.* **1996**, *96*, 1533.

[4] V. Kriegisch, C. Lambert, *Top. Curr. Chem.* **2005**, published online.

[5] R. M. Crooks, A. J. Ricco, *Acc. Chem. Res.* **1998**, *31*, 219.

[6] T. E. Mallouk, J. D. Harrison, *Interfacial Design and Chemical Sensing*, American Chemical Society, Washington, DC, **1994**.

[7] S. Flink, C. J. M. van Weggel, D. N. Reinhoudt, *Adv. Mater.* **2000**, *12*, 1315.

[8] L. Haussling, W. Knoll, H. Ringsdorf, F. J. Schmitt, J. Yang, *Makromol. Chem., Macromol. Symp.* **1991**, *46*, 145.

[9] I. Willner, S. Rubin, *Angew. Chem. Int. Ed. Engl.* **1996**, *35*, 367.

[10] A. Dhirani, P.-H. Lin, P. Guyot-Sionnest, R. W. Zehner, L. R. Sita, *J. Chem. Phys.* **1997**, *106*, 5249.

[11] T. Kondo, S. Horiuchi, I. Yagi, S. Yw, K. Uosaki, *J. Am. Chem. Soc.* **1999**, *121*, 391.

[12] R. Naraoka, G. Kaise, K. Kajikawa, H. Okawa, H. Ikezawa, K. Hashimoto, *Chem. Phys. Lett.* **2002**, *362*, 26.

[13] E. Mishina, Y. Miyakita, Q.-K. Yu, S. Nakabayashi, H. Sakaguchi, *J. Chem. Phys.* **2002**, *117*, 4016.

[14] K. Tsuboi, K. Seki, Y. Ouchi, K. Fujita, K. Kajikawa, *Jpn. J. Apll. Phys.* **2003**, *42*, 607.

[15] I. Willner, M. Lion-Dagan, S. Marx-Tibbon, E. Katz, *J. Am. Chem. Soc.* **1995**, *117*, 6581.

[16] I. Willner, M. Lion-Dagan, E. Katz, *J. Chem. Soc., Chem. Commun.* **1996**, 623.

[17] I. Willner, *Acc. Chem. Res.* **1997**, *30*, 347.

[18] I. Willner, B. Willner, *Coord. Chem. Rev.* **2003**, *245*, 139.

[19] T. Kondo, T. Kanai, K. Uosaki, *Langmuir* **2001**, *17*, 6317.

[20] Z. Wang, M. J. Cook, A.-M. Nygard, R. D. A., *Langmuir* **2003**, *19*, 3779.

[21] L. Haussling, H. Ringsdorf, F. J. Schmitt, W. Knoll, *Langmuir* **1991**, *7*, 1837.

[22] F. P. Zamborini, R. M. Crook, *Langmuir* **1998**, *14*, 3279.

[23] Z. J. Donhauser, B. A. Mantooth, K. F. Kelly, L. A. Bumm, J. D. Monnell, J. J. Stapleton, D. W. Price Jr., A. M. Rawlett, D. L. Allara, J. M. Tour, P. S. Weiss, *Science* **2001**, *292*, 2303.

[24] D. L. Feldheim, C. D. Keating, *Chem. Soc. Rev.* **1998**, *27*, 1.

[25] J. H. Fendler, *Chem. Mater.* **2001**, *13*, 3196.

[26] M. A. Reed, J. Chen, A. M. Rawlett, D. W. Price Jr., J. M. Tour, *Appl. Phys. Lett.* **2001**, *78*, 3735.

[27] H. Imahori, Y. Sakata, *Eur. J. Org. Chem.* **1999**, 2445.

[28] H. Imahori, Y. Mori, Y. Matano, *J. Photochem. Photobiol., C* **2003**, *4*, 51.

[29] T. Otsubo, Y. Aso, K. Takimiya, *J. Mater. Chem.* **2002**, *12*, 2565.

[30] N. L. Abbott, J. P. Folkers, G. M. Whitesides, *Science* **1992**, *257*, 1380.

[31] G. P. Lopez, H. A. Biebuyck, C. D. Frisbie, G. M. Whitesides, *Science* **1993**, *260*, 647.

[32] C. B. Gorman, H. A. Biebuyck, G. M. Whitesides, *Chem. Mater.* **1995**, *7*, 252.

[33] L. F. Rozsnyai, M. S. Wrighton, *Langmuir* **1995**, *11*, 3913.

[34] K. C. Chan, T. Kim, J. K. Schoer, R. M. Crooks, *J. Am. Chem. Soc.* **1995**, *117*, 5875.

[35] C. M. Bell, H. C. Yang, T. E. Mallouk, in *Materials Chemistry* (Eds.: L. V. Interrante, L. A. Caspar, A. B. Ellis), American Chemical Society, Washington, DC, **1995**, pp. 211.

[36] J.-H. Fuhrhop, J. Köning, in *Membranes and Molecular Assemblies: The Synkinetic Approach, Monographs in Supramolecular Chemistry* (Ed.: J. F. Stoddart), Freie Univerisität, Berlin, **1995**, pp. 149.

[37] D. Roy, J. Fendler, *Adv. Mater.* **2004**, *16*, 479.

[38] M.-C. Daniel, D. Astruc, *Chem. Rev.* **2004**, *104*, 293.

[39] P. V. Kamat, *J. Phys. Chem. B* **2002**, *106*, 7729.

[40] E. Dulkeith, A. C. Morteani, T. Niedereichholz, T. A. Klar, J. Feldmann, S. A. Levi, F. C. J. M. van Veggel, D. N. Reinhoudt, M. Möller, D. I. Gittins, *Phys. Rev. Lett.* **2002**, *89*, 203002.

[41] X.-M. Li, V. Paraschiv, J. Huskens, D. N. Reinhoudt, *J. Am. Chem. Soc.* **2003**, *125*, 4279.

[42] K. R. Gopidas, J. K. Whitesell, M. A. Fox, *J. Am. Chem. Soc.* **2003**, *125*, 14168.

[43] K. R. Gopidas, J. K. Whitesell, M. A. Fox, *J. Am. Chem. Soc.* **2003**, *125*, 6491.

[44] V. Subramanian, E. E. Wolf, P. V. Kamat, *J. Am. Chem. Soc.* **2004**, *126*, 4943.

[45] B. I. Ipe, K. George Thomas, S. Barazzouk, S. Hotchandani, P. V. Kamat, *J. Phys. Chem. B* **2002**, *106*, 18.

[46] P. K. Sudeep, B. I. Ipe, K. George Thomas, M. V. Geroge, S. Barazzouk, S. Hotchandani, P. V. Kamat, *Nano Lett.* **2002**, *2*, 29.

[47] B. L. Frankamp, A. K. Boal, V. M. Rotello, *J. Am. Chem. Soc.* **2002**, *124*, 15146.

[48] A. Verma, H. Nakade, J. M. Simard, V. M. Rotello, *J. Am. Chem. Soc.* **2004**, *126*, 10806.

[49] E. Jeoung, V. M. Rotello, *J. Supramol. Chem.* **2002**, *2*, 53.

[50] R. Hong, T. Emrick, V. M. Rotello, *J. Am. Chem. Soc.* **2004**, *126*, 13572.

[51] A. K. Boal, V. M. Rotello, *J. Am. Chem. Soc.* **2000**, *122*, 734.

[52] A. K. Boal, V. M. Rotello, *Langmuir* **2000**, *16*, 9527.

[53] S. A. Levi, A. Mourran, J. P. Spatz, F. C. J. M. van Veggel, D. N. Reinhoudt, M. Möller, *Chem. Eur. J.* **2002**, *8*, 3808.

[54] K. G. Thomas, B. I. Ipe, P. K. Sudeep, *Pure Appl. Chem.* **2002**, *74*, 1731.

[55] K. G. Thomas, P. V. Kamat, *Acc. Chem. Res.* **2003**, *36*, 888.

[56] T. Hasobe, H. Imahori, P. V. Kamat, S. Fukuzumi, *J. Am. Chem. Soc.* **2003**, *125*, 14962.

[57] S. Flink, F. C. J. M. van Veggel, D. N. Reinhoudt, *J. Phys. Org. Chem.* **2001**, *14*, 407.

[58] M. Crego-Calama, D. N. Reinhoudt, *Adv. Mater.* **2001**, *13*, 1171.

[59] S. Flink, F. C. J. M. van Veggel, D. N. Reinhoudt, *Chem. Commun.* **1999**, 2229.

[60] N. J. van der Veen, S. Flink, M. A. Deij, R. J. M. Egberink, F. C. J. M. van Veggel, D. N. Reinhoudt, *J. Am. Chem. Soc.* **2000**, *122*, 6112.

[61] A. Berlin, G. Zotti, *Macromol. Rapid Commun.* **2000**, *21*, 301.

[62] H. Imahori, S. Fukuzumi, *Adv. Funct. Mater.* **2004**, *14*, 525.

[63] I. Taniguchi, K. Toyoshima, H. Yamaguchi, Y. K., *J. Chem. Soc., Chem. Commun.* **1982**, 1032.

[64] R. G. Nuzzo, D. L. Allara, *J. Am. Chem. Soc.* **1983**, *105*, 4481.

[65] I. Langmuir, *J. Am. Chem. Soc.* **1917**, *39*, 1848.

[66] K. B. Blodgett, *J. Am. Chem. Soc.* **1935**, *57*, 1007.

[67] R. M. Metzger, *Chem. Rev.* **2003**, *103*, 3803.

[68] M. Lahav, T. Gabriel, A. N. Shipway, I. Willner, *J. Am. Chem. Soc.* **1999**, *121*, 258.

[69] L. A. J. Chrisstoffels, A. Adronov, J. M. J. Frechet, *Angew. Chem. Int. Ed. Engl.* **2000**, *39*, 2163.

[70] F. Schreiber, *Prog. Surf. Sci.* **2000**, *65*, 151.

[71] E. Delamarche, B. Michel, *Thin Solid Films* **1996**, *273*, 54.

[72] E. Delamarche, B. Michel, H. A. Biebuyck, C. Gerber, *Adv. Mater.* **1996**, *8*, 719.

[73] T. Pradeep, N. Sandhyarani, *Pure Appl. Chem.* **2002**, *74*, 1593.

[74] D. K. Schwartz, *Annu. Rev. Phys. Chem.* **2001**, *52*, 107.

[75] H. O. Finklea, *J. Electroanal. Chem.* **1996**, *19*, 109.

[76] A. C. Templeton, W. P. Wuelfing, R. W. Murray, *Acc. Chem. Res.* **2000**, *33*, 27.

[77] M. J. Hostetler, R. W. Murray, *Curr. Opin. Colloid Interface Sci.* **1997**, *2*, 42.

[78] T. Ishida, *Chemistry of Nanomolecular Systems: Towards the Realization of Molecular Devices*, Springer, Berlin, **2003**.

[79] G. Y. Liu, J. A. Rodriguez, J. Dvorak, J. Hrbek, T. Jirsak, *Surf. Sci.* **2002**, *505*, 295.

[80] L. H. Dubois, R. G. Nuzzo, *Ann. Phys. Chem.* **1992**, *43*, 437.

[81] G. E. Poirier, *Chem. Rev.* **1997**, *97*, 1117.

[82] H. Sellers, A. Ulman, Y. Shnidman, J. E. Eilers, *J. Am. Chem. Soc.* **1993**, *115*, 9389.

[83] M. Zharinkov, S. Frey, H. Rong, Y.-J. Yang, K. Heister, M. Buck, M. Grunze, *Phys. Chem. Chem. Phys.* **2000**, *2*, 3359.

[84] H. Imahori, H. Norieda, Y. Nishimura, I. Yamazaki, K. Higuchi, N. Kato, T. Motohiro, H. Yamada, K. Tamaki, M. Arimura, Y. Sakata, *J. Phys. Chem. B* **2000**, *104*, 1253.

[85] M. S. Boeckl, A. L. Bramblett, K. D. Hauch, T. Sasaki, B. D. Ratner, J. W. Rogers Jr., *Langmuir* **2000**, *16*, 5644.

[86] G. Kalyuzhny, A. Vaskevich, G. Ashkenasy, A. Shanzer, I. Rubinstein, *J. Phys. Chem. B* **2000**, *104*, 8238.

[87] R. W. Owens, D. A. Smith, *Langmuir* **2000**, *16*, 562.

[88] M. Kawasaki, T. Sato, T. Yoshimoto, *Langmuir* **2000**, *16*, 5409.

[89] H. Imahori, Y. Nishimura, H. Norieda, H. Karita, I. Yamazaki, Y. Sakata, S. Fukuzumi, *Chem. Commun.* **2000**, 661.

[90] H. Yamada, H. Imahori, Y. Nishimura, I. Yamazaki, S. Fukuzumi, *Chem. Commun.* **2000**, 1921.

[91] H. Imahori, H. Norieda, S. Ozawa, K. Ushida, H. Yamada, T. Azuma, K. Tamaki, Y. Sakata, *Langmuir* **1998**, *14*, 5335.

[92] H. Imahori, T. Hasobe, H. Yamada, Y. Nishimura, I. Yamazaki, S. Fukuzumi, *Langmuir* **2001**, *17*, 4925.

[93] K. Shimazu, M. Takechi, H. Fujii, M. Suzuki, H. Saiki, T. Yoshimura, K. Uosaki, *Thin Solid Films* **1996**, *273*, 250.

[94] T. Yamada, M. Nango, T. Ohtsuka, *J. Electroanal. Chem.* **2002**, *528*, 93.

[95] H. Yuan, l. K. Woo, *J. Porphyrins Phthalocyanines* **1997**, *1*, 189.

[96] J. E. Hutchinson, T. A. Postlethwaite, C.-h. Chen, K. W. Hathcock, R. S. Ingram, W. Ou, R. W. Linton, R. W. Murray, D. A. Tyvoll, L. L. Chng, J. P. Collman, *Langmuir* **1997**, *13*, 2143.

[97] J. Zak, H. Yuan, M. Ho, K. Woo, M. D. Porter, *Langmuir* **1993**, *9*, 2772.

[98] T. A. Postlethwaite, J. E. Hutchinson, K. W. Hathcock, R. W. Murray, *Langmuir* **1995**, *11*, 4109.

[99] A. L. Bramblett, M. S. Boeckl, K. D. Hauch, B. D. Ratner, T. Sasaki, J. W. Rogers Jr., *Surf. Interface Anal.* **2002**, *33*, 506.

[100] D. A. Offord, S. B. Sachs, M. S. Ennis, T. A. Eberspacher, J. H. Griffin, C. E. D. Chidsey, J. P. Collman, *J. Am. Chem. Soc.* **1998**, *120*, 4478.

[101] G. Ashkenasy, G. Kalyuzhny, J. Libman, I. Rubinstein, A. Shanzer, *Angew. Chem. Int. Ed. Engl.* **1999**, *38*, 1257.

[102] T. Kondo, T. Ito, S.-i. Nomura, K. Uosaki, *Thin Solid Films* **1996**, *284-285*, 652.

[103] T. Kondo, M. Yanagida, S.-i. Nomura, M. Takahashi, K. Uosaki, *J. Electroanal. Chem.* **1997**, *438*, 121.

[104] D. T. Gryko, C. Clausen, J. S. Lindsay, *J. Org. Chem.* **1999**, *64*, 8635.

[105] D. T. Gryko, C. Clausen, K. M. Roth, N. Dontha, D. F. Bocian, W. G. Kuhr, J. S. Lindsey, *J. Org. Chem.* **2000**, *65*, 7345.

[106] K. M. Roth, D. T. Gryko, C. Clausen, J. Li, J. S. Lindsey, W. G. Kuhr, D. F. Bocian, *J. Phys. Chem. B* **2002**, *106*, 8639.

[107] A. Balakumar, A. B. Lysenko, C. Carcel, V. L. Malinovskii, D. T. Gryko, K.-H. Schweikart, R. S. Loewe, A. A. Yasseri, Z. Liu, D. F. Bocian, J. S. Lindsey, *J. Org. Chem.* **2004**, *69*, 1435.

[108] L. Wei, K. Padmaja, W. J. Youngblood, A. B. Lysenko, J. S. Lindsey, D. F. Bocian, *J. Org. Chem.* **2004**, *69*, 1461.

[109] L. Cai, Y. Yao, J. Yang, D. W. Price, Jr., J. M. Tour, *Chem. Mater.* **2002**, *14*, 2905.

[110] K. Kobayashi, S. Imabayashi, H. Fujita, K. Nonaka, T. Kakiuchi, H. Sasabe, W. Knoll, *Bull. Chem. Soc. Jpn.* **2000**, *73*, 1993.

[111] K. Kobayashi, M. Shimizu, T. Nagamune, H. Sasabe, Y. Fang, W. Knoll, *Bull. Chem. Soc. Jpn.* **2002**, *75*, 1707.

[112] J. D. Wright, *Prog. Surf. Sci.* **1989**, *31*, 1.

[113] A. W. Snow, W. R. Barger, *Phthalocyanines - Properties and Applications*, VCH, New York, **1989**.

[114] T. R. E. Simpson, M. J. Cook, M. C. Petty, S. C. Thorpe, D. A. Russell, *Analyst* **1996**, *121*, 1501.

[115] M. J. Cook, *Pure Appl. Chem.* **1999**, *71*, 2145.

[116] I. Chambrier, M. J. Cook, D. A. Russell, *Synthesis* **1995**, 1283.

[117] D. J. Revell, I. Chambrier, M. J. Cook, D. A. Russell, *J. Mater. Chem.* **2000**, *10*, 31.

[118] K.-H. Schweikart, V. L. Malinovskii, A. A. Yasseri, J. Li, A. B. Lysenko, D. F. Bocian, J. S. Lindsay, *Inorg. Chem.* **2003**, *42*, 7431.

[119] C. A. Mirkin, W. B. Cladwell, *Tetrahedron* **1996**, *52*, 5113.

[120] H. Imahori, T. Azuma, S. Ozawa, H. Yamada, K. Ushida, A. Ajavakom, H. Norieda, Y. Sakata, *Chem. Commun.* **1999**, 557.

[121] H. Imahori, T. Azuma, A. Ajavakom, H. Norieda, H. Yamada, Y. Sakata, *J. Phys. Chem. B* **1999**, *103*, 7233.

[122] D. Hirayama, K. Takimiya, Y. Aso, T. Otsubo, T. Hasobe, H. Yamada, H. Imahori, S. Fukuzumi, Y. Sakata, *J. Am. Chem. Soc.* **2002**, *124*, 532.

[123] B. Liedberg, Z. Yang, I. Engquist, M. Wirde, U. Gelius, G. Götz, P. Bäuerle, R.-M. Rummel, C. Ziegler, W. Göpel, *J. Phys. Chem. B* **1997**, *101*, 5951.

[124] A. Natansohn, P. Rochon, *Chem. Rev.* **2002**, *102*, 4139.

[125] H. Nishihara, *Bull. Chem. Soc. Jpn.* **2004**, *77*, 407.

[126] R. Wang, T. Iyoda, L. Jiang, D. A. Tryk, K. Hashimoto, A. Fujishima, *J. Electroanal. Chem.* **1997**, *438*, 213.

[127] R. Wang, T. Iyoda, D. A. Tryk, K. Hashimoto, A. Fujishima, *Langmuir* **1997**, *13*, 4644.

[128] A. Zhang, J. Qin, J. Gu, Z. Lu, *Thin Solid Films* **2000**, *375*, 242.

[129] M. A. Fox, J. K. Whitesell, A. J. McKerrow, *Langmuir* **1998**, *14*, 816.

[130] M. A. Fox, W. Li, M. Wooten, A. J. McKerrow, J. K. Whitesell, *Thin Solid Films* **1998**, *327-329*, 477.

[131] E. Soto, J. C. MacDonald, C. G. F. Cooper, W. G. McGimpsey, *J. Am. Chem. Soc.* **2003**, *125*, 2838.

[132] K. Fujita, M. Hara, H. Sasabe, W. Knoll, K. Tsuboi, K. Kajikawa, K. Seki, Y. Ouchi, *Langmuir* **1998**, *14*, 7456.

[133] H. A. Frank, *The photochemistry of carotenoids, Vol. 8*, Kluwer, Dordrecht, **1999**.

[134] G. Leatherman, E. N. Durantini, D. Gust, T. A. Moore, S. Stone, Z. Zhou, P. Rez, Y. Z. Liu, S. M. Lindsay, *J. Phys. Chem. B* **1999**, *103*, 4006.

[135] D. Liu, G. J. Szulczewski, L. D. Kispert, A. Primak, T. A. Moore, D. Gust, *J. Phys. Chem. B* **2002**, *106*, 2933.

[136] T. Morita, S. Kimura, S. Kobayashi, *J. Am. Chem. Soc.* **2000**, *122*, 2850.

[137] Z. Li, T. P. Fehlner, *Inorg. Chem.* **2003**, *42*, 5715.

[138] E. Katz, I. Willner, *Langmuir* **1997**, *13*, 3364.

[139] U. Haas, C. Thalacker, J. Adams, J. Fuhrmann, S. Riethmüller, U. Beginn, U. Ziener, M. Möller, R. Dobrawa, F. Würthner, *J. Mater. Chem.* **2003**, *13*, 762.

[140] S. Fukuzumi, H. Imahori, *Electron Transfer in Chemistry*, Wiley-VCH, Weinheim, **2000**.

[141] J. E. Hutchinson, T. A. Postlethwaite, R. W. Murray, *Langmuir* **1993**, *9*, 3277.

[142] M. Lion-Dagan, E. Katz, I. Willner, *J. Chem. Soc., Chem. Commun.* **1994**, 2741.

[143] M. Lahav, E. Katz, A. Doron, F. Patolsky, I. Willner, *J. Am. Chem. Soc.* **1999**, *121*, 862.

[144] H. Chen, Y. Li, F. Huo, Z. Wang, X. Zhang, *Chem. Lett.* **2003**, *32*, 1094.

[145] C. G. F. Cooper, J. C. MacDonald, E. Soto, W. G. McGimpsey, *J. Am. Chem. Soc.* **2004**, *126*, 1032.

[146] P. Qu, G. J. Meyer, in *Electron Transfer in Chemistry, Vol. 4* (Ed.: V. Balzani), VCH-Verlag, Weinheim, **2001**, pp. 353.

[147] K. Uosaki, T. Kondo, X.-Q. Zhang, M. Yanagida, *J. Am. Chem. Soc.* **1997**, *119*, 8367.

[148] H. Imahori, S. Ozawa, K. Ushida, M. Takahashi, T. Azuma, A. Ajavakom, T. Akiyama, M. Hasegawa, S. Taniguchi, T. Okada, Y. Sakata, *Bull. Chem. Soc. Jpn.* **1999**, *72*, 485.

[149] H. Imahori, H. Yamada, S. Ozawa, K. Ushida, Y. Sakata, *Chem. Commun.* **1999**, 1165.

[150] I. Willner, E. Katz, *Angew. Chem. Int. Ed. Engl.* **2000**, *39*, 1181.

[151] D. Dulic, S. J. van der Molen, T. Kudernac, H. T. Jonkman, J. J. D. de Jong, T. N. Bowden, J. van Esch, B. L. Feringa, B. J. van Wees, *Phys. Rev. Lett.* **2003**, *91*, 207402.

[152] D. G. Zhu, M. C. Petty, M. Harris, *Sens. Actuators, B* **1990**, *2*, 265.

[153] T. R. E. Simpson, D. A. Russell, I. Chambrier, M. J. Cook, A. B. Horn, S. C. Thorpe, *Sens. Actuators, B* **1995**, *29*, 353.

[154] T. R. E. Simpson, D. J. Revell, M. J. Cook, D. A. Russell, *Langmuir* **1997**, *13*, 460.

[155] S. Wang, Y. Liu, X. Huang, G. Yu, D. G. Zhu, *J. Phys. Chem. B* **2003**, *107*, 12639.

[156] J. M. Tour, *Acc. Chem. Res.* **2000**, *33*, 791.

[157] C. J. Yu, Y. Chong, J. F. Kayyem, M. Gozin, *J. Org. Chem.* **1999**, *64*, 2070.

[158] S. E. Creager, C. J. Yu, C. Bamdad, S. O'Connor, T. MacLean, E. Lam, Y. Chong, G. T. Olsen, J. Luo, M. Gozin, J. F. Kayyem, *J. Am. Chem. Soc.* **1999**, *121*, 1059.

[159] S. B. Sachs, S. P. Dudek, R. P. Hsung, L. R. Sita, J. F. Smalley, M. D. Newton, S. W. Feldberg, C. E. D. Chidsey, *J. Am. Chem. Soc.* **1997**, *119*, 10563.

[160] S. E. Creager, T. T. Wooster, *Anal. Chem.* **1998**, *70*, 4257.

[161] S. P. Dudek, H. D. Sikes, C. E. D. Chidsey, *J. Am. Chem. Soc.* **2001**, *123*, 8033.

[162] H. D. Sikes, J. F. Smalley, S. P. Dudek, A. R. Cook, M. D. Newton, C. E. D. Chidsey, S. W. Feldberg, *Science* **2001**, *291*, 1519.

[163] D. S. Seferos, D. A. Banach, N. A. Alcantar, J. N. Israelachvili, G. Bazan, *J. Org. Chem.* **2004**, *69*, 1110.

[164] C. Creutz, *Prog. Inorg. Chem.* **1983**, *30*, 1.

[165] N. S. Hush, *Coord. Chem. Rev.* **1985**, *64*, 135.

[166] M. D. Newton, R. J. Cave, *Mol. Electron.* **1997**, 73.

[167] R. J. Cave, M. D. Newton, *Chem. Phys. Lett.* **1996**, *249*, 15.

[168] R. J. Cave, M. D. Newton, *J. Chem. Phys.* **1997**, *106*, 9213.

[169] C. Creutz, B. S. Brunschwig, N. J. Sutin, *J. Phys. Chem. B* **2005**, *109*, 10251.

[170] J. F. Smalley, H. O. Finklea, C. E. D. Chidsey, M. R. Linford, S. E. Creager, J. P. Ferraris, K. Chalfant, T. Zawodzinsk, S. W. Feldberg, M. D. Newton, *J. Am. Chem. Soc.* **2003**, *125*, 2004.

[171] J. F. Smalley, S. B. Sachs, C. E. D. Chidsey, S. P. Dudek, H. D. Sikes, S. Creager, C. J. Yu, S. W. Feldberg, M. D. Newton, *J. Am. Chem. Soc.* **2004**, *126*, 14620.

[172] W. B. Davis, W. A. Svec, M. A. Ratner, M. R. Wasielewski, *Nature* **1998**, *396*, 60.

[173] L. Wei, D. Syomin, R. S. Loewe, J. S. Lindsey, F. Zaera, D. F. Bocian, *J. Phys. Chem. B* **2005**, *109*, 6323.

[174] A. A. Yasseri, D. Syomin, V. L. Malinovskii, R. S. Loewe, J. S. Lindsey, F. Zaera, D. F. Bocian, *J. Am. Chem. Soc.* **2004**, *126*, 11944.

[175] L. Wei, D. Syomin, R. S. Loewe, J. S. Lindsey, F. Zaera, D. F. Bocian, *J. Phys. Chem. B* **2005**, *109*, 6323.

[176] A. A. Yasseri, D. Syomin, R. S. Loewe, J. S. Lindsey, F. Zaera, D. F. Bocian, *J. Am. Chem. Soc.* **2004**, *126*, 15603.

[177] C. Hortholary, F. Minc, C. Coudret, J. Bonvoisin, J.-P. Launay, *Chem. Commun.* **2002**, 1932.

[178] S. Sek, A. Sepiol, A. Tolak, A. Misicka, R. Bilewicz, *J. Phys. Chem. B* **2004**, *108*, 8102.

[179] H. O. Finklea, D. D. Hanshew, *J. Am. Chem. Soc.* **1992**, *114*, 3173.

[180] H. O. Finklea, M. S. Ravenscroft, D. A. Snider, *Langmuir* **1993**, *9*, 223.

[181] C. E. D. Chidsey, *Science* **1991**, *251*, 919.

[182] K. Weber, S. E. Creager, *Anal. Chem.* **1994**, *66*, 3164.

[183] K. Weber, L. Hockett, S. Creager, *J. Phys. Chem. B* **1997**, *101*, 8286.

[184] L. Tender, M. T. Carter, R. W. Murray, *Anal. Chem.* **1994**, *66*, 3173.

[185] T. M. Nahir, R. A. Clark, E. F. Bowden, *Anal. Chem.* **1994**, *66*, 2595.

[186] S. E. Creager, T. T. Wooster, *Anal. Chem.* **1998**, *70*, 4257.

[187] J. J. Sumner, S. E. Creager, *J. Am. Chem. Soc.* **2000**, *122*, 11914.

[188] P. F. Barbara, T. J. Meyer, M. A. Ratner, *J. Phys. Chem.* **1996**, *100*, 13148.

[189] S. P. Dudek, H. D. Sikes, C. E. D. Chidsey, *J. Am. Chem. Soc.* **2001**, *123*, 8033.

[190] R. J. Crutchley, *Adv. Inorg. Chem.* **1994**, *41*, 273.

[191] C. Lambert, G. Nöll, *Angew. Chem. Int. Ed. Engl.* **1998**, *37*, 2107.

[192] S. F. Nelsen, R. F. Ismaligov, *Science* **1997**, *278*, 846.

[193] W. B. Davis, M. R. Wasielewski, M. A. Ratner, V. Mujica, A. Nitzan, *J. Phys. Chem. A* **1997**, *101*, 6158.

[194] D. Segal, A. Nitzan, W. B. Davis, M. R. Wasielewski, M. A. Ratner, *J. Phys. Chem. B* **2000**, *104*, 3817.

[195] S. Dapperheld, E. Steckhan, K.-H. G. Brinkhaus, T. Esch, *Chem. Ber.* **1991**, *124*, 2557.

[196] G. Jones, D.-X. Yan, D. J. Goszotola, S. R. Greenfield, M. R. Wasielewski, *J. Am. Chem. Soc.* **1999**, *121*, 11016.

[197] M. Holzapfel, C. Lambert, C. Selinka, D. Stalke, *J. Chem. Soc. Perkin Trans. 2* **2002**, 1553.

[198] A. J. Bard, L. R. Faulkner, *Electrochemical Methods*, Wiley, New York, **1980**.

[199] J. R. MacDonald, *Impedance Spectroscopy: Emphasizing Solid Materials and Systems*, Wiley, New York, **1987**.

[200] J. R. Macdonald, *J. Electroanal. Chem.* **1987**, *223*, 25.

[201] T. Lötzbeyer, W. Schuhmann, H.-L. Schmidt, *J. Electroanal. Chem.* **1995**, *395*, 341.

[202] H. Zimmermann, A. Lindgren, W. Schuhmann, L. Gorton, *Chem. Eur. J.* **2000**, *6*, 592.

[203] J. J. Sumner, S. E. Creager, *J. Phys. Chem. B* **2001**, *105*, 8739.

[204] C. E. D. Chidsey, C. R. Bertozzi, T. M. Putvinksi, A. M. Mujsce, *J. Am. Chem. Soc.* **1990**, *112*, 4301.

[205] H. O. Finklea, *Electroanal. Chem.* **1996**, *19*, 109.

[206] J. J. Sumner, K. S. Weber, L. A. Hockett, S. E. Creager, *J. Phys. Chem. B* **2000**, *104*, 7449.

[207] J. Li, K. Schuler, S. E. Creager, *J. Electrochem. Soc.* **2000**, *147*, 4584.

[208] R. A. Marcus, *J. Chem. Phys.* **1965**, *43*, 679.

[209] C.-P. Hsu, R. A. Marcus, *J. Phys. Chem.* **1997**, *106*, 584.

[210] S. Creager, C. J. Yu, C. Bamdad, S. O'Connor, T. MacLean, E. Lam, Y. Chong, G. T. Olsen, J. Y. Luo, M. Gozin, J. F. Kayyem, *J. Am. Chem. Soc.* **1999**, *121*, 1059.

[211] M. D. Newton, N. Sutin, *Annu. Rev. Phys. Chem.* **1984**, *35*, 294.

[212] J. F. Smalley, S. W. Feldberg, C. E. D. Chidsey, M. R. Linford, M. D. Newton, Y.-P. Liu, *J. Phys. Chem.* **1995**, *99*, 13141.

[213] T. A. Eberspacher, J. P. Collman, C. E. D. Chidsey, D. L. Donohue, H. Van Ryswyk, *Langmuir* **2003**, *19*, 3814.

[214] A. Terfort, *Institute of Inorganic Chemistry, University of Hamburg, Germany*.

[215] L. Eberson, *Electron Transfer Reactions in Organic Chemistry*, Springer-Verlag, Berlin Heidelberg, **1987**.

[216] S. Amthor, B. Noller, C. Lambert, *Chem. Phys.* **2005**, in press.

[217] H. O. Finklea, L. Liu, M. S. Ravenscroft, *J. Phys. Chem.* **1996**, *100*, 18852.

[218] E. R. Biehl, T. Daniel, P. C. Reeves, S. Lapis, *J. Heterocyclic Chem.* **1974**, *11*, 247.

[219] R. Engel, Universität Regensburg **1999**.

[220] C. S. Krämer, K. Zeitler, T. J. J. Müller, *Org. Lett.* **2000**, *2*, 3723.

[221] J. Wu, C. Chi, X. Wang, X. Zhang, J. Li, F. Wang, *Synth. Comm.* **2000**, *30*, 4293.

[222] A. Blaszczyk, M. Elbing, M. Mayor, *Org. Biomol. Chem.* **2004**, *2*, 2722.

[223] S. Takahashi, Y. Kuroyama, K. Sonogashira, N. Hagihara, *Synthesis* **1980**, 628.

[224] W. P. Wuelfing, R. W. Murray, *J. Phys. Chem. B* **2002**, *106*, 3139.

[225] Y. T. Tao, C. C. Wu, J. Y. Eu, W. L. Lin, *Langmuir* **1997**, *13*, 4018.

[226] S. C. Chang, I. Chao, Y. T. Tao, *J. Am. Chem. Soc.* **1994**, *116*, 6792.

[227] B. Geiß„, University of Würzburg, oral communication.

[228] J. M. Tour, A. M. Rawlett, M. Kozaki, Y. Yao, R. C. Jagessar, S. M. Dirk, D. W. Price, M. A. Reed, C.-W. Zhou, J. Chen, W. Wang, I. Campbell, *Chem.-Eur. J.* **2001**, *7*, 5118.

[229] Z. Zhu, J. S. Moore, *J. Org. Chem.* **2000**, *65*, 116.

[230] U. H. F. Bunz, *Chem. Rev.* **2000**, *100*, 1605.

[231] U. Ziener, A. Godt, *J. Org. Chem.* **1997**, *62*, 6137.

[232] M. R. Akula, G. W. Kabalka, *J. Labelled Cpd. Radiopharm.* **1999**, *42*, 959.

[233] J.-J. Hwang, J. M. Tour, *Tetrahedron* **2002**, *58*, 10387.

[234] O. Dannenberger, M. Buck, M. Grunze, *J. Phys. Chem. B* **1999**, *103*, 2202.

[235] K. A. Peterlinz, R. Gerogiadis, *Langmuir* **1996**, *12*, 4731.

[236] D. S. Karpovich, G. J. Blanchard, *Langmuir* **1994**, *10*, 3315.

[237] A. P. H. J. Schenning, A. C. Tsipis, S. C. J. Meskers, D. Beljonne, E. W. Meijer, J.-L. Bredas, *Chem. Mater.* **2002**, *14*, 1362.

[238] G. Sauerbrey, *Z. Phys.* **1959**, *155*, 206.

[239] D. Buttry, in *A Series of Advances in Electroanalytical Chemistry* (Eds.: A. Bard, M. Dekker), **1991**, pp. 23.

[240] *Operation and Service Manual for QCM 200*, Stanford Research Systems, **2004**.

[241] A.-A. Dhirani, R. W. Zehner, R. P. Hsung, P. Guyot-Sionnest, L. R. Sita, *J. Am. Chem. Soc.* **1996**, *118*, 3319.

[242] J. J. Stapleton, P. Harder, T. A. Daniel, M. D. Reinard, Y. Yao, D. W. Price, J. M. Tour, D. L. Allara, *Langmuir* **2003**, *19*, 8245.

[243] F.-R. F. Fan, R. Y. Lai, J. Cornil, Y. Karzazi, J.-L. Bredas, L. Cai, L. Cheng, Y. Yao, D. W. Price Jr., S. M. Dirk, J. M. Tour, A. Bard, *J. Am. Chem. Soc.* **2004**, *126*, 2568.

[244] P. L. Burn, A. Kraft, D. R. Baigent, D. D. C. Bradley, A. R. Brown, R. H. Friend, R. W. Gymer, A. B. Holmes, R. W. Jackson, *J. Am. Chem. Soc.* **1993**, *115*, 10117.

[245] M. Bixon, J. Jortner, *Advances in Chemical Physics, Vol. 106, Electron Transfer - From Isolated Molecules to Biomolecules, Part I*, Wiley, New York, **1999**.

[246] V. Balzani, *Electron Transfer in Chemistry, Vol. 1-5*, Wiley-VCH, Weinheim, **2001**.

[247] N. Krauß, *Curr. Opin. Chem. Biol.* **2003**, *7*, 540.

[248] M. Hervas, J. A. Navarro, M. A. De la Rosa, *Acc. Chem. Res.* **2003**, *36*, 798.

[249] R. Harrer, *Chem. Unserer Zeit* **2003**, *37*, 234.

[250] J. Barber, *Quart. Rev. Biophys.* **2003**, *36*, 71.

[251] W. Lubitz, F. Lendzian, R. Bittl, *Acc. Chem. Res.* **2002**, *35*, 313.

[252] G. L. Closs, L. T. Calcaterra, N. J. Green, K. W. Penfield, J. R. Miller, *J. Phys. Chem.* **1986**, *90*, 3673.

[253] Z. R. Grabowski, K. Rotkiewicz, W. Rettig, *Chem. Rev.* **2003**, *103*, 3899.

[254] M. N. Paddon-Row, *Acc. Chem. Res.* **1994**, *27*, 18.

[255] J. Herbich, B. Brutschy, in *Electron Transfer in Chemistry, Vol. 4* (Ed.: V. Balzani), Wiley-VCH, Weinheim, **2001**, p. 697.

[256] J. M. Warman, P. Matthijs, J. W. Verhoeven, M. N. Paddon-Row, in *Advances in Chemical Physics, Vol. 106, Electron Transfer - From Isolated Molecules to Biomolecules, Part 1* (Eds.: M. Bixon, J. Jortner), Wiley, New York, **1999**, p. 571.

[257] B. Wegewijis, J. W. Verhoeven, in *Advances in Chemical Physics, Vol. 106, Electron Transfer - From Isolated Molecules to Biomolecules, Part 1* (Eds.: M. Bixon, J. Jortner), Wiley, New York, **1999**, p. 221.

[258] L. Jones II, M. S. Farahat, *Adv. Elec. Trans. Chem.* **1993**, *3*, 1.

[259] J. L. Sessler, V. L. Capuano, K. Kubo, M. R. Johnson, D. J. Magda, A. H. Harriman, *NATO ASI Ser., Ser. C* **1992**, *376*, 375.

[260] J. W. Verhoeven, M. N. Paddon-Row, J. M. Warman, *NATO ASI Ser., Ser. C* **1992**, *376*, 271.

[261] H. Imahori, Y. Sakata, *Adv. Mater.* **1997**, *9*, 537.

[262],, Wiley-VCH, Weinheim, **2001**.

[263] D. Gust, T. A. Moore, A. L. Moore, *J. Photochem. Photobiol. B* **2000**, *58*, 63.

[264] J.-C. Chambron, J.-P. Sauvage, J.-P. Collin, P. Gavina, V. Heitz, M. Linke, A. Livoreil, *NATO ASI Ser., Ser. C* **1999**, *527*, 23.

[265] D. M. Kaschak, S. A. Johnson, C. C. Waraksa, J. Pogue, T. E. Mallouk, *Coord. Chem. Rev.* **1999**, *185-186*, 403.

[266] J.-C. Chambron, J.-P. Collin, J.-O. Dalbavie, C. O. Dietrich-Buchecker, V. Heitz, F. Odobel, N. Solladie, J.-P. Sauvage, *Coord. Chem. Rev.* **1998**, *178-180*, 1299.

[267] I. Willner, E. Kaganer, E. Joselevich, H. Durr, E. David, M. J. Gunter, M. R. Johnston, *Coord. Chem. Rev.* **1998**, *171*, 261.

[268] P. Piotrowiak, *Chem. Soc. Rev.* **1999**, *28*, 143.

[269] A. H. Harriman, *Photochemistry* **1998**, *29*, 425.

[270] P. Seta, E. Bienvenue, A. L. Moore, T. A. Moore, D. Gust, *Electrochim. Acta* **1989**, *34*, 1723.

[271] N. S. Hush, *Progr. Inorg. Chem.* **1967**, *8*, 391.

[272] N. Sutin, *Progr. Inorg. Chem.* **1983**, *30*, 441.

[273] J.-P. Launay, *Chem. Soc. Rev.* **2001**, *30*, 386.

[274] B. S. Brunschwig, C. Creutz, N. Sutin, *Chem. Soc. Rev.* **2002**, *31*, 168.

[275] S. F. Nelsen, *Chem.-Eur. J.* **2000**, *6*, 581.

[276] K. D. Demadis, C. M. Hartshorn, T. J. Meyer, *Chem. Rev.* **2001**, *101*, 2655.

[277] S. F. Nelsen, H. Chang, J. J. Wolff, J. Adamus, *J. Am. Chem. Soc.* **1993**, *115*, 12276.

[278] S. F. Nelsen, J. Adamus, J. J. Wolff, *J. Am. Chem. Soc.* **1994**, *116*, 1589.

[279] S. F. Nelsen, R. F. Ismagilov, Y. Teki, *J. Am. Chem. Soc.* **1998**, *120*, 2200.

[280] S. F. Nelsen, R. F. Ismagilov, D. R. Powell, *J. Am. Chem. Soc.* **1998**, *120*, 1924.

[281] S. F. Nelsen, H. Q. Tran, M. A. Nagy, *J. Am. Chem. Soc.* **1998**, *120*, 298.

[282] S. F. Nelsen, D. A. Trieber II, R. F. Ismagilov, Y. Teki, *J. Am. Chem. Soc.* **2001**, *123*, 5684.

[283] S. F. Nelsen, R. F. Ismagilov, K. Gentile, D. R. Powell, *J. Am. Chem. Soc.* **1999**, *121*, 7108.

[284] S. F. Nelsen, R. F. Ismagilov, D. A. Trieber II, *Science* **2000**, *278*, 846.

[285] R. D. Williams, J. T. Hupp, M. T. Ramm, S. F. Nelsen, *J. Phys. Chem. B* **1999**, *103*, 11172.

[286] J. Bonvoisin, J.-P. Launay, W. Verbouwe, M. Van der Auweraer, F. C. De Schryver, *J. Phys. Chem.* **1996**, *100*, 17079.

[287] C. Lambert, G. Nöll, *J. Am. Chem. Soc.* **1999**, *121*, 8434.

[288] C. Lambert, G. Nöll, *Angew. Chem.* **1998**, *110*, 2239.

[289] C. Lambert, W. Gaschler, E. Schmälzlin, K. Meerholz, C. Bräuchle, *J. Chem. Soc. Perkin Trans. 2* **1999**, 577.

[290] C. Lambert, G. Nöll, F. Hampel, *J. Phys. Chem. A* **2001**, *105*, 7751.

[291] C. Lambert, C. Risko, V. Coropceanu, J. Schelter, S. Amthor, N. E. Gruhn, J. Durivage, J.-L. Brédas, *J. Am. Chem. Soc.* **2005**, *127*, 8508.

[292] C. Lambert, G. Nöll, J. Schelter, *Nature Materials* **2002**, *1*, 69–73.

[293] C. Lambert, G. Nöll, *J. Chem. Soc. Perkin Trans. 2* **2002**, 2039.

[294] C. Lambert, S. Amthor, J. Schelter, *J. Phys. Chem. A* **2004**, *108*, 6474.

[295] J. Bonvoisin, J.-P. Launay, C. Rovira, J. Veciana, *Angew. Chem.* **1994**, *106*, 2190.

[296] J. Sedo, D. Ruiz, J. Vidal-Gancedo, C. Rovira, J. Bonvoisin, J.-P. Launay, J. Veciana, *Synth. Met.* **1997**, *85*, 1651.

[297] C. Rovira, D. Ruiz-Molina, O. Elsner, J. Vidal-Gancedo, J. Bonvoisin, J.-P. Launay, J. Veciana, *Chem. Eur. J.* **2001**, *7*, 240.

[298] A. Heckmann, C. Lambert, M. Goebel, R. Wortmann, *Angew. Chem. Int. Ed. Engl.* **2004**, *43*, 5851.

[299] K. Lahlil, A. Moradpour, C. Bowlas, F. Menou, P. Cassoux, J. Bonvoisin, J.-P. Launay, G. Dive, D. Dehareng, *J. Am. Chem. Soc.* **1995**, *117*, 9995.

[300] S. F. Rak, L. L. Miller, *J. Am. Chem. Soc.* **1992**, *114*, 1388.

[301] S. V. Lindeman, S. V. Rosokha, D. Sun, J. K. Kochi, *J. Am. Chem. Soc.* **2002**, *124*, 843.

[302] S. V. Rosokha, D.-L. Sun, J. K. Kochi, *J. Phys. Chem.* **2002**, *106*, 2283.

[303] M. Thelakkat, *Macromol. Mater. Eng.* **2002**, *287*, 442.

[304] M. Thelakkat, R. Fink, F. Haubner, H.-W. Schmidt, *Macromol. Symp.* **1997**, *125*, 157.

[305] P. M. Borsenberger, D. S. Weiss, *Organic Photoreceptors for Imaging Systems*, Marcel Dekker, New York, **1993**.

[306] T. Braig, D. C. Müller, M. Groß, K. Meerholz, O. Nuyken, *Macromol. Rapid Commun.* **2000**, *21*, 583.

[307] C. Giebeler, H. Antoniadis, D. D. C. Bradley, Y. Shirota, *Appl. Phys. Lett.* **1998**, *72*, 2448.

[308] M. Redecker, D. D. C. Bradley, M. Inbasekaran, W. W. Wu, E. P. Woo, *Adv. Mater.* **1999**, *11*, 241.

[309] C. W. Tang, *Appl. Phys. Lett.* **1984**, *48*, 183.

[310] C. W. Tang, S. A. van Slyke, *Appl. Phys. Lett.* **1987**, *51*, 913.

[311] E. S. Kolb, R. A. Gaudiana, P. G. Metha, *Macromolecules* **1996**, *29*, 2359.

[312] H. Fujikawa, S. Tokito, Y. Taga, *Synth. Met.* **1997**, *91*, 161.

[313] K. Kaeriyama, M. Suda, M. Sato, Y. Osawa, M. Ishikawa, M. Kawai, *JP 63168974* **1988**.

[314] M. Takeuchi, M. Kobayashi, R. Shishikawa, T. Sakai, H. Nakamura, H. Konuma, *JP 6127906* **1986**.

[315] W. E. Moerner, S. M. Silence, *Chem. Rev.* **1994**, *94*, 127.

[316] H. Sato, T. Wada, H. Shirane, *Patent JP 10333195* **1998**.

[317] A. Hirao, K. Matsumoto, T. Tsukamoto, H. Nishizawa, *Patent JP 2003099979* **2003**.

[318] Y. Nishikitani, M. Kobayashi, S. Uchida, T. Kubo, *Electrochim. Acta* **2001**, *46*, 2035.

[319] H. J. Byker, *Patent US 4902108* **1990**.

[320] A. M. Horgan, *Patent US 4047948* **1997**.

[321] A. M. Horgan, *Patent US 4047949* **1977**.

[322] A. M. Horgan, *Patent US 4078925* **1978**.

[323] A. M. Horgan, *Patent US 4081274* **1978**.

[324] M. Stolka, J. F. Yanus, D. M. Pai, *Patent DE 2734990* **1978**.

[325] M. Stolka, J. F. Yanus, D. M. Pai, *J. Phys. Chem.* **1984**, *88*, 4707.

[326] N. S. Hush, *Electrochim. Acta* **1968**, *13*, 1005.

[327] N. S. Hush, *Chem. Phys.* **1975**, *10*, 361.

[328] N. S. Hush, *Chem. Phys.* **1989**, *134*, 323.

[329] J. R. Reimers, N. S. Hush, *Chem. Phys.* **1989**, *134*, 323.

[330] S. F. Nelsen, M. D. Newton, *J. Phys. Chem. A* **2000**, *104*, 10023.

[331] P. Day, *Endeavour* **1970**, *29*, 45.

[332] M. B. Robin, P. Day, *Adv. Inorg. Chem.* **1967**, *10*, 247.

[333] C. Creutz, M. D. Newton, N. J. Sutin, *J. Photochem. Photobiol. A* **1994**, *82*, 47.

[334] K. Y. Wong, P. N. Schatz, *Prog. Inorg. Chem.* **1981**, *28*, 369.

[335] B. S. Brunschwig, N. Sutin, in *Electron Transfer in Chemistry, Vol. 2*, 1 ed. (Ed.: V. Balzani), VCH, Weinheim, **2001**, pp. 583.

[336] P. Siemsen, R. C. Livingston, F. Diederich, *Angew. Chem.* **2000**, *112*, 2740.

[337] C. S. Krämer, T. J. J. Müller, *Eur. J. Org. Chem.* **2003**, 3534.

[338] M. Rudolph, S. W. Feldberg„, Bioanalytical Systems, Inc., West Lafayette (U.S.A.), **2000**.

[339] F. A. Neugebauer, S. Bamberger, W. R. Groh, *Chem. Ber.* **1975**, *108*, 2406.

[340] W. Schmidt, E. Steckhan, *Chem. Ber.* **1980**, *113*, 577.

[341] G. Nöll, Dissertation thesis, Universität Regensburg **2001**.

[342] J. Schelter, Dissertation thesis, Universität Würzburg **2003**.

[343] J. V. Lockard, J. I. Zink, D. A. Trieber, A. E. Konradsson, M. N. Weaver, S. F. Nelsen, *J. Phys. Chem. A* **2005**, *109*, 1205.

[344] J. Salbeck, Universität Regensburg **1988**.

[345] H. Kiesele, *Anal. Chem.* **1980**, *52*, 2230.

[346] R. Carlier, J. Simonet, *Bull. Soc. Chim. Fr.* **1988**, *5*, 831.

[347] Autorenkollektiv, *Organikum*, VEB Deutscher Verlag der Wissenschaften, Berlin, **1988**.

[348] K. Sonogashira, Y. Tohda, N. Hagihara, *Tetrahedron Lett.* **1975**, *16*, 4467.

[349] M. Nishiyama, T. Yamamoto, Y. Koie, *Tetrahedron Lett.* **1998**, *39*, 617.

[350] T. Yamamoto, M. Nishiyama, Y. Koie, *Tetrahedron Lett.* **1998**, *39*, 2367.

[351] T. Hundertmark, A. F. Littke, S. L. Buchwald, G. C. Fu, *Org. Lett.* **2000**, *2*, 1729.

[352] T. W. Greene, P. G. M. Wuts, *Protective Groups in Organic Synthesis, 2nd Edition*, John Wiley & Sons, New York, **1991**.

[353] H. B. Goodbrand, N.-X. Hu, *J. Org. Chem.* **1999**, *64*, 670.

[354] M. V. Jovanovic, E. R. Biehl, *J. Org. Chem.* **1984**, *49*, 1905.

[355] H. Meier, D. Ickenroth, U. Stalmach, K. Koynov, A. Bahtiar, C. Bubeck, *Eur. J. Org. Chem.* **2001**, 4431.

[356] W. B. Caldwell, D. J. Campbell, K. Chen, B. R. Herr, C. A. Mirkin, A. Malik, M. K. Burbin, P. Dutta, K. G. Huang, *J. Am. Chem. Soc.* **1995**, *117*, 6071.

[357] A. J. Moore, L. M. Goldenberg, M. R. Bryce, M. C. Petty, J. Moloney, J. A. K. Howard, M. J. Joyce, S. N. Port, *J. Org. Chem.* **2000**, *65*, 8269.

[358] S. Ebdrup, *J. Chem. Soc. Perkin Trans. 1* **1998**, 1147.

13 Formula Table

13.1 Ferrocene Compounds

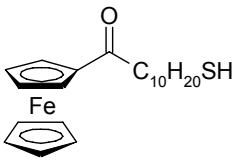

1

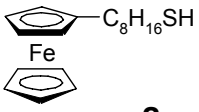

2

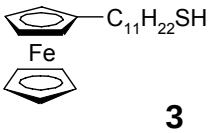

3

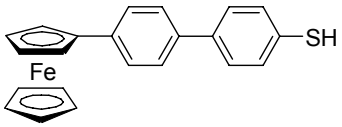

4

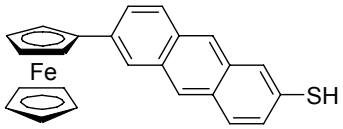

5

13.2 Different Redox Centres

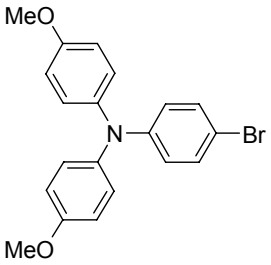

6

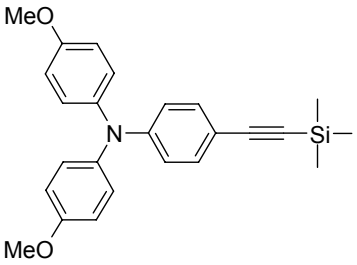

7

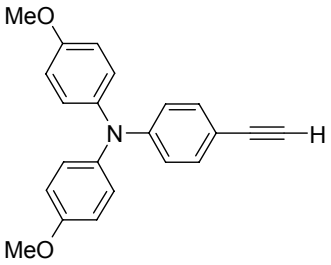

8

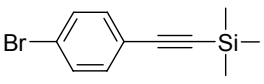

9

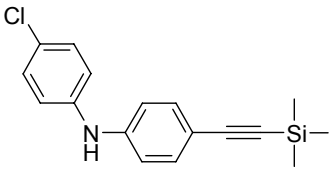

10

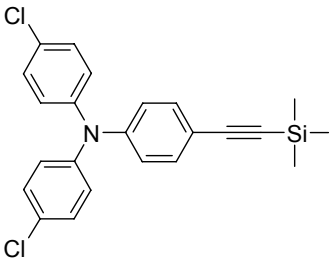

11

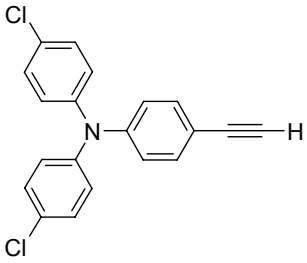

12

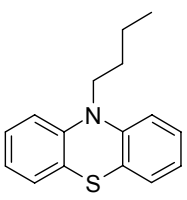

13

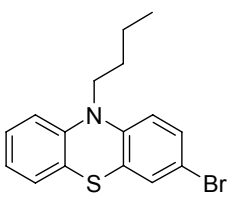

14

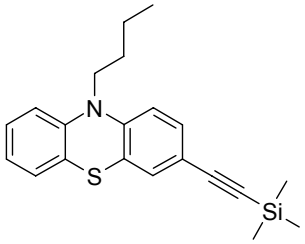

15

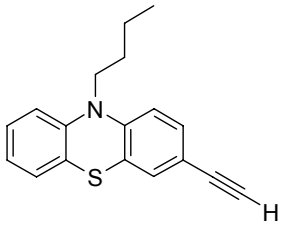

16

13.3 Anchor Functions

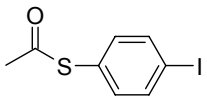

17

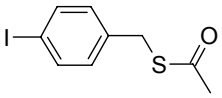

18

13.4 Different Bridge Units

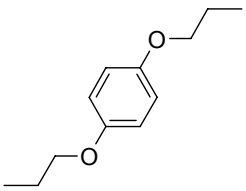

19

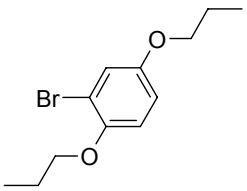

20

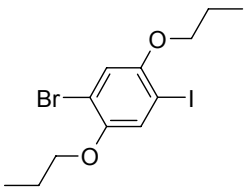

21

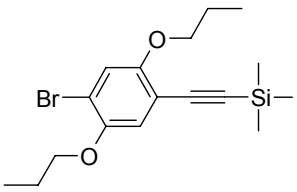

22

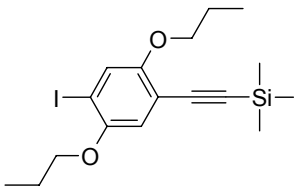

23

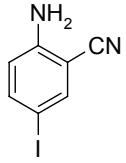

24

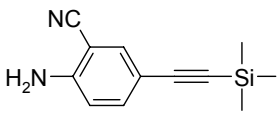

25

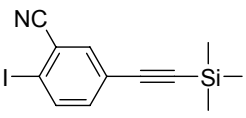

26

13.5 Redox Active Thiols with Saturated Bridge Units

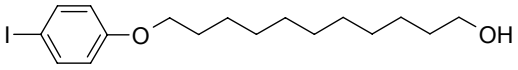

27

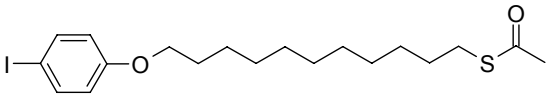

28

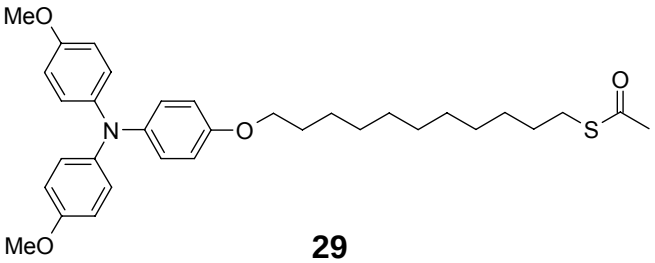

29

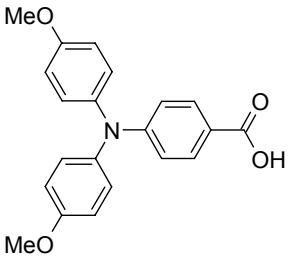

30

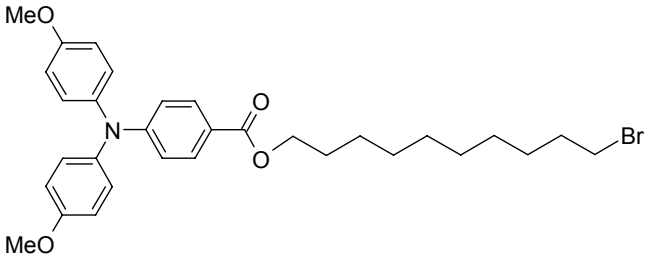

31

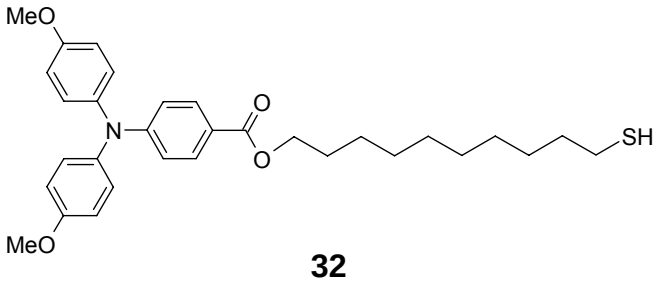

32

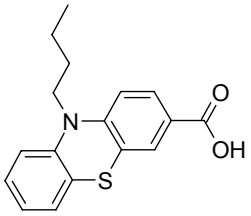

33

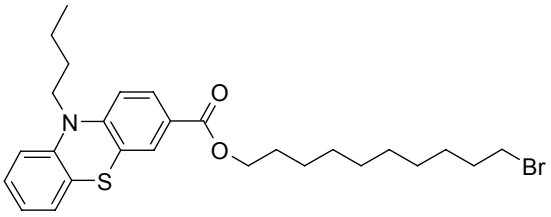

34

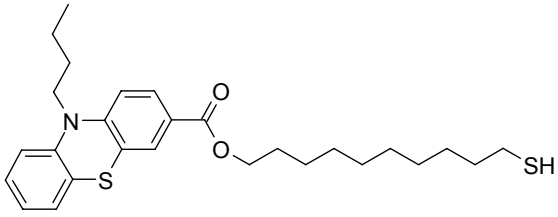

35

13.6 Redox Active Thiols with Unsaturated Bridge Units

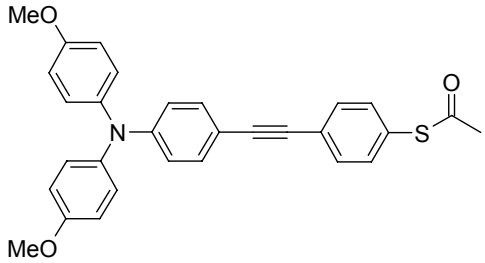

36

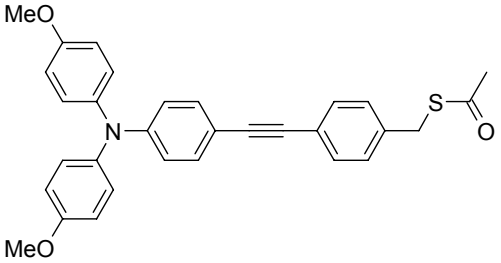

37

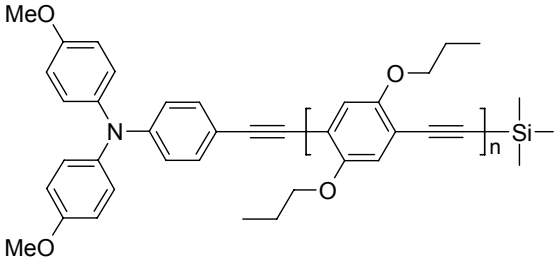

n	1	2
	38	**41**

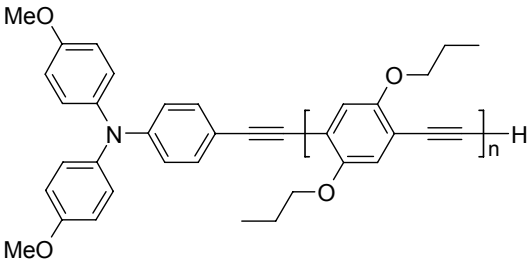

n	1	2
	39	**42**

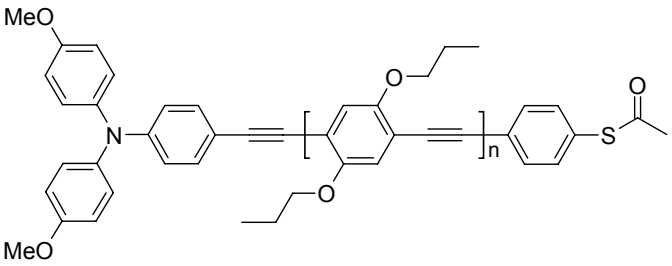

n	1	2
	40	**43**

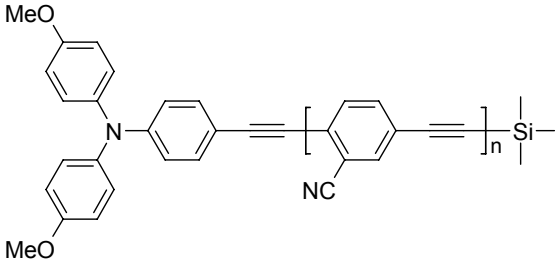

n	1	2	3
	44	**47**	**50**

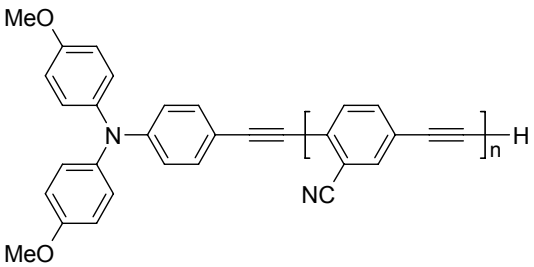

n	1	2	3
	45	**48**	**51**

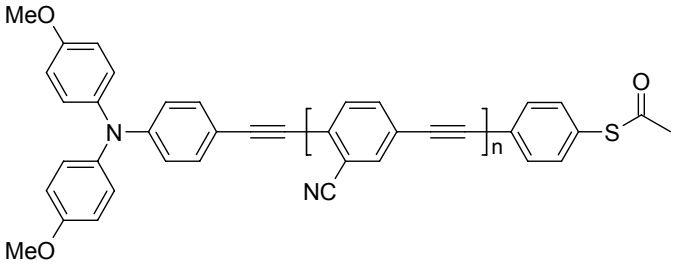

n	1	2	3
	46	**49**	**52**

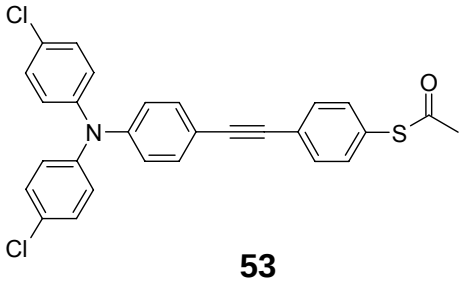

53

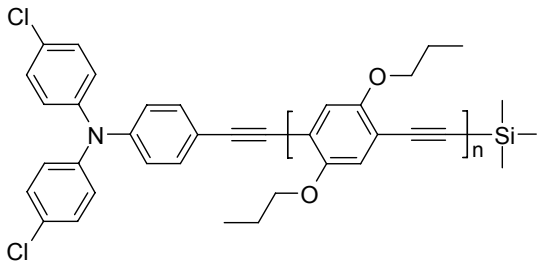

n	1	2	3
	54	**57**	**60**

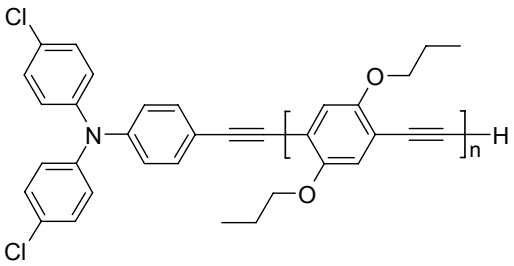

n	1	2	3
	55	**58**	**61**

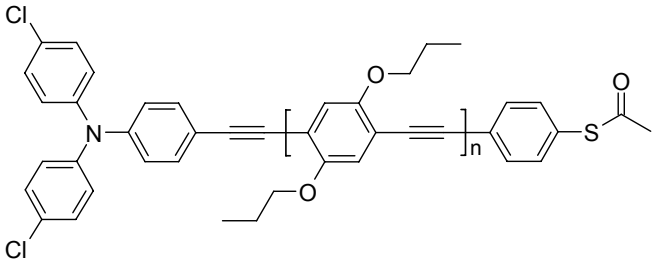

n	1	2	3
	56	**59**	**62**

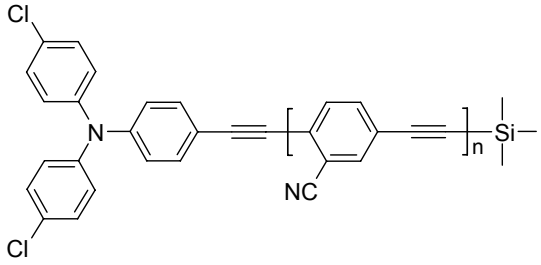

n	1	2	3
	63	**66**	**69**

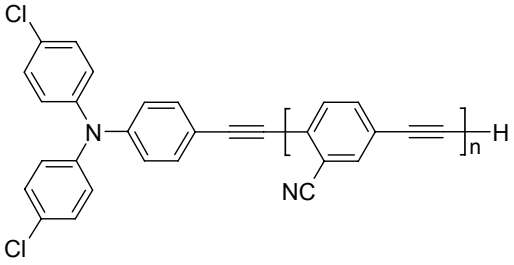

n	1	2	3
	64	**67**	**70**

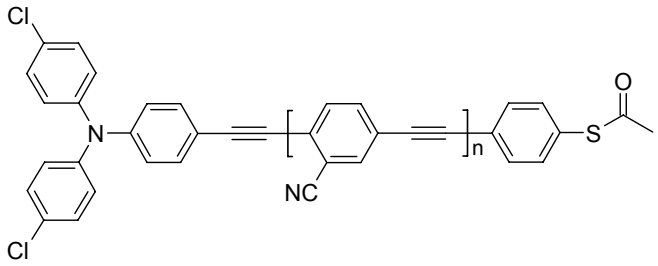

n	1	2	3
	65	**68**	**71**

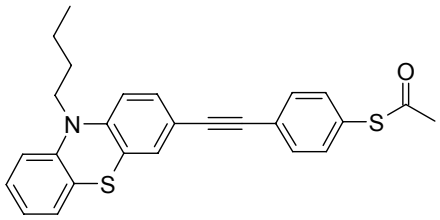

72

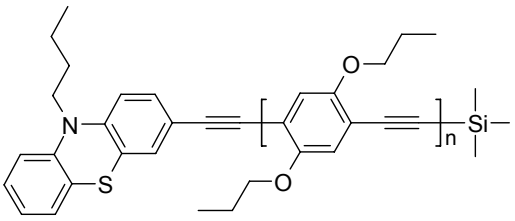

n	1	2	3
	73	**76**	**79**

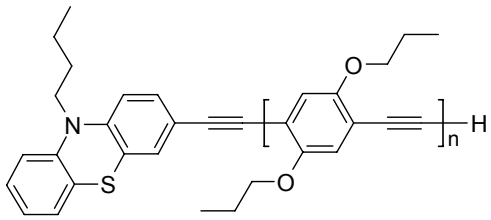

n	1	2	3
	74	**77**	**80**

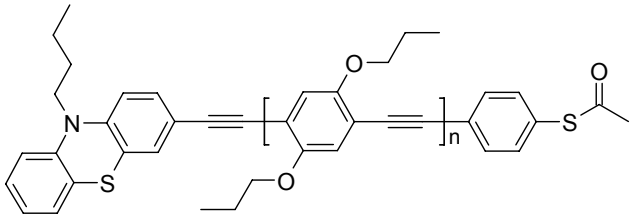

n	1	2	3
	75	**78**	**81**

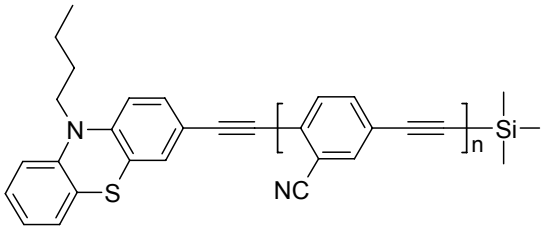

n	1	2
	82	**85**

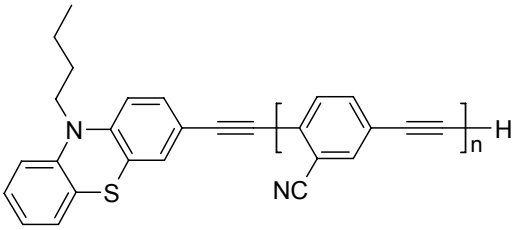

n	1	2
	83	**86**

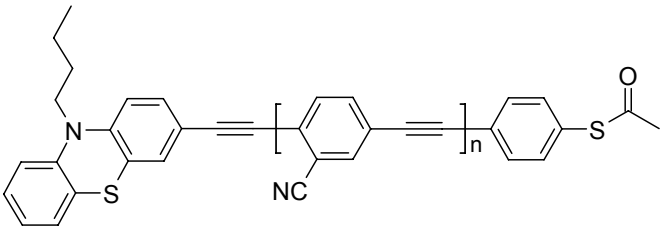

n	1	2
	84	**87**

13.7 Bistriarylamine- and Bisphenothiazinechromophores

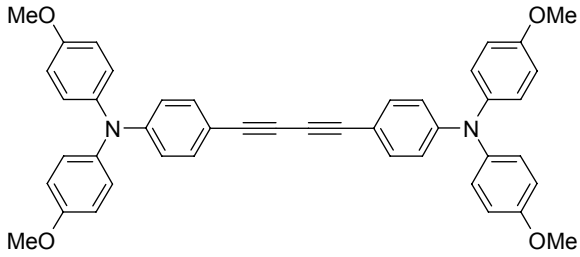

88

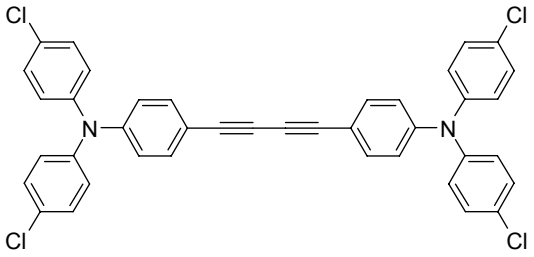

89

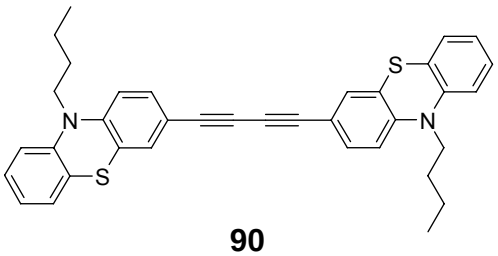

90

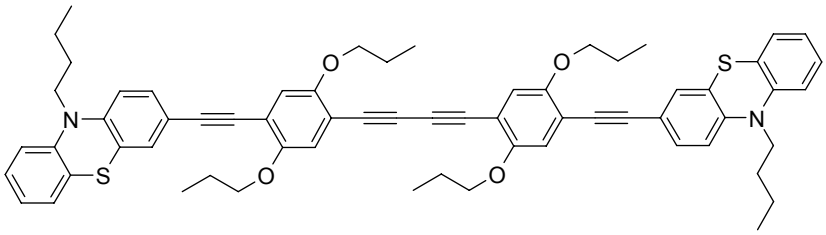

91

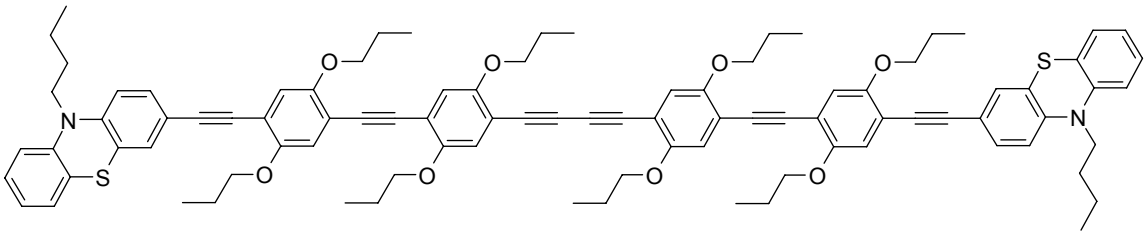

92

Zusammenfassung

Ziel dieser Arbeit war es, den Einfluß „aktiver“ Brückeneinheiten auf den Elektronentransfer (ET) innerhalb organischer Donor-Brücke-Elektrode Einheiten in selbstorganisierenden Monolagen (SAM) mittels spektroskopischer und elektrochemischer Methoden zu untersuchen.

Um Erfahrung bezüglich der Präparation der SAMs und den Meßmethoden zur Bestimmung der ET Geschwindigkeiten zu erhalten, wurden im ersten Teil dieser Arbeit die Ferrocenalkylthiole **1** – **3** und die Ferrocenarylthiole **4** und **5** als Modelverbindungen für Untersuchungen herangezogen.

Cyclovoltammetrische Messungen belegen, dass homogene, gemischte Monolagen aus redoxaktiven Verbindungen und redoxinaktiven Alkylthiolen gebildet werden. Die von *Creager et al.* bestimmten ET Raten der Ferrocenalkylthiole **1** – **3** konnten hierbei verifiziert werden [1]. Wie erwartet erfolgt eine Abnahme der ET Geschwindigkeit bei einer Kettenverlängerung des Alkylspacers von **2** nach **3**. Eine unterschiedliche Konnektivität zwischen Redoxzentrum und Alkylspacer, z. B. die Einführung einer Carbonyl-Funktion im Falle von **1**, unter Beibehaltung der Kettenlänge zeigt keinen bemerkbaren Einfluß auf den ET. Trotzt vergleichbaren Abstands der aromatischen Ferrocenthiole **4** und **5** zu der C_8-Alkyl-Verbindung **2** zwischen Redoxzentrum und Elektrode, weisen diese aufgrund ihrer starken Konjugation sehr hohe ET Geschwindigkeiten auf. Die elektronischen Kopplungsfaktoren selbst deuten auf einen nichtadiabtischen ET zwischen Redoxzentrum und Elektrode hin. Wie erwartet kommt es zu einem Anwachsen der Kopplungsfaktoren bei sich verkürzender Kettenlänge oder bei Einführung konjugierter Spacersysteme. Zusammenfassend kann gesagt werden, dass Erfahrungen hinsichtlich der Präparation der Monolagen gesammelt, die gemessenen ET Raten für der literaturbekannten Verbindungen **1** – **3** bestätigt und diese Informationen auf die konjugierten Verbindungen **4** und **5** angewandt werden konnten.

Im zweiten Teil wurden die Triarylamin- (**29**, **32**) und Phenothiazinalkylthiole (**35**) bezüglich ihres ET Verhaltens in gemischten Monolagen untersucht.

Mittels Cyclovoltammetrie konnte gezeigt werden, daß einheitlich geformte, verdünnte Monolagen vorliegen. Die ET Raten der Triarylamin- (**29**, **32**) und Phenithiazinalkylthiole (**35**) sind jedoch um den Faktor 10 bis 100 höher als vergleichbare

Ferrocenalkylthiole gleicher Kettenlänge [1, 2], wohingegen für Monolagen, welche [Ru(bpy)2(pp)]$^+$-Alkythiole enthalten, äquivalente Werte gefunden wurden [3]. Die ET Geschwindigkeit wird von zwei Parametern beeinflusst: dem elektronischen Kopplungsmatrixelement $|V_{ab}|$ und der Regorganisationsenergie λ [4]. Die ET Geschwindigkeit in Donor-substituierten Alkylthiolen wird hauptsächlich durch die Reorganisationsenergie λ [3] beeinflusst und sogar kleine Änderungen dieser zeigen eine große Auswirkung auf die zu untersuchenden Prozesse. Aus diesem Grund wird eine Zunahme der ET Geschwindigkeit von Ferrocen (hohe Reorganisationsenergie) über die Phenothiazinverbindung **35** und [Ru(bpy)2(pp)]$^+$ zu den Triarylaminchromophoren **29** und **32** (niedrige Reorganisationsenergie) beobachtet. Weiterhin spielt, im Gegensatz zu Beobachtung von *Creager et al.* an äquivalenten Ferrocenverbingungen, die Anbindung des Redoxzentrums an den Alkylspacer eine bedeutende Rolle. Im Falle der elektronenreichen Ether-verbrückten Verbindung **29** wird der ET nicht alleine durch die Reorganisationsenergie λ, sondern ebenso durch mesomere Effekte bestimmt. Bei **29** kommt es durch Lokalisation der positiven Ladung nahe der Ether Funktion formal zu einer Kettenverkürzung um eine „Methyleneinheit“, welche schließlich in höheren ET Geschwindigkeiten resultiert.

Im dritten Teil dieser Dissertation wurde ein Serie „molekularer Drähte“ bestehend aus Methoxy- oder Chlorid-substituierten Triarylamin- und Phenothiazinverbindungen mit unterschiedlichen Brückeneinheiten und Brückenlängen zwischen Redoxzentrum und Ankerfunktion dargestellt und im Hinblick auf ihr ET Verhalten untersucht.

Durch cyclovoltammetrische und UV/Vis-spektroskopische Untersuchungen konnte gezeigt werden, dass sowohl die Oxidationspotentiale als auch die energetischen Zustände der Chromophore recht gut durch Einführung unterschiedlicher Redoxzentren und Brückeneinheiten beeinflusst werden können. Trotz erfolgreicher Kontrolle der Dichte der Chromophoreinheiten in den gemischten Monolagen konnte nur für die Verbindungen **49**, **52** und **87** mit Nitril-substituierten Brückeneinheiten verlässliche ET Geschwindigkeiten erhalten werden. Bei diesen Chromphoren ist ein Absinken der ET Geschwindigkeit bei zunehmender Dichte der redoxaktiven Moleküle in den gemischten Monolagen zu beobachten, welche auf eine Änderung der Adsorptionsgeometrie hindeutet. Bei zunehmender Packungsdichte der Chromophore führt dies zu einer aufrechteren Stellung der redoxaktiven Spezies. Für alle anderen Verbindungen konnten keine Werte aufgrund der zu schnellen ET Geschwindigkeiten ermittelt werden. Konformelle, wie auch

die sehr geringe Abstandsabhängigkeit des ET, resultieren in hohen ET Geschwindigkeiten [5] oder auch ungünstige HOMO-LUMO Energien bezüglich des Donors, der Brücke und der Elektrode sind Gründe für dieses Verhalten. Die Tatsache, dass Verbindung **49** und **52** beinahe die gleichen Geschwindigkeitskonstanten des ETs unabhängig von der Anzahl der Brückeneinheiten (n = 2, n = 3) besitzen, deutet darauf hin, dass ein Hopping-Prozess stattfindet, bei welchem eine geringere Längenabhängigkeit des ETs als bei eine Superexchange-Mechanismus zu erwarten ist. Das es nicht möglich ist die Meßmethode bei ET Geschwindigkeiten größer als 10^5 s^{-1} anzuwenden und auch die Verwendung spektroelektrochemischer Methoden oder der Fast-Scan Cyclovoltammetrie kein Erfolg aufgrund der Instabilität der redoxaktiven Monolagen brachten, muß bei zukünftigen Arbeiten ein besonderes Augenmerk auf die Synthese analoger, gesättigter Verbindungen gelegt werden, bei welchen langsamere ET Geschwindigkeiten zu erwarten sind.

Im letzten Teil dieser Arbeit wurden die Bistriarylamin- und Bisphenothiazinverbindungen **88** – **92** mit verschiedenen Redoxzentren und unterschiedlich langen Spacern und ihre korrespondierenden Radikalkationen und –dikationen bezüglich ihrer elektronischen Kopplung V_{AB} und ihrer Zugehörigkeit zu gemischtvalenten Chromophoren der *Robin/Day* Klasse I – III untersucht. Die Ergebnisse der cyclovoltammetrischen Untersuchungen zeigen, dass nur eine geringe Kopplung zwischen den Triarylamin- und Phenothiazinzentren der Verbindungen **88** und **90** vorliegen. Zudem nimmt die Kopplung innerhalb der homologen Reihe der Bisphenothiazinchromophore von **90** nach **92** bei zunehmender Brückenverlängerung ab. Die Analyse der IV-CT-Banden von **88** und **90** weist darauf hin, dass diese Verbindungen als Übergang zwischen *Robin/Day* Klasse II und III anzusehen sind. Für Verbindungen **89**, **91** und **92** wurde ein komplett anderes Verhalten während der Oxidation gefunden und es konnten keine IV-CT-Bande beobachtet werden. Die UV/Vis-Spektroskopie zeigt, dass im Falle von $\mathbf{89}^{1+}$ ein optisch induzierter Ladungstransfer von der Brückeneinheit zum Triarylamin stattfindet, während die Phenothiazinverbindungen **91** und **92** direkt zum Dikation oxidiert werden. Im zuletzt genannten System kann ein optisch induzierter Ladungstransfer von der Phenothiazineinheit zur Brücke beobachtet werden. Zur Auswertung und zur Untersuchung von V_{AB} wurde hierbei ein Drei-Niveau-Model [6], welches sowohl die direkte als auch die brückenvermittelte Kopplung in die Analyse der CT-Bande mit einbezieht, angewandt.

[1] J. J. Sumner, K. S. Weber, L. A. Hockett, S. E. Creager, *J. Phys. Chem. B* **2000**, *104*, 7449.

[2] K. Weber, L. Hockett, S. Creager, *J. Phys. Chem. B* **1997**, *101*, 8286.

[3] C. Hortholary, F. Minc, C. Coudret, J. Bonvoisin, J.-P. Launay, *Chem. Commun.* **2002**, 1932.

[4] C.-P. Hsu, R. A. Marcus, *J. Phys. Chem.* **1997**, *106*, 584.

[5] W. B. Davis, W. A. Svec, M. A. Ratner, M. R. Wasielewski, *Nature* **1998**, *396*, 60.

[6] C. Lambert, S. Amthor, J. Schelter, *J. Phys. Chem. A* **2004**, *108*, 6474.

Publications

How Delocalized Is *N,N,N',N'*-Tetraphenylphenylenediamine Radical Cation? An Experimental and Theoretical Study on the Electronic and Molecular Structure, A. V. Szeghalmi, M. Erdmann, V. Engel, M. Schmitt, S. Amthor, V. Kriegisch, G. Nöll, R. Stahl, C. Lambert, D. Leusser, D. Stalke, M. Zabel, J. Popp, *J. Am. Chem. Soc.* **2004**, *126*, 7834.

Self-Assembled Monolayers of Chromophores on Gold Surfaces, V. Kriegisch, C. Lambert, *Top. Curr. Chem.* **2005**, published online.

Synthesis and Linear Optical Properties of Tris(catecholate)-Metal(III,IV)-Complexes with Acceptor-Substituted Ligands for Nonlinear Optics, V. Kriegisch, C. Lambert, *Eur. J. Inorg. Chem.* **2005**, accepted.

Poster Presentations

Tris(catecholate)-metal(III,IV)-complexes with Acceptor-substituted Ligands for Nonlinear Optics, Volker M. Kriegisch, Christoph Lambert, *Fifth International Symposium on Functional π-Electron Systems*, Ulm **2002**.

A Theoretical and Experimental Study on the Intervalence Charge Transfer System [*p*-$(Ph_2N)_2$-C_6H_4]$^+$[$SbCl_6$]$^-$, A. V. Szeghalmi, M. Schmitt, W. Kiefer, S. Amthor, V. Kriegisch, G. Nöll, R. Stahl, C. Lambert, D. Leusser, D. Stalke, *Conference on Electron Density: Measurement, Calculation, Application*, Würzburg **2002**.

Electron Transfer in Self Assembled Monolayers (SAM), V. Kriegisch, C. Lambert, Z. Chen, A. Lohr, F. Würthner, A. Terfort, B. Zeysing, *Sixth International Symposium of the Volkswagen-Stiftung on Intra- and Intermolecular Electron Transfer*, Köln **2003**.

Electron Transfer in Self Assembled Monolayers (SAM), V. Kriegisch, C. Lambert, A. Hofmann, Z. Chen, A. Lohr, F. Würthner *Gordon Research Conference "Electron Donor Acceptor Interactions"*, Newport, USA **2004**.

Lectures

Electron Transfer in Self Assembled Monolayers (SAM), V. Kriegisch, *Graduiertenkolleg 690 Electron Density: Theory and Experiment*, Würzburg **2003**.

Electron Transfer in Self Assembled Monolayers (SAM), V. Kriegisch, *KOPO'03*, Blaubeuren **2003**.

Curriculum Vitae

Persönliche Daten

Volker Kriegisch
geboren am 09.08.1975 in Ingolstadt
ledig, ortsungebunden

Schulbildung

1982 – 1986	Grundschule Schonungen
1986 – 1995	Alexander-von-Humboldt-Gymnasium, Schweinfurt **Abschluss: Abitur**

Wehrdienst

07/1995 – 04/1996	2. Instandsetzungsbataillon 8, Volkach

Hochschulausbildung

10/1996 – 12/2001	Studium der Chemie an der Universität Würzburg
10/1998	**Chemie-Vordiplom**
03/2001 – 12/2001	Diplomarbeit bei Prof. Dr. C. Lambert am Institut für Organische Chemie der Universität Würzburg Thema: **Darstellung und Charakterisierung Akzeptor-substituierter Triscatechol-Metall-Komplexe**
12/2001	**Chemie-Diplom**
01/2001 – 10/2005	Doktorarbeit bei Prof. Dr. C. Lambert am Institut für Organische Chemie der Universität Würzburg Thema: **Electron Transfer in Self Assembled Monolayers (SAM)**

Auslandsaufenthalt

03/2000 – 07/2000	Fortgeschrittenenpraktikum bei Dr. K .McCullough in Organischer Chemie an der Herrioth-Watt-University in Edinburgh, Schottland

Praktische Tätigkeiten

05/1999 – 07/1999	Studentische Hilfskraft des Medizinerpraktikums, Universität Würzburg
03/2001 – 03/2005	Verantwortlicher Ausbilder der Auszubildenden im Arbeitskreis Prof. Dr. Lambert

10/2002 – 03/2004	Assistent des Medizinerpraktikums, Universität Würzburg
05/2003 – 07/2003	Tutoriumsleiter des Tutoriums für Lehramtskandidaten des Faches Chemie für Gymnasien, Universität Würzburg

Stipendien

10/1997 – 12/2001	Stipendium der Bosch-Stiftung
01/2002 – 06/2002	Stipendium des Graduiertenkollegs „Elektronendichte“
07/2002 – 06/2004	Stipendium des Fonds der Chemischen Industrie

Auszeichnungen

06/1999	Vordiplom – Fakultätspreis der Fakultät für Chemie und Pharmazie, Universität Würzburg
06/2002	Diplom – Fakultätspreis der Fakultät für Chemie und Pharmazie, Universität Würzburg

Berufliche Tätigkeit

seit 10/2005	Leitender Mitarbeiter im Bereich Produktion und Verfahrenstechnik der Forschungs- und Entwicklungsabteilung bei Wolff Cellulosics, Bayer Material Science Company, Walsrode

Danksagung

Bedanken möchte ich mich bei allen, die am Gelingen dieser Arbeit großen Anteil hatten:

Herrn Dr. M. Grüne und *Frau E. Ruckdeschel* für die Aufnahme der NMR-Spektren und für bereitwillige Auskunft und Hilfe bei den alltäglichen Meßschwierigkeiten.

Herrn C.-P. Kneis, für die Durchführung der Elementaranalysen. Erfreulicherweise hatte ich sogar einmal ein „Vierer" auf Anhieb – der Sechser im Lotto der Elementaranalyse.

Herrn Dr. M. Büchner und *Herrn F. Dadrich*, für die Aufnahme der Massenspektren und für so manch lustige und „längere" Unterhaltung.

Herrn M. Ramold, der beim Anblick von mir und vor allem Rainer gleich in eine Art Schockzustand versetzt wurde, da er wieder einmal die Befürchtung hatte, vor beinahe unlösbare Aufgaben gestellt zu werden. Ohne seine Fähigkeiten wären nicht nur so manche Elektroden noch Zukunftsmusik.

Ein besonderer Dank gilt *Herrn Dipl.-Ing. B. Brunner*, der mir immer mit Rat und Tat bezüglich Computer bei Seite stand und sich auch immer wieder über unsere Meßanordnung wunderte – so ganz nach der Devise: „Für was braucht man den noch eine dritte Elektrode? Ach, ist mir auch egal, das ist eure Sache!"

Allen anderen Angestellten hier im Hause, *Frau Dreher*, *Frau Krug*, *Frau Lange*, *Frau Schreiber*, *Herrn Braun*, *Herrn Förtsch*, *Herrn Fromm*, *Herrn Heilmann*, unserem Glasbläser *Herrn Ludwig*, *Herrn Meckel*, *Herrn Möckel*, *Herrn Rauch*, *Herrn Reich*, und *Herrn Dr. Stadler* die bei großen und kleinen Schwierigkeiten sofort hilfsbereit waren und durch Ihre Arbeit meine sehr erleichterten.

Besonderer Dank gebührt den Mitgliedern des Arbeitskreises *Lambert* für die lockere Arbeitsatmosphäre, die große Hilfsbereitschaft, die Grillabende, die Federweißenzeit, die Weinproben und auch die Weißwurstfrühstücke. Diese Auflistung soll aber nicht darüber hinwegtäuschen, dass nur gefeiert wurde, es wurde ebenfalls viel gearbeitet. Auch wenn es sowohl Höhen als auch Tiefen gab, so war es eine wirklich schöne Zeit, welche ich nicht missen möchte. Besonders die Kanutour im Altmühltal wird unvergesslich bleiben. Es wäre so viel zu erzählen oder zu erwähnen, manchmal sind es nur Kleinigkeiten, dies ist leider unmöglich, aber wenigstens bleibt die gemeinsame Erinnerung und das Erlebnis. Ein besonderer Dank gilt:

Herrn Prof. Dr. Lambert für seine Unterstützung während der gesamten Zeit in seinem Arbeitskreis. Nicht nur ich, sondern auch alle anderen wurden immer wieder von seinem Wissen, sowohl im Bereich der allgemeinen Chemie, als auch in der Elektrochemie und aller möglichen und unmöglichen spektroskopischen Methoden und von seinen Ideen überrascht. Seine ständige Erreichbarkeit und Hilfsbereitschaft bei Messproblemen ist nicht hoch genug einzuschätzen.

Meinen gesamten Azubis *Kristina*, *Manuela*, *Tatjana*, *Veronika*, *Vilija*, *David* und *Florian* (*Floh*), hier auch *Andre* nicht zu vergessen (obwohl er für Sascha gearbeitet hat) welche unermüdlich für mich synthetisiert haben und nach der fünften Wiederholung auch die Nase voll hatten. Ihre Leistung für mich war wirklich unbezahlbar und ohne sie wäre der Umfang meiner präparativen Arbeit nicht möglich gewesen. Ich wünsche Euch allen viel Erfolg in eurer Zukunft, sei es bei eurem Studium oder bei eurem weiteren beruflichen und persönlichen Werdegang.

Ein ganz großer Dank geht an meine „Effis“ *Mandy*, *Andi* und *Christoph,* welche mich jeweils sechs Wochen „ertragen“ mussten und ebenfalls ein fester Bestandteil meiner Arbeit waren und zum Gelingen beitrugen. Auch euch weiterhin viel Erfolg.

Auch unserem Postdoc, *Hongchao* oder auch *Holidayhong* genannt, sei gedankt. Ich möchte nur nicht wissen, wie das Bild der Deutschen bei Hong durch Sascha geprägt wurde, ich sage nur: „Hello Hong, how was the dog?“ (Zitat Sascha) und wie sich dies auf die Beziehungen zu China zukünftig auswirken wird.

Jetzt zu unseren letzten Diplomanden, *Dörte*, *Christian* und *Conny*, welche zu meinem Ende hin in diesen AK nochmals frischen Wind hereinbrachten. *Dörte*, passe auf, wer weiterhin manchmal hinter dir steht (übrigens: „Dirty Harry" müssen wird doch noch irgendwann einmal ansehen) und zum *Gefreiten Müller* sage ich nur: still gestanden oder tiefste Gangart. Mit Diplomanden hat man schon so sein Kreuz, da darf man sogar noch in meinem Alter an Liegestütze-Wettbewerben teilnehmen, nur um nicht sein Gesicht zu verlieren. Aber wenigstens war der *Gefreite Müller* danach glücklich eine mehr zu Stande gebracht zu haben (Mitarbeiter müssen eben glücklich gemacht werden, damit sie weiterhin Freude an der Arbeit haben). Auch lernen sie kaum aus Fehlern, obwohl man schon vorher sagt, dass etwas nicht funktionieren kann, wird dem älteren, erfahrenen Doktoranden nicht geglaubt, stimmts *Marco*. Ich denke aber, das war vor allem auch, um uns Altdoktoranden in einer stressigen Zeit etwas zu erheitern, jedenfalls ist es euch gelungen.

Sascha danke ich zum einen für seine bloße Anwesenheit und für das Leben, dass er in diesen AK brachte. Seine Ausführungen über das weibliche Geschlecht, so manche Diskussion und tänzerische Princeinterpretation mit Gesangseinlage sind legendär. Schreiben kann ich hier über deine Lieblingsthemen nichts näheres, da ich nicht möchte, dass meine Dissertation der Zensur anheim fällt, am besten drückt es dieses Wort aus: „Puhhh!". In diesem Sinne bleibt nur zu sagen: „Des muschde dir ma gebbe!". Einen riesigen Dank für die unermüdliche Korrektur meiner Arbeit.

Unserer guten Seele und Laborantin *Roswitha*, welche immer wieder Ordnung in unser Durcheinander brachte. Ich hoffe, dass du den Kampf gegen Windmühlen, sprich die Unsauberkeit unseres Seminarraums, gewinnen wirst.

Zudem *Marco*, meinen Labornachbarn, der sich durch die Zulassungsarbeit bei uns nicht hat abschrecken lassen und zur Promotion wieder zurückkam. Seine heitere und lockere Art brachte Schwung ins Labor, auch wenn er hin und wieder einmal „mit der Gesamtsituation unzufrieden" war. Zudem auch vielen Dank für die schnelle Korrektur meiner Dissertation.

Meinen Mitstreitern, *Rainer* und *Stephan*, die mich bereits durch das Studium begleitet und auch mit gelitten haben. Ich werde auf alle Fälle dem traditionellen freitäglichen Frühstück

mit Rainer nachtrauern. Rainer, erinnere dich vor allem immer an eine Frage im Hesse/Schrader bezüglich der Mitarbeiter oder auch an den unvergesslichen Abend in der „Mai-Thai Bar“ in Ulm. Stephans Wissen über Wein und Essen ist legendär, wodurch nicht nur ich einiges hinzulernen konnte. Seine theoretischen Ausführungen über sein Dissertationsthema beim Mittagessen, bei welchen der Rest schon nach dem zweiten Satz nicht mehr durchstieg, waren immer wieder köstlich anzuhören. Ich glaube, hier konnte nur noch unser Chef folgen. Danke für eure uneigennützliche Hilfe in jeder Situation. Ohne euch beide wäre es definitiv langweiliger gewesen und es hätte einiges gefehlt.

Dann wäre da noch unser AK-Pärchen *Babs* und *Dirk*, besser bekannt unter dem Titel: Das fleißige Geißlein, dass über die rauschenden Bäche springt (Zitat: Prof. Dr. Ch. Lambert). Die Fahrradtouren, die gemeinsame Theaterbesuche oder Frühstücke sind jetzt leider vorbei. Die überragende Organisation von Feiern hast du, Babs, schon wirklich spitze gemeistert und damit auch erheblich zum Zusammenhalt des AKs beigetragen. Ebenfalls ein riesiger Dank bei der Hilfe so mancher kleinerer oder größerer Probleme. Leider, Dirk, ist die „Klopferei“ zum Schluß etwas auf der Strecke geblieben, aber ich hoffe, wir kommen nochmals dazu - die Kreide in Hannover wartet auf dich.

Wen habe ich denn noch vergessen? Ach ja, welch unverzeihlicher Fehler, unsere Lehrämtlerin *Simone*, auch Simon, klein Seimen, Wally, …. genannt, welche im AK Lambert anfing, nach Friedberg auswanderte, zu ein „paar“ Prüfungen zurückkam, einen kleinen Abstecher nach Australien einlegte und schließlich Würzburg Richtung Hamburg den Rücken kehrte. Entgegengesetzter könnte diese Lage zu deinem Wunschgebiet Freiburg nicht sein. Dich zu übersehen oder nicht zu bemerken war wirklich schwierig. Meist wie ein Wirbelwind, manchmal (eher seltener) etwas ruhiger, aber nie um einen entsprechenden Spruch verlegen, wurde der AK aufgemischt. Für deine Zukunft und für deine Dissertation wünsche ich dir viel Erfolg und alles erdenkliche Gute. Danke übrigens auch für die mithilfe bei der Korrektur meiner Doktorarbeit.

Zudem gebührt auch Dank an zwei Australier, Ngari und eine mir nicht nähere namentlich bekannte Person, welche ebenfalls Teile meiner Arbeit verbesserten. Es ist eigentlich schon recht witzig, wenn man bedenkt, dass dieses Dokument dazu um den halben Erdball wandern musste.

Dank auch an *Jörg*, meinen „Fahrradkollegen“ für seine heitere und wirklich lustige Art. Vielleicht schaffen wir es ja doch noch irgendwann einmal ein Rennen zusammen zu fahren – meinen Sturz habe ich allerdings schon hinter mir.

Spezieller Dank gilt meinen Studienfreunden *Andrea*, *Andi*, *Christian* (das Fehnoxy-Radikal) und im Speziellen Schmitti (sorry Rainer). Es war eine wirklich herrliche Zeit mit euch, auch wenn ein Teil dieser Konstellation nach Bayreuth abgewandert ist. Die Besuche im AK Malisch sind natürlich jetzt auch Geschichte. Manche meiner Kollegen meinten ja, ich solle mich nicht in die Höhle des Löwen, sprich die AC, wagen, aber geschadet hat es weder euch, Andi und Schmitti, noch mir. Ich wünsche euch ebenfalls für die Zukunft und eure Bewerbungen alles erdenklich Gute – solche Freunde muß man erst einmal haben.

Vielen Dank meiner Schwester *Martina* für alles Unmögliche und für die Verbesserung des sprachlichen Teils meiner Arbeit. Inhaltlich hast Du mit Sicherheit genauso viel verstanden wie bei meiner Diplomarbeit, aber tröste Dich, wenn du dies willst, dann kannst du nochmals mit einem Chemiestudium beginnen – der kleine Bruder hilft dir dabei.

Der größte Dank gilt allerdings meinen Eltern für den moralischen und finanziellen Rückhalt, ohne den diese Arbeit und mein Studium nicht zustande gekommen wären. Würde ich es in Worte fassen müssen, was ich meinen Eltern zu verdanken habe und was sie mir bedeuten, würde dies ohne Probleme den Umfang dieser Arbeit sprengen.

Erklärung

Hiermit erkläre ich an Eides statt, daß ich die Dissertation „ELECTRON TRANSFER PROCESSES BETWEEN ORGANIC REDOX CENTRES AND ELECTRODES VIA ACTIVE BRIDGES IN SELF-ASSEMBLED MONOLAYERS“ selbständig angefertigt und keine anderen als die von mir angegebenen Quellen und Hilfsmittel benutzt habe.

Ich erkläre außerdem, daß diese Dissertation weder in gleicher oder anderer Form bereits in einem anderen Prüfungsverfahren vorgelegen hat.

Ich habe früher außer den mit dem Zulassungsgesuch urkundlich vorgelegten Graden keine weiteren akademischen Grade erworben oder zu erwerben versucht.

Würzburg, den

Volker Kriegisch